

Parasitic nematodes of marine fishes from Palmyra Atoll, East Indo-Pacific, including a new species of *Spinitectus* (Nematoda, Cystidicolidae)

David González-Solís^{1,2,*}, Lilia C. Soler-Jiménez^{3,*},
M. Leopoldina Aguirre-Macedo³, John P. McLaughlin⁴, Jenny C. Shaw⁴,
Anna K. James⁴, Ryan F. Hechinger⁵, Armand M. Kuris⁴,
Kevin D. Lafferty^{4,6}, Víctor M. Vidal-Martínez³

1 El Colegio de la Frontera Sur, unidad Chetumal. Av. Centenario Km 5.5, Chetumal, Quintana Roo 77014, México **2** Institute of Parasitology, Biology Centre of the Academy of Sciences of the Czech Republic, Branišovská 31, 370 05 České Budějovice, Czech Republic **3** Laboratorio de Patología Acuática, Centro de Investigación y de Estudios Avanzados, Mérida. Antigua carretera a Progreso km. 6, Cordemex, Mérida, Yucatán, México **4** Department of Ecology, Evolution and Marine Biology and Marine Science Institute, University of California, Santa Barbara, CA 93106, USA **5** Scripps Institution of Oceanography-Marine Biology Research Division, University of California, San Diego, La Jolla, California 92093, USA **6** Western Ecological Research Center, U.S. Geological Survey, Marine Science Institute, University of California, Santa Barbara CA 93106, USA

Corresponding author: Victor M. Vidal-Martínez (vvidal@cinvestav.mx)

Academic editor: Nic Smol | Received 23 July 2019 | Accepted 27 October 2019 | Published 27 November 2019

<http://zoobank.org/8951A3F9-FDD0-4041-8BEA-BDA48C1B616C>

Citation: González-Solís D, Soler-Jiménez LC, Aguirre-Macedo ML, McLaughlin JP, Shaw JC, James AK, Hechinger RF, Kuris AM, Lafferty KD, Vidal-Martínez VM (2019) Parasitic nematodes of marine fishes from Palmyra Atoll, East Indo-Pacific, including a new species of *Spinitectus* (Nematoda, Cystidicolidae). ZooKeys 892: 1–26. <https://doi.org/10.3897/zookeys.892.38447>

Abstract

Here, we present the results of a taxonomic survey of the nematodes parasitizing fishes from the lagoon flats of Palmyra Atoll, Eastern Indo-Pacific. We performed quantitative parasitological surveys of 653 individual fish from each of the 44 species using the intertidal sand flats that border the atoll's lagoon. We provide morphological descriptions, prevalence, and mean intensities of the recovered seven species of adult nematode (*Pulchrascaris chiloscyllyi*, Capillariidae gen. sp., *Cucullanus bourdini*, *Cucullanus oceanien-sis*, *Pseudascarophis* sp., *Spinitectus* (*Paraspinitectus*) *palmyraensis* sp. nov., *Philometra pellucida*) and three larval stages (*Pulchrascaris* sp., *Hysterothylacium* sp., *Cucullanus* sp.). We recorded: *Pulchrascaris chiloscyllyi*

* Contributed equally as the first authors

from *Carcharhinus melanopterus*; Capillariidae gen. sp. from *Chaetodon lunula*, *Lutjanus fulvus*, and *Ellochelone vaigiensis*; *Cucullanus bourdini* from *Arothron hispidus*; *Cucullanus oceanensis* from *Abudefduf sordidus*; *Pseudascarophis* sp. from *Chaetodon auriga*, *Chaetodon lunula*, and *Mulloidichthys flavolineatus*; *Spinitectus (Paraspinitectus) palmyraensis* **sp. nov.** from *Albula glossodonta*; *Philometra pellucida* from *Arothron hispidus*; and three larval forms, *Pulchrascaris* sp. from *Acanthurus triostegus*, *Acanthurus xanthopterus*, *Rhinecanthus aculeatus*, *Platybelone argalus*, *Carangoides ferdau*, *Carangoides orthogrammus*, *Caranx ignobilis*, *Caranx melampygus*, *Caranx papuensis*, *Chaetodon auriga*, *Chanos chanos*, *Amblygobius phalaena*, *Asterropteryx semipunctata*, *Valencienea sexguttata*, *Kyphosus cinerascens*, *Lutjanus fulvus*, *Lutjanus monostigma*, *Ellochelone vaigiensis*, *Mulloidichthys flavolineatus*, *Upeneus taeniopterus*, *Gymnothorax pictus*, *Abudefduf septemfasciatus*, *Abudefduf sordidus*, and *Stegastes nigricans*; *Hysterothylacium* sp. type MD from *Acanthurus triostegus*, *Carangoides ferdau*, *Chaetodon lunula*, *Chanos chanos*, *Kyphosus cinerascens*, *Abudefduf sordidus*, and *Arothron hispidus*; and *Cucullanus* sp. from *Caranx ignobilis*. *Spinitectus (Paraspinitectus) palmyraensis* **sp. nov.** (Cystidicolidae) is described from the intestine of roundjaw bonefish *Albula glossodonta*. All the nematode species reported in this study represent new geographical records. We discuss how our survey findings compare to other areas of the Indo-Pacific, and the way the relatively numerical dominance of trophically transmitted larval stages likely reflect the intact food web of Palmyra Atoll, which includes a large biomass of large-bodied top predator sharks and ray-finned fishes.

Keywords

Cucullanus, *Hysterothylacium*, *Paraspinitectus*, *Philometra*, *Pseudascarophis*, *Pulchrascaris*

Introduction

Few studies have surveyed the parasites of all the fish species found in a habitat. In the Eastern Indo-Pacific, several studies have reported parasitic nematodes of marine fishes from Australia, French Polynesia, Okinawa (Japan), Palawan (Philippines) Indonesia, off New Caledonia, and the Hawaiian Islands (Johnston and Mawson 1951; Schmidt 1969; Deardorff et al. 1982; Lester and Sewell 1989; Bruce and Cannon 1990; Hasegawa et al. 1991; Rigby et al. 1997, 1999; Morand and Rigby 1998; Justine 2007; Lafferty et al. 2008; Moravec and Justine 2010; Palm and Bray 2014; Moravec and Justine 2018). Most studies focus on a single host species or a particular nematode genus, and a few include several large fish species (Justine 2007, 2010; Justine et al. 2012; Palm and Bray 2014). The survey by Lafferty et al. (2008) is the only one to examine parasitic nematodes of marine fishes in Palmyra Atoll, listing helminths from five fish species in the fore-reef (a habitat adjacent to the one we surveyed); however, their analysis was limited to broad patterns of richness and abundance of morphospecies, conservatively grouped into broad taxonomic categories.

Palmyra Atoll is one of the northern Line Islands located in the Eastern Indo-Pacific marine ecoregion (Spalding et al. 2007), 1680 km south-south-west of Hawaii. It is a National Wildlife Refuge managed by the US Fish and Wildlife Service (The Nature Conservancy 2006), where visitation is restricted to a small staff and a few visiting scientists or volunteers. All fishing has been prohibited at Palmyra since it became a US National Wildlife Refuge in 2000, and before that, the atoll's remoteness kept fishing pressure low (Stevenson et al. 2007).

This study is part of a larger project to understand the structure and function of the Palmyra Atoll's food webs. This paper is a companion to three others examining different fish parasite taxa (Vidal-Martínez et al. 2012, 2017; Soler-Jiménez et al. 2019) from Palmyra's lagoon flats. As such, our survey adds to the few published, detailed species descriptions or host records from this Central Indo-Pacific region (Palm and Bray 2014). The specific primary contributions of this study are 1) morphological descriptions, prevalence estimates, mean intensities, and host records for the nematode species recovered from the fish species sampled on the lagoonal flats of Palmyra Atoll, and, 2) a morphological description of a new nematode in the genus *Spinitectus*.

Methods

Individual fish were captured between 13 October and 10 November 2009, and 22 June and 28 July 2010, by seine, spear, and hook and line from the intertidal sand flats bordering the lagoon of Palmyra Atoll (05°53'00"N, 162°05'00"W). Immediately after capture, the fish were separated and anaesthetised individually with 0.5 ml/L of 2-phenoxyethanol (Sigma, St. Louis, MO, USA) in plastic bags with lagoon water and transported to the laboratory facility of the Palmyra Atoll Research Consortium (PARC). Total length and weight (g) were recorded for each individual fish. Subsequently, cavities, musculature, and all internal organs were examined for metazoan parasites in a standardized way to permit a complete estimate of the nematodes intensity (Shaw et al. 2005), using squash plates and a dissection microscope with a total magnification of 40×. Nematodes were isolated, washed in physiological saline, fixed in 4% hot formalin or 70% ethanol, labelled and stored in vials for later evaluation. The remaining specimens were flattened and cleared in a mixture of glycerine and water in different proportions, to study the morphology of structures under a compound microscope (Olympus BX-53, Olympus Corporation, Tokyo, Japan). For scanning electron microscopy (SEM), specimens were postfixed in 1% osmium tetroxide (in phosphate buffer), dehydrated through a graded acetone series, critical-point-dried, and sputter-coated with gold; they were examined using a JEOL JSM-7401F scanning electron microscope at an accelerating voltage of 4 kV (GB low mode). Measurements were made on the images at 1,000× magnification using ImageJ software (v. 1.43, April 2010). All measurements are in micrometres, unless otherwise indicated. Prevalence and mean intensity concepts were applied following Bush et al. (1997). Type and voucher specimens of each species were deposited in the Helminthological Collection of the Laboratory of Parasitology, at Centre for Research and Advanced Studies, National Polytechnic Institute, Mérida, Yucatán, México (CHCM).

Results

A total of 653 individual fish from 44 species were examined (Table 1), 28 of which were parasitized by at least one parasitic nematode species (Table 2). *Abudefduf sordidus*

Table 1. Fish species examined from the lagoon flats of the Palmyra Atoll. *N* = number of fish examined; Max = maximum length reported for that fish species in FishBase (<http://www.fishbase.se>); range = total length range of the fish examined.

Host examined	Fish common name	<i>N</i>	Infected hosts	Max (cm)	Range (cm)
Acanthuridae					
<i>Acanthurus triostegus</i> (Linnaeus, 1758)	Convict surgeonfish	50	7	27	10–18
<i>Acanthurus xanopterus</i> Valenciennes, 1835	Yellowfin surgeonfish	20	3	70	20–40
Albulidae					
<i>Albula glossodonta</i> (Forsskål, 1775)	Roundjaw bonefish	24	13	90	37–58
Pogonidae					
<i>Cheilodipterus quinquelineatus</i> Cuvier, 1828	Five-lined cardinalfish	5	0	13	5–6
Balistidae					
<i>Pseudobalistes flavimarginatus</i> (Rüppell, 1829)	Yellowmargin triggerfish	4	0	60	17–53
<i>Rhinecanthus aculeatus</i> (Linnaeus, 1758)	White-banded triggerfish	18	2	30	8–24
Belonidae					
<i>Platybelone argalus argalus</i> (Lesueur, 1821)	Keeltail needlefish	2	1	50	9–36
Carangidae					
<i>Carangoides ferdau</i> (Forsskål, 1775)	Blue trevally	5	4	75	33–38
<i>Carangoides orthogrammus</i> (Jordan & Gilbert, 1882)	Island trevally	3	2	75	25–35
<i>Caranx ignobilis</i> (Forsskål, 1775)	Giant trevally	4	4	170	56–79
<i>Caranx melampygus</i> Cuvier, 1833	Bluefin trevally	6	6	117	31–66
<i>Caranx papuensis</i> Alleyne & MacLeay, 1877	Brassy trevally	5	2	88	12–41
Carcharhinidae					
<i>Carcharhinus melanopterus</i> (Quoy & Gaimard, 1824)	Blacktip reef shark	5	4	200	46–219
Chaetodontidae					
<i>Chaetodon auriga</i> Forsskål, 1775	Threadfin butterflyfish	13	5	23	12–19
<i>Chaetodon lunula</i> (Lacepède, 1802)	Raccoon butterflyfish	14	11	20	11–16
Chanidae					
<i>Chanos chanos</i> (Forsskål, 1775)	Milkfish	5	2	180	31–57
Gobiidae					
<i>Amblygobius phalaena</i> (Valenciennes, 1837)	Whitebarred goby	18	6	15	1.3–7
<i>Asterropteryx semipunctata</i> Rüppell, 1830	Starry goby	12	1	6	2–4
<i>Gnatholepis anjerensis</i> (Bleeker, 1851)	Eye-bar goby	2	0	8	2–3
<i>Istigobius decoratus</i> (Herre, 1927)	Decorated goby	5	0	13	7–11
<i>Istigobius ornatus</i> (Rüppell, 1830)	Ornate goby	26	0	11	3–6
<i>Istigobius rigilius</i> (Herre, 1953)	Rigilius goby	1	0	11	4
<i>Oplopomus oplopomus</i> (Valenciennes, 1837)	Spinecheek goby	26	0	10	2–7
<i>Psilopomus prolatus</i> Watson & Lachner, 1985	Longjaw shrimpgoby	11	0	6	2–4
<i>Valenciennea sexguttata</i> (Valenciennes, 1837)	Sixspot goby	14	1	14	2–9
Hemiramphidae					
<i>Hemiramphus depauperatus</i> Lay & Bennett, 1839	Tropical half-beak fish	20	0	40	20–34
Kyphosidae					
<i>Kyphosus cinerascens</i> (Forsskål, 1775)	Blue sea chub	2	2	50	35–38
Lutjanidae					
<i>Lutjanus fulvus</i> (Forster, 1801)	Blacktail snapper	26	13	40	7–26
<i>Lutjanus monostigma</i> (Cuvier, 1828)	One spot snapper	6	3	60	17–37
Mugilidae					
<i>Crenimugil crenilabis</i> (Forsskål, 1775)	Fringelip mullet	42	0	60	8–45

Host examined	Fish common name	N	Infected hosts	Max (cm)	Range (cm)
<i>Ellochelon vaigiensis</i> (Quoy & Gaimard, 1825)	Squairetail mullet	54	7	63	3–32
<i>Osteomugil engeli</i> (Bleeker, 1858)	Kanda	63	0	30	1–20
Mullidae					
<i>Mulloidichthys flavolineatus</i> (Lacepède, 1801)	Yellowstripe goatfish	52	6	43	8–37
<i>Upeneus taeniopterus</i> Cuvier, 1829	Finstripe goatfish	5	3	33	1–30
Muraenidae					
<i>Gymnothorax pictus</i> (Ahl, 1789)	Paintspotted moray	7	1	140	41–70
Ophichthidae					
<i>Myrichthys colubrinus</i> (Boddaert, 1781)	Harlequin snake eel	3	0	97	33–65
Pinguipedidae					
<i>Paraperis lata</i> Randall & McCosker, 2002	Y-barred sandperch	13	0	21	2–3
Pomacentridae					
<i>Abudefduf septemfasciatus</i> (Cuvier, 1830)	Banded sergeant	12	1	23	14–20
<i>Abudefduf sordidus</i> (Forsskål, 1775)	Blackspot sergeant	18	4	24	14–19
<i>Chrysiptera glauca</i> (Cuvier, 1830)	Grey demoiselle	3	0	12	8–10
<i>Stegastes nigricans</i> (Lacepède, 1802)	Dusky farmerfish	10	1	14	8–10
Serranidae					
<i>Epinephelus merra</i> Bloch, 1793	Honeycomb grouper	2	0	32	13–24
Sphyrnidae					
<i>Sphyrna barracuda</i> (Edwards, 1771)	Great barracuda	2	0	200	65–76
Tetraodontidae					
<i>Arothron hispidus</i> (Linnaeus, 1758)	White-spotted puffer	15	7	50	17–49

(Forsskål) (Pomacentridae), *Arothron hispidus* (Linnaeus) (Tetraodontidae) and *Chaetodon lunula* (Lacepède) (Chaetodontidae) each harbored three nematode species. *Acanthurus triostegus* (Linnaeus) (Acanthuridae), *Carangoides ferdau* (Forsskål) (Carangidae), *Chaetodon auriga* Forsskål (Chaetodontidae), *Chanos chanos* (Forsskål) (Chanidae), *Kyphosus cinerascens* (Forsskål) (Kipposidae), *Ellochelon vaigiensis* (Quoy & Gaimard) (Mugilidae), *Lutjanus fulvus* (Forster) (Lutjanidae) and *Mulloidichthys flavolineatus* (Lacepède) (Mullidae) served as host for two nematode species. All other infected fish species hosted a single nematode species. Sixteen fish species were found free of any nematode parasite (Table 1).

A total of 10 nematode taxa belonging to six families were found. Seven nematode species were adults and three were larvae (Table 2). A brief taxonomic description of each species with their respective prevalences and mean intensities is presented below.

Family Anisakidae Railliet & Henry, 1912

Pulchrascaris Vicente & Santos, 1972

Pulchrascaris chiloscyllyi (Johnston & Mawson, 1951) Deardorff, 1987

Description. Male (1 mature specimen, measurements of one young specimen in parenthesis): elongate, relatively large nematodes, 68.01 (20.36) mm long, 767 (388) wide. Cuticular alae distinct. Lips small, greatly reduced, with tooth-like structures. Nerve ring located at first third of esophagus length, 503 (380); deirids posterior to

Table 2. Parasitic nematodes of fishes from the lagoon flats of Palmyra Atoll and their infection parameters; *N* = number of fish examined. *Larval forms.

	Hosts	<i>N</i>	Infected hosts	Prevalence (%)	Mean intensity (±SD)
Anisakidae					
<i>Pulchrascaris chiloscyllyii</i>	<i>Carcharhinus melanopterus</i>	5	4	80	35 ± 26.5
<i>Pulchrascaris</i> sp.*	<i>Acanthurus triostegus</i>	50	4	8	2.3 ± 1.9
	<i>Acanthurus xanthopterus</i>	20	3	15	1.3 ± 0.6
	<i>Rhinecanthus aculeatus</i>	18	2	11.1	1
	<i>Platybelone argalus</i>	2	1	50	10
	<i>Carangoides ferdau</i>	5	2	40	42 ± 58
	<i>Carangoides orthogrammus</i>	3	2	67	52.5 ± 72.8
	<i>Caranx ignobilis</i>	4	4	100	71.3 ± 106.5
	<i>Caranx melampygus</i>	6	6	100	53.7 ± 106.4
	<i>Caranx papuensis</i>	5	2	40	8 ± 9.9
	<i>Chaetodon auriga</i>	13	1	8	1
	<i>Chanos chanos</i>	5	1	20	2
	<i>Amblygobius phalaena</i>	18	6	33	7.2 ± 8.6
	<i>Asterropteryx semipunctata</i>	12	1	8	3
	<i>Valencienea sexguttata</i>	14	1	7	1
	<i>Kyphosus cinerascens</i>	2	1	50	7
	<i>Lutjanus fulvus</i>	26	12	46	5.2 ± 3.7
	<i>Lutjanus monostigma</i>	6	3	50	4.7 ± 3.2
	<i>Ellochelone vaigiensis</i>	54	4	7	1.5 ± 0.6
	<i>Mulloidichthys flavolineatus</i>	52	5	10	1.4 ± 0.4
	<i>Upeneus taeniopterus</i>	5	3	60	3.7 ± 1.5
<i>Gymnothorax pictus</i>	7	1	14	3	
<i>Abudefduf septemfasciatus</i>	12	1	8	1	
<i>Abudefduf sordidus</i>	18	1	6	1	
<i>Stegastes nigricans</i>	10	1	10	1	
<i>Hysterothylacium</i> sp. type MD*	<i>Acanthurus triostegus</i>	50	3	6	1.7 ± 0.6
	<i>Carangoides ferdau</i>	5	2	40	1.0
	<i>Chaetodon lunula</i>	14	7	50	3.3 ± 1.6
	<i>Chanos chanos</i>	5	1	20	6
	<i>Kyphosus cinerascens</i>	2	1	50	2
	<i>Abudefduf sordidus</i>	18	1	6	3
<i>Arothron hispidus</i>	15	3	20	7.0 ± 5.0	
Capillariidae					
Capillariidae gen. sp.	<i>Chaetodon lunula</i>	14	2	14	2.5 ± 0.7
	<i>Lutjanus fulvus</i>	26	1	4	1
	<i>Ellochelone vaigiensis</i>	54	3	6	1.7 ± 0.6
Cucullanidae					
<i>Cucullanus bourdini</i>	<i>Arothron hispidus</i>	15	7	47	6 ± 4.7
<i>Cucullanus oceaniensis</i>	<i>Abudefduf sordidus</i>	18	2	11	1.5 ± 0.7
<i>Cucullanus</i> sp.*	<i>Caranx ignobilis</i>	4	1	25	2
Cystidicolidae					
<i>Spinitectus</i> (<i>Paraspinitectus</i>) <i>palmyraensis</i> sp. nov.	<i>Albula glossodonta</i>	24	13	54	3.2 ± 4.0
<i>Pseudascarophis</i> sp.	<i>Chaetodon auriga</i>	13	4	31	1
	<i>Chaetodon lunula</i>	14	2	14	3 ± 2.8
	<i>Mulloidichthys flavolineatus</i>	52	1	2	1
Philometridae					
<i>Philometra pellucida</i>	<i>Arothron hispidus</i>	15	6	40	20.8 ± 31.4

level of nerve ring, 604, both from anterior body end. Excretory pore between base of subventral lips. Esophagus cylindrical, 2.96 (1.95) mm long, with large ventriculus at posterior end, 3.38 (2.12) mm long, and without ventricular appendage. Intestinal caecum anteriorly directed, somewhat larger than ventriculus, 3.57 (2.36) mm long. Spicules equal, similar, alate, 1.48 mm long; gubernaculum absent. Caudal papillae 51 pairs: 42 precloas pairs (some subventral and other sublateral), 4 adcloacal subventral pairs, 5 postcloacal (including phasmids). One single, ventral papilla on the anterior cloacal lip. Three cuticular plates immediately posterior to cloacal opening, with serrate edges. Tail conical, short, 298 (182) long.

Fourth-stage larva (1 specimen): Length of body 11.56 mm long, 233 wide. Esophagus, ventriculus and intestinal caecum 1.25, 0.93, 1.08 mm, respectively. Nerve ring 275, deirids 355, both from the cephalic end. Tail 126 long.

Host. *Carcharhinus melanopterus* (Quoy & Gaimard) (Carcharhinidae).

Site of infection. Intestine.

Prevalence and mean intensity. 80 and 35 ± 26.5 ($n = 5$).

Specimens deposited. CHCM no. 619 (voucher) (1 vial, 1 specimen ♀).

Remarks. These specimens are morphologically similar to *P. chiloscyllii* (reported as *Terranova chiloscyllii*), originally found in *Chiloscyllium punctatum* Müller & Henle and *Mustelus antarcticus* Günther (reported as *Emissola antarctica*) from the Central Queensland coast (Johnston and Mawson 1951). This species was redescribed by Deardorff (1987) from *Sphyrna lewini* (Griffith) and *Sphyrna zygaena* (Linnaeus) (Sphyrnidae) off Hawaii, Alabama and South Africa, and later recorded in *Trianodon obesus* (Rüppell) (Carcharhinidae) and *C. melanopterus* from the Solomon Islands and the Maldives by Bruce and Cannon (1990). Our specimens are somewhat larger than those described earlier, but this difference is consistent with intraspecific variability.

Pulchrascaris sp.

Description. Third-stage larva (12 specimens): relatively long nematodes 6.99–12.42 mm long and 172–452 wide, whitish with lateral cuticular alae. Lips weakly developed and bearing a larval, ventral tooth, 5–12 long. Nerve ring encircling esophagus in its anterior third, 173–302 from anterior body end. Deirids slightly posterior to nerve ring, 225–273 from cephalic end. Excretory pore at base of subventral lip. Esophagus relatively long, 636–1,414 with elongated ventriculus at posterior end, 388–1,371 long. Intestinal caecum anteriorly directed and somewhat larger than ventriculus, 389–1,384 long. Tail conical, 99–179 long, without ornamentations. Some specimens with a single papilla at 1.65–5.78 mm from posterior end of body.

Hosts. *Acanthurus sordidus*, *A. triostegus*, *Acanthurus xanthopterus* Valenciennes (Acanthuridae), *Rhinecanthus aculeatus* (Linnaeus) (Balistidae), *Platybelone argalus argalus* (Lesueur) (Belonidae), *C. ferdau*, *Carangoides orthogrammus* (Jordan & Gilbert), *Caranx ignobilis* (Forsskål), *Caranx melampygus* Cuvier, *Caranx papuensis* Alleyne

& MacLeay (all Carangidae), *Amblygobius phalaena* (Valenciennes), *Asterropteryx semipunctata* Rüppell, *Valenciennesia sexguttata* (Valenciennes) (all Gobiidae), *M. flavolineatus*, *Upeneus taeniopterus* Cuvier (Mullidae), *Gymnothorax pictus* (Ahl) (Muraenidae), *L. fulvus*, *Lutjanus monostigma* (Cuvier) (Lutjanidae), *Abudefduf septemfasciatus* (Cuvier), *Stegastes nigricans* (Lacepède) (Pomacentridae), *C. auriga*, *C. chanos*, *K. cinerascens*, *E. vaigiensis*.

Site of infection. Mesenteries.

Prevalence and mean intensity. 5.6 and 1 ($n = 18$) to *A. sordidus*, 8 and 2.3 ± 1.9 ($n = 50$) to *A. triostegus*, 15 and 1.3 ± 0.6 ($n = 20$) to *A. xanthopterus*, 11.1 and 1 ($n = 18$) to *R. aculeatus*, 50 and 10 ($n = 2$) to *P. argalus*, 40 and 42 ± 58 ($n = 5$) to *C. ferdau*, 66.7 and 52.5 ± 72.8 ($n = 2$) to *C. orthogrammus*, 100 and 71.3 ± 106.5 ($n = 4$) to *C. ignobilis*, 100 and 53.7 ± 106.4 ($n = 6$) to *C. melampygu*, 40 and 8 ± 9.9 ($n = 5$) to *C. papuensis*, 33.3 and 7.2 ± 8.6 ($n = 18$) to *A. phalaena*, 8.3 and 3 ($n = 12$) to *A. semipunctata*, 7.1 and 1 ($n = 14$) to *V. sexguttata*, 9.6 and 1.4 ± 0.4 ($n = 52$) to *M. flavolineatus*, 60 and 3.7 ± 1.5 ($n = 5$) to *U. taeniopterus*, 14.3 and 3 ($n = 7$) to *G. pictus*, 46.2 and 5.2 ± 3.7 ($n = 26$) to *L. fulvus*, 50 and 4.7 ± 3.2 ($n = 6$) to *L. monostigma*, 8.3 and 1 ($n = 12$) to *A. septemfasciatus*, 10 and 1 ($n = 10$) to *S. nigricans*, 7.7 and 1 ($n = 13$) to *C. auriga*, 20 and 2 ($n = 5$) to *C. chanos*, 50 and 7 ($n = 2$) to *K. cinerascens*, 7.4 and 1.5 ± 0.6 ($n = 54$) to *E. vaigiensis*.

Specimens deposited. CHCM no. 620 (voucher) (1 vial, 1 specimen ♀) (from *A. triostegus*), CHCM no. 621 (voucher) (1 vial, 2 specimens ♂ ♀) (from *C. auriga*), CHCM no. 622 (voucher) (1 vial, 1 specimen ♀) (from *K. cinerascens*), CHCM no. 623 (voucher) (1 vial, 1 specimen ♀) (from *L. fulvus*).

Remarks. These larvae belong to the genus *Pulchrascaris* because of the position of the excretory pore between the subventral lips, absence of ventricular appendage, elongate esophagus, relatively large ventriculus, and intestinal caecum anteriorly directed and somewhat larger than ventriculus. Deardorff (1987) mentioned that differentiation of third stage larvae of the genera *Pulchrascaris* and *Terranova* is difficult, since lips are not well developed at that stage. We found one adult male, a young female and one larva of the species *P. chiloscyllyi* in the blacktip reef shark *C. melanopterus*, which occurs in the same area and feeds on some small reef fishes (Froese and Pauly 2014). Larvae identified as *Pulchrascaris* sp. are identical to those in the shark, and they could belong to the same species, but until studies on the life cycle or molecular analysis are carried out, we considered them as separate taxa. All fishes reported here probably act as intermediate or paratenic hosts and elasmobranchs are the definitive hosts. Jabbar et al. (2012) reported larval anisakid nematodes from several teleosts from the Great Barrier Reef, including larvae named as *Terranova* sp. type II in *C. papuensis*. Those nematodes differ from the present ones in the length and ratio of the intestinal caecum and ventriculus. Larval nematodes reported as *Terranova* sp. type I and *Terranova* sp. type Hawaii B (HB) (Cannon 1977; Deardorff et al. 1982; Palm and Bray 2014) should be considered as *Pulchrascaris* sp. according to the ratios of their esophageal appendages. All fish parasitized by these larvae in the present work represent new host records.

Family Raphidascarididae Hartwich, 1954

Hysterothylacium sp. type MD of Deardorff & Overstreet, 1981 (larval type VIII of Shamsi et al., 2011)

Description. Third-stage larva (5 specimens): medium-sized nematodes, 3.00–8.64 mm long, 100–267 wide. Cuticular lateral alae extending along whole length of worm. Poorly developed lips, small, 18 long and 19 wide. Esophagus 270–680 long, with almost spherical ventriculus at distal part, 59–75 long and 57–87 wide. Ventricular appendage 481–595 long; intestinal caecum small, anteriorly directed, 67–274 long. Ratio for length of ventricular appendage and intestinal caecum 1: 2.10–7.73. Nerve ring at 116–279 from anterior end of body. Excretory pore slightly anterior to nerve ring, 137–198 from cephalic end. Deirids 395 from anterior end (observed in only 1 specimen). Tail conical, 121–227 long, with small spine-like mucron at tip.

Hosts. *Acanthurus triostegus*, *C. ferdau*, *C. lunula*, *C. chanos*, *K. cinerascens*, *A. sordidus*, and *A. hispidus*.

Site of infection. Mesenteries and liver.

Prevalence and mean intensity. 6 and 1.7 ± 0.6 ($n = 50$) to *A. triostegus*, 40 and 1.0 ± 0.0 ($n = 5$) to *C. ferdau*, 50 and 3.3 ± 1.6 ($n = 14$) to *C. lunula*, 20 and 6 ($n = 5$) to *C. chanos* and 50 and 2 ($n = 2$) to *K. cinerascens*, 5.6 and 3 ($n = 18$) to *A. sordidus*, 20 and 7.0 ± 5.0 ($n = 15$) to *A. hispidus*.

Specimens deposited. CHCM no. 624 (voucher) (1 vial, 1 specimen ♀) (from *Chaetodon lunula*), CHCM no. 625 (voucher) (1 vial, 2 specimens ♂ ♀) (from *K. cinerascens*).

Remarks. Because of the presence of a small intestinal caecum, long ventricular appendage, rounded ventriculus and small mucron on the tail tip, these larvae are morphologically similar to those described by Deardorff and Overstreet (1981) and the type HA of Deardorff et al. (1982) in the Gulf of Mexico and the Hawaiian Island, respectively. Recently, Shamsi et al. (2011) proposed a new classification for larvae occurring in fishes off Australia according to their molecular characterization. Morphometrically, larvae from America and the Australian region were practically identical. *Arothron hispidus*, *C. lunula*, and *K. cinerascens* represent new host records.

Family Capillariidae Railliet, 1915

Capillariidae gen. sp.

Description. Gravid female (1 damaged specimen, measurements of 1 young female in parentheses): long, thin and slender nematodes, 9.42 (8.80) mm long and 26 (37) wide. Muscular esophagus – (335). Stichosome formed by 4–6 (5) stichocytes. Eggs with polar plugs, thick-walled, 49–55 × 20–24 (–). Tail very short, 7 (6) long.

Hosts. *Chaetodon lunula*, *L. fulvus*, and *E. vaigiensis*.

Site of infection. Stomach.

Prevalence and mean intensity. 14.3 and 2.5 ± 0.7 ($n = 14$) to *C. lunula*, 3.8 and 1 ($n = 26$) to *L. fulvus*, 5.6 and 1.7 ± 0.6 ($n = 54$) to *E. vaigiensis*.

Specimens deposited. CHCM no. 626 (voucher) (1 vial, 1 specimen ♀) (from *Chaetodon lunula*), CHCM no. 627 (voucher) (1 vial, 2 specimens ♂ ♀) (from *L. fulvus*).

Remarks. Specimens were damaged, but it was possible to observe the most important features to allocate them to the family Capillariidae, such as esophagus divided in muscular and glandular parts (stichosome), eggs with polar plugs, and the general shape of body. Since males are unknown, it is impossible to determine their generic or specific identity. This is the first capillariid nematode reported in *C. ignobilis* and the second for the family Carangidae in the southwestern Pacific Ocean, which was recorded in *Carangoides oblongus* (Cuvier) (Carangidae) off New Caledonia (Moravec and Justine 2010). Palm and Bray (2014) only recorded *Capillaria* eggs in the musculature from *Bathygobius fuscus* (Rüppell) (Gobiidae) in Hawaii.

Family Cucullanidae Cobbold, 1864

Cucullanus bourdini Petter & Le Bel, 1992

Description. Male (5 specimens): medium-sized nematodes, 8.11–12.87 mm long, 223–413 wide. Esophagus 777–1,003 long and 126–240 wide at its posterior end. Anterior part of esophagus forming pseudocapsule (esophastome) 228–275 long and 129–185 wide. Nerve ring surrounding esophagus at its first third, 267–368 from anterior body end. Excretory pore beyond posterior end of esophagus, cervical papillae on distal end of esophagus or slightly posterior to it, 969–1,215 and 671–937, respectively, from cephalic end. Well-developed precloacal pseudosucker present, its distal part at 626–942 from posterior body end. Cloacal opening elevated. Eleven pairs of caudal papillae: 3 subventral, pedunculate precloacal pairs (first pair sometimes anterior to sucker and sometimes over anterior border), 4 adcloacal pairs (3 subventral, 1 lateral), 4 postcloacal pairs, including phasmids (1 subdorsal, 1 lateral, 2 subventral). One single papilla on anterior cloacal lip. Spicules similar, equal, alate, 982–1,543 with supporting structures along almost their whole length. Gubernaculum well-sclerotized, 116–140 long. Right and left postdeirids 3.94–6.37 and 1.92–3.27 mm, respectively, from posterior end of body. Tail conical 187–236 long, with pointed tip.

Gravid females (5 specimens, measurements of 1 young female in parentheses): body length 13.72–15.90 (5.23) mm long and 472–500 (220) wide. Esophagus 999–1,087 (600) long, 227–263 (106) wide at its posterior end. Esophastome 250–311 (197) long, 169–201 (129) wide. Nerve ring, excretory pore and deirids 318–367 (250), 1,150–1,377 (902), 805–971 (614), respectively, from anterior end of body. Vulva postequatorial 7.97–9.35 (3.30) from anterior end of body, with somewhat elevated lips and posteriorly directed muscular vagina. Eggs oval, 53–71 × 34–46 (–) in size, non-larvated. Tail conical, 294–385 (204) long.

Host. *Arothron hispidus*.

Site of infection. Intestine.

Prevalence and mean intensity. 46.7 and 6 ± 4.7 ($n = 15$).

Specimens deposited. CHCM no. 628 (voucher) (1 vial, 1 specimen ♀).

Remarks. The measurements of these nematodes are similar to those of *C. bourdini*, a species described from lutjanid fishes off New Caledonia (Petter and Le Bel 1992; Moravec and Justine 2011), although it was also reported from *Balistapus undulatus* Park (Balistidae) and *Myripristis kuntee* Valenciennes (Holocentridae) from the French Polynesia (Morand and Rigby 1998). They have overlapping measurements of the body length of males, spicules, gubernaculum, and similar number and distribution of caudal papillae, although there are some differences in female body length, which could be considered to represent intraspecific variability. Apparently, this nematode is not host-specific (see Moravec and Justine 2011), since it has been reported from four different fish families to date. This is the first record of *C. bourdini* in *A. hispidus* and the second for a tetraodontiform fish.

***Cucullanus oceaniensis* Moravec, Sasal, Würtz & Taraschewski, 2005**

Description. Male (1 specimen): medium-sized nematodes, whitish. Body length 6.22 mm, 183 wide. Muscular esophagus 678 long and 112 wide at its posterior part. Anterior end of esophagus forming a pseudobuccal capsule (esophastome), 214 long and 153 wide. Nerve ring slightly posterior to esophastome, 275 from anterior end of body. Deirids anterior to posterior end of esophagus, excretory pore posterior to it, at 609 and 797, respectively, from cephalic end. Eleven pairs of caudal papillae (including phasmids): 3 subventral precloacal pairs, 4 adcloacal pairs (3 subventral, 1 lateral), 4 postcloacal pairs (3 subventral, 1 lateral). A single, ventral papilla on the anterior cloacal lip. Spicules equal, similar, alate, 374 long. Gubernaculum well sclerotized, 112 long. Ventral precloacal sucker well developed, posterior margin at 690 from posterior end of body. Postdeirids 1.71 mm from tail tip. Tail conical with pointed tip, 112 long.

Host. *Abudefduf sordidus*.

Site of infection. Intestine.

Prevalence and mean intensity. 11.1 and 1.5 ± 0.7 ($n = 18$).

Specimens deposited. CHCM no. 629 (voucher) (1 vial, 1 specimen ♀).

Remarks. This single male is morphologically similar to *C. bourdini* and *C. oceaniensis*, two species described from lutjanids off New Caledonia and *Anguilla marmorata* Quoy & Gaimard (Anguillidae) in Polynesia and Melanesia (Petter and Le Bel 1992; Moravec et al. 2005). The number and distribution of caudal papillae of this male are practically the same as those of the above-mentioned species, although much more similar to that of *C. oceaniensis*. However, we found some differences in body (6.22 vs 10.6–14.0 and 7.14–9.51 mm) and spicule lengths (374 vs 740–1,000 and 819–1,020 μ m) of the present male. These differences could be related to the suitability of the fish hosts, since apparently the adult males in *C. bourdini* and *C. oceaniensis* are able to fully develop in lutjanids, while *A. sordidus* might act as a paratenic or not preferential

host for this nematode, since maturity was not fully reached. According to the original descriptions of *C. bourdini* and *C. oceaniensis*, these two species share many morphometric values and have never been compared (see Petter and Le Bel 1992; Moravec et al. 2005; Moravec and Justine 2011). An examination of the type material of both species should be carried out to elucidate their possible synonymy.

***Cucullanus* sp.**

Description. Third-stage larva (2 specimens): small nematodes, 1.45–1.53 long, 50–51 wide. Esophagus 333–352 long, 38–39 wide at its posterior part. Esophastome 60–65 long and 44–50 wide. Nerve ring 139–151, excretory pore 374–413 and deirids 262. Excretory pore posterior to distal end of esophagus, deirids on its posterior end of esophagus or slightly anterior to it. Tail elongate, 105–113 long, with pointed tip.

Host. *Caranx ignobilis*

Site of infection. Intestine.

Prevalence and mean intensity. 25 and 2 ($n = 4$).

Specimens deposited. CHCM no. 630 (voucher) (1 vial, 1 specimen ♀).

Remarks. These were two very small and poorly developed cucullanid larvae and it was not possible to identify them to species. Perhaps, they represent new infections, or this fish acts as paratenic host. These are the first cucullanid nematodes reported from *C. ignobilis* and the family Carangidae in the Indo-Pacific Ocean.

Family Cystidicolidae Skryabin, 1946

***Pseudascarophis* sp.**

Description. Gravid female (1 specimen): large, whitish nematode, 18.20 mm long, 158 wide. Anterior end rounded with two large rounded pseudolabia. Vestibule relatively short, 159 long, with anterior prostom and posterior part forming a transverse ring on anterior end of esophagus. Muscular esophagus short, narrow, 258 long; glandular part broader, 5 times longer than muscular one, 1.52 mm long. Nerve ring encircling muscular esophagus at its first third, 206 from anterior body end. Deirids small, bifurcated, situated between second and third thirds of vestibule length, 109 from anterior end of body. Excretory pore posterior to level of nerve ring, 220 from cephalic end. Vagina muscular directed posteriorly. Vulva pre-equatorial, 8.74 mm from anterior end of body, with not elevated lips. Fully developed eggs, thick-walled, larvated, without filaments, $31\text{--}36 \times 24\text{--}29$. Tail elongate, 239 long, with rounded tip.

Hosts. *Chaetodon auriga*, *C. lunula*, and *M. flavolineatus*.

Site of infection. Stomach.

Prevalence and mean intensity. 30.8 and 1 ($n = 13$) to *C. auriga*, 14.3 and 3 ± 2.8 ($n = 14$) to *C. lunula*, 1.9 and 1 ($n = 52$) *M. flavolineatus*.

Specimens deposited. CHCM no. 631 (voucher) (1 vial, 1 specimen ♀) (from *C. auriga*), CHCM no. 632 (voucher) (1 vial, 2 specimens ♂ ♀) (from *M. flavolineatus*).

Remarks. The presence of rounded pseudolabia, bifurcated deirids, and elongate tail with rounded tip, make this female similar to those of the genus *Pseudoascarophis*. Nematodes belonging to this genus were originally reported in *K. cinerascens* from off Japan and later found in *Parupeneus chrysopleuron* (Temminck & Schlegel) (Mullidae), *Genypterus chilensis* (Guichenot) (Ophidiidae), *Kyphosus sectatrix* (Linnaeus) (Kyphosidae) from China, Chile, Brazil, respectively (Ko et al. 1985; Solov'eva 1996; Muñoz and George-Nascimento 2001; Pereira et al. 2013). Therefore, this find represents new host and geographical records. Since only one female was recovered, it is impossible to identify it to species.

***Spinitectus (Paraspinitectus) palmyraensis* González-Solís & Vidal-Martínez, sp. nov.**
<http://zoobank.org/AB52DF93-B3F2-4C78-A221-7720368266C8>

Figs 1–3

Description. General: medium-sized nematodes with transverse rings of markedly long, posteriorly directed spines. First ring situated at level of base of prostom (Figs 1C, 2D), other rings extending posteriorly to mid-length of body. Spination is weakly visible in the posterior end of body (Figs 1H, 3C, G). Rings 1–4 with 11–14 uninterrupted spines, rings 5–12 with 13–17 interrupted spines at lateral side of body, rings 13–14 with 13–15 discontinuous spines in number and shape (Fig. 1A), rings 15 and posteriormost rings with 6 relatively large spines with a pore-like in their bases (Fig. 3B). In some specimens, anteriormost rings incomplete, asymmetrical and not forming a circle or with some missing spines (Fig. 1F, G), sometimes with double spines (Fig. 1E). Spines from rings 1–15 not overlapping each other, spines of more posterior rings overlapping (Fig. 3A). Cuticle transversely striated forming elevated rings (Figs 2D–E, 3A). The oral aperture oval surrounded by four submedian labia, which form continuous dorsal and ventral margins around the mouth. Two dorsal and two ventral submedian sublabia, curved and attached by their bases to surface of labia. There are two lateral, highly reduced pseudolabia without internal extensions. Two pairs of submedian cephalic papillae are present and a pair of lateral, barely visible amphids are situated outside the oral aperture (Figs 1B, 2A–C). Vestibule straight, rather long, with anterior end distinctly distended to form funnel-shaped prostom in lateral view (Fig. 1A, F). Esophagus clearly divided into muscular portion and posterior glandular, much longer and slightly wider portion. Nerve ring encircles muscular esophagus near its anterior end, situated between 8th and 9th rings of cuticular spines (Fig. 1A, F). Excretory pore situated between 9th and 10th rings of spines (Figs 1A, F, 2E). Small, trifurcated deirids situated just anterior to first ring of spines (Figs 1A, C, F, 2F). Tail of both sexes conical.

Male (4 specimens, measurements of holotype in parenthesis): length of body 3.90–5.50 (4.92) mm, maximum width 89–115 (103). First cuticular ring 31–33 (33)

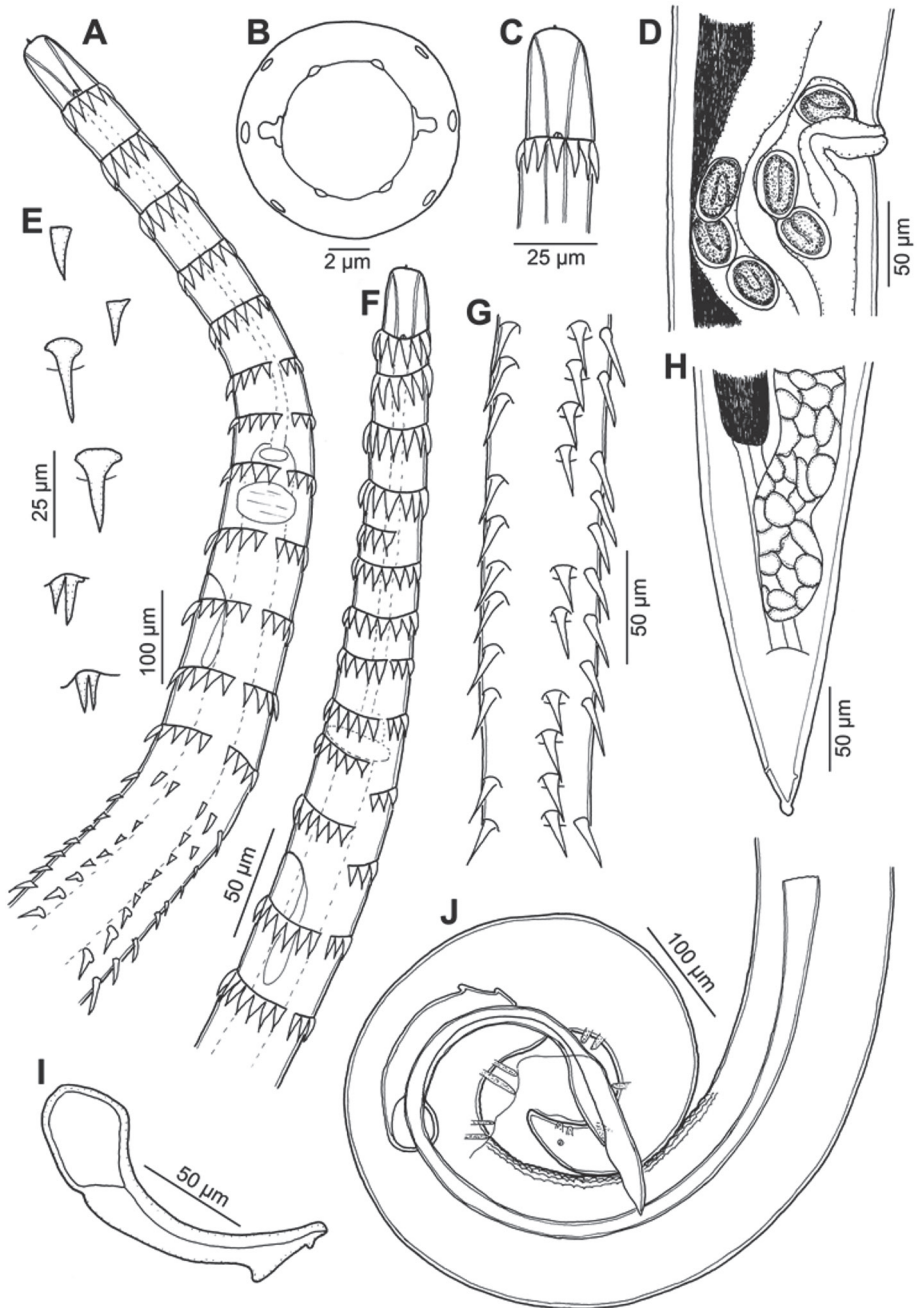


Figure 1. *Spinitectus* (*Paraspinitectus*) *palmyraensis* sp. nov. **A** anterior extremity of male, lateral view **B**, **C** cephalic end, apical and lateral views, respectively **D** region of vulva, lateral view **E** spines from different parts of body **F** anterior end, showing incomplete rows of spines **G** region of mid-body, showing missing spines **H** tail of female, ventral view **I** small spicule, lateral view **J** posterior end of male, lateral view.

from anterior extremity, armed with 11–14 (12) spines, 10–14 (12) long. Larger spines 22–23 (22–23) are at the level of the glandular esophagus. Vestibule including prostom 188–213 (188) long; prostom 21–28 (28) long and 7–9 (8) wide. Muscular esophagus 251–278 (261) long; glandular esophagus 0.82–1.55 (0.93) mm long, 32–41 (33) wide; length ratio of both parts of esophagus 1:3.2–4.2 (3.5). Entire esophagus and vestibule represent 28–31 (29)% of whole body length. Nerve ring and excretory pore 212–223 (223) and 233–254 (254), respectively, from anterior extremity. Deirids 30–32 (32) from anterior end of body. Posterior end of body ventrally curved, provided with well-developed caudal alae reaching posteriorly to end of tail (Figs 1J, 3C–F). Well-developed longitudinal, ventral cuticular ridges (area rugosa) present in precloacal region, formed by 9 lines in its most anterior part, 10 at middle and 3 near cloacal opening (Figs 1J, 3C, E). Precloacal papillae: 4 pairs of subventral, pedunculate, close to each other and equally distributed papillae present. Postcloacal papillae: 6 pairs of subventral pedunculate papillae, although second pair slightly laterally displaced. One pair of lateral papillae situated between two last pairs of subventrals (probably representing phasmids) (Figs 1J, 3D–F). Spicules dissimilar and unequal; large (left) spicule 673–766 (713) long, striated, with expanded proximal end 31–39 (39) wide, and bifurcated distal part. Small (right) spicule boat-shaped, 126–155 (126) long, with narrowed, ventrally bent distal end and two dorsal protuberances (Fig. 1I, J). Length ratio of spicules 1: 4.4–5.6 (5.6). Tail 123–160 (141) long, with blunt tip (Fig. 3F).

Gravid female (4 specimens; measurements of allotype in parentheses): body length 5.89–7.14 (6.26) mm, maximum width 129–143 (143). First cuticular ring 27–31 (27) from anterior extremity, 11–14 spines 12–15 (12) long. Larger spines 12–14 (12–14) at the level of the glandular esophagus. Vestibule including prostom 183–211 (183) long; prostom 23–28 (28) long and 7–9 (7) wide. Muscular esophagus 273–300 (289) long; glandular esophagus 0.908–1.165 (1.165) mm long, 38–46 (46) wide; length ratio of both parts of esophagus 1: 3.3–4.1 (4). Entire esophagus and vestibule with prostome represents 23–26 (26)% of whole body length. Nerve ring and excretory pore 206–231 (206) and 219–266 (206), respectively, from anterior extremity. Deirids 26–30 (26) from anterior end. Vulva with slightly elevated lips, postequatorial, situated at 4.24–4.82 (4.58) mm from anterior extremity, representing 67–73 (73)% of body length. Vagina muscular, directed posteriorly from vulva (Fig. 1D). Ovaries extending slightly anterior to anus level (Fig. 1H). Eggs in uterus oval, thick-walled (4–5 wide), smooth; larvated eggs 35–42 × 23–27 (34–41 × 25–27) (Fig. 1D). Tail conical, 73–102 (73) long, with lateral phasmids and knob-like appendage at tip, 7–9 long, separated from body by a narrow constriction (Figs 1H, 3G, H).

Etymology. The specific name of this nematode relates to the collection locality (Palmyra Atoll).

Type-host. *Albula glossodonta* (Forsskål) (Albulidae).

Site of infection. Intestine.

Type-locality. Palmyra Atoll, Eastern Indo-Pacific Ocean.

Prevalence and mean intensity. 54.2 and 3.2 ± 4.0 ($n = 24$).

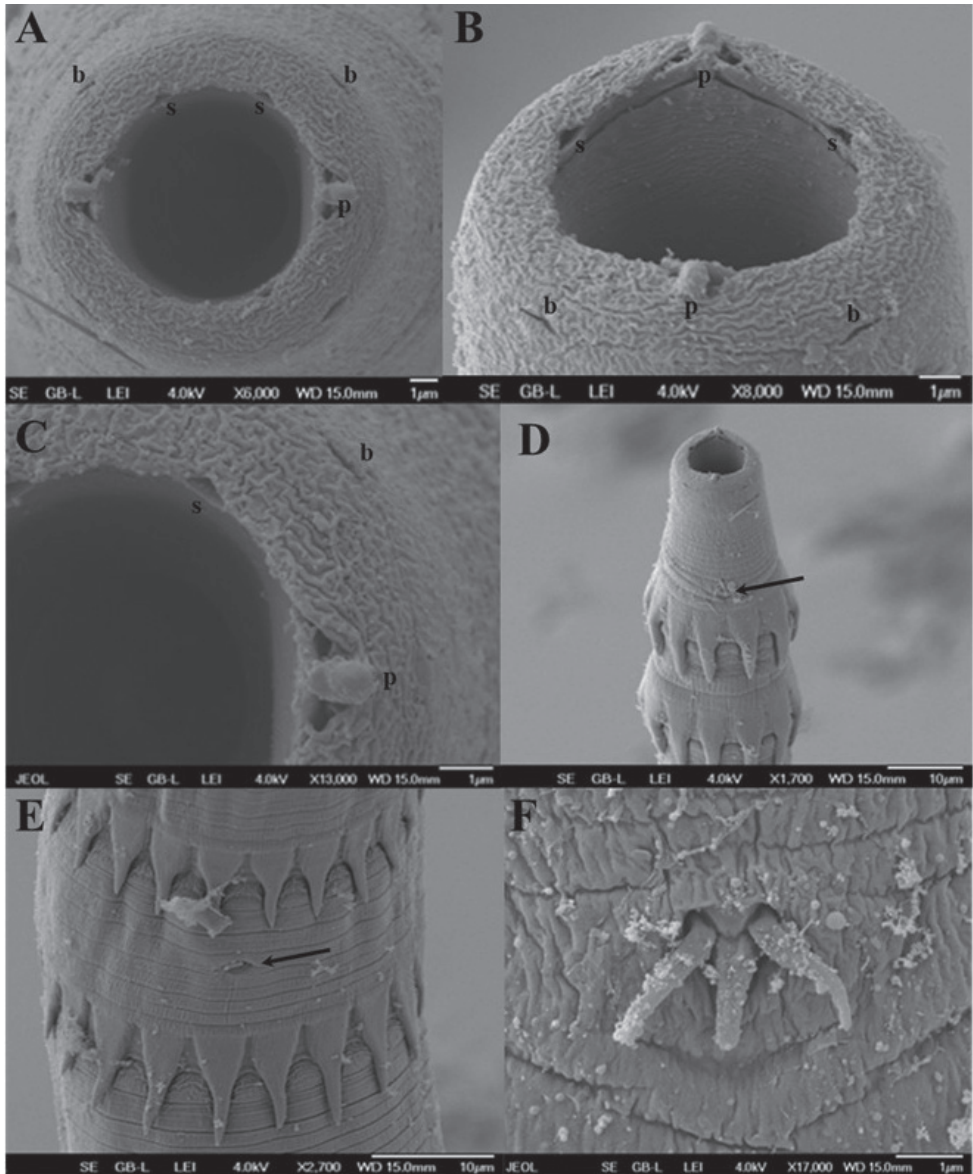


Figure 2. *Spinitectus* (*Paraspinitectus*) *palmyraensis* sp. nov. scanning electron micrographs. **A, B** anterior end of gravid female, apical and subapical views, respectively **C** detail of mouth, apical view **D** anterior end body, lateral view (arrow indicates deirids) **E** region of excretory pore, ventral view (arrow indicates the excretory pore) **F** deirids. Abbreviations: **b** submedian papilla, **l** labium, **p** pseudolabium, **s** sublabium.

Specimens deposited. Holotype and paratype (in SEM stub) specimens in the Helminthological Collection of the Institute of Parasitology, Academy of Sciences of the Czech Republic, Ceske Budejovice (no. N-1073) and CHCM no. 633 (allotype) (1 vial, 1 specimen ♀).

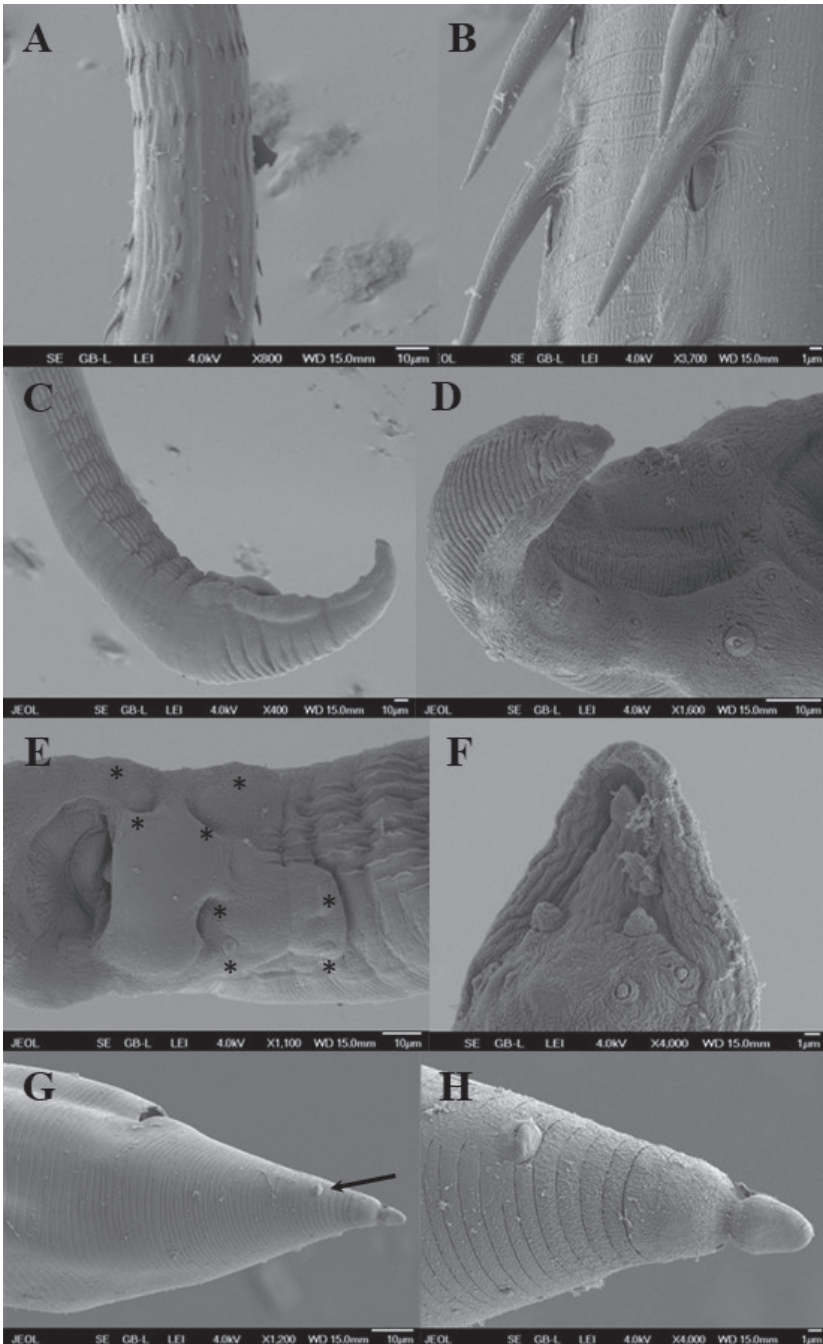


Figure 3. *Spinitectus (Paraspinitectus) palmyraensis* sp. nov. scanning electron micrographs. **A** transition zone of spination, lateral view **B** larger spines with pore-like on bases **C** posterior end of male showing area rugosa, sublateral view **D** tail of male, ventral view **E** region of cloaca, ventral view (asterisks indicate precloacal papillae) **F** tail tip of male, ventral view **G** posterior end female, lateral view (arrow indicates phasmid) **H** detail of tail tip.

Remarks. According to Moravec (2007), Moravec and Justine (2009), and Moravec and Klimpel (2009), the genus *Spinitectus* is one of the 24 valid genera within the family Cystidicolidae. This genus is represented by a large number of species described mainly from freshwater and marine fishes (Moravec et al. 2002) and includes the monotypic subgenus *Paraspinitectus* (Moravec and Justine 2009).

Due to the presence of markedly reduced pseudolabia in the oral opening and a body covered by spinose rings, the nematodes herein described were assigned to the subgenus *Paraspinitectus*, as diagnosed by Moravec and Justine (2009). The subgenus was created based on the structure of the oral opening of a lone female nematode reported as *Spinitectus* (*Paraspinitectus*) sp. collected from *A. glossodonta*, off New Caledonia. *Spinitectus beaveri*, a species originally described from *Albula vulpes* (Linnaeus) (Albulidae) in Biscayne Bay, Florida (Overstreet 1970) and later examined by SEM by Jilek and Crites (1982), had similar structure to the oral opening, and thus became the type species of the subgenus. The former was reported in the same host and geographical region (southern Pacific Ocean), while the latter was described from a congeneric host (*A. vulpes*) and different geographical region (off Florida). They both have very similar morphological characteristics to *S. (P.) palmyraensis* sp. nov., although, the new species differs from *S. (P.) beaveri* in the length of right spicule (673–766 vs 390–430 μm), vestibule (188–213 vs 80–90 μm), different pattern in the distribution and number of spinose rings, position of nerve ring (between rings 9–10 vs 3–7), and number of caudal papillae. The new species differs from *Spinitectus (P.)* sp. in the position of nerve ring (between rings 10–11), excretory pore (rings 9–10 vs 14–15) as well as the distribution pattern of spinose rings.

Interestingly even though the three species within *Paraspinitectus* occur in closely related hosts, morphological differences are evident among species of *Spinitectus* parasitizing albulid fishes around the world. Potentially, ecological differences of their hosts or habitats are substantial enough to select for this interspecific variability.

Morphological features as reduced pseudolabia, small triangular sublabia in the oral opening, trifurcated deirids (probably also present in *Spinitectus (P.)* sp.), and spinose rings with two different patterns of arrangement are common to the three known forms assigned to the subgenus. These characteristics support the validity of the subgenus *Paraspinitectus* and highlight the need for detailed SEM examination of cystidicolid specimens to determine the substantial intraspecific differences when comparing among species.

Within the Cystidicolidae there is a recently created genus, *Ascarophisnema* Moravec & Justine, 2010 with remarkable similarities with the new species. Similarities between the *Ascarophisnema* and *Spinitectus* include trifurcated deirids (only reported in these two genera), the structure of the oral opening, and the number and distribution of caudal papillae. Although the presence of spinose rings in *Spinitectus* clearly set it apart from *Ascarophisnema*. Probably, both genera are closely related but a phylogenetic analysis using molecular and morphological data is needed to clarify this situation.

This is the second nominal species reported within the subgenus *Paraspinitectus* and represents a new geographical record (southern Pacific region), since the previous report was a generically identified female from the same host species.

Family Philometridae Baylis & Daubney, 1926***Philometra pellucida* (Jägerskiöld, 1893) Yorke & Maplestone, 1926**

Description. Gravid female (3 specimens, measurements of 3 subgravid females in parentheses): large, yellowish nematodes, 111.42–140.70 (37.84–48.64) mm long, 0.94–3.29 (0.336–0.649) mm wide, with smooth cuticle and both ends rounded. Esophagus with anterior bulbous inflation, 220–267 (147–181) long and 163–182 (130–162) wide, with spacious lumen. Esophagus 1.59–2.06 (1.41–1.50) mm long, with dorsal esophageal gland not well demarcated, extended anteriorly to level of nerve ring. Esophageal gland with cell nucleus located at mid-length, at 0.915–1.07 (–) mm from anterior extremity. Small ventriculus 80–111 (50–80) long and 79–142 (75–85) wide, opening into intestine through valve. Nerve ring encircling esophagus just posterior to its anterior bulb, 279–407 (239–246) from anterior body end. Deirids and excretory pore not visible. Intestine brownish, straight and almost reaching the posterior end of body, forming ligament 325–690 (547–594) long, attached to the body wall near the caudal end. Ovaries extending near both ends of body. Uterus filled with larval mass (in gravid females) and developing embryos and eggs (in subgravid females). Larvae from uterus 345–492 long, with elongated tail. Posterior end of body rounded.

Host. *Arothron hispidus*.

Site of infection. Body cavity.

Prevalence and mean intensity. 40 and 20.8 ± 31.4 ($n = 15$).

Specimens deposited. CHCM no. 634 (voucher) (1 vial, 1 specimen ♀).

Remarks. Due to the presence of the anterior inflation of the esophagus, weakly demarcated esophageal gland, its occurrence in the body cavity of a congeneric fish host (*A. hispidus*) and close geographical region (Southeastern Pacific Ocean), these females were identified as *P. pellucida*. Gravid females showed similar morphometric features than those reported by Jägerskiöld (1893, 1894). They represent new host (*A. hispidus*) and geographical records (Palmyra Atoll).

Discussion

The present study is the first detailed survey of the diversity and ecological attributes of the parasitic nematodes infecting fishes at Palmyra Atoll. Consistent with observations of the monogenean and parasitic copepod fauna of Palmyra Atoll fishes (Vidal-Martinez et al. 2017; Soler-Jiménez et al. 2019), parasitic nematode species richness at Palmyra Atoll appears low (10 species in 44 host fish) compared with others Indo-Pacific regions. In fact, several of the fish species we examined (16 of 44) were not parasitized by nematodes at all, even with large sample sizes for some fish species (e.g. *Osteomugil engeli* (Bleeker) (Mugilidae) $n = 63$, *Istigobius ornatus* (Rüppell) (Gobiidae) $n = 26$). Other fish species such as *C. melanopterus*, *C. melampygus*, *C. papuensis*, and *E. vaigiensis* with a single species of nematodes infecting them in this study (Table 1),

have previous records of *Terranova* type II (larvae), *Anisakis typica*, *Hysterothylacium* type II (larvae), and *Camallanus carangis* (Deardorff et al. 1982; Moravec et al. 2006; Shamsi et al. 2011; Jabbar et al. 2012). Likewise, the nematode *Spirocamallanus colei* has been reported from *A. triostegus* (Rigby et al. 1997).

At a broad geographical scale, the most likely hypothesis to account for the paucity of parasitic nematodes at Palmyra Atoll is its geographical remoteness. Indeed, Palmyra Atoll apparently would show a pattern similar to that suggested by the island biogeography theory, where the large distance from the presumed centre of origin of Indo-West Pacific fishes and their parasites (the Austro-Malayan-Philippine region) would result in a low number of both fish and nematode parasite species. Further support for this explanation is the low species richness of fishes of the Line Islands, including Palmyra Atoll (Gosline 1971) compared to other coral atolls in the Indo-West Pacific region (e.g. Adler 1992). A similar pattern has been suggested for other groups of parasites of marine fish from the lagoonal flats of Palmyra Atoll such as monogeneans and parasitic copepods (Vidal-Martínez et al. 2017; Soler-Jiménez et al. 2019).

In our samples from the lagoonal flats of Palmyra Atoll, of the 10 nematode species recovered, seven were in the adult stage and three were larvae (Table 2). However, from the 43 fish species sampled, 24 were infected by larval stages of *Pulchrascaris* sp., followed by *Hysterothylacium* infecting seven fish species, *Pseudascaphis* sp. in three fish species, and *Cucullanus* in one species. The rest of the nematodes in Table 2 were adults and infected only one host species in low numbers. Because this is the most important pattern in the present study, it frames the rest of our discussion in the context of the life cycles of these nematodes.

The most likely explanation for the numerical dominance of the larval stages of nematodes is the lack of fishery activity at Palmyra Atoll and the substantial biomass of large, piscivorous sharks and ray-finned fishes (Lafferty et al. 2008). That means that the life cycles and transmission of nematodes of both elasmobranch and bony fishes acting as definitive hosts occur given the lack of selective removal of these hosts. This pattern at Palmyra Atoll agrees with the findings of Lafferty et al. (2008) for Kiritimati Island and Wood et al. (2015) at the Line Islands in the equatorial Pacific, as well as Marzoug et al. (2012) in the Mediterranean Sea, and Vidal-Martínez et al. (2019) in the Yucatan Peninsula, Gulf of Mexico. These authors have suggested that the completion of the life cycles of helminths such as cestodes using sharks as definitive hosts could be at risk due to overfishing. In the present study we have an opposite pattern where the lack of removal of the definitive hosts is the most likely explanation for the high number of larval nematodes using fishes as second intermediate hosts. We observed a similar pattern of abundant larval metacercarial stages in fishes at Palmyra (Vidal-Martínez et al. 2012).

The life cycle of the members of the *Pulchrascaris* genus is unknown but being an anisakid nematode, it should include small marine crustaceans as first intermediate hosts, fishes as second intermediate hosts and elasmobranch fishes as definitive hosts (Deardorff 1987; Moravec et al. 1995). In our study, the black tip shark *C. melanopterus* was infected with *Pulchrascaris chiloscylli*, and this shark is clearly acting as de-

finitive host. All other 24 bony fish species in Table 2 are most likely acting as second intermediate host of *P. chiloscylli* and all other potential species of the same genus that could be present at Palmyra Atoll.

Hysterothylacium sp. larval stages were parasitizing seven fish species from the intertidal lagoon at Palmyra Atoll (Table 2). This nematode species is also a member of the Anisakidae (Moravec et al. 1995; Vidal-Martínez et al. 2001). Therefore, its life cycle should include small marine crustaceans as first intermediate hosts, marine bony fishes as second intermediate hosts, and carnivorous marine fishes as definitive hosts (Moravec et al. 1995; Vidal-Martínez et al. 2001). It is not surprising to find a long list of infected hosts with larvae of *Hysterothylacium* sp. in Palmyra Atoll because there are at least 60 marine fish species acting as intermediate hosts from nearby locations such as the Hawaiian Islands (Palm and Bray 2014).

Pseudascarophis sp. was also an adult nematode infecting three fish species (Table 2). Unfortunately, most of the material was lost, and the present description was based in only one gravid female. The life cycles of this species and that of the adult nematode *S. palmyrensis* sp. nov. are unknown. However, both nematodes belong to the family Cystidicolidae, from which several life cycles have been described. Briefly, eggs of Cystidicolidae contain fully developed first stage larvae, and crustaceans such as shrimps, crabs, and amphipods, as well as nymphal stages of aquatic insects (probably Ephemeroptera), act as first intermediate hosts. In these intermediate hosts, the nematodes have two molts, and fish acquire third stage larvae when they eat infected crustaceans (Anderson 2000).

The life cycle of the unidentified nematodes of the family Capillaridae is also unknown. However, based on the extant literature on the life cycles of the members of this family, it is likely that they use oligochaetes as first intermediate hosts (Kutzer and Otte 1966). Several authors, experimentally fed fish (*Salmo gairdneri*) with infected oligochaetes and obtained mature capillarid specimens of *Schulmanella petruschewskii* after six months (Kutzer and Otte 1966; Anderson 2000; Moravec 2001).

There were three species of the genus *Cucullanus* infecting fishes from the sand flats of Palmyra Atoll (Table 2), two as adults and a one a larva. Knowledge on the life cycle of the members of this genus is scarce (Anderson 2000). However, there is evidence to suggest the use of an intermediate host has been replaced by a histotropic phase in the definitive host (Gibson 1972; Anderson 2000). This means that if the fish eats eggs or first stage larvae occurring in the environment, the rest of the development occurs entirely in the definitive host.

The life cycle of *Philometra pellucida* (Table 2) is unknown, but information on other members of this genus suggest that copepods should be the first intermediate hosts (Moravec 1998; Anderson 2000). Once the fish eats infected copepods, the parasite develops until reaching sexual maturity in their preferred microhabitat (in this case, in the body cavity).

In conclusion, despite the relatively low species richness of parasitic nematodes in the lagoonal flats at Palmyra Atoll, which is due to its remoteness, there were very interesting patterns at the local level, especially those related with the numerical domi-

nance of larval stages of nematodes. Apparently, the lack of fishing at the atoll since 2001 (https://www.fws.gov/refuge/palmyra_atoll/) and its selective removal of definitive hosts such as sharks and piscivorous bony fishes applied is the most likely explanation for the high number of larval nematodes using fishes as second intermediate hosts.

Acknowledgements

We thank to the staff of the Laboratory of Electron Microscopy, Institute of Parasitology, Biology Centre of the Academy of Sciences of the Czech Republic, České Budějovice for technical assistance and Blanka Škoriková from the same institution for help in preparing drawings and plates. This study was partially supported by the Czech Science Foundation (Project no. P505/12/G112). This work was supported by the National Council of Science and Technology of Mexico – Mexican Ministry of Energy – Hydrocarbon Trust, project (201441). This is a contribution of the Gulf of Mexico Research Consortium (CIGoM). We acknowledge and thank the Palmyra Atoll National Wildlife Refuge, US Fish and Wildlife Service, Department of the Interior, the Nature Conservancy, and the United States Geological Survey for their support. We deeply thank the Nature Conservancy staff and US Fish and Wildlife staff who were friendly and helpful. We are particularly indebted to Franklin Viola, Amanda Meyer, Brad Kintz, Aaron Kierzek, Jan Eber, Anthony Wilson, Lynette Williams, Kathy Wilson, and Clara Viva-Rodríguez. We also thank Gareth Williams and Ingrid Knapp for sharing their field knowledge. This work also benefitted from a grant from the Marisla Foundation and a US National Science Foundation Grant (DEB-0224565). Any use of trade, product, or firm names in this publication is for descriptive purposes only and does not imply endorsement by the US Government.

References

- Adler GH (1992) Endemism in birds of tropical Pacific islands. *Evolutionary Ecology* 6: 296–306. <https://doi.org/10.1007/BF02270966>
- Anderson RC (2000) *Nematode Parasites of Vertebrates: Their Development and Transmission* (2nd edn). CABI Publishing, Wallingford, 650 pp. <https://doi.org/10.1079/9780851994215.0000>
- Bruce NL, Cannon LRG (1990) Ascaridoid nematode from sharks from Australia and the Solomon Islands, Southwestern Pacific Ocean. *Invertebrate Taxonomy* 4: 763–783. <https://doi.org/10.1071/IT9900763>
- Bush A, Lafferty K, Lotz J, Shostak A (1997) Parasitology meets ecology on its own terms: Margolis et al. revisited. *The Journal of Parasitology* 83: 575–583. <https://doi.org/10.2307/3284227>
- Cannon LRG (1977) Some larval ascaridoids from south-eastern Queensland marine fishes. *International Journal for Parasitology* 7: 233–243. [https://doi.org/10.1016/0020-7519\(77\)90053-4](https://doi.org/10.1016/0020-7519(77)90053-4)

- Deardorff TL (1987) Redescription of *Pulchrascaris chiloscyllyi* (Johnston and Mawson, 1951) [sic] (Nematoda: Anisakidae), with comments on species in *Pulchrascaris* and *Terranova*. Proceedings of the Helminthological Society of Washington 54(1): 28–39.
- Deardorff TL, Kliks MM, Rosenfeld ME, Rychlinski RA, Desowitz RS (1982) Larval ascariid nematodes from fishes near the Hawaiian Islands, with comments on pathogenicity experiments. Pacific Science 36(2): 187–201. <http://hdl.handle.net/10125/419>
- Deardorff TL, Overstreet RM (1981) Larval *Hysterothylacium* (= *Thynnascaris*) (Nematoda: Anisakidae) from fishes and invertebrates in the Gulf of Mexico. Proceedings of the Helminthological Society of Washington 48(2): 113–126.
- Froese R, Pauly D (2014) FishBase. <http://www.fishbase.org> [Accessed on: 2019-6-7]
- Gibson DI (1972) Contributions to the life histories and development of *Cucullanus minutus* Rudolphi, 1819 and *C. heterochrous* Rudolphi, 1802 (Nematoda: Ascaridida). Bulletin of the British Museum (Natural History) Zoology 22: 153–170.
- Gosline WA (1971) The zoogeographic relationships of Fanning Island inshore fishes. Pacific Science 25: 282–289. <http://hdl.handle.net/10125/4243>
- Hasegawa H, Williams EH, Bunkley-Williams L (1991) Nematode parasites from marine fishes of Okinawa, Japan. Journal of the Helminthological Society of Washington 58(2): 186–197.
- Jabbar A, Asnoussi A, Norbury LJ, Eisenbarth A, Shamsi S, Gasser RB, Lopata AL, Beveridge I (2012) Larval anisakid nematodes in teleost fishes from Lizard Island, northern Great Barrier Reef, Australia. Marine and Freshwater Research 63: 1283–1299. <https://doi.org/10.1071/MF12211>
- Jägerskiöld LA (1893) Bidrag till kännedom om nematoderma. Akademisk Afhandling, Stockholm, 86 pp. [+ 5 pls] <https://doi.org/10.5962/bhl.title.46828>
- Jägerskiöld LA (1894) Beiträge zur Kenntniss der Nematoden. Zoologische Jahrbücher. Abteilung für Anatomie und Ontogenie der Tiere Abteilung für Anatomie und Ontogenie der Tiere 7: 449–532. [pls 26–28]
- Jilek R, Crites JL (1982) Comparative morphology of the North American species of *Spinitectus* (Nematoda: Spirurida) analyzed by scanning electron microscopy. Transactions of the American Microscopical Society 101: 126–134. <https://doi.org/10.2307/3225764>
- Johnston TH, Mawson PM (1951) Report on some parasitic nematodes from the Australian Museum. Records of the Australian Museum 22(4): 289–297. <https://doi.org/10.3853/j.0067-1975.22.1951.609>
- Justine J-L (2007) Fish parasites: Platyhelminthes (Monogenea, Digenea, Cestoda) and Nematodes, reported from off New Caledonia. In: Payri CE, Richer de Forges B (Eds) Compendium of marine species of New Caledonia. Documents Scientifiques et Techniques 117, (2nd edn), IRD Nouméa, 183–198.
- Justine JL (2010) Parasites of coral reef fish: how much do we know? With a bibliography of fish parasites in New Caledonia. The Belgian Journal of Zoology 140(Suppl.): 155–190.
- Justine JL, Beveridge I, Boxshall GA, Bray RA, Miller TL, Moravec F, Trilles JP, Whittington ID (2012) An annotated list of fish parasites (Isopoda, Copepoda, Monogenea, Digenea, Cestoda, Nematoda) collected from Snappers and Bream (Lutjanidae, Nemipteridae, Caesionidae) in New Caledonia confirms high parasite biodiversity on coral reef fish. Aquatic Biosystems 8: 22. <https://doi.org/10.1186/2046-9063-8-22>

- Ko RC, Margolis L, Machida M (1985) *Pseudoascarophis kyphosi* n. gen., n. sp. (Nematoda: Cystidicolidae) from the stomach of the fish *Kyphosus cinerascens* (Forskål) [sic] from Japan. Canadian Journal of Zoology 63(11): 2684–2688. <https://doi.org/10.1139/z85-401>
- Kutzer E, Otte E (1966) *Capillaria petruschewskii* (Schulman, 1948), Morphologie, Biologie und Pathogene Bedeutung. Zeitschrift für Parasitenkunde 28: 16–30. <https://doi.org/10.1007/BF00260526>
- Lafferty KD, Shaw JC, Kuris AM (2008) Reef fishes have higher parasite richness at unfished Palmyra Atoll compared to fished Kiritimati Island. EcoHealth 5(3): 338–345. <https://doi.org/10.1007/s10393-008-0196-7>
- Lester RJG, Sewell KB (1989) Checklist of parasites from Heron Island, Great Barrier Reef. Australian Journal of Zoology 37: 101–128. <https://doi.org/10.1071/ZO9890101>
- Marzoug D, Boutiba Z, Kostadinova A, Pérez-del-Olmo A (2012) Effects of fishing on parasitism in a sparid fish: contrasts between two areas of the Western Mediterranean. Parasitology International 61: 414–20. <https://doi.org/10.1016/j.parint.2012.02.002>
- Morand S, Rigby MC (1998) Cucullanin nematodes from coral reef fishes of French Polynesia, with a description of *Cucullanus faliexae* n. sp. (Nematoda: Chitwoodchabaudiidae). Journal of Parasitology 84: 1213–1217. <https://doi.org/10.2307/3284677>
- Moravec F, Vidal Martínez VM, Aguirre Macedo ML (1995) Some helminth parasites of *Epinephelus morio* (Pisces: Serranidae) from the Peninsula of Yucatan, Mexico. Studies of the Natural History of the Caribbean Region 72: 55–68.
- Moravec F (1998) Nematodes of Freshwater Fishes of the Neotropical Region. Academia, Praha, 464 pp.
- Moravec F (2001) Trichinelloid Nematodes Parasitic in Cold-blooded Vertebrates. Academia, Praha, 430 pp.
- Moravec F, Justine J-L, Rigby MC (2006) Some camallanid nematodes from marine perciform fishes off New Caledonia. Folia Parasitologica 53(3): 223–239. <https://doi.org/10.14411/fp.2006.029>
- Moravec F (2007) Some aspects of the taxonomy and biology of adult spirurine nematodes parasitic in fishes: a review. Folia Parasitologica 54: 239–257. <https://doi.org/10.14411/fp.2007.033>
- Moravec F, García-Magaña L, Salgado-Maldonado G (2002) *Spinitectus tabascoensis* sp. nov. (Nematoda, Cystidicolidae) from *Ictalurus furcatus* (Pisces) in southeastern Mexico. Acta Parasitologica 47: 224–227. <https://doi.org/10.1590/S0074-02762010000100007>
- Moravec F, Justine J-L (2009) Two cystidicolids (Nematoda, Cystidicolidae) from marine fishes off New Caledonia. Acta Parasitologica 54: 341–349. <https://doi.org/10.2478/s11686-009-0058-7>
- Moravec F, Justine J-L (2010) Some trichinelloid nematodes from marine fishes off New Caledonia, including description of *Pseudocapillaria novaecaledoniensis* sp. nov. (Capillariidae). Acta Parasitologica 55: 71–80. <https://doi.org/10.2478/s11686-010-0005-7>
- Moravec F, Justine J-L (2011) Cucullanid nematodes (Nematoda: Cucullanidae) from deep-sea marine fishes off New Caledonia, including *Dichelyne etelidis* n. sp. Systematic Parasitology 78: 95–108. <https://doi.org/10.1007/s11230-010-9281-8>

- Moravec F, Justine J-L (2018) *Rasheedia* n. nom. (Nematoda, Physalopteridae) for *Bulbocephalus* Rasheed, 1966 (a homonym of *Bulbocephalus* Watson, 1916), with description of *Rasheedia heptacanthi* n. sp. and *R. novaecaledoniensis* n. sp. from perciform fishes off New Caledonia. *Parasite* 25: 39. <https://doi.org/10.1051/parasite/2018033>
- Moravec F, Klimpel S (2009) Two new species of cystidicolid nematodes from the digestive tract of the deep-sea fish *Coryphaenoides mediterraneus* (Giglioli) (Macrouridae) from the Mid-Atlantic Ridge. *Systematic Parasitology* 73: 37–47. <https://doi.org/10.1007/s11230-009-9182-x>
- Moravec F, Sasal P, Würtz J, Taraschewski H (2005) *Cucullanus oceaniensis* sp. n. (Nematoda: Cucullanidae) from Pacific eels (*Anguilla* spp.). *Folia Parasitologica* 52: 343–348. <https://doi.org/10.14411/fp.2005.047>
- Muñoz G, George-Nascimento M (2001) *Pseudascarophis genypteri* n. sp. (Nematoda: Cystidicolidae) parasite from the red ling *Genypterus chilensis* off Chile. *Journal of Parasitology* 87: 1106–1111. <https://doi.org/10.2307/3285241>
- Overstreet RM (1970) *Spinitectus beaveri* sp. n. (Nematoda: Spiruroidea) from the bonefish, *Albula vulpes* (Linnaeus), in Florida. *Journal of Parasitology* 56: 128–130. <https://doi.org/10.2307/3277468>
- Palm HW, Bray RA (2014) *Marine Fish Parasitology in Hawaii*. Westarp and Partner Digitaldruck, Hohenwaelesleben, 302 pp.
- Pereira FB, Pereira AN, Timi JT, Luque JL (2013) *Pseudascarophis brasiliensis* sp. nov. (Nematoda: Cystidicolidae) parasitic in the Bermuda chub *Kyphosus sectatrix* (Perciformes: Kyphosidae) from southeastern Brazil. *Memórias do Instituto Oswaldo Cruz* 108: 476–480. <https://doi.org/10.1590/S0074-0276108042013013>
- Petter A-J, Le Bel J (1992) Two new species in the genus *Cucullanus* (Nematoda – Cucullanidae) from the Australian region. *Memórias do Instituto Oswaldo Cruz* 87: 201–206. <https://doi.org/10.1590/S0074-02761992000500038>
- Rigby MC, Holmes JC, Cribb TH, Morand S (1997) Patterns of species diversity in the gastrointestinal helminths of a coral reef fish, *Epinephelus merra* (Serranidae), from French Polynesia and the South Pacific Ocean. *Canadian Journal of Zoology* 75: 1818–1827. <https://doi.org/10.1139/z97-811>
- Rigby MC, Lo CM, Cribb TH, Euzet L, Faliex E, Galzin R, Holmes JC, Morand S (1999) Checklist of the parasites of coral reef fishes from French Polynesia, with considerations on their potential role in these fish communities. *Cybium: International Journal of Ichthyology* 23(3): 273–284.
- Schmidt GD (1969) Nematode parasites of Oceanica V. Four species from fishes of Palawan, P.I., with a proposal for *Oceanicucullanus* Gen.nov [sic]. *Parasitology* 59: 389–396. <https://doi.org/10.1017/S0031182000082354>
- Shamsi S, Eisenbarth A, Saptarshi S, Beveridge I, Gasser RB, Lopata AL (2011) Occurrence and abundance of anisakid nematode larvae in five species of fish from southern Australian waters. *Parasitology Research* 108: 927–934. <https://doi.org/10.1007/s00436-010-2134-1>
- Shaw JC, Aguirre-Macedo L, Lafferty KD (2005) An efficient strategy to estimate intensity and prevalence: sampling metacercariae in fishes. *Journal of Parasitology* 91(3): 515–522. <https://doi.org/10.1645/GE-385R2>

- Soler-Jiménez LC, Morales-Sern FN, Aguirre-Macedo ML, McLaughlin JP, Jaramillo AJ, Shaw JC, James AK, Hechinger RF, Kuris AM, Lafferty KD, Vidal-Martínez VM (2019) Parasitic copepods (Crustacea, Hexanauplia) on fishes from the lagoon flats of Palmyra Atoll, Central Pacific. *ZooKeys* 833: 85–106. <https://doi.org/10.3897/zookeys.833.30835>
- Solov'eva GF (1996) *Pseudascarophis tropica* n. sp. (Nematoda: Spirurida), a parasite of South China Sea fishes. *Parazitologiya* 25: 556–558.
- Spalding MD, Fox HE, Allen GR, Davidson N, Ferdaña ZA, Finlayson M, Halpern BS, Jorge MA, Lombana A, Lourie SA, Martin KD, McManus E, Molnar J, Recchia CA, Robertson J (2007) Marine ecoregions of the world: a bioregionalization of coastal and shelf areas. *BioScience* 57: 573–583. <https://doi.org/10.1641/B570707>
- Stevenson C, Katz LS, Micheli F, Block B, Heiman KW, Perle C, Weng K, Dunbar R, Witting J (2007) High apex predator biomass on remote Pacific islands. *Coral Reefs* 26: 47–51. <https://doi.org/10.1007/s00338-006-0158-x>
- The Nature Conservancy (2006) The Nature Conservancy in Palmyra Atoll. <http://www.nature.org/wherewework/asiapacific/palmyra/> [Accessed on: 2019-07-23]
- Vidal-Martínez VM, Aguirre-Macedo ML, Scholz T, González-Solís D, Mendoza-Franco E (2001) Atlas of the Helminth Parasites of Cichlid fishes of Mexico. Academia, Praha, 166 pp.
- Vidal-Martínez VM, Aguirre-Macedo ML, McLaughlin JP, Hechinger RF, Jaramillo AG, Shaw JC, James AK, Kuris AM, Lafferty KD (2012) Digenean metacercariae of fishes from the lagoon flats of Palmyra Atoll, Eastern Indo-Pacific. *Journal of helminthology* 86(4): 493–509. <https://doi.org/10.1017/S0022149X11000526>
- Vidal-Martínez VM, Soler-Jiménez LC, Aguirre-Macedo ML, McLaughlin J, Jaramillo AG, Shaw JC, James A, Hechinger RF, Kuris AM, Lafferty KD (2017) Monogenea of fishes from the lagoon flats of Palmyra Atoll in the Central Pacific. *ZooKeys* 713: 1–23. <https://doi.org/10.3897/zookeys.713.14732>
- Vidal-Martínez VM, Velázquez-Abunader I, Centeno-Chalé OA, May-Tec AL, Soler-Jiménez LC, Pech D, Mariño-Tapia I, Enriquez C, Zapata-Pérez O, Herrera-Silveira J, Hernández-Mena DI, Herzka SZ, Ordoñez-López U, Aguirre-Macedo ML (2019) Metazoan parasite infracommunities of the dusky flounder (*Syacium papillosum*) as bioindicators of environmental conditions in the continental shelf of the Yucatan Peninsula, Mexico. *Parasites & Vectors* 12: 277. <https://doi.org/10.1186/s13071-019-3524-6>
- Wood CL, Baum JK, Reddy SM, Trebilco R, Sandin SA, Zgliczynski BJ, Briggs AA, Micheli F (2015) Productivity and fishing pressure drive variability in fish parasite assemblages of the Line Islands, equatorial Pacific. *Ecology* 96: 1383–1398. <https://doi.org/10.1890/13-2154.1>

A new species and new records of *Onchidium* slugs (Gastropoda, Euthyneura, Pulmonata, Onchidiidae) in South-East Asia

Benoît Dayrat¹, Tricia C. Goulding^{1,2}, Munawar Khalil³,
Deepak Apte⁴, Shau Hwai Tan^{5,6}

1 Pennsylvania State University, Department of Biology, Mueller Laboratory 514, University Park, PA 16802, USA **2** Current address: Bernice Pauahi Bishop Museum, 1525 Bernice St, Honolulu, HI 96817, USA **3** Department of Marine Science, Universitas Malikussaleh, Reuleut Main Campus, Kecamatan Muara Batu, North Aceh, Aceh, 24355, Indonesia **4** Bombay Natural History Society, Hornbill House, Opp. Lion Gate, Shaheed Bhagat Singh Road, Mumbai 400 001, Maharashtra, India **5** Marine Science Laboratory, School of Biological Sciences, Universiti Sains Malaysia, 11800 Minden Penang, Malaysia **6** Centre for Marine and Coastal Studies, Universiti Sains Malaysia, 11800 Minden Penang, Malaysia

Corresponding author: *Benoît Dayrat* (bad25@psu.edu)

Academic editor: *N. Yonow* | Received 29 August 2019 | Accepted 8 October 2019 | Published 27 November 2019

<http://zoobank.org/5F543780-6E6C-4353-BF6E-FD0E252D63AE>

Citation: Dayrat B, Goulding TC, Khalil M, Apte D, Tan SH (2019) A new species and new records of *Onchidium* slugs (Gastropoda, Euthyneura, Pulmonata, Onchidiidae) in South-East Asia. ZooKeys 892: 27–57. <https://doi.org/10.3897/zookeys.892.39524>

Abstract

A new species, *Onchidium melakense* Dayrat & Goulding, **sp. nov.**, is described, bringing the total to four known species in the genus *Onchidium* Buchannan, 1800. *Onchidium melakense* is a rare species with only nine individuals found at three mangrove sites in the Andaman Islands and the Strait of Malacca (western Peninsular Malaysia and eastern Sumatra). The new species is delineated based on mitochondrial (COI and 16S) and nuclear (ITS2 and 28S) DNA sequences as well as comparative anatomy. Each *Onchidium* species is characterized by a distinct color and can easily be identified in the field, even in the Strait of Malacca where there are three sympatric *Onchidium* species. An identification key is provided. In addition, *Onchidium stuxbergi* (Westerlund, 1883) is recorded for the first time from eastern Sumatra, and *Onchidium pallidipes* Tapparone-Canefri, 1889, of which the type material is described and illustrated here, is regarded as a new junior synonym of *O. stuxbergi*.

Keywords

Biodiversity, integrative taxonomy, Malacca Strait, mangrove, systematic revisions

Introduction

Onchidiids are true slugs (lacking an internal shell) which breathe air with a lung and die if they are immersed in water for a few hours. Most species are found in the intertidal zone, but a few species are adapted to high-elevation rainforest up to 1,850 meters (Dayrat 2010). Onchidiids are found worldwide, but the highest species diversity is in South-East Asia, especially in mangroves where onchidiids are among the most abundant animals. Onchidiid slugs are most closely related to veronicellids, which are also true slugs but which, unlike onchidiids, are fully terrestrial, and to Stylommatophora, the land snails and slugs (Dayrat et al. 2011).

The taxonomy of the Onchidiidae has been in a state of chaos for many years (Dayrat 2009). In the past few years, the Dayrat laboratory has been revising the taxonomy of the entire family one clade at a time (Dayrat et al. 2016, 2017, 2018, 2019a, b; Dayrat and Goulding 2017; Goulding et al. 2018a, b, c). We follow an integrative approach to taxonomy based on: 1) a re-examination of all types available and a comprehensive review of the nomenclature to address the application of all existing species- and genus-group names; 2) extensive field work to observe species in their habitat and to collect fresh material (we visited more than 300 sites worldwide); and, 3) species delineation using DNA sequences to complement comparative anatomy.

As the type genus of the family, *Onchidium* Buchannan, 1800 was the focus of our first revision (Dayrat et al. 2016). In the past, the generic name *Onchidium* was traditionally used by default for many onchidiid species, because relationships among onchidiid species were very confusing. In total, 80 species were described using *Onchidium* in the original binomial (Dayrat 2009). However, the revision of the genus *Onchidium* showed that it included only three species (Dayrat et al. 2016): the type species *O. typhae* Buchannan, 1800, *O. reevesii* (J. E. Gray, 1850), and *O. stuxbergi* (Westerlund, 1883). Except for *Onchidium nigrum* Plate, 1893 and *Onchidium pallidipes* Tapparone-Canefri, 1889, both junior synonyms of *O. stuxbergi*, all other species binomials with *Onchidium* as a generic name refer to species that actually belong to other onchidiid genera or to nomina dubia which cannot be placed in any onchidiid genus (Dayrat et al. 2016, 2017, 2018, 2019a, b; Dayrat and Goulding 2017; Goulding et al. 2018a, b, c).

Onchidium slugs can be identified in the field thanks to two external features: large, conical, pointed papillae on the dorsal notum and very long and thin ocular tentacles. These two traits are synapomorphies of *Onchidium* which are not found in any other onchidiids. In the present contribution, we describe the new species *Onchidium melakense* Dayrat & Goulding. It is a rare species for which we found only nine individuals at three mangrove sites (out of the dozens of sites that we explored in the region). One individual was collected in the Andaman Islands. Eight individuals were collected in the Strait of Malacca: four individuals in the Matang mangrove near Kuala Sepatang in western Peninsular Malaysia, and four individuals in Sinaboi Island, a small uninhabited island in eastern Sumatra. *Onchidium melakense* is supported by mitochondrial (COI and 16S) and nuclear (ITS2 and 28S) DNA sequences and comparative anatomy. Each *Onchidium* species is characterized by a distinct color so the three *Onchidium* species that are sympatric in the Strait of Malacca can easily be

identified: *Onchidium melakense* is characterized by a light brown dorsal notum and a perfectly white hyponotum. An identification key to *Onchidium* species is provided.

In addition, *Onchidium stuxbergi* is recorded for the first time from eastern Sumatra. Also, *Onchidium pallidipes* Tapparone-Canefri, 1889, of which the type material is described and illustrated here, is regarded as a new junior synonym of *O. stuxbergi*. Finally, for the first time, a plate illustrates precisely the range of individual variation for the intestinal loops of each *Onchidium* species: intestinal loops are of type II in *O. typhae* and of type III in the three other species.

Materials and methods

Collecting

All specimens were collected by the authors in the past few years, except six specimens from China for which sequences were obtained from GenBank (Table 1). Collecting field parties were led by Benoît Dayrat in the Andaman Islands (India) and Peninsular Malaysia and by Munawar Khalil in Sumatra (Indonesia). Sites were accessed by car or by boat. Although each site was explored for an average of two hours, the exact time spent at each site also depended on the time of the low tide, the weather conditions, etc. Photographs were taken to document the kind of mangrove being visited as well as the diverse microhabitats where specimens were collected.

Specimens were individually numbered and photographed in their respective habitat. At each site, we endeavored to sample as much diversity as possible. In addition to numbering individually the specimens that looked different, we also numbered individually specimens that looked similar so that we could test for the presence of cryptic diversity. Importantly, a piece of tissue was cut for all specimens individually numbered (for DNA extraction) and the rest of each specimen was relaxed (using magnesium chloride) and fixed (using 10% formalin or 70% ethanol) for comparative anatomy.

Specimens

Eighteen specimens were already included in our revision of the genus *Onchidium* and are included in the molecular analyses here to demonstrate the existence of a new species and of a new record for *O. stuxbergi* (Table 1). Their mitochondrial COI and 16S sequences are from our revision of *Onchidium*, but their nuclear ITS2 and 28S sequences are new. All mitochondrial and nuclear sequences for the 10 specimens representing a new species or a new record are new. Overall, mitochondrial COI and 16S sequences are provided for 28 individuals and nuclear 28S and ITS2 sequences are provided for 12 of those 28 individuals (excluding outgroups). All DNA sequences were generated by us except for the mitochondrial sequences of six individuals from China obtained from GenBank (Table 1).

Table 1. DNA extraction numbers and GenBank accession numbers for all the specimens included in the present study. The letter H next to an extraction number indicates the holotype.

Species	DNA #	Voucher	Locality	COI	16S	ITS2	28S
<i>Onchidium melakense</i>	1105	BNHS 94	Andaman, India	–	MN528066	–	–
	1720	UMIZ 00001	Sumatra, Indonesia	MN528057	MN528067	MN527565	MN527530
	1723	UMIZ 00001	Sumatra, Indonesia	MN528058	MN528068	–	–
	1769	UMIZ 00001	Sumatra, Indonesia	MN528059	MN528069	MN527566	MN527531
	1771	UMIZ 00001	Sumatra, Indonesia	MN528060	MN528070	MN527567	MN527532
	5978	USMMC 00076	Peninsular Malaysia	MN528061	MN528071	–	–
	5979 H	USMMC 00075	Peninsular Malaysia	MN528062	MN528072	MN527568	MN527533
	5981	USMMC 00076	Peninsular Malaysia	MN528063	MN528073	MN527569	MN527534
	5982	USMMC 00076	Peninsular Malaysia	MN528064	MN528074	–	–
	<i>O. reevesii</i>	S871	ASTM-Mo-S871	China (22°30'N)	JN543161*	JN543097*	–
S831		ASTM-Mo-S831	China (24°24'N)	JN543160*	JN543096*	–	–
S853		ASTM-Mo-S853	China (27°29'N)	JN543164*	JN543100*	–	–
S821		ASTM-Mo-S821	China (33°20'N)	JN543162*	JN543098*	–	–
S802		ASTM-Mo-S802	China (34°46'N)	JN543157*	JN543093*	–	–
<i>O. stuxbergi</i>	971	USMMC 00006	Peninsular Malaysia	KX179514*	KX179531*	MN527562	MN527527
	1770	UMIZ 00002	Sumatra, Indonesia	MN528056	MN528065	–	–
	1048	BDMNH	Brunei	KX179515*	KX179532*	MN527563	MN527528
	3251	PNM 041199	Bohol, Philippines	KX179517*	KX179534*	–	–
	3363	PNM 041202	Bohol, Philippines	KX179518*	KX179535*	MN527564	MN527529
	5602	ITBZC IM 00001	Vietnam	KX179519*	KX179536*	–	–
	5605	ITBZC IM 00002	Vietnam	KX179520*	KX179537*	MG958721*	MG971211*
	S891	ASTM-Mo-S891	China (19°56'N)	JN543155*	JN543091*	–	–
<i>O. typhae</i>	1064	BNHS 82	West Bengal, India	–	KX179528*	–	–
	1089	BNHS 82-1089	Andaman, India	KX179512*	KX179529*	–	–
	1109	BNHS 21-1109	Andaman, India	KX179513*	KX179530*	–	–
	967	USMMC 00003	Peninsular Malaysia	KX179510*	KX179526*	MN527560	MN527525
	965	USMMC 00005	Peninsular Malaysia	KX179509*	KX179525*	MG958720*	MG971210*
	1007	ZRC.MOL.6396	Singapore	KX179511*	KX179527*	MN527561	MN527526
<i>Alionchis jaitloensis</i>	5137	UMIZ 00117	Indonesia, Halmahera	MG953528*	MG953538*	MG953548*	MK122918*
<i>Marmaronchis vaiigiensis</i>	1183	ZRC.MOL.3007	Singapore	MK122812*	MK122854*	MK122877*	MK122910*
<i>M. marmoratus</i>	5409	MNHN-IM-2013-15764	PNG, Madang	MK122838*	MK122859*	MK122893*	MK122915*
<i>Melayonchis aileanae</i>	970	USMMC 00018	Peninsular Malaysia	KX240033*	KX240057*	MK122902*	MK125514*
<i>M. annae</i>	1010	ZRC.MOL.6502	Singapore	KX240015*	KX240039*	MK122903*	MK122919*
<i>M. eloisae</i>	1011	ZRC.MOL.6499	Singapore	KX240026*	KX240050*	MK122904*	MK125515*
<i>M. siongkiati</i>	1002	ZRC.MOL.6501	Singapore	KX240020*	KX240044*	MK122905*	MK122920*
<i>Paromoionchis penangensis</i>	957	USMMC 00061	Peninsular Malaysia	MH055078*	MH055137*	MH055255*	MH055293*
<i>P. tumidus</i>	963	USMMC 00057	Peninsular Malaysia	MH054946*	MH055101*	MH055194*	MH055266*
<i>Onchidella celtica</i>	5013	MNHN-IM-2014-6891	France	MG958715*	MG958717*	MK122906*	MK122921*
<i>O. nigricans</i>	1524	AM C468921.002	Australia, NSW	MG970878*	MG970944*	MK122908*	MK122923*
<i>Onchidina australis</i>	1523	AM C468918.002	Australia, NSW	KX179548*	KX179561*	MG958719*	MG971209*
<i>Peronia</i> sp.	706	UF 303653	USA, Hawaii	HQ660038*	HQ659906*	MG958722*	MG971212*
	696	UF 352288	Japan, Okinawa	HQ660043*	HQ659911*	MG958871*	MG958883*
<i>Peronia tenera</i>	960	USMMC 00039	Peninsular Malaysia	MG958740*	MG958796*	MG958840*	MG958874*
<i>P. zulfigari</i>	924	USMMC 00048	Peninsular Malaysia	MG958760*	MG958816*	MG958853*	MG958876*
<i>Plateindex luteus</i>	1001	ZRC.MOL.10179	Singapore	MG958714*	MG958716*	MG958718*	MG958888*
<i>Wallaconchis ater</i>	3272	PNM 041222	Philippines, Bohol	MG970809*	MG970910*	MG971132*	MG971185*
<i>W. sinantui</i>	2740	UMIZ 00059	Indonesia, Ambon	MG970713*	MG970881*	MG971093*	MG971161*

* Sequences (including all sequences of the outgroups) from our former publications (Dayrat et al. 2011, 2016, 2017, 2018, 2019a, b; Dayrat and Goulding 2017; Goulding et al. 2018a, b, c). Sequences from China were obtained from GenBank (Sun et al. 2014) where they are misidentified as *Onchidium struma*, a *nomen nudum*.

Abbreviations: Australian Museum, Sydney (AM); Aquatic Science and Technology Museum of Shanghai Ocean University (ASTM); Brunei Darussalam Museum of Natural History (BDMNH); Bombay Natural History Society, India (BNHS); Institute of Tropical Biology, Zoology Collection, Vietnam Academy of Science and Technology (ITBZC); Muséum national d'Histoire naturelle, Paris, France (MNHN); National Museum of the Philippines, Manila (PNM); University of Florida, Gainesville (UF); Universitas Malikussaleh, North Aceh, Sumatra, Indonesia (UMIZ); Universiti Sains Malaysia Mollusc Collection, Penang, Malaysia (USMMC); Zoological Reference Collection, Lee Kong Chian Natural History Museum, National University of Singapore (ZRC).

DNA extraction numbers unique to each individual are indicated in phylogenetic analyses as well as lists of material examined and figure captions (numbers are between brackets). Size (length/width) is indicated in millimeters (mm) for each specimen. Many additional specimens were examined in the context of our revision of the family, including all available types (the types of *Onchidium pallidipes* Tapparone-Canefri, 1889 and *Onchidium multinotatum* Plate, 1893, are addressed in detail in the discussion) and hundreds of onchidiids representing all the known genera and nearly all known species. The ten specimens representing a new species and a new record were deposited as vouchers in institutions in the countries of origin: Bombay Natural History Society, Mumbai, (India); Universitas Malikussaleh, North Aceh, Sumatra (Indonesia); Universiti Sains Malaysia, Penang (Malaysia).

Museum collection abbreviations

MNHN	Muséum national d'Histoire naturelle, Paris, France;
NMNH	National Museum of Natural History, Smithsonian Institution, Washington, DC, USA;
SMNH	Swedish Museum of Natural History, Stockholm, Sweden;
UMIZ	Universitas Malikussaleh, North Aceh, Sumatra, Indonesia;
USMMC	Universiti Sains Malaysia, Mollusk Collection, Penang, Malaysia;
ZMB	Museum für Naturkunde, Berlin, Germany;
ZMH	Zoologisches Museum, Hamburg, Germany.

Anatomical preparations and descriptions

Both the external morphology and the internal anatomy were studied. All anatomical observations were made under a dissecting microscope and drawn with a camera lucida. Radulae and male reproductive organs were prepared for scanning electron microscopy (Zeiss SIGMA Field Emission Scanning Electron Microscopy). Radulae were cleaned in 10% NaOH for a week, rinsed in distilled water, briefly cleaned in an ultrasonic water bath (less than a minute), sputter-coated with gold-palladium and examined by SEM. Soft parts (penis, accessory penial gland, etc.) were dehydrated in ethanol and critical point dried before coating.

The detailed anatomy of the type species, *Onchidium typhae*, can be found in our revision of *Onchidium* (Dayrat et al. 2016). To avoid unnecessary repetition, the description of anatomical features that are virtually identical between *Onchidium* species (e.g., position of female opening, position of anus, size of hyponotum relative to total width, nervous system, heart, and stomach) is not repeated here. However, all the characters that are useful for species comparison (e.g., color of live animals, radular formulae, intestinal loops, and reproductive system) are described for the new species. Special attention has been given to illustrating the holotype of the new species and its habitat, including an image of its type locality.

DNA extraction and PCR amplification

DNA was extracted using a phenol-chloroform extraction protocol with cetyltrimethyl-ammonium bromide (CTAB). The mitochondrial cytochrome *c* oxidase I region (COI) and 16S region were amplified using the following universal primers: LCO1490 (5'-3') GGT CAA CAA ATC ATA AAG ATA TTG G, and HCO2198 (5'-3') TAA ACT TCA GGG TGA CCA AAR AAY CA (Folmer et al. 1994), 16Sar-L (5'-3') CGC CTG TTT ATC AAA AAC AT (Palumbi 1996), and the modified Palumbi primer 16S 972R (5'-3') CCG GTC TGA ACT CAG ATC ATG T (Dayrat et al. 2011). The nuclear ITS2 region and 28S region were amplified with the following primers: LSU-1 (5'-3') CTA GCT GCG AGA ATT AAT GTG A, and LSU-3 (5'-3') ACT TTC CCT CAC GGT ACT TG (Wade and Mordan 2000), 28SC1 (5'-3') ACC CGC TGA ATT TAA GCA T (Hassouna et al. 1984), and 28SD3 (5'-3') GAC GAT CGA TTT GCA CGT CA (Vonnemann et al. 2005). The 25 µl PCRs for COI and 16S contained 15.8 µl of water, 2.5 µl of 10X PCR Buffer, 1.5 µl of 25 mM MgCl₂, 0.5 µl of each 10 µM primer, 2 µl of dNTP Mixture, 0.2 µl (1 unit) of TaKaRa Taq (Code No. R001A), 1 µl of 20 ng/µl template DNA, and 1 µl of 100X BSA (Bovine Serum Albumin). The PCRs for ITS2 used the reagents in the same amounts as COI and 16S, except that water was reduced to 14.8 µl and the amount of 100X BSA was increased to 2 µl. The PCRs for 28S included 14.8 µl of water, 2.5 µl of 10X PCR Buffer, 0.5 µl of each 10 µM primer, 1 µl of dNTP Mixture, 5 µl of Q solution (which includes MgCl₂) and 0.5 µl of 20 ng/µl template DNA. The thermopprofile used for COI and 16S was: 5 minutes at 94 °C; 30 cycles of 40 seconds at 94 °C, 1 minute at 46 °C, and 1 minute at 72 °C; and a final extension of 10 minutes at 72 °C. The thermopprofile used for ITS2 was: 1 minute at 96 °C; 35 cycles of 30 seconds at 94 °C, 30 seconds at 50 °C, and 1 minute at 72 °C; and a final extension of 10 minutes at 72 °C. The thermopprofile used for 28S was: 4 minutes at 94 °C; 38 cycles of 50 seconds at 94 °C, 1 minute at 52 °C, and 2 minutes 30 seconds at 72 °C; and a final extension of 10 minutes at 72 °C. The PCR products were cleaned with ExoSAP-IT (Affymetrix, Santa Clara, CA, USA) prior to sequencing. Untrimmed sequenced fragments represented approximately 680 bp for COI, 530 bp for 16S, 740 bp for ITS2, and 1000 bp for 28S.

Phylogenetic analyses

Chromatograms were consulted to resolve rare ambiguous base calls. DNA sequences were aligned using Clustal W in MEGA 7 (Kumar et al. 2016). Nineteen onchidiid species outside *Onchidium* were selected as outgroups from our previous studies (Dayrat et al. 2011, 2016, 2017, 2018, 2019a, b; Dayrat and Goulding 2017; Goulding et al. 2018a, b, c): *Alionchis jailoloensis* Goulding & Dayrat in Goulding et al. 2018a, *Marmaronchis marmoratus* (Lesson, 1831), *Marmaronchis vaigiensis* (Quoy & Gaimard, 1825), *Melayonchis aileenae* Dayrat & Goulding in Dayrat et al. 2017, *Melayonchis annae* Dayrat in Dayrat et al. 2017, *Melayonchis eloisae* Dayrat in Dayrat et al. 2017, *Melayonchis siongiati* Dayrat &

Goulding in Dayrat et al. 2017, *Onchidella celtica* (Cuvier in Audouin and Milne-Edwards 1832), *Onchidella nigricans* (Quoy & Gaimard, 1832), *Onchidina australis* (Semper, 1880), *Paromoionchis daemelii* (Semper, 1880), *Paromoionchis tumidus* (Semper, 1880), *Peronia* sp. (Hawaii), *Peronia* sp. (Okinawa), *Peronina tenera* (Stoliczka, 1869), *Peronina zulfigari* Goulding & Dayrat in Goulding et al. 2018c, *Platevindex luteus* (Semper, 1880), *Wallaconchis ater* (Lesson, 1831), and *Wallaconchis sinanui* Goulding & Dayrat in Goulding et al. 2018b. All new DNA sequences were deposited in GenBank and vouchers deposited in museum collections (Table 1). The ends of each alignment were trimmed. Alignments of mitochondrial (COI and 16S) sequences and nuclear (ITS2 and 28S) sequences were concatenated separately in order to test whether these two data sets support the same relationships. The concatenated mitochondrial alignment included 986 nucleotide positions: 582 (COI) and 404 (16S). The concatenated ITS2 and 28S alignment included 1467 nucleotide positions: 472 (ITS2) and 995 (28S).

Two independent sets of phylogenetic analyses were performed: 1) Maximum Likelihood and Bayesian analyses with concatenated mitochondrial COI and 16S sequences; 2) Maximum Parsimony analyses with concatenated nuclear ITS2 and 28S sequences. Maximum Parsimony analyses were conducted in PAUP v 4.0 (Swofford 2002) with gaps coded as a fifth character state, and 100 bootstrap replicates conducted using a full heuristic search. Prior to Maximum Likelihood and Bayesian phylogenetic analyses, the best-fitting evolutionary model was selected for each locus separately using the Model Selection option from Topali v2.5 (Milne et al. 2004): a GTR + G model was independently selected for COI and 16S. Maximum Likelihood analyses were performed using PhyML (Guindon and Gascuel 2003) as implemented in Topali. Node support was evaluated using bootstrapping with 100 replicates. Bayesian analyses were performed using MrBayes v3.1.2 (Ronquist and Huelsenbeck 2003) as implemented in Topali, with five simultaneous runs of 1.5×10^6 generations each, sample frequency of 100, and burn in of 25% (and posterior probabilities were also calculated). Topali did not detect any issue with respect to convergence. All analyses were run several times and yielded the same result.

In addition, another set of analyses was performed with only COI sequences. Genetic distances between COI sequences were calculated in MEGA 7 as uncorrected p-distances. COI sequences were also translated into amino acid sequences in MEGA using the invertebrate mitochondrial genetic code to check for the presence of stop codons (no stop codon was found).

Results

Molecular phylogenetic analyses (Figs 1, 2)

DNA sequences were used to test species limits within *Onchidium*. The monophyly of *Onchidium* is recovered in all analyses. In the analyses based on mitochondrial COI and 16S concatenated sequences, four least-inclusive units are reciprocally monophyl-

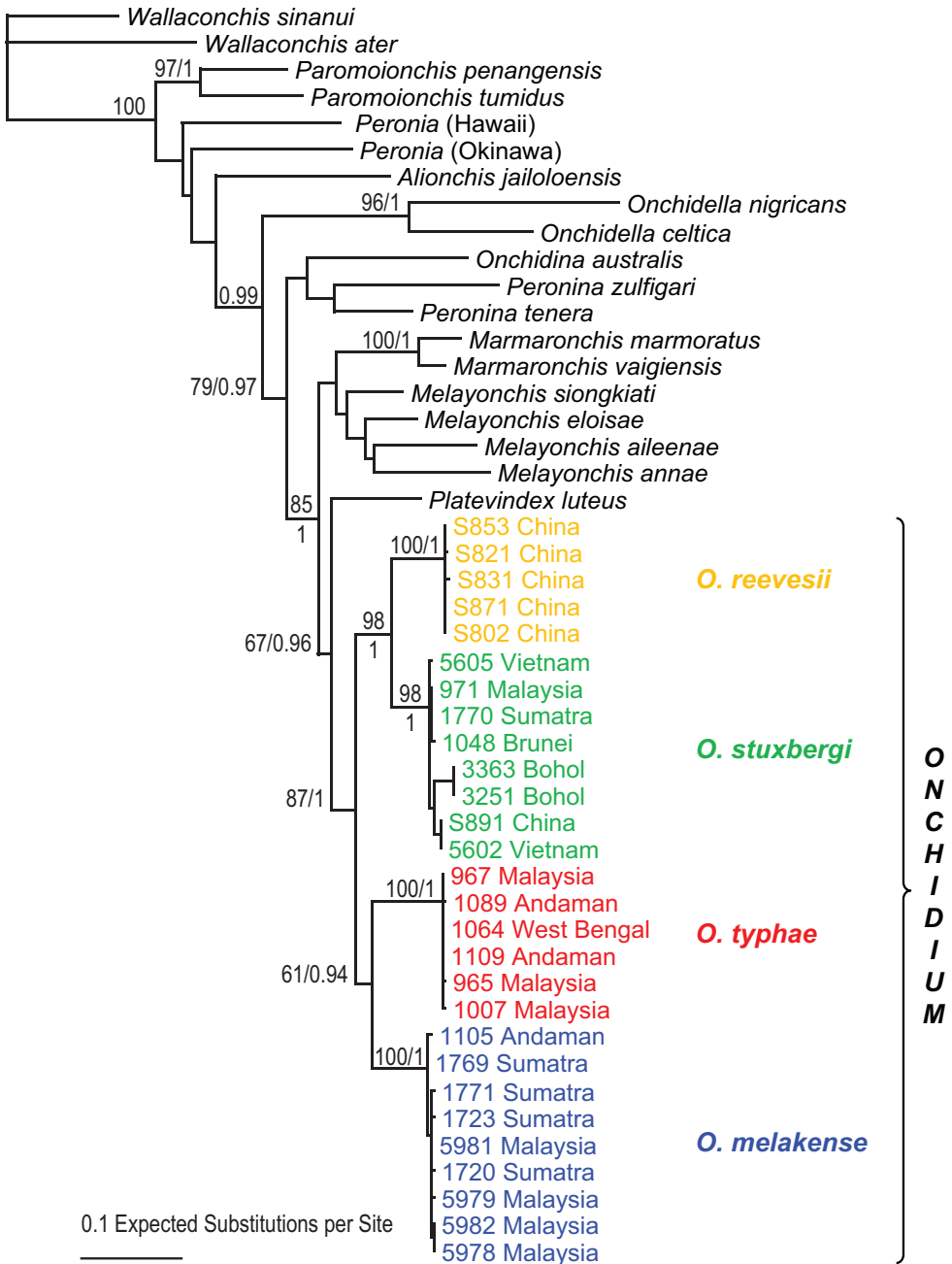


Figure 1. Phylogenetic tree showing the relationships between *Onchidium* individuals based on mitochondrial COI and 16S DNA sequences. Numbers by the nodes are the bootstrap values (Maximum Likelihood analysis) and the posterior probabilities (Bayesian analysis); only significant numbers (> 65% and > 0.9) are indicated. All other sequences serve as outgroups. Information on specimens can be found in the lists of material examined and Table 1. The colors used for each *Onchidium* species are the same as those used in Figs 2–4.

strongly supported with bootstrap values of 100. *Onchidium reevesii* could not be included in the nuclear analyses because ITS2 sequences for the specimens from China are not available in GenBank (Table 1).

Pairwise genetic divergences (Fig. 3)

Pairwise genetic distances (between COI sequences) support the existence of four species of *Onchidium* as least-inclusive molecular units (Table 2). The intra-specific genetic distances are all below 3.2% (within *O. stuxbergi*). The inter-specific distances vary from 8.6% (between *O. reevesii* and *O. stuxbergi*) to 14.3% (between *O. reevesii* and *O. typhae*). So, overall, the distance gap between the four *Onchidium* species is between 3.2% and 8.6%.

Comparative anatomy

Due to its distinctive external color, the new species was immediately recognized in the field as new to science. It also differs in internal anatomy from the three other known species. In particular, the penial sheath in the male copulatory apparatus is short and straight while coiled in the three other species (Table 3).

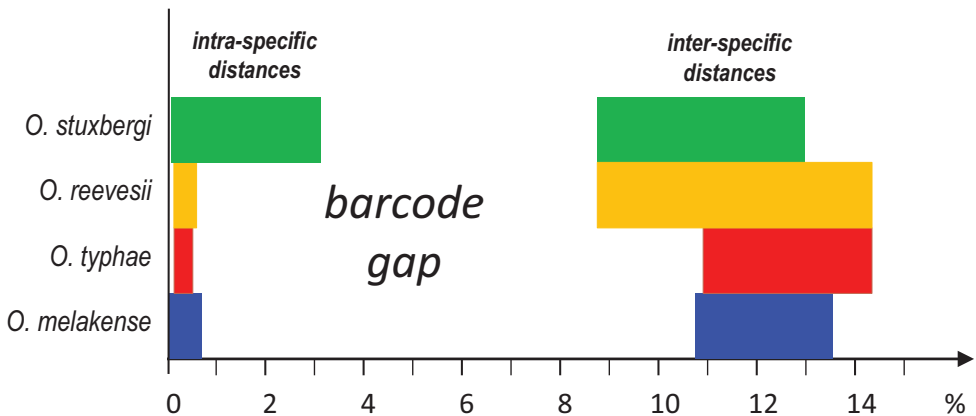


Figure 3. Diagram to help visualize pairwise genetic distances between COI sequences within and between *Onchidium* species (Table 2). Ranges of minimum to maximum distances are indicated (in percentages). For instance, the intra-specific divergences within *O. typhae* are between 0.1 and 0.4%, while the inter-specific divergences between *O. typhae* and the three other species are between 10.9 and 14.3%. Overall, the distance gap between all four *Onchidium* species is between 3.2 and 8.6%. The colors used for each *Onchidium* species are the same as those used in Figs 1, 2, and 4.

Table 2. Pairwise genetic distances between mitochondrial COI sequences in *Onchidium*. Ranges of minimum to maximum distances are indicated (in percentage). For instance, the intra-specific divergences within *O. typhae* are between 0.1 and 0.4%, while the inter-specific divergences between *O. typhae* and *O. stuxbergi* are between 11.4 and 12.9%.

Species	<i>O. typhae</i>	<i>O. stuxbergi</i>	<i>O. melakense</i>	<i>O. reevesii</i>
<i>O. typhae</i>	0.1–0.4	–	–	–
<i>O. stuxbergi</i>	11.4–12.9	0.0–3.2	–	–
<i>O. melakense</i>	10.9–11.9	10.7–13.0	0.0–0.7	–
<i>O. reevesii</i>	13.4–14.3	8.6–10.1	12.6–13.5	0.1–0.5

Table 3. Morphological differences among *Onchidium* species. All traits are subject to individual variation. Information regarding *O. stuxbergi* and *O. typhae* is from Dayrat et al. (2016). Information regarding *O. reevesii* is from Dayrat et al. (2016) for the holotype, and from Wang et al. (2018) for non-type material. For the type of intestinal loops, the orientation of the transitional loop (TL) is provided. For the radular formulae, the range of number of rows (e.g., 60 to 80 rows in *O. melakense*) and the range of number of lateral teeth per half row (e.g., 70 to 110 in *O. melakense*) are provided. The number of radular rows was not described in *O. reevesii* by Wang et al. (2018).

Species	<i>O. melakense</i>	<i>O. reevesii</i>	<i>O. stuxbergi</i>	<i>O. typhae</i>
Size	Up to 45 mm	Up to 67 mm	Up to 55 mm	Up to 65 mm
Dorsal color	Light brown	Brown	Brown, occasionally black	Brownish
Foot color	Pale yellow-beige	Whitish or light yellow	Bright orange	Grey to yellow, sometimes greenish
Hyponotum color	White	Light grey or beige-white	Greyish to yellowish, sometimes greenish	Grey to yellow, sometimes greenish
Black dots on hyponotum	Absent	Present	Present	Absent
Type of intestinal loops	III, TL from 1 to 5 o'clock	III, TL at 2 o'clock	III, TL from 1 to 8 o'clock	II, TL from 8 to 9 o'clock
Radular formulae	60/80, 70/110	62/110 (lateral teeth only)	50/70, 68/80	53/65, 65/80
Penial gland spine length	Up to 1.1 mm	No data available	Up to 2 mm	Up to 1.2 mm
Penial sheath	Short and straight	Long and heavily coiled in spirals	Long and heavily coiled in spirals	Long and heavily coiled in spirals
Insertion of retractor muscle in visceral cavity	Middle	Posterior third	Posterior third	Near the heart (India) & posterior half (everywhere else)
Anterior retractor muscle	Present (occasionally absent)	Absent	Present (possibly occasionally absent)	Absent

Systematics and anatomical descriptions

Family Onchidiidae Rafinesque, 1815

Genus *Onchidium* Buchannan, 1800

Onchidium Buchannan, 1800: 132.

Labella Starobogatov, 1970: 45; Starobogatov 1976: 211. Replacement name for *Elophilus* Labbé, 1935, preoccupied by *Elophilus* Meigen, 1803 [Diptera].

Type species. *Onchidium typhae* Buchannan, 1800, by monotypy.

Gender. Neuter, gender of the final component of *Onchidium*, a name formed from the masculine Greek word ὁ ὄγκος (mass, tumor) and the neuter Latin suffix *-ium* (ICZN 1999: Article 30.1.1).

Diagnosis. Body not flattened. No dorsal gills. Dorsal eyes present on notum. Large, conical, pointed papillae present on notum. Retractable, central papilla (with three or four dorsal eyes) present but not significantly larger than surrounding papillae. Eyes at tip of extremely long ocular tentacles. Male opening below right ocular tentacle and slightly to its left. Transversal protuberance on oral lobes present. Foot wide. Pneumostome medial, on average in middle between foot margin and notum margin. Intestinal loops of types II and III. Rectal gland present. Accessory penial gland present with a hollow spine but no muscular sac. Penis with hooks.

Distinctive features. In the field, *Onchidium* slugs differ from all other onchidiids by the presence of large, conical, pointed papillae on the dorsal notum. However, papillae can only be observed when animals remain undisturbed. In disturbed (and preserved) animals, papillae remain pointed but become minute. However, the best feature to identify *Onchidium* slugs in the field is the presence of very long and thin ocular tentacles (up to 20 mm). Papillae can definitely be confused between genera but *Onchidium* slugs are (almost) the only ones with such long eye tentacles. Very long ocular tentacles are also present in *Alionchis jailoloensis* but they are much thicker (in diameter) than those of *Onchidium*. Also, *Alionchis jailoloensis* is so far only known from Halmahera (where *Onchidium* is not found) and lacks the large, conical, pointed papillae that are typical of *Onchidium*. Finally, in *Alionchis*, the pneumostome is always located exactly at the margin of the notum. Therefore, *Onchidium* slugs cannot be confused with *Alionchis* slugs.

Distribution. From northeastern India (West Bengal) to the Philippines, including the Strait of Malacca, Singapore, Thailand, Vietnam, eastern Borneo, and China (Fig. 4).

Remarks. The diagnosis and the distinctive features provided above are slightly updated from Dayrat et al. (2016). The synonymy of *Labbella* (replacement name for *Elophilus*) with *Onchidium* was already discussed by Dayrat et al. (2016). In brief, *Labbella ajuthiae* (Labbé, 1935), the type species of *Labbella*, is a junior synonym of *Onchidium stuxbergi* (Westerlund, 1883). Therefore, both *Labbella* and *Onchidium* apply to the same clade. We remark a detail concerning the nomenclatural status of *Elophilus* Meigen, 1803. Under plenary powers of the Commission (ICZN 1993: 256), the generic name *Elophilus* Meigen, 1803 was “suppressed for the purposes of the Principle of Priority but not for those of the Principle of Homonymy.” So, even though *Elophilus* Meigen, 1803, was placed on the Official Index of Rejected and Invalid Generic Names in Zoology, *Elophilus* Labbé, 1935 remains a junior homonym of *Elophilus* Meigen, 1803, hence the necessity of the replacement name *Labbella*. Also, note that the publication date for *Labbella* by Starobogatov is 1970 instead of 1976 (Dayrat 2009; Dayrat et al. 2016).

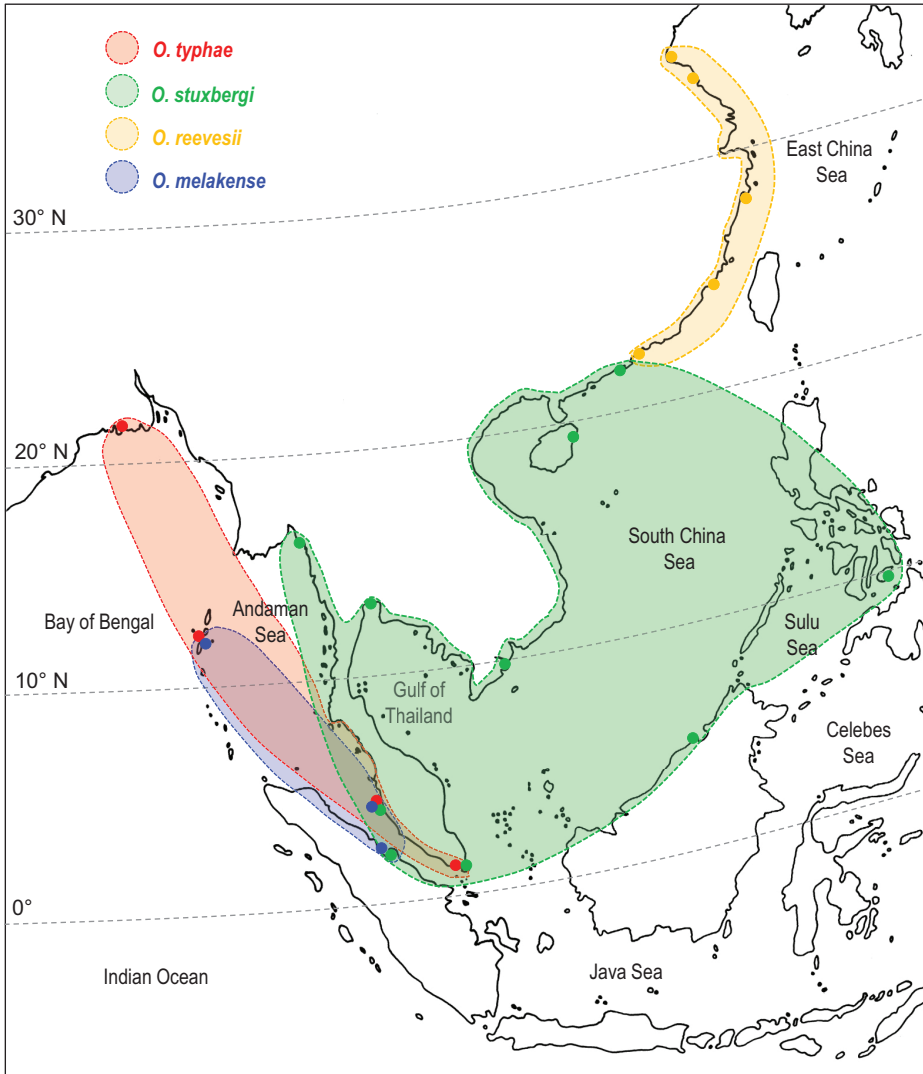


Figure 4. Geographic distribution of the four known *Onchidium* species. Dots correspond to known records. The colors used for each *Onchidium* species are the same as those used in Figs 1–3.

***Onchidium melakense* Dayrat & Goulding, sp. nov.**

<http://zoobank.org/D7C0CD7A-C888-407B-9E36-C1544835B355>

Figs 5–11, 13G, H

Type material. Holotype. MALAYSIA • holotype, designated here, 45/25 mm [5979 H]; Peninsular Malaysia, Kuala Sepatang; 04°50.605'N, 100°38.133'E; 28 Jul 2016; B Dayrat and field party leg.; st 258, old forest with tall *Rhizophora* trees, high in the tidal zone (ferns), in educational mangrove preserve; USMMC 00075.

Additional material examined. INDIA – **Andaman Islands** • 1 specimen 25/15 mm [1105]; Middle Andaman, Rangat, Shyamkund; 12°28.953'N, 92°50.638'E; 11 Jan 2011; B Dayrat and field party leg.; st 57, by a large river, deep mangrove with tall trees, small creeks, and many muddy logs; BNHS 94. MALAYSIA – **Peninsular Malaysia** • 3 specimens 30/20 mm [5978], 35/18 mm [5981], and 35/30 mm [5982]; same collection data as for the holotype; USMMC 00076. INDONESIA – **Sumatra** • 4 specimens 27/20 mm [1723], 25/22 mm [1720], 35/20 mm [1769], and 40/20 mm [1771]; Pulau Sinaboi; 02°18.145'N, 100°59.309'E; 8 Oct 2012; M Khalil and field party leg.; st 73, mangrove forest with medium *Rhizophora* and *Avicennia* trees, logs, hard mud; UMIZ 00001.

Distribution (Fig. 4). Western Peninsular Malaysia (type locality), eastern Sumatra (Indonesia), and Andaman Islands (India).

Etymology. *Onchidium melakense* is named after the Strait of Malacca or 'Selat Melaka' in Malay: *melakense* is a Latinized adjective that agrees in gender (neuter) with the generic name (ICZN 1999: Art. 31.2). The mangrove gastropod diversity of the Strait of Malacca is extraordinarily rich. For instance, three of the four known *Onchidium* species are sympatric there: *O. typhae*, *O. stuxbergi*, and the new species *O. melakense*. The fourth species, *O. reevesii*, is restricted to the Chinese coast (Fig. 4).

Habitat (Fig. 5). *Onchidium melakense* was found under a log (type locality, Peninsular Malaysia), inside crevices of a muddy log (Sumatra) and on the cemented wall of a bridge over a mangrove creek (Andaman Islands). Most individuals were hidden and could not have been found if logs had not been turned over and thoroughly searched inside. This search, however, should be done with caution because pit vipers often like to rest near logs in mangroves (Fig. 5D). *Onchidium melakense* does not seem to particularly favor the habitat where *O. typhae* and *O. stuxbergi* are most commonly found, i.e., the surface of muddy trunks, logs, and *Thalassina* lobster mounds. Even though *O. typhae* and *O. stuxbergi* can be found at the same sites as *O. melakense* (they are found in the Matang mangrove, where the type locality of *O. melakense* is located), they do not share exactly the same micro-habitats. Clearly, all these species hide in crevices at high tide but, unlike *O. typhae* and *O. stuxbergi*, *O. melakense* appears to remain hidden at low tide as well.

Abundance. *Onchidium melakense* is a rare species. In total, we found only nine individuals: four individuals at the type locality in Peninsular Malaysia, four individuals at one site in eastern Sumatra, and a single individual in the Andaman Islands.

Color and external morphology of live animals (Figs 6, 7). Live animals are not covered with mud and the color of their dorsum can normally be seen. The dorsum is homogeneously light brown. The hyponotum is distinctly white. The foot is pale yellow-beige. The ocular tentacles are dark grey and are extremely long (up to 2 cm) when animals are undisturbed. The head is grey. Large, conical, pointed papillae (which are typical of *Onchidium* species) are present but can only be seen when the animal remains undisturbed for a long time. Some of these papillae bear dorsal eyes. When animals are disturbed, papillae immediately retract and become minute (although they remain pointed). A central papilla (with three or four dorsal eyes), fully retractable within the dorsal notum, is also present but is not particularly more



Figure 5. Habitats, *Onchidium melakense* **A** type locality, Peninsular Malaysia, Kuala Sepatang, old forest with tall *Rhizophora* trees, high in the tidal zone (ferns), in educational mangrove preserve (st 258) **B** Sumatra, Pulau Sinaboi, mangrove forest with medium *Rhizophora* and *Avicennia* trees, dead logs, hard mud (st 73) **C** old log with crevices which *O. melakense* typically favors (st 73) **D** mangrove pit viper (arrow) resting by a log (st 73).

prominent than surrounding papillae. Crawling individuals are up to 45 mm long. Preserved specimens no longer display the distinct color seen in live animals: the dorsal notum remains light brown and the hyponotum remains white, but the foot of preserved animals is whitish.

Digestive system (Figs 7, 9). Examples of radular formulae are presented in Table 4. The median cusp of the rachidian tooth is always present; its lateral cusps (on its lateral sides) can be conspicuous. The intestine is of type III, with a transitional loop oriented to the right, approximately from 1 to 5 o'clock (for a comparison of intestinal types between *Onchidium* species, see the Discussion).

Reproductive system (Fig. 10A). The receptaculum seminis (caecum) is bent, ovate and elongated. The spermatheca is spherical-ovate and connects to the oviduct through a short duct with one loop. The oviduct and the deferent duct are narrow and straight. A vaginal gland is absent.

Copulatory apparatus (Figs 10, 11). The male anterior organs consist of the penial complex (penial papilla, penial sheath, deferent duct, and retractor muscle) and the accessory penial gland (flagellum and hollow spine). The penial complex and the ac-

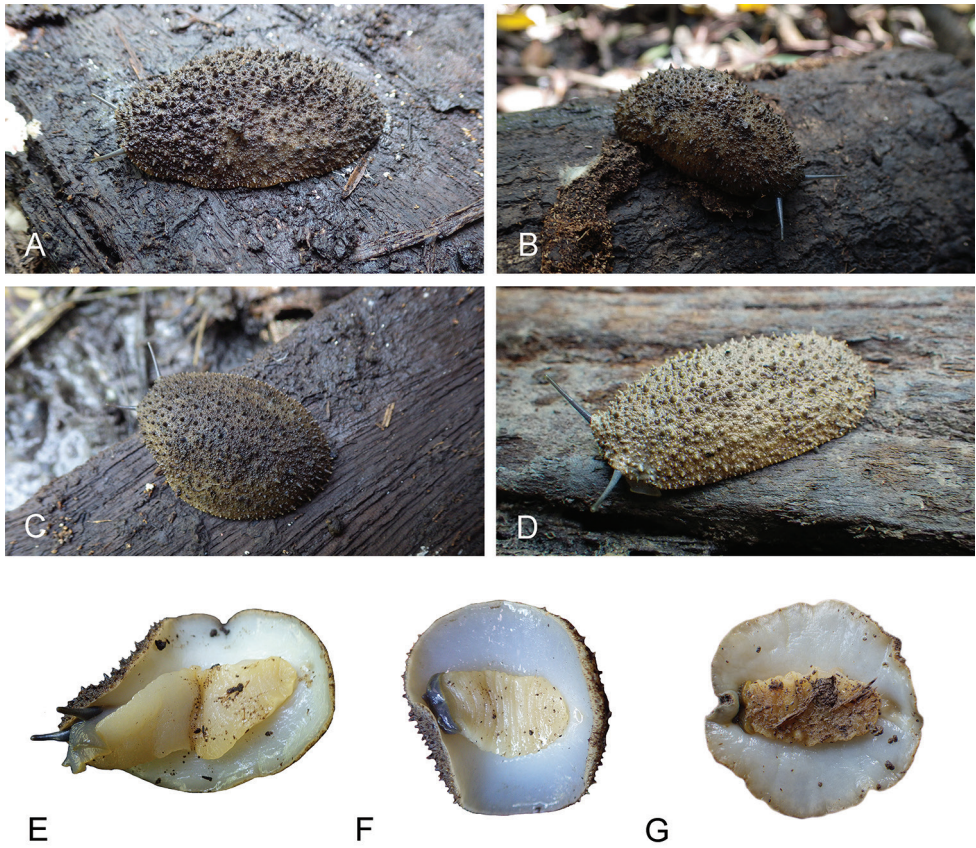


Figure 6. Live animals, *Onchidium melakense* **A** dorsal view, holotype, 45 mm long [5979], Peninsular Malaysia (USMMC 00075) **B** dorsal view, 30 mm long [5978], Peninsular Malaysia (USMMC 00076) **C** dorsal view, 35 mm long [5981], Peninsular Malaysia (USMMC 00076) **D** dorsal view, 35 mm long [1769], Sumatra (UMIZ 00001) **E** ventral view, same as A **F** ventral view, same as C **G** dorsal view, 40 mm long [1771], Sumatra (UMIZ 00001).

cessory penial gland share the same vestibule and male opening. The flagellum of the penial gland is coiled. Distally, it ends in a hard, hollow spine. The hollow spine is narrow, elongated, and slightly curved. Its length varies from 0.8 to 1.1 mm. Its diameter is approximately 50 μm for most of its length (but approximately 140 μm at its conical base). The hollow spine does not open directly into the proximal region of the vestibule. There is a transversal, flat disc at the distal end of the flagellum (approximately 0.4 mm in diameter) through which the hollow spine must protrude in order to be outside and shared with the partner (Fig. 11D).

The penial sheath is short (less than 5 mm) and straight, not coiled in spirals. The (posterior) retractor muscle is longer than the penial sheath and inserts at about the middle of the visceral cavity floor. An additional, anterior retractor muscle is present (and occasionally absent) in the distal part of the penial sheath. The deferent duct is highly convoluted with many loops. The penis is made of two distinct parts. The

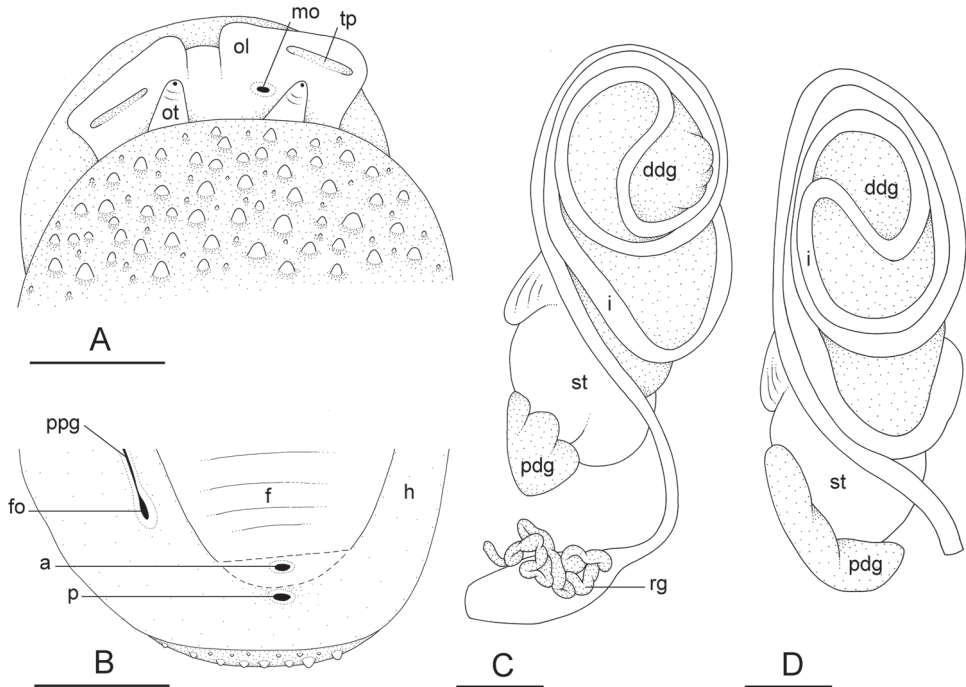


Figure 7. External morphology and digestive system, *Onchidium melakense*, Peninsular Malaysia **A–C** holotype [5979] (USMMC 00075) **D** [5978] (USMMC 00076) **A** dorsal, anterior view **B** posterior, ventral view (dotted lines indicate where the foot was cut to show the anus) **C** digestive system, dorsal view **D** digestive system, dorsal view. Abbreviations: a anus, ddg dorsal lobe of digestive gland, f foot (pedal sole), fo female opening, h hyponotum, i intestine, mo male opening, ol oral lobe, ot ocular tentacle, p pneumostome, pdg posterior lobe of the digestive gland, ppg peripodial groove, rg rectal gland, st stomach, tp transversal protuberance (on oral lobe). Scale bars: 5 mm (**A–C**), 3 mm (**D**).

Table 4. Radular formulae for *Onchidium melakense*. Each formula follows the same format: number of rows \times number of lateral teeth per left half row – 1 (rachidian tooth) – number of lateral teeth per right half row. Each DNA extraction number corresponds to one individual. The letter H next to an extraction number indicates the holotype.

DNA extraction number	Voucher	Radular formula	Specimen length (mm)
5979 H	USMMC 00075	80 \times 110-1-110	45
5982	USMMC 00076	80 \times 90-1-90	35
1723	UMIZ 00001	75 \times 90-1-90	27
5981	USMMC 00076	65 \times 70-1-70	35
1720	UMIZ 00001	60 \times 85-1-85	25

proximal part is a hollow, solid, flexible stalk with no hooks; its length varies from 1.2 to 1.8 mm and its diameter from 100 μ m to 200 μ m. The distal part is short (up to approximately 0.8 mm long), soft, and covered with penial hooks internally. Penial hooks are inside the tube-like penis when the penis is retracted inside the penial sheath. During copulation, the penis is everted like a glove and the hooks are then on the outside. Penial hooks are conical, curved, pointed, and up to 60 μ m long.

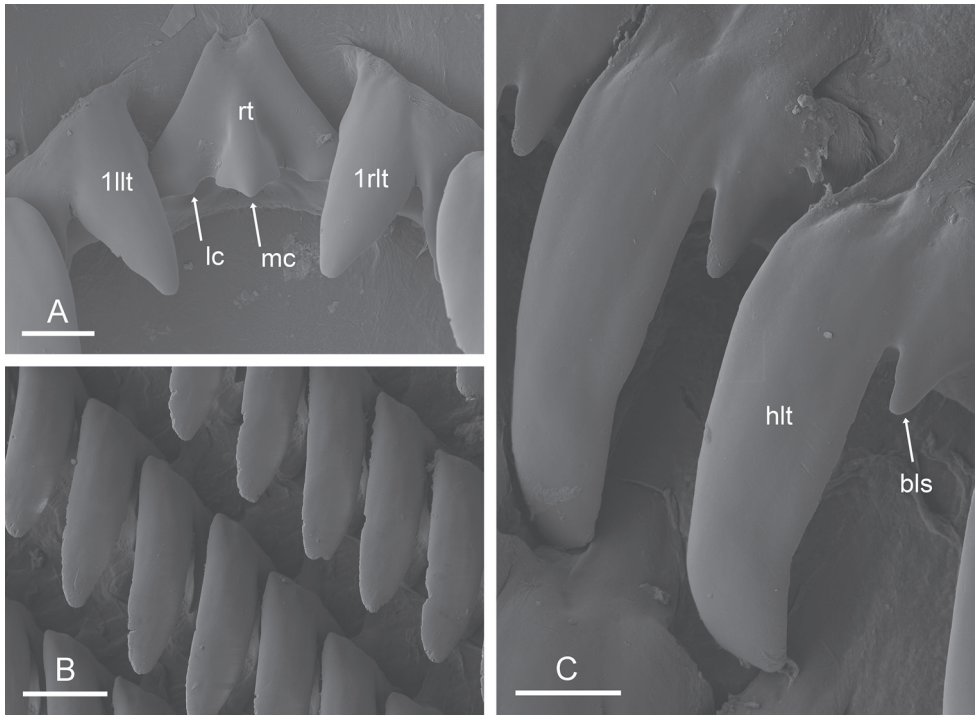


Figure 8. Radula, *Onchidium melakense*, Peninsular Malaysia, holotype [5979] (USMMC 00075) **A** rachidian and innermost lateral teeth **B** right lateral teeth **C** right lateral teeth. Abbreviations: 1llt first left lateral tooth, 1rlt first right lateral tooth, bls basal lateral spine, hlt hook of lateral tooth, lc lateral cusp of rachidian tooth, mc median cusp of rachidian tooth, rt rachidian tooth. Scale bars: 10 μm (**A**), 20 μm (**B, C**).

Diagnostic features. Externally, *Onchidium melakense* differs from all other *Onchidium* species by its color. *Onchidium melakense* is the only known species with a light brown dorsal notum, a pale yellow-beige foot, and a white hyponotum (see Table 3 and the Identification key). Internally, *O. melakense* is the only known species with a short and straight penial sheath, while in other species the penial sheath is long and coiled in spirals (Table 3). Other traits are helpful as well but may not be as diagnostic as the penial sheath. For instance, intestinal loops help distinguish *O. melakense* from *O. typhae* but not from *O. stuxbergi* (Table 3).

Remarks. A new species name is needed because no existing name applies to the species described here, based on the examination of all the type specimens available in the Onchidiidae, a careful study of all the original descriptions, and our ongoing taxonomic revision of every genus of the family (Dayrat et al. 2016, 2017, 2018, 2019a, b; Dayrat and Goulding 2017; Goulding et al. 2018a, b, c). Moreover, based on its known distribution (Andaman Islands, eastern Sumatra, western Peninsular Malaysia), *O. melakense* is expected to be found in other places, such as the Nicobar Islands. However, *O. melakense* is rare, at least in comparison to its two sympatric species, *O. typhae* and *O. stuxbergi*.

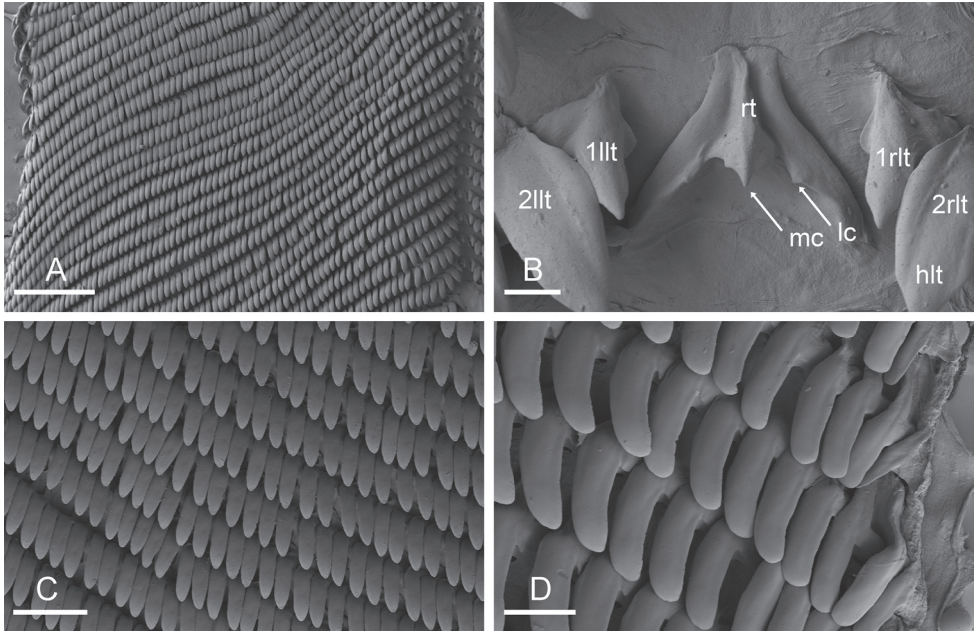


Figure 9. Radula, *Onchidium melakense*, Sumatra (UMIZ 00001) **A** left, half rows, [1720] **B** rachidian and innermost lateral teeth, [1720] **C** lateral teeth, [1723] **D** outermost, lateral teeth, [1723]. Abbreviations: 1llt first left lateral tooth, 1rlt first right lateral tooth, 2llt second left lateral tooth, 2rlt second right lateral tooth, hlt hook of lateral tooth, lc lateral cusp of rachidian tooth, mc median cusp of rachidian tooth, rt rachidian tooth. Scale bars: 200 μm (**A**), 10 μm (**B**), 60 μm (**C**), 20 μm (**D**).

Large populations (with dozens of individuals) of *O. typhae* were encountered (Dayrat et al. 2016). In the field, *O. typhae* and *O. stuxbergi* can be found by looking at the muddy surface of trunks, logs, and lobster mounds, while *O. melakense* can be found only if one actively searches for it under and inside logs.

Onchidium stuxbergi (Westerlund, 1883)

Figs 12B, C, 13C–E

Vaginulus stuxbergi Westerlund, 1883: 165; Westerlund 1885, 191–192, pl. 2, fig. 2a–c.

Onchidium stuxbergi (Westerlund, 1883): Dayrat et al. 2016: 21–32, figs 9–16.

Onchidium pallidipes Tapparone-Canefri, 1889: 329–331. Syn. nov.

Onchidium nigrum Plate, 1893: 188–190, pl. 8, fig. 31a, pl. 10, fig. 53, pl. 11, fig. 75; Hoffmann 1928: 78; Labbé 1934: 223–224, figs 58–61.

Elophilus ajuthiae Labbé, 1935: 312–317, figs 1–3. *Elophilus* Labbé, 1935, preoccupied by *Elophilus* Meigen, 1803 [Diptera], was replaced by *Labella* Starobogatov, 1970.

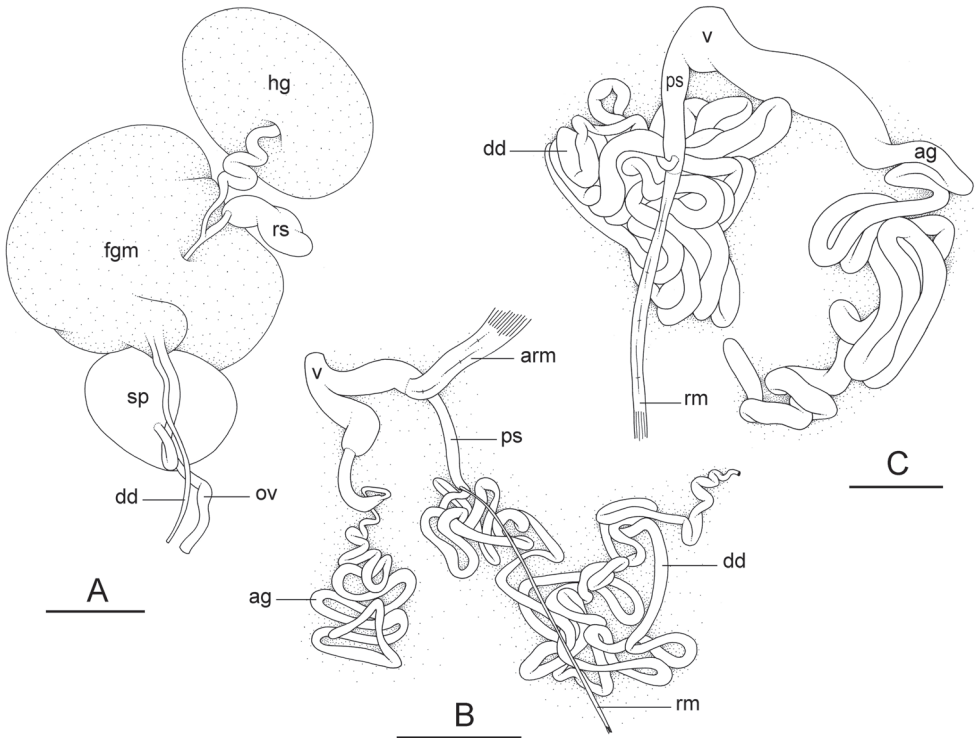


Figure 10. Reproductive system, *Onchidium melakense* **A, B** Peninsular Malaysia, holotype [5979] (USMMC 00075) **C** Sumatra, [1723] (UMIZ 00001) **A** posterior, hermaphroditic, reproductive parts **B** anterior, male, copulatory parts **C** anterior, male, copulatory parts. Abbreviations: ag accessory penial gland, arm anterior penial retractor muscle, dd deferent duct, fgm female gland mass, hg hermaphroditic gland, ov oviduct, ps penial sheath, rm penial retractor muscle, rs receptaculum seminis, sp spermatheca, v vestibule. Scale bars: 4 mm (**A**), 5 mm (**B**), 2 mm (**C**).

Type material. *Lectotype and paralectotypes* (*Vaginulus stuxbergi*). BRUNEI DARUSSALAM • lectotype, 43/25 mm; Brunei Bay, northwestern Borneo; SMNH 1334. • 11 paralectotypes, 35/30 to 15/12 mm; SMNH 1334, SMNH 7523. For detailed information, see Dayrat et al. (2016: 22).

Lectotype and paralectotypes (*Onchidium pallidipes*). MYANMAR • lectotype, 15/12 mm, designated here; Moulmein, Tenasserim [now Mawlamyine, Tanintharyi]; USNM 127328. • 1 paralectotype, 12/9 mm; same collection data as for the lectotype; ZMH 27467/1. • 1 paralectotype, 10/5 mm; same collection data as for the lectotype; ZMB/Moll 47190. The lectotype is poorly-preserved but its dorsal notum bears some faint traces of what could have been dorsal papillae similar to those found in *Onchidium*; its copulatory apparatus and its digestive system are drawn for the present study (Fig. 12B, C). One paralectotype is completely destroyed (ZMB/Moll 47190): it likely dried and it cannot be identified. The other paralectotype is an immature specimen with no male or female reproductive system (ZMH 27467/1), but its intestinal loops are exactly identical to those of the lectotype. Labels of the three type specimens

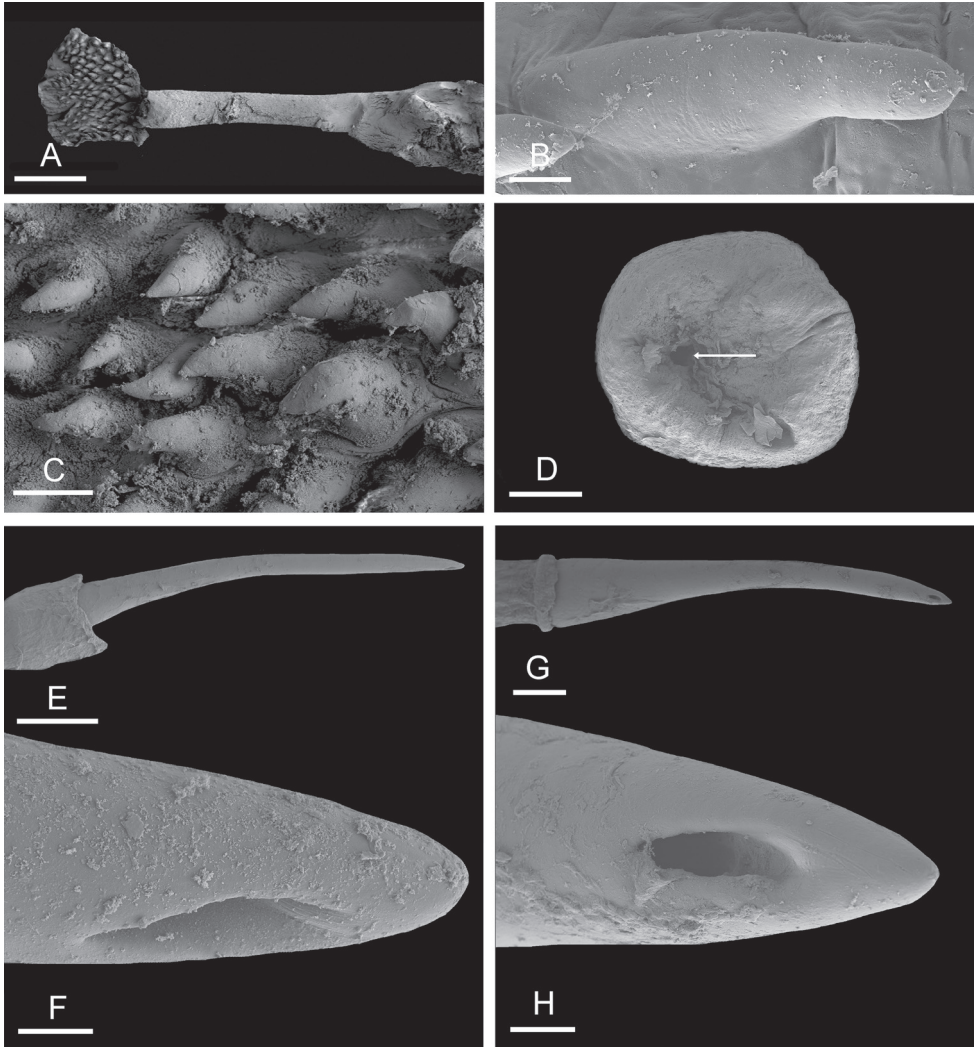


Figure 11. Male, anterior, copulatory parts, *Onchidium melakense* **A, C** Sumatra, [1723] (UMIZ 00001) **B, E, F** Peninsular Malaysia, holotype [5979] (USMMC 00075) **D, G, H** Peninsular Malaysia, holotype [5982] (USMMC 00076) **A** stalk and penial hooks **B** penial hook **C** penial hooks **D** flat disc at distal end of flagellum of penial accessory gland (the arrow indicates the hole through which the hollow spine protrudes) **E** hollow spine **F** hollow spine tip **G** hollow spine **H** hollow spine tip. Scale bars: 300 μm (**A**), 10 μm (**B, C, F**), 100 μm (**D, G, H**), 200 μm (**E**).

indicate Moulmein as locality. All three type specimens seem to be from the same locality according to the original description (Tapparone-Canefri 1889: 330), and are preserved in three different museum collections.

Holotype (*Onchidium nigrum*). BORNEO • holotype, 40/30 mm, by monotypy; unidentified area on the island of Borneo; ZMB/Moll 22749. For detailed information, see Dayrat et al. (2016: 23).

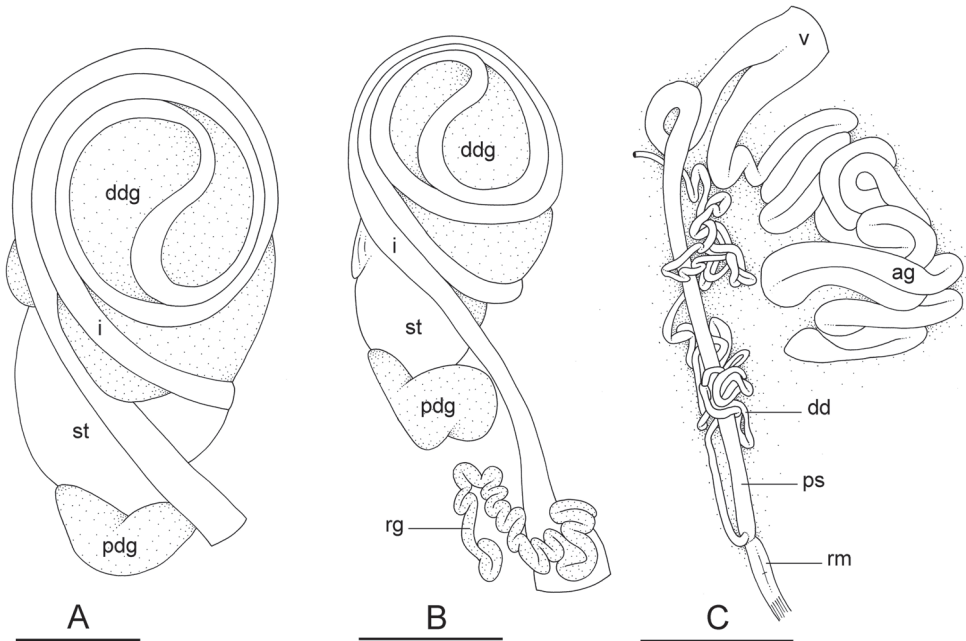


Figure 12. Name-bearing types of *Onchidium multicolor* and *Onchidium pallidipes* **A** digestive system, type III with a transitional loop at 2 o'clock (based on marks left by the intestine in the digestive gland), dorsal view, holotype, *O. multicolor* (ZMB/Moll 240117) **B** digestive system, type III with a transitional loop at 2 o'clock, dorsal view, lectotype, *O. pallidipes* (NMNH 127328) **C** anterior, male, copulatory parts, lectotype, *O. pallidipes* (NMNH 127328). Abbreviations: ag accessory penial gland, dd deferent duct, ddg dorsal lobe of digestive gland, i intestine, pdg posterior lobe of the digestive gland, ps penial sheath, rg rectal gland, rm penial retractor muscle, st stomach, v vestibule. Scale bars: 3 mm (**A, B**), 2 mm (**C**).

Syntypes (*Labbella ajuthiae*). THAILAND • 3 syntypes 20/17 mm, 20/15 mm, and 20/14 mm; Chao Phraya River, Ayutthaya Province; brackish waters; MNHN-IM-2000-22965. For detailed information, see Dayrat et al. (2016: 23).

Additional material examined. INDONESIA – Sumatra • 1 specimen 23/14 mm [1775]; Dumai; 01°42.838'N, 101°23.286'E; 9 Oct 2012; M Khalil and field party leg.; st 74, mangrove forest just behind abandoned buildings, high intertidal, with many *Thalassina* mounds and small creeks; UMIZ 00003.

Distribution. (Fig. 4). Myanmar (type locality of *O. pallidipes*, new record), and eastern Sumatra (new record). Other known records are in Singapore, Sabah and western Peninsular Malaysia (Malaysia), Brunei Darussalam, Bohol (Philippines), Vietnam, Thailand (Gulf of Thailand), and southern China up to 22°10'N (Dayrat et al. 2016: 24).

Habitat. In eastern Sumatra, *O. stuxbergi* was found on a muddy log, one of the habitats in which it is known to live (Dayrat et al. 2016: 24). In the original description of *O. pallidipes*, it is indicated that the slugs were found under the plant debris of sugar cane (Tapparone-Canefri 1889: 330), which is an unusual but possible habitat.

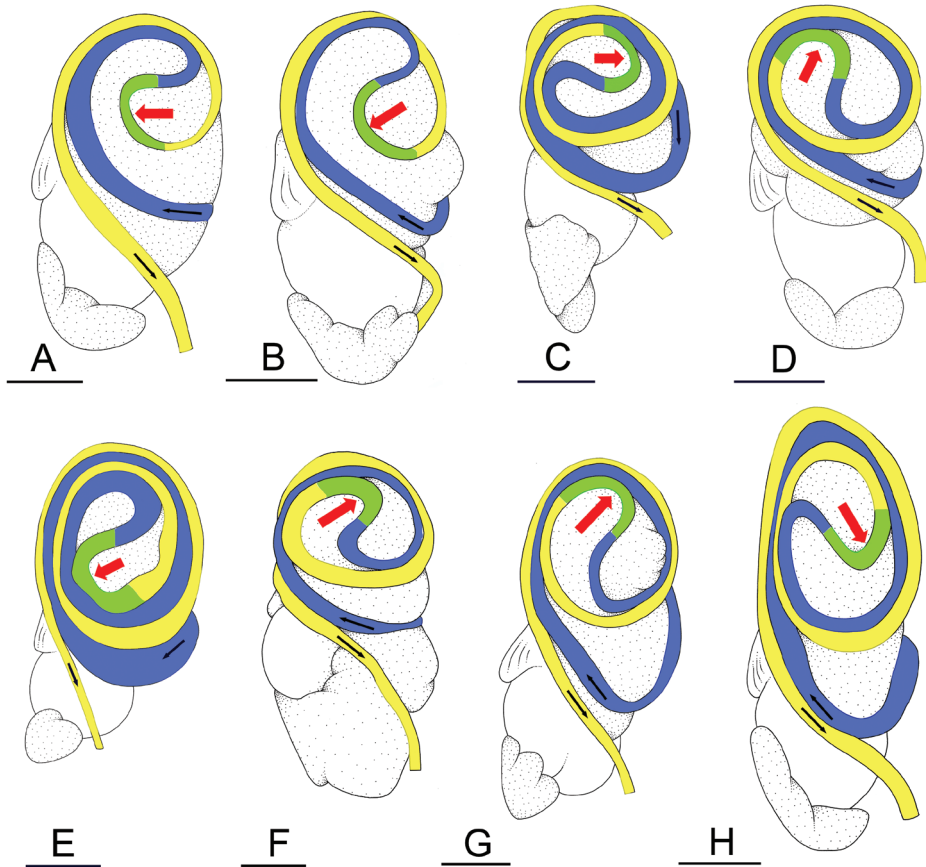


Figure 13. Types of intestinal loops in the genus *Onchidium*. Small black arrows indicate the direction of the intestinal transport, which starts in the blue loop. A blue loop turns clockwise. A yellow loop turns counterclockwise. A green loop is transitional in between a blue loop and a yellow loop. The orientation of the transitional (green) loop is indicated with a red arrow. Details on individuals of *O. reevesii*, *O. typhae*, *O. stuxbergi* can be found in Dayrat et al. (2016) **A** *O. typhae*, type II with a transitional loop at 9 o'clock, [1007] **B** *O. typhae*, type II with a transitional loop at 8 o'clock (from Dayrat et al. 2016: fig. 5E) **C** *O. stuxbergi*, type III with a transitional loop at 3 o'clock (from Dayrat et al. 2016: fig. 11B) **D** *O. stuxbergi*, type III with a transitional loop at 1 o'clock, (PNM 041200) **E** *O. stuxbergi*, type III with a transitional loop at 8 o'clock, [5605] **F** *O. reevesii*, holotype, type III with a transitional loop at 2 o'clock (from Dayrat et al. 2016: fig. 14A) **G** *O. melakense*, type III with a transitional loop at 1 o'clock, holotype [5979] (USMMC 00075) **H** *O. melakense*, type III with a transitional loop at 5 o'clock, [5978] (USMMC 00076). Scale bars: 3 mm (**A, H**), 5 mm (**B, C, E–G**), 4 mm (**D**).

Abundance. The present record from eastern Sumatra confirms that *O. stuxbergi* is not found in high densities (a few individuals at most) even though it is found at many sites across its distribution range.

Remarks. Given its known records on the other side of the Strait of Malacca (western Peninsular Malaysia) and Singapore, *Onchidium stuxbergi* was expected to be present in eastern Sumatra. Anatomically, *Onchidium stuxbergi* in Sumatra is indis-

tinguishable from the individuals found elsewhere. Also, the DNA sequences of the individual from eastern Sumatra are nested within the rest of the species (Fig. 1).

A detailed discussion on the synonymy of *Labbella ajuthiae* and *Onchidium nigrum* with *O. stuxbergi* can be found in Dayrat et al. (2016). The type material of *Onchidium pallidipes* was briefly addressed in a study on the genus *Melayonchis* Dayrat & Goulding in Dayrat et al. 2017. At the time, it was thought that *O. pallidipes* was a *nomen dubium*. However, the dissection of far more onchidiid species in the past few years has revealed that the coiled penial sheath of the lectotype of *O. pallidipes* (Fig. 12C) is typical of what is observed only in *Onchidium* (except for the new *Onchidium* species described here, in which the penial sheath is short and straight). Also, the poorly-preserved dorsal notum of the lectotype of *O. pallidipes* bears some faint traces of what could have been papillae similar to those found in *Onchidium*. So, now, it is considered that the name *Onchidium pallidipes* applies to an *Onchidium* species. Note that this application is exclusively based on the lectotype (designated here) because a paralectotype is destroyed and the other paralectotype is an immature specimen.

Onchidium typhae is supposedly present in Myanmar because it is known from West Bengal eastward all the way to Singapore (Fig. 4). However, *O. pallidipes* cannot apply to *O. typhae* because the intestinal loops of *O. typhae* are always of type II (see below, Fig. 13A, B). Given the intestinal loops of type III of its lectotype (Fig. 12B), *O. pallidipes* applies to *O. stuxbergi*, also characterized by intestinal loops of type III (Fig. 13C–E). The hollow spine of the accessory penial gland of the lectotype of *O. pallidipes* is 2.7 mm long, which is slightly outside the range known so far in *O. stuxbergi* (0.5 to 2 mm), but that character is expected to vary. No additional retractor muscle fibers were found in the distal part of the male apparatus of the lectotype of *O. pallidipes* (Fig. 12C), even though they are known to be present in *O. stuxbergi* (Dayrat et al. 2016: fig. 11C). However, the lack of an anterior, retractor muscle in the lectotype of *O. pallidipes* can be explained by the fact that it is relatively small (15 mm long) and poorly-preserved. Also, this trait was found to vary in *O. melakense* and it is possible that it also varies in *O. stuxbergi*, especially among small individuals. Finally, it is worth pointing out that Tapparone-Canefri (1889: 330) selected the specific name *pallidipes* to refer to the “pale foot” of the preserved specimens he examined for the original description. Tapparone-Canefri (1889: 330) did not have access to information on live animals but he suggested that the foot was “probably ocher in living specimens,” which fits well with *O. stuxbergi* (of which the foot is bright orange).

In the future, if fresh material collected from the type locality of *O. pallidipes* is shown to form its own reciprocally-monophyletic unit using both mitochondrial and nuclear DNA sequences, and if it is shown to be anatomically fully compatible with the lectotype of *O. pallidipes* (especially regarding the length of the spine of the accessory penial gland), then *O. pallidipes* could become a valid name for a distinct *Onchidium* species endemic to the eastern Andaman Sea. This hypothesis cannot be completely ruled out at this stage. However, given the data currently available and all the reasons given above, we regard *O. pallidipes* as a junior synonym of *O. stuxbergi*.

The name *Onchidium multinotatum* Plate, 1893 needs to be briefly discussed. Its type locality is Cavite, Manila, in Luzon, Philippines. The original description is quite detailed, as often with Plate, but the holotype (30/15 mm), by monotypy (ZMB/Moll 240117), is very poorly preserved because it likely dried for a while. Only a few destroyed pieces of the digestive system remain in the empty body wall. Some of the features that Plate described could unfortunately not be checked (rectal gland present, accessory penial gland present, penial gland spine 4 mm long, penis 30 mm long). Plate separated the intestine from the digestive gland but described intestinal loops of type II. However, marks left by the intestine on the dorsal aspect of the digestive glands suggest that the intestinal loops of *O. multinotatum* were of type III (Fig. 12A). Given the critical uncertainty regarding the type of intestinal loops and that traits described by Plate cannot be checked, *Onchidium multinotatum* is regarded as a *nomen dubium*. *Onchidium multinotatum* could apply to *O. stuxbergi*, but that is not certain. We collected many onchidiids from the Philippines, including in Batangas, just south of Manila in Luzon, and the only species that could match the anatomy of *O. multinotatum* (acknowledging some uncertainty) is *O. stuxbergi*. Unfortunately, the type locality of *O. multinotatum* is in a part of Manila which is now completely developed and we could not collect onchidiids there.

Identification key

A key based on external characters is provided to help identify *Onchidium* slugs in the field. Information on the color of live individuals of *O. typhae* and *O. stuxbergi* is from Dayrat et al. (2016). Information on the color of live individuals of *O. reevesii* is from Wang et al. (2018).

- | | | |
|---|--|------------------------|
| 1 | The foot is bright orange | <i>O. stuxbergi</i> |
| – | The foot is not bright orange..... | 2 |
| 2 | The hyponotum is pure white and the dorsum is light brown | <i>O. melakense</i> ** |
| – | The hyponotum is not pure white and the dorsum is brown | 3 |
| 3 | The hyponotum is light grey or beige-white, the foot is whitish or light yellow, and the dorsum is brown..... | <i>O. reevesii</i> *** |
| – | The hyponotum and the foot vary between greyish and yellowish, and sometimes even greenish, and the dorsum is brown..... | <i>O. typhae</i> **** |

* Known distribution: Myanmar, western Peninsular Malaysia, eastern Sumatra, Thailand (Gulf of Thailand), Vietnam, eastern Borneo, Philippines, and southernmost tropical China (up to 22°10'N).

** Known distribution: Andaman Islands, western Peninsular Malaysia, and eastern Sumatra.

*** Known distribution: subtropical China, from 22°30'N to 34°36'N.

**** Known distribution: West Bengal, Andaman Islands, western Peninsular Malaysia, and Singapore.

Discussion

Onchidium slugs can easily be identified in the field at the generic and specific levels. Indeed, all live *Onchidium* slugs are characterized by two external features that distinguish them from other onchidiids: large, conical, pointed papillae, and very long and thin ocular tentacles (easily up to 20 mm). Also, each *Onchidium* species is characterized by a distinct color and, even though *O. stuxbergi*, *O. typhae*, and *O. melakense* are sympatric, they cannot be confused (see the Identification key above, and Table 3). The only other genus in which species can be easily distinguished in the field is *Melayonchis* Dayrat & Goulding in Dayrat et al. 2017, but, in most other onchidiid genera, such as *Peronina*, *Wallaconchis*, or *Paromoionchis*, species are cryptic externally. This could suggest that *Onchidium* and *Melayonchis* species are relatively older and that there has been enough time for external differences to accumulate. Finally, the discovery of *O. melakense* suggests that additional, rare, endemic *Onchidium* species possibly still are unknown, especially in the region of the Strait of Malacca, which seems to be its center of highest diversity.

Our molecular phylogenetic analyses (Figs 1, 2) indicate that *O. stuxbergi* and *O. reevesii* are most closely related, which is supported by the fact that their hyponotum bears black dots (absent in *O. typhae* and *O. melakense*, Table 3). As of today, *O. stuxbergi* and *O. reevesii* do not overlap geographically even though they get very close in southern China (Fig. 4). Their speciation is possibly related to adaptation to warm (*O. stuxbergi*) and colder (*O. reevesii*) waters.

Our knowledge of *O. reevesii* is based on the re-description of the holotype (Dayrat et al. 2016: 32–35) as well as a recent re-description of fresh material by Wang et al. (2018). The latter study begs discussion here. The foot sole of *O. reevesii* is said to be “whitish or light yellow” within the body of the species description (Wang et al. 2018: 2). In the discussion, some individuals from Cixi City, Zhejiang Province, are also mentioned with a yellow foot (Wang et al. 2018: 6). It is unclear whether those specimens from Cixi City belong to *O. reevesii*. However, it cannot be excluded that the color of the foot sole of *O. reevesii* might vary from white to yellow, instead of light yellow. More importantly, according to Wang et al. (2018: 6): “On the basis of COI sequences we misidentified two distinct species as *Onchidium* ‘struma’ (Sun et al. 2014). These were *O. reevesii* and *O. hongkongense*.” That is incorrect: Dayrat et al. (2016: 35) demonstrated that Sun et al. (2014) applied the *nomen nudum* *Onchidium* ‘struma’ to *O. reevesii* and *O. stuxbergi*. Also, Dayrat et al. (2019a: 22) showed that *Onchidium hongkongense* Britton, 1984 is a junior synonym of *Paromoionchis tumidus* (Semper, 1880) and therefore does not apply to an *Onchidium* species. Finally, the individuals misidentified as *Paraonchidium reevesii* (J.E. Gray, 1850) by Sun et al. (2014) actually belong to *Paromoionchis tumidus* (Dayrat et al. 2019a: 44): the combination *Paraonchidium reevesii* is erroneous because the species described as *Onchidium reevesii* by J.E. Gray (1850) belongs to the genus *Onchidium*, based on the re-description of its holotype (Dayrat et al. 2016: 32–35), and also because *Paraonchidium* Labbé, 1934 is a junior synonym of *Onchidina* Semper, 1882 (Dayrat and Goulding 2017: 123).

In onchidiids, types of intestinal loops are defined based on the pattern of the intestine on the dorsal aspect of the digestive gland. Plate (1893) first distinguished four types of intestinal loops (types I to IV) and Labbé (1934) later added a type V. Only the types II and III are found in *Onchidium* (Table 3). The type species, *O. typhae*, is characterized by intestinal loops of type II, and the three other species are characterized by intestinal loops of type III. The different types of intestinal loops and their individual variation are best revealed by coloring with a different color different sections of the intestine (Dayrat et al. 2019b): a clockwise intestinal loop is colored in blue, a counterclockwise intestinal loop is colored in yellow, and a transitional loop between them is colored in green (Fig. 13).

The intestine first appears dorsally on the right side and starts by forming a clockwise (blue) loop (Fig. 13). In intestinal loops of type II, the clockwise (blue) loop makes approximately a complete circle. As a result, the transitional (green) loop is oriented to the left, typically at 9 o'clock (horizontal red arrow, Fig. 13A). In *Onchidium*, intestinal loops of type II are found only in *O. typhae*, in which the orientation of the transition loop varies approximately between 8 and 9 o'clock (Fig. 13A, B). In intestinal loops of type III, the clockwise (blue) loop is longer and rotates more than in a type II. As a result, the transitional (green) loop is oriented to the right, typically at 3 o'clock (horizontal red arrow, Fig. 13C). In *O. stuxbergi*, the orientation of the transitional (green) loop varies from 1 to 8 o'clock (red arrow, Fig. 13C–E). In *O. reevesii*, the orientation of the transitional (green) loop is approximately at 2 o'clock (red arrow, Fig. 13F). In *O. melakense*, the orientation of the transitional (green) loop varies from 1 to 5 o'clock (red arrow, Fig. 13G, H). A few preliminary remarks on the distribution of types of intestinal loops in genera of onchidiid slugs can be found in Dayrat et al. (2019b). A more thorough discussion regarding types of intestinal loops will be provided after our revisions of *Peronia* and *Platevindex* are published (in preparation).

Acknowledgements

We are grateful to associate editor Nathalie Yonow and reviewers Adrienne Jochum and Pierre Lozouet for constructive comments that helped improve the manuscript. Accessing field sites would have been impossible without help from local fishermen and villagers. We would like to thank the collection managers and curators of various institutions for sending us specimens on loan for examination in the present study: Virginie Héros (Muséum national d'Histoire naturelle, Paris); Chad Walter (Smithsonian Institution, Washington DC); Karin Kronstedt, Elin Sigvaldadottir, Emily Dock Åkerman, Anna Persson, and Anders Warén (Swedish Museum of Natural History, Stockholm); Thomas von Rintelen, Christine Zorn, and Matthias Glaubrecht formerly (Museum für Naturkunde, Berlin); Bernhard Hausdorf (Zoologisches Museum, Hamburg). Collecting was overseen by Deepak Apte in India, by Munawar Khalil in Indonesia, and by Shaw Hwai Tan in Malaysia. We are grateful to Rahul C. Salunkhe and Yogesh Shouche (Bombay Natural History Society, Mumbai, India, and National

Center for Cell Science, Pune, India) for their help with the DNA sequencing of the specimens from India, and we thank Vishal Bhave for his help collecting slugs in the Andaman Islands. We thank the Ministry of Research, Technology and Higher Education, Republic of Indonesia (Ristek-Dikti) for issuing a research permit to BD (Ristek #134/SIP/FRP/E5/Dit.KI/VI/2017). We also wish to thank the Universitas Malikussaleh, North Aceh, Sumatra, Indonesia, for being our homebase institution in Indonesia. This work was supported by the Eberly College of Science at the Pennsylvania State University and by a REVSYS (Revisionary Syntheses in Systematics) award to BD from the US National Science Foundation (DEB 1419394).

References

- Audouin V, Milne-Edwards H (1832–1834) Recherches Pour Servir à L'histoire Naturelle du Littoral de la France (Vol. 2). Crochard, Paris. <https://doi.org/10.5962/bhl.title.43796>
- Britton KM (1984) The Onchidiacea (Gastropoda, Pulmonata) of Hong Kong with a worldwide review of the genera. *Journal of Molluscan Studies* 50: 179–191. <https://doi.org/10.1093/oxfordjournals.mollus.a065863>
- Buchanan F (1800) An account of the *Onchidium*, a new genus of the class of vermes, found in Bengal. *Transactions of the Linnean Society of London* 5: 132–134. [pl 5] <https://doi.org/10.1111/j.1096-3642.1800.tb00584.x>
- Cretella M (2010) The complete collation and dating of the section *Zoologie* of the *Coquille* voyage. *Bollettino Malacologico* 46: 83–103.
- Dayrat B (2009) Review of the current knowledge of the systematics of Onchidiidae (Mollusca: Gastropoda: Pulmonata) with a checklist of nominal species. *Zootaxa* 2068: 1–26. <https://doi.org/10.11646/zootaxa.2068.1.1>
- Dayrat B (2010) Anatomical re-description of the terrestrial onchidiid slug *Semperoncis montana* (Plate, 1893). *Malacologia* 52: 1–20. <https://doi.org/10.4002/040.052.0101>
- Dayrat B, Conrad M, Balayan S, White TR, Albrecht C, Golding R, Gomes S, Harasewych MG, Frias Martins AM de (2011) Phylogenetic relationships and evolution of pulmonate gastropods (Mollusca): new insights from increased taxon sampling. *Molecular Phylogenetics and Evolution* 59: 425–437. <https://doi.org/10.1016/j.ympev.2011.02.014>
- Dayrat B, Goulding TC (2017) Systematics of the onchidiid slug *Onchidina australis* (Mollusca: Gastropoda: Pulmonata). *Archiv für Molluskenkunde* 146: 121–133. <https://doi.org/10.1127/arch.moll/146/121-133>
- Dayrat B, Goulding TC, Apte D, Bhave V, Comendador J, Ngô XQ, Tan SK, Tan SH (2016) Integrative taxonomy of the genus *Onchidium* Buchanan, 1800 (Mollusca, Gastropoda, Pulmonata, Onchidiidae). *ZooKeys* 636: 1–40. <https://doi.org/10.3897/zookeys.636.8879>
- Dayrat B, Goulding TC, Apte D, Bhave V, Ngô XQ (2017) A new genus and four new species of onchidiid slugs from South-East Asia (Mollusca: Gastropoda: Pulmonata: Onchidiidae). *Journal of Natural History* 51: 1851–1897. <https://doi.org/10.1080/00222933.2017.1347297>
- Dayrat B, Goulding TC, Khalil M, Lozouet P, Tan SH (2018) Systematic revision one clade at a time: A new genus of onchidiid slugs from the Indo-West Pacific (Gastropoda: Euthyneura: Onchidiidae). *Raffles Bulletin of Zoology* 66: 814–837.

- Dayrat B, Goulding TC, Khalil M, Apte D, Bourke AJ, Comendador J, Tan SH (2019a) A new genus and three new species of mangrove slugs from the Indo-West Pacific (Gastropoda: Euthyneura: Onchidiidae). *European Journal of Taxonomy* 500: 1–77. <https://doi.org/10.5852/ejt.2019.500>
- Dayrat B, Goulding TC, Khalil M, Comendador J, Ngô XQ, Tan SK, Tan SH (2019b) A new genus of air-breathing marine slugs from South-East Asia (Gastropoda: Pulmonata: Onchidiidae). *ZooKeys* 877: 31–80. <https://doi.org/10.3897/zookeys.877.36698.figure1>
- Folmer O, Black M, Hoeh W, Lutz R, Vrijenhoek R (1994) DNA primers for amplification of mitochondrial cytochrome c oxidase subunit I from diverse metazoan invertebrates. *Molecular Marine Biology and Biotechnology* 3: 294–299.
- Goulding TC, Khalil M, Tan SH, Dayrat B (2018a) A new genus and a new species of onchidiid slugs from eastern Indonesia (Gastropoda: Euthyneura: Onchidiidae). *Raffles Bulletin of Zoology* 66: 337–349.
- Goulding TC, Khalil M, Tan SH, Dayrat B (2018b) Integrative taxonomy of a new and highly-diverse genus of onchidiid slugs from the Coral Triangle (Gastropoda: Pulmonata: Onchidiidae). *ZooKeys* 763: 1–111. <https://doi.org/10.3897/zookeys.763.21252>
- Goulding TC, Tan SH, Tan SK, Apte D, Bhawe V, Narayana S, Salunkhe R, Dayrat B (2018c) A revision of *Peronina* Plate, 1893 (Gastropoda: Euthyneura: Onchidiidae) based on mitochondrial and nuclear DNA sequences, morphology, and natural history. *Invertebrate Systematics* 32: 803–826. <https://doi.org/10.1071/IS17094>
- Gray JE (1850) Figures of molluscos animals selected from various authors. Etched for the use of students by M. E. Gray. (Vol. 4). Longman, Brown, Green and Longmans, London, 219 pp.
- Guindon S, Gascuel O (2003) A simple, fast, and accurate algorithm to estimate large phylogenies by maximum likelihood. *Systematic Biology* 52: 696–704. <https://doi.org/10.1080/10635150390235520>
- Hassouna N, Mithot B, Bachellerie JP (1984) The complete nucleotide sequence of mouse 28S rRNA gene. Implications for the process of size increase of the large subunit rRNA in higher eukaryotes. *Nucleic Acids Research* 12: 3563–3583. <https://doi.org/10.1093/nar/12.8.3563>
- Hoffmann H (1928) Zur Kenntnis der Onchidiiden. *Zoologische Jahrbücher* 55: 29–118.
- ICZN (1993) Opinion 1747. *Bulletin of Zoological Nomenclature* 50: 256–258.
- ICZN (1999) International Code of Zoological Nomenclature (4th edn.). The International Trust for Zoological Nomenclature, London, 306 pp.
- Kumar S, Stecher G, Tamura K (2016) MEGA7: Molecular Evolutionary Genetics Analysis version 7.0 for bigger datasets. *Molecular Biology and Evolution* 33(7): 1870–1874. <https://doi.org/10.1093/molbev/msw054>
- Labbé A (1934) Les Silicodermés Labbé du Muséum d'Histoire Naturelle de Paris. Première partie: classification, formes nouvelles ou peu connues. *Annales de l'Institut Océanographique* 14: 173–246.
- Labbé A (1935) Sur une forme nouvelle de Silicoderme, *Elophilus ajuthiae* nov. Gen. nov. sp. *Bulletin de la Société Zoologique de France* 60: 312–317.
- Lesson RP (1830–1831) Voyage autour du monde, Exécuté par Ordre du Roi, sur La Corvette de Sa Majesté, La Coquille, pendant les années 1822, 1823, 1824 et 1825, sous le ministère et conformément aux Instructions de S.E.M. le Marquis de Clermont-Tonnerre, Ministre de la Marine; Et publié sous les auspices de son Excellence Mgr le Cte de Chabrol, Ministre

- de la Marine et des Colonies, par M.L.I. Duperrey, Capitaine de Frégate, Chevalier de Saint-Louis et Membre de la Légion d'Honneur, Commandant de l'Expédition. Zoologie, par M. Lesson. Tome Second. 1re Partie. Arthus Bertrand, Libraire-Editeur, Paris, 1–471. [pls 1–16] [pp 241–471 published on November 15, 1831; plates on mollusks published between January 9, 1830 and December 22, 1831; plate 14 published on November 15, 1831; see Cretella 2010] <https://doi.org/10.5962/bhl.title.57936>
- Meigen JW (1803) Versuch einer neuen Gattungs Eintheilung der europäischen zweiflügligen Insekten. *Magazin für Insektenkunde* 2: 259–281. <https://www.biodiversitylibrary.org/bibliography/69243#/summary>
- Milne I, Wright F, Rowe G, Marshal DF, Husmeier D, McGuire G (2004) TOPALi: Software for Automatic Identification of Recombinant Sequences within DNA Multiple Alignments. *Bioinformatics* 20: 1806–1807. <https://doi.org/10.1093/bioinformatics/bth155>
- Palumbi SR (1996) Nucleic acid II: The polymerase chain reaction. In: Hillis DM, Moritz C, Mable BK (Eds) *Molecular Systematics* (2 edn.). Sinauer Press Sunderland, Massachusetts Associates, Inc., 205–247.
- Plate L von (1893) Studien über opisthopneumone Lungenschnecken, II, Die Oncidiiden. *Zoologische Jahrbücher, Anatomie und Ontogenie der Thiere* 7: 93–234. [pls 7–12] <https://biodiversitylibrary.org/page/11175213>
- Quoy JRC, Gaimard JP (1824–1826) Zoologie. Voyage autour du Monde entrepris par ordre du Roi, sous le ministère et conformément aux instructions de S. Exc. M. Le Vicomte du Bouchage, secrétaire d'État au Département de la Marine, exécuté sur les corvettes de S. M. l'Uranie et la Physicienne, pendant les années 1817, 1818, 1819 et 1820; publié par M. Louis de Freycinet. Pillet Aîné, Paris, 672 pp. [pp 425–496 published in 1825; for collation, see Sherborn & Woodward 1901] <https://doi.org/10.5962/bhl.title.15862>
- Quoy JRC, Gaimard JP (1832–1833) Zoologie. Tome Second. Voyage de découvertes de l'As-trolabe exécuté par ordre du Roi, pendant les années 1826–1827–1828–1829, sous le commandement de M. J. Dumont d'Urville. J. Tastu, Paris, 686 pp. [pp 1–320 published in 1832 and pp 321–686 published in 1833; for collation, see Sherborn & Woodward 1901] <https://doi.org/10.5962/bhl.title.2132>
- Rafinesque CS (1815) *Analyse de la Nature ou tableau de l'univers et des corps organisés*. Palermo, 223 pp. <https://doi.org/10.5962/bhl.title.106607>
- Ronquist F, Huelsenbeck JP (2003) MrBayes 3: Bayesian phylogenetic inference under mixed models. *Bioinformatics* 19: 1572–1574. <https://doi.org/10.1093/bioinformatics/btg180>
- Semper C (1880–1885) Dritte Familie, Onchidiidae [for Onchidiidae]. In: Semper C (Ed.) *Reisen im Archipel der Philippinen, Zweiter Theil. Wissenschaftliche Resultate. Dritter Band. Landmollusken*. CW Kreidel's Verlag, Wiesbaden, 251–264 [1880], 265–290 [1882], [pls 19–20, 22–23 [1880], pl 21 [1882], pls 24–27 [1885]] <https://biodiversitylibrary.org/page/32630046>
- Sherborn CD, Woodward BB (1901) Notes on the dates of publication of the natural history portions of some French voyages. Part I. 'Amérique méridionale'; 'Indes orientales'; 'Pôle Sud' ('Astrolabe' and 'Zéléé'); 'La Bonite'; 'La Coquille'; and 'L'Uranie et Physicienne'. *Annals and Magazine of Natural History* 7(40): 388–392. <https://doi.org/10.1080/00222930108678490>

- Starobogatov YI (1970) Fauna Molliuskov i Zoogeograficheskoe Raionirovanie Kontinental'nykh Vodoemov Zemnogo Shara [The Molluscan Fauna and Zoogeographical Zoning of the Continental Water Bodies of the World]. Nauka, Leningrad, 372 pp. [in Russian]
- Starobogatov YI (1976) Composition and taxonomic position of marine pulmonate mollusks. Soviet Journal of Marine Biology 4: 206–212.
- Stoliczka F (1869) The malacology of Lower Bengal. Journal of the Asiatic Society of Bengal 38: 86–111.
- Sun B, Chen C, Shen H, Zhang K, Zhou N, Qian J (2014) Species diversity of Onchidiidae (Eupulmonata: Heterobranchia) on the mainland of China based on molecular data. Molluscan Research 34: 62–70. <https://doi.org/10.1080/13235818.2013.868860>
- Swofford DL (2002) PAUP: Phylogenetic Analysis Using Parsimony, Version 4.0b10. Sinauer, Sunderland.
- Tapparone-Canefri C (1889) Viaggio di Leonardo Fea in Birmanica e Regioni vicini; XVIII Molluschi terrestri e d'acqua dolce. Annali del Museo Civico di Storia Naturale, Genova 27: 295–359. <https://www.biodiversitylibrary.org/bibliography/7929#/summary>
- Vonnemann V, Schrödl M, Klussmann-Kolb A, Wägele H (2005) Reconstruction of the phylogeny of the Opisthobranchia (Mollusca: Gastropoda) by means of 18S and 28S rRNA gene sequences. Journal of Molluscan Studies 71: 113–125. <https://doi.org/10.1093/mollus/eyi014>
- Wade CM, Mordan PB (2000) Evolution within the gastropod molluscs; using the ribosomal RNA gene-cluster as an indicator of phylogenetic relationships. Journal of Molluscan Studies 66: 565–570. <https://doi.org/10.1093/mollus/66.4.565>
- Wang D, Xu G, Qian J, Shen H, Zhang K, Guan J (2018) A morphological description of *Onchidium reevesii* (Gastropoda: Eupulmonata: Systellommatophora). Molluscan Research 38: 218–225. <https://doi.org/10.1080/13235818.2018.1428780>
- Westerlund CA (1883) Noch einige von der Vega-Expedition gesammelte Mollusken. Nachrichtenblatt der deutschen malakozoologischen Gesellschaft 15: 164–166. <https://biodiversitylibrary.org/page/31121809>
- Westerlund CA (1885) Land- och sötvatten-mollusker insamlade under Vega-Expeditionen. Vega-Expeditionens Vetenskapliga Iakttagelser 4: 191–192. [pl 4]

A new species of *Gordius* (Phylum Nematomorpha) from terrestrial habitats in North America

Christina Anaya¹, Andreas Schmidt-Rhaesa², Ben Hanelt³, Matthew G. Bolek¹

1 Department of Integrative Biology, 501 Life Sciences West, Oklahoma State University, Stillwater, Oklahoma 74078, USA **2** Zoological Museum and Institute, Biocenter Grindel, Martin-Luther-King-Platz 3, University of Hamburg, 20146 Hamburg, Germany **3** Center for Evolutionary and Theoretical Immunology, Department of Biology, 163 Castetter Hall, University of New Mexico, Albuquerque, New Mexico 87131-0001, USA

Corresponding author: Christina Anaya (christina.anaya@okstate.edu)

Academic editor: Y. Mutafchiev | Received 6 August 2019 | Accepted 21 October 2019 | Published 27 November 2019

<http://zoobank.org/43ADAED6-F21A-45F1-BE8A-B30C4211CDA6>

Citation: Anaya C, Schmidt-Rhaesa A, Hanelt B, Bolek MG (2019) A new species of *Gordius* (Phylum Nematomorpha) from terrestrial habitats in North America. ZooKeys 892: 59–75. <https://doi.org/10.3897/zookeys.892.38868>

Abstract

Freshwater hairworms (class Gordiida) are members of the phylum Nematomorpha that use terrestrial arthropods as definitive hosts but reside as free-living adult worms in rivers, lakes, or streams. The genus *Gordius* consists of 90 described species, of which three species were described from freshwater habitats in North America. In this paper we describe a new species of *Gordius* from terrestrial habitats in Oklahoma, Texas, and Louisiana, United States. Oddly, each year hundreds of adult free-living worms appear after bouts of heavy rain on streets, sidewalks, and lawns during the winter season, when terrestrial arthropod hosts are not active. The new species is described based on morphological characters of adults and non-adult stages including the egg strings, eggs, larvae, and cysts. Adult males have a unique row of bristles on the ventral inner side of each tail lobe and a circular pattern of bristles on the terminal end of each lobe, which distinguishes them from all other described North American species of *Gordius*. The egg string, larval, and cyst morphology of this new species conform to previous descriptions of non-adult hairworm stages for the genus *Gordius*. However, the eggs of this new species of hairworm are unique, as they contain an outer shell separated by distinct space from a thick inner membrane. The consistent occurrence of this gordiid in terrestrial habitats, along with its distinct egg morphology, suggests that this new species of hairworm has a terrestrial life cycle.

Keywords

eggs, Gordiida, hairworm, life cycles, North America, Oklahoma, soil

Introduction

The Phylum Nematomorpha, commonly known as hairworms or Gordian worms, or simply gordiids, are parasites of terrestrial arthropods with a complex life cycle that includes a free-living and parasitic phase with multiple hosts (Carvalho 1942; Townsend 1970; Blair 1983; Poinar and Brockerhoff 2001; Hanelt et al. 2005). However, their short lifespan, cryptic coloration, and hiding behavior makes hairworms difficult to collect for biodiversity studies (May 1919; Hanelt et al. 2015). An analysis of all known life cycles indicates that juvenile gordiids infect terrestrial arthropods from which free-living adults emerge into freshwater habitats, such as streams, rivers, and lakes (May 1919; Hanelt et al. 2005; Bolek et al. 2015). After emerging from their arthropod host, dioecious species mate and females deposit egg strings in aquatic habitats (Bolek et al. 2013). Within weeks, larvae develop, hatch, infect, and encyst indiscriminately within a variety of aquatic vertebrate and invertebrate animals (Hanelt and Janovy 2003). Some of these infected animals, such as aquatic insect larvae, act as paratenic (transport) hosts by carrying cysts to land where they are consumed by omnivorous or predatory definitive hosts including millipedes, crickets, beetles, cockroaches, and mantids (Bolek et al. 2015).

Although first described more than 300 years ago, gordiids have been identified as one of the most understudied groups of parasites (Poulin 1998). Currently, it is hypothesized that only 18% of the estimated 2000 gordiid species have been described (Bolek et al. 2015). Because of their life cycle that includes an aquatic environment where worms emerge as free-living adults from their arthropod host, sampling for hairworms and discovering their true biodiversity has been challenging (Hanelt et al. 2005). However, during the last 15 years, advances in sampling, culturing, and barcoding techniques for gordiids have resulted in the descriptions of more than 50 new species including a parthenogenetic species (Bolek et al. 2010; Schmidt-Rhaesa and Prous 2010; Hanelt et al. 2012; Bolek et al. 2013a; Chiu et al. 2017; Swanteson-Franz et al. 2018).

At present, approximately 360 gordiid species have been described from across the world within 18 extant and two extinct genera (Schmidt-Rhaesa 2013; Bolek et al. 2015; Yadav et al. 2018). Of those, the genus *Gordius* Linnaeus, 1758 is the second largest in terms of described species, with 90 valid species distributed across the world (Schmidt-Rhaesa 2010, 2013). The diagnostic characters for the genus *Gordius* are based on male characteristics and include a semicircular or parabolic cuticular fold posterior of the cloacal opening, known as the postcloacal crescent, and a bilobed posterior end with rounded posterior tips. The posterior end of females is rounded, with a terminal cloacal opening. The anterior end is distinctly tapering, with a white tip, known as a calotte, followed by a brown or black collar usually present in both sexes of most species. Additionally, various combinations of a dark ventral and/or dorsal line, and/or white spots on the cuticle are often present on free-living male and/or female worms of several species (Schmidt-Rhaesa 2010). However, compared to other gordiid genera, the genus *Gordius* contains few cuticular structures, such as areoles, that demonstrate intraspecific and interspecific variability making species identification difficult (Schmidt-Rhaesa 2013).

The majority of *Gordius* diversity has been identified from the palearctic region which harbors 71% of *Gordius* diversity with the remaining 29% distributed throughout the world with the exception of Antarctica (Schmidt-Rhaesa 2010). Currently three valid species of *Gordius* have been described from the Nearctic region representing 4% of *Gordius* species. These include *Gordius attoni* Redlich, 1980, *Gordius difficilis* Smith, 1994, and *Gordius robustus* Leidy, 1851 (Schmidt-Rhaesa et al. 2003; Schmidt-Rhaesa 2010, 2013; Schmidt-Rhaesa et al. 2016). Of those, *G. robustus* is one of the most commonly reported and widely distributed hairworm species in North America (Schmidt-Rhaesa et al. 2003; Schmidt-Rhaesa 2010). However, recent sampling efforts across North America for *G. robustus*, combined with molecular data indicate that *G. robustus* is a complex of at least eight distinct species (Hanelt et al. 2015).

Based on genetic data, one of the eight species, identified as clade 7 by Hanelt et al. (2015), occurs in Oklahoma, Texas, and Louisiana. In this article, we describe free-living adults of this new species of *Gordius* collected from locations in Oklahoma, Texas, and Louisiana using light and scanning electron microscopy. In addition, we describe the non-adult life stages, including the egg strings, eggs, larvae and cysts. Finally, based on morphological characteristics of non-adult stages, and the occurrence of adult free-living worms of this new species in terrestrial habitats, we provide evidence and suggest that this new species of gordiid has a terrestrial life cycle.

Materials and methods

Field collections

A total of 39 female and 194 male free-living hairworms were collected from two suburban locations in the city of Stillwater, OK, USA (36.12091, -97.03669; 36.13653, -97.04266). All free-living worms were collected after bouts of heavy rain from streets, sidewalks, or lawns between November-December 2014 and January-March 2015. In addition, each location was searched for potential definitive arthropod hosts by visually scanning the locations when worms were present. All specimens were placed in 950 ml glass jars containing aged tap water and transported to the laboratory at Oklahoma State University. A subsample of adult worms was processed for morphological characters; whereas the remaining worms were allowed to mate to obtain non-adult life stages (see below). Additionally, two male specimens from a single location in Montgomery, Texas (30.38988, -95.69552) and one male from Baton Rouge, Louisiana (30.40661, -91.18734) were collected by citizen scientists and sent to us as per the instructions on our website (www.nematomorpha.net) and its Report-A-Worm feature.

Biological material and microscopy

Adults. Length, width, color, and color pattern (presence of a calotte, dark pigmented ring, and spots on the cuticle) were recorded for all male and female individuals col-

lected from Stillwater, OK. Lengths of worms were obtained by placing individuals on a ruler without stretching the specimen and measured to the nearest 1 mm. The width of each worm was obtained using an Olympus SZ1145 Stereomicroscope and a calibrated ocular micrometer. Posterior ends of males were then photographed with a Sony Cybershot camera and the angle of postcloacal crescent was measured using ImageJ software (Schneider et al. 2012).

For scanning electron microscopy (SEM), four female and six male worms collected from Oklahoma and two males collected from Texas were imaged as described by Harkins et al. (2016). Briefly, live worms were preserved in 70% ethanol at room temperature and 5–10 mm sections of the anterior, posterior, and mid-body regions of each worm were cut with a razorblade. Specimens were then dehydrated in increasing concentrations of ethanol (70 %, 85 %, 95 %, 100 %), dried using hexamethyldisilazane (HDMS) according to Harkins et al. 2016, mounted on aluminum stubs, sputter coated with gold palladium, and examined with an FEI Quanta 600 field emission gun ESEM (ThermoFisher Scientific, Hillsboro, OR) with Exev EDS and HKL EBSD or a JEOL 5800LV SEM at 15 kV (JEOL Ltd., Tokyo, Japan). All terminology for adult worms follows Schmidt-Rhaesa (2010).

Obtaining non-adult stages. A subset of single male and female worms from Stillwater, OK were paired and placed in 110 × 35 mm Stender dishes filled with filtered and aged tap-water (Szymgiel et al. 2014). Observations were made daily on the mating and oviposition behavior of worms. After males deposited a sperm drop on the posterior end of females, females were isolated and allowed to deposit egg strings in individual Stender dishes filled with aged tap-water. Egg strings were rinsed in a solution of 1-part 5.25 % chlorine bleach to 250-parts water to prevent fungal growth and visually observed over a period of 2–5 weeks for larval maturation, indicated by a color change in egg strings from white to yellow in color. After hatching a subset of larvae was pipetted into 0.2 mL microtubes and stored at -80 °C for snail infections according to Bolek et al. (2013b). To obtain cysts, *Physa acuta* (Draparnaud, 1805) snails were reared in the laboratory according to Szymgiel et al. (2014). A subset of hatched larvae was thawed, collected with a Pasteur pipette and approximately 100–200 larvae were pipetted into 48, 1.5 ml well-plates filled with 1 mm of aged tap water. A single laboratory reared *Physa acuta* snail was then added to each well. Snails fed on the larvae mixture for 48 hours and snails were then maintained in 3.75 L jars filled with aerated aged tap water and fed on a diet of frozen lettuce and Tetra Min fish food for a period of four weeks. To evaluate cyst development, every week for a period of four weeks post infection (WPI), a subsample of snails was placed in labeled and capped 50 ml plastic centrifuged tubes, filled with approximately 35 ml of aged tap water, and frozen at -80 °C following the protocol of Bolek et al. (2013b). The gastropod nomenclature is according to Wethington and Lydeard (2007).

Morphology of egg strings, eggs, and larvae. Photographs were taken of two-day old egg strings in Stender dishes and a plastic ruler as a reference using a Sony Cybershot camera and the length and width of 20 egg strings was measured using ImageJ software. Individual developed eggs, and two-day old larvae after hatching were prepared as live wet mounts and observed using an Olympus BX–51 upright research

microscope (Olympus, Tokyo, Japan) configured for bright field and Nomarski differential interference contrast (DIC) microscopy with plain fluorite objectives at 400× to 1000× total magnification. Measurements of developed eggs with larvae were taken from captured digital images using an Olympus 5-megapixel digital camera and ImageJ software. Briefly, for developed eggs, 5 mm sections of egg strings were placed on microscope slides in a drop of water, covered with a coverslip without crushing, and observed for general morphology with an Olympus BX-51 upright research microscope and the length and width was recorded for 30 eggs. For larvae, the length and width of the preseptum, postseptum, pseudointestine, and stylets was measured for 30 individuals following the protocols of Szymgiel et al. (2014).

Morphology of cysts. Laboratory infected and post frozen snails were processed for gordiid cysts following Harkins et al. (2016). Briefly, all frozen snails were thawed, each snail's body was removed from its shell using a dissection microscope with forceps and pressed between two slides (Harkins et al. 2016). A wet mount was prepared by removing the top slide and adding a drop of water and covering the flattened tissue with a coverslip. Slides were then examined with an Olympus BX-51 microscope as described for eggs and larvae. Thirty cysts were digitally photographed at 1000× total magnification and the length and width of the cyst, cyst wall and encysted larvae were obtained using ImageJ software. Finally, the folding pattern of all encysted larvae was recorded. Procedures and terminology for cyst stages of gordiids follows Hanelt and Janovy (2002), Szymgiel et al. (2014) and Harkins et al. (2016).

Larval preparation for SEM and larval characters. Pieces of egg strings with developed larvae and hatched larvae suspended in water, were pipetted onto Poly-L-Lysine coated coverslips placed in 1.5 ml plastic well plates and fixed in a solution of alcohol, formalin, and acetic acid. Fixed larvae were dehydrated in a graded series of ethanol in each plastic well with 0.5 ml of 30 %, 50 % and 70 % ethanol for 30 min each, followed by dripping 1 ml of 100% ethanol into the well over a period of an hour, 1 ml of ethanol was then removed from the well and the process repeated three additional times (Harkins et al. 2016). Finally, specimens were dried using HDMS, mounted on aluminum stubs, coated with gold palladium, and examined with an FEI Quanta 600 field emission gun ESEM with Evex EDS and HKL EBSD housed at Oklahoma State University. The following morphological surface characteristics were recorded for at least 30 individual larvae: number of terminal spines on the postseptum, the number and relative size of cuticular hooks on the preseptum, the proboscis orientation (dorso-ventrally or laterally compressed) and the number and orientation of spines on the proboscis. External morphological characteristics for larvae examined with SEM followed terminology by Szymgiel et al. (2014). All measurements are reported as a mean \pm 1 standard deviation followed by the range.

Egg morphology of aquatic gordiids. To compare the egg morphology of the new species to eggs of aquatic gordiids, we examined egg photomicrographs from our personal collections for three species/genera of aquatic hairworms. All species examined were collected from streams as free-living adults or cysts that were reared in crickets in the laboratory. These included *Gordius difficilis* from Waukesha County, Wisconsin, USA (42.966229, -88.364328), *Neochordodes occidentalis* Montgomery, 1898 from Pima

County, Arizona, USA (31.8655, -109.1905) and *Paragordius obamai* Hanelt, Bolek, and Schmidt-Rhaesa 2012 from Nyanza province, Kenya (-0.1519, 34.4455). Information on how eggs were obtained and processed is reported in Bolek and Coggins (2002), Hanelt et al. (2012) and Szmygiel et al. (2014). Briefly, pieces of egg strings of each hair-worm species were placed on a microscope slide with a drop of water and covered with a cover slip. Most eggs were examined using DIC microscopy. However, some eggs were examined with bright field microscopy and in this case, a drop of Nile Blue was added to the wet mount to visualize the inner egg content.

Taxonomy

Gordius terrestris sp. nov.

<http://zoobank.org/6A529B7C-147D-450D-B3AA-D3A4E82305AC>

Type locality. A suburban lawn in the City of Stillwater, Payne County, Oklahoma; USA (36.12091, -97.03669; approximate altitude: 276–296 m).

Holotype. Male collected on 5 December 2014. Deposited in the Museum of Southwestern Biology (MSB) Parasite Division, University of New Mexico (UNM), New Mexico, USA with accession number MSB:Para:29147.

Paratypes. Female specimen collected on 5 December 2014, from the type locality. Deposited into the MSB Parasite Division, accession number MSB:Para:29148. Paratypes: two males collected 14 January 2003 in Montgomery, Texas (30.38988, -95.69552). Deposited into the MSB Parasite Division, accession numbers MSB:Para:19257 and MSB:Para:19258.

Other material deposited. Larvae and egg strings with hatching larvae on SEM stubs obtained from laboratory cultures from Oklahoma collected worms. Deposited into the Museum of Southwestern Biology (MSB) Parasite Division, University of New Mexico (UNM), New Mexico, USA with accession number MSB:Para:29149.

Host. Natural definitive host is unknown, and no arthropod hosts were found during times when adult free-living worms were present.

Etymology. The new species is named after the terrestrial habitat from which all adult free-living individuals were collected.

Distribution. Stillwater, Oklahoma (36.12091, -97.03669; 36.13653, -97.04266), Montgomery, Texas (30.38988, -95.69552) and Baton Rouge, Louisiana (30.40661, -91.18734).

Link to molecular data. GenBank accession numbers for mitochondrial (CO1 and cytb) and ribosomal (partial 28S, ITS1, 5.8S and ITS2) DNA sequences for the Louisiana (KM382307; KM382349; KM382400), Oklahoma (KM382308 and KM382309; KM382350) and Texas (KM382351; KM382401 and KM382402; KM382403 and KM382310; KM382352; KM382404) samples of *G. terrestris* sp. nov. were published in Hanelt et al. (2015) but are provided in this description for consistency.

Material examined. Adults ($N = 233$), eggs, larvae, and cysts. Eight adult males, six from Oklahoma and two from Texas, and four adult females from Oklahoma were

imaged using SEM; and other male and female individuals were examined using DIC and bright field microscopy for color pattern. Additionally, egg, larvae, and cyst stages were imaged using SEM and/or DIC microscopy.

Description of male. Adult free-living males were creamy white to dark brown in color and contained distinct white spots throughout the length of the body (Fig. 1D). A dark dorsal and ventral medial line was present along the length of the cuticle being most distinct in the mid-body region (Fig. 1D). Males were 258 ± 73 (122–470; $N = 194$) mm in length and 0.6 ± 0.1 (0.4–0.9) mm in width. The anterior end was tapered and contained a white calotte followed by a dark collar (Fig. 1A, B). The cuticle was variable among individuals but contained one type of areole distributed on the anterior, midbody, and/or posterior regions of the body with various bristles distributed among the areoles (Figs 1C, F, I; 2E–G). Areoles were weakly developed, polygonal in shape, and 9–12 μm in diameter (Figs 1C, F, I; 2E–G). The posterior end of males contained two terminal tail lobes which were 0.50 ± 0.1 (0.4–0.7) mm long and 0.2 ± 0.04 (0.17–0.3 mm) wide (Figs 1G, H; 2A–D). Each tail lobe contained a distinct row of bristles on the ventral inner side and distinct bristles distributed in a circular pattern on the terminal ends of each lobe (Fig. 2D). Additionally, the inner side of the lobes were darkly pigmented compared to the lighter creamy white color of each lobe (Fig. 1G). The cloacal opening was round and situated ventrally in a broad nonareolar field above the postcloacal crescent (Figs 1G, H; 2B, C). The postcloacal crescent was situated between the proximal ends of the two tail lobes and was dark brown in color (Fig. 1G) and had an angle of $111 \pm 9^\circ$ (102–126°) (see Figs 1G, H; 2B–D).

Description of female. Adult free-living females were creamy white to dark brown, and contained dark dorsal and ventral lines along the length of the body. Females were 246 ± 41 (211–336; $N = 39$) mm long by 1.0 ± 0.1 (0.7–1.3) mm wide. The anterior end was tapered and contained a white calotte followed by a dark collar (Fig. 3A, B). Areoles were weakly developed, polygonal in shape, and 11–13 μm in diameter with branching bristles being scattered across the cuticle (Fig. 3C, F, I). The posterior end of females was round and cylindrical in shape and darkly pigmented on the terminal end (Fig. 3G, H). The cloaca was round in shape and located on the terminal end.

Description of mating, oviposition, egg strings, and eggs. When placed together, male and female worms immediately formed Gordian knots. Males moved up and down the female's body with their coiled posterior end. Once the male's bifurcated tail was in proximity of the female's cloaca, the male deposited a mass of sperm on the female's posterior end. Egg strings were deposited within 7–30 days after copulation. Newly deposited egg strings were white in color and deposited in a continuous string that broke as it emerged from the female's cloaca into short segments (Fig. 4A). Deposited egg strings were 7 ± 4 (2–19) mm in length and 1.2 ± 0.3 (0.8–1.9) mm in width. Over two to three weeks the white eggs strings darkened to a tan color and contained fully developed larvae within eggs (Fig. 4C, D). Developed eggs were tightly aggregated together within egg strings and spherical to elliptical in shape (Fig. 4B, C). Eggs were 55 ± 7 (42–72) μm long by 55 ± 7 (43–68) μm wide. Each egg contained an outer shell separated by distinct space from a thick inner membrane (Fig. 4B–D). The distinct inner membrane was 38 ± 3 (29–42) μm long by 39 ± 4 (30–45) μm wide.

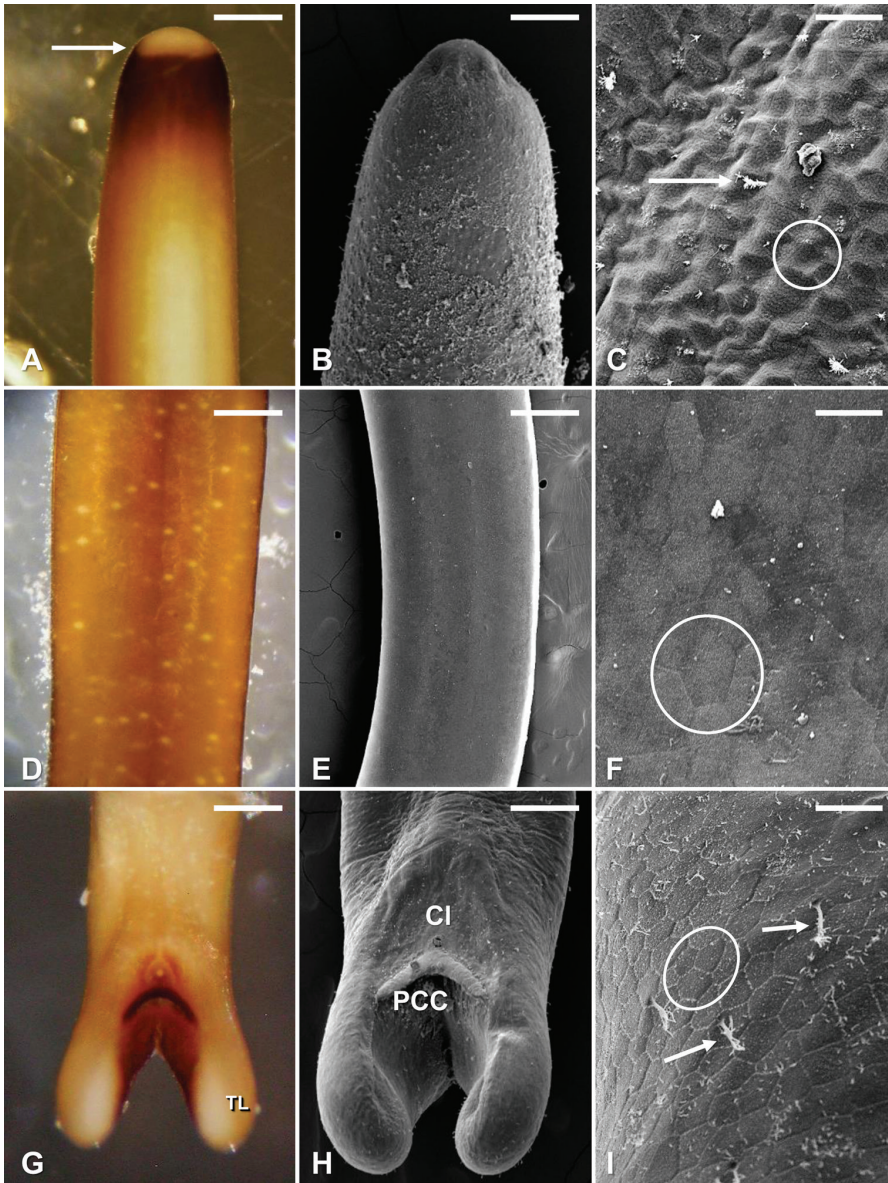


Figure 1. *Gordius terrestris* sp. nov., adult male from Stillwater, Oklahoma, light (**A, D, G**) and SEM (**B, C, E, F, H, I**) photomicrographs **A** anterior body region showing typical color pattern, showing the distinct calotte (arrow) and dark ring **B** anterior end, dorsal view **C** areole pattern on the anterior body region. Note the weakly developed areoles (circle) and the presence of bristles (arrows) **D** midbody region, dorsal view, showing distinct white spots and medial line **E** Midbody region, dorsal view, showing typical cuticular pattern **F** areole pattern on the midbody region; note the weakly developed polygonal shaped areoles (circle) **G** posterior body region, ventral view, showing distinct coloration; note the darkly pigmented postcloacal crescent and dark pigmentation on inner sides of the tale lobes (TL) **H** ventral view of the posterior region, showing the cloaca (Cl) and postcloacal crescent (PCC) **I** areole pattern on the posterior body region; note the weakly developed polygonal shaped areoles (circle) and the bristles (arrows). Scale bars: 210 μm (**A**); 130 μm (**B**); 18 μm (**C**); 220 μm (**D, G**); 290 μm (**E**); 10 μm (**F**); 175 μm (**H**); 20 μm (**I**).

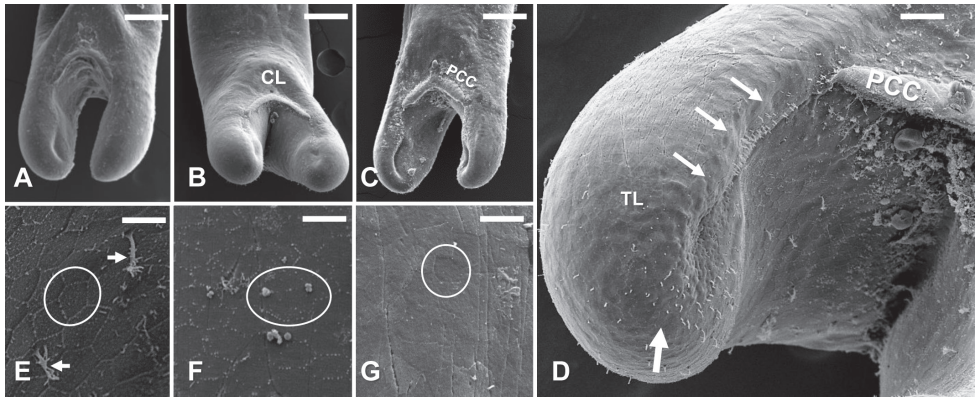


Figure 2. *Gordius terrestris* sp. nov., adult males from Stillwater, Oklahoma, SEM photomicrographs **A–C** posterior body region, ventral view, note the variation in the shape of tail lobes and postcloacal crescents (PCC) below the cloaca (CL) **D** tail lobe showing the distinct row of bristles beginning below the postcloacal crescent (PCC) and progressing on the ventral inner side (small arrows) of the tail lobe (TL); and bristles distributed in a circular pattern on the terminal end (large arrow) of the tail lobe **E–G** variation in the weakly developed polygonal shaped areoles (circles) on the posterior body region of different male individuals; note the branching bristles (arrows) in **E**. Scale bars: 175 μm (**A–C**); 75 μm (**D**); 8 μm (**E–G**).

Description of larvae. Larvae of *G. terrestris* sp. nov. possessed a cylindrical body divided by a septum into two regions, the preseptum and a postseptum (Fig. 5A, B). The preseptum was 30 ± 6 (22–40) μm in length and 20 ± 2 (16–26) μm in width and contained an eversible proboscis supported with three internal stylets which were 17 ± 4 (10–25) μm in length and 5 ± 1.3 (2–8) μm in width (Fig. 5B). The postseptum was 106 ± 12 (76–127) μm in length and 20 ± 18 (15–23) μm in width and contained a clearly visible pseudointestine. The pseudointestine was an elongated oval structure, subdivided into two portions (Fig. 5A). The pseudointestine was 80 ± 10 (57–104) μm in length and 12 ± 2 (10–17) μm in width.

Externally, larvae were superficially annulated with a single spine located on the posterior region of the postseptum (Fig. 5C). The preseptum had three sets of cuticular hooks (Fig. 5D). The outer ring of hooks contained seven hooks, two of which were fused proximally and located on the ventral side (Fig. 5D). The middle and inner rings contained six hooks each (Fig. 5D). The eversible proboscis contained three pairs of spines and one terminal spine on the distal end of the left lateral, right lateral and dorsal sides (Fig. 5E, F).

Cyst development and morphology. After being ingested by snails, larvae develop into cysts and became distributed throughout the snail tissues. During cyst formation the content of the larval pseudointestine was emptied and larvae folded their postseptum twice around the preseptum (Fig. 6D–F). The posterior end of the postseptum always reached the posterior end of the preseptum and protruding spines were never visible on the anterior end of fully formed cysts (Fig. 6A, B). Fully formed cysts of *G. terrestris* sp. nov. were observed in laboratory exposed snails 2–3 WPI and possessed a clear cyst wall of unknown composition with a distinct inner layer surrounding the

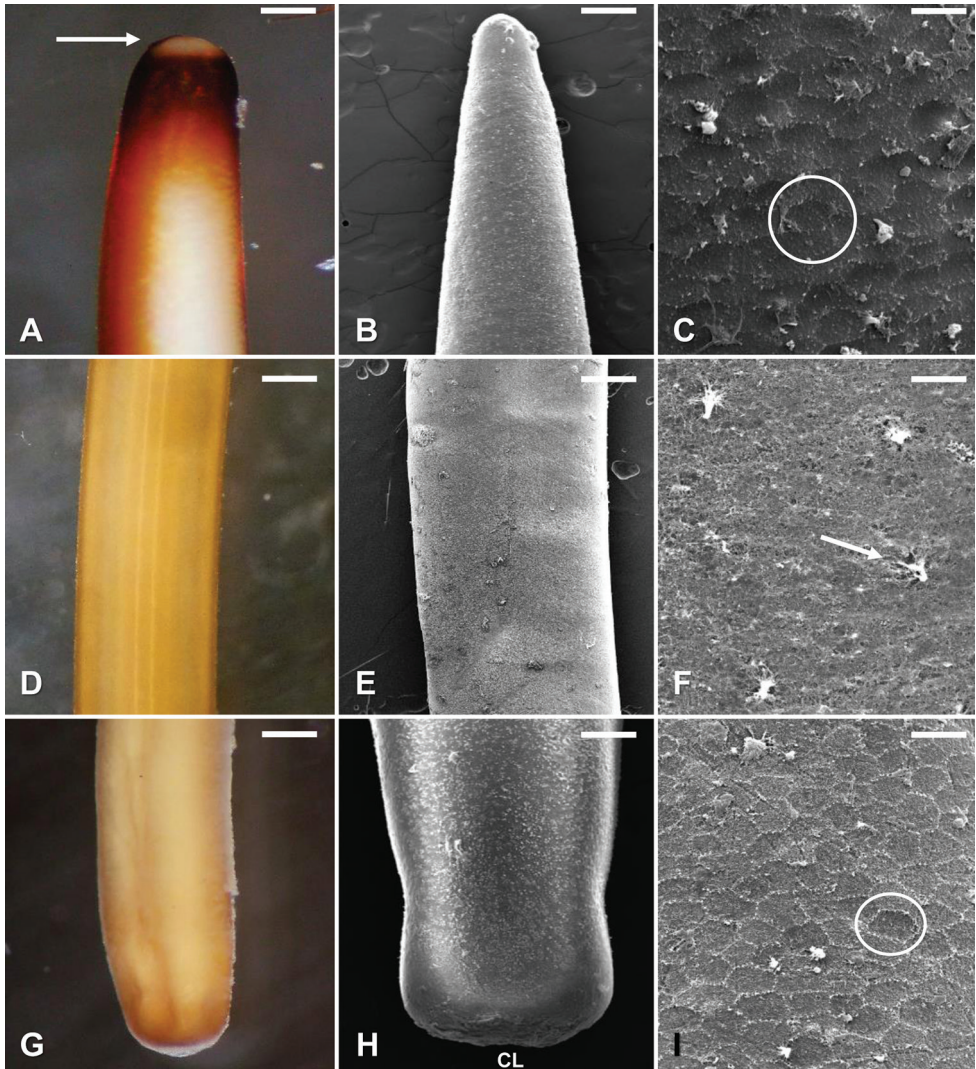


Figure 3. *Gordius terrestris* sp. nov., adult females from Stillwater, Oklahoma, light (**A, D, G**) and SEM (**B, C, E, F, H, I**) photomicrographs **A** anterior body region showing typical color pattern, showing the distinct calotte (arrow) followed by a dark ring **B** anterior end, dorsal view **C** areole pattern on the anterior body region; note the weakly developed polygonal shaped areoles (circle) **D** midbody region, lateral view, showing typical color pattern **E** midbody region, dorsal view showing typical cuticular pattern **F** midbody region, dorsal view, showing finer details of the cuticle; note the branching bristles (arrow) **G** posterior body region, ventral view, showing typical coloration **H** posterior body region, ventral view showing the location of the cloaca (CL) **I** posterior body region, areole pattern on the posterior body region; note the weakly developed polygonal shaped areoles (circle). Scale bars: 160 μm (**A**); 150 μm (**B**); 10 μm (**C**); 440 μm (**D, G**); 330 μm (**E**); 15 μm (**F, I**); 190 μm (**H**).

folded larva (Fig. 6A, B). Cysts were 102 ± 16.7 (68–131) μm in total length and 101 ± 13 (72–140) μm in total width (Fig. 6B). Folded larvae inside of the cyst were 29 ± 7 (17–39) μm in length and 31 ± 5 (18–43) μm in width.

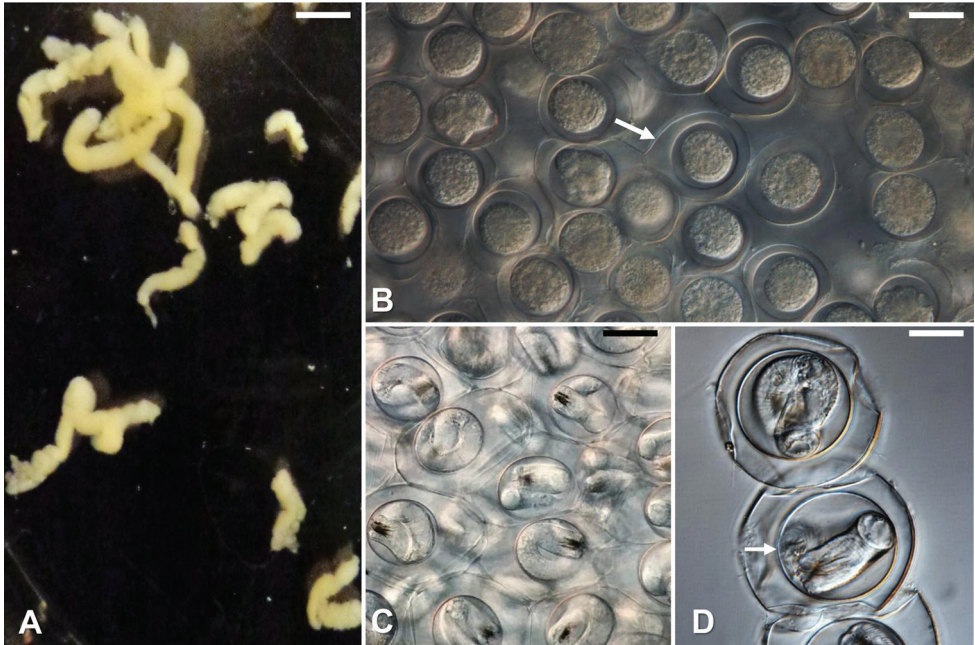


Figure 4. *Gordius terrestris* sp. nov., eggs and egg strings, light photomicrographs **A** newly deposited egg strings **B** egg string segment showing tightly aggregated undeveloped eggs; note the eggshell (arrow) **C** segment of an egg string showing developing larvae within eggs **D** eggs with fully developed larvae; note the distinct space between the eggshell and the thick inner membrane. Scale bars: 4 mm (**A**); 40 µm (**B**); 25 µm (**C**); 20 µm (**D**).

Diagnosis and taxonomic comments. *Gordius terrestris* sp. nov. has unique morphological features which warrant placing it as a new species and make it distinct from the other three described Nearctic species of *Gordius*. *Gordius terrestris* sp. nov. differs morphologically from *G. difficilis* by lacking distinct pre-cloacal bristles which are present in males of *G. difficilis* (Bolek and Coggins 2002). Additionally, *G. terrestris* sp. nov. has distinct polygonal areoles and therefore differs morphologically from the description of *G. robustus* which has a smooth cuticle (Schmidt-Rhaesa et al. 2003). Although, *G. attoni* and *G. terrestris* sp. nov. both have polygonal shaped areoles and distinct white spots on the cuticle of males, *G. attoni* areoles contain microscopic processes which are absent on the areoles of *G. terrestris* sp. nov. (Redlich 1980; Schmidt-Rhaesa et al. 2003). In addition, male *G. terrestris* sp. nov. contain an aggregation of bristles on the ventral inner side of each tale lobe posterior of the postcloacal crescent and distinct bristles distributed in a circular pattern on the terminal ends of each lobe, which are not present in male *G. attoni*, *G. difficilis* or *G. robustus* (Redlich 1980; Smith 1994; Bolek and Coggins 2002; Schmidt-Rhaesa et al. 2003; Schmidt-Rhaesa 2010). Finally, published molecular data by our group on *G. terrestris* sp. nov., *G. attoni* and seven other undescribed species of *Gordius* collected across the United States and one undescribed species from Mexico, indicate that *G. terrestris* sp. nov. (described as clade 7) is genetically distinct from all other *Gordius* species for which genetic data

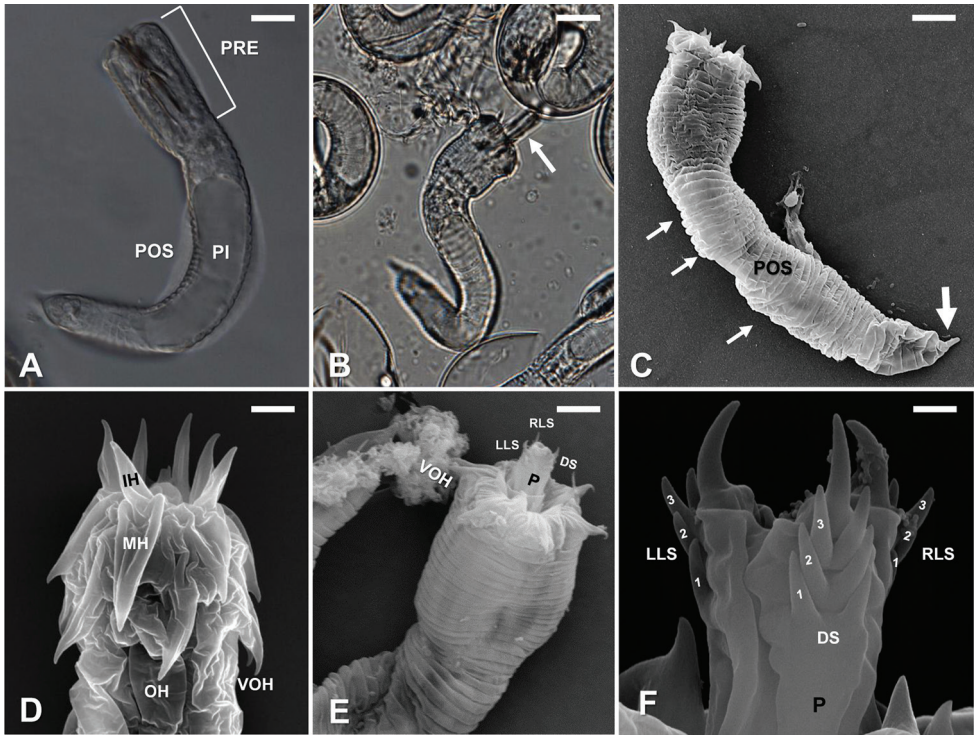


Figure 5. *Gordius terrestris* sp. nov., larvae, light (**A**, **B**) and SEM (**C**–**F**) photomicrographs **A** live larva, showing the preseptum (PRE), postseptum (POS) and pseudointestine (PI) **B** recently hatched larvae showing everted proboscis (arrow) **C** larva note the superficial annulations (small arrows) and a single terminal spine located (large arrow) on the posterior region of the postseptum (POS) **D** preseptum, showing the arrangement of three sets of cuticular hooks, including outer hooks (OH), middle hooks (MH) and inner hooks (IH); and fused ventral outer hooks (VOH) **E** anterior end with the eversible proboscis (P); note the distinct spines on the distal end of the left lateral side (LLS), right lateral side (RLS) and dorsal side (DS) in respect to the ventral outer hooks (VOH) **F** partially everted proboscis (P) showing pairs of small spines (numbers) and a larger terminal spine on the distal end of the left lateral (LLS), right lateral (RLS) and dorsal sides (DS). Scale bars: 12 μm (**A**); 13 μm (**B**); 8 μm (**C**); 2.5 μm (**D**); 6 μm (**E**) 0.8 μm (**F**).

are available (Hanelt et al. 2015). Mitochondrial CO1 genetic distances indicate that *G. terrestris* sp. nov. differs by 8–21 % in the CO1 genetic distance from the other seven undescribed species of *Gordius* from the United States and one from Mexico and by 17% from *G. attoni*, but only differs by 1.5 % within individuals collected from Oklahoma, Texas, and Louisiana (Hanelt et al. 2015).

Although, the distribution of the cuticular bristles on tail lobes of male *G. terrestris* sp. nov. distinguish it from all other described North American species of *Gordius*, several European species including *Gordius helveticus* Schmidt-Rhaesa, 2010, *Gordius karwendeli* Schmidt-Rhaesa, 2010, *Gordius spiridonovi* Spiridonovi, 1984, *Gordius terminosetosus* Schmidt-Rhaesa, 2010, and *Gordius zwicki* Schmidt-Rhaesa, 2010 also contain cuticular bristles on tail lobes (Schmidt-Rhaesa 2010; Schmidt-Rhaesa and Prous 2010). Of those, the distribution pattern of cuticular bristles on tail lobes of male *G. terrestris* sp. nov. is

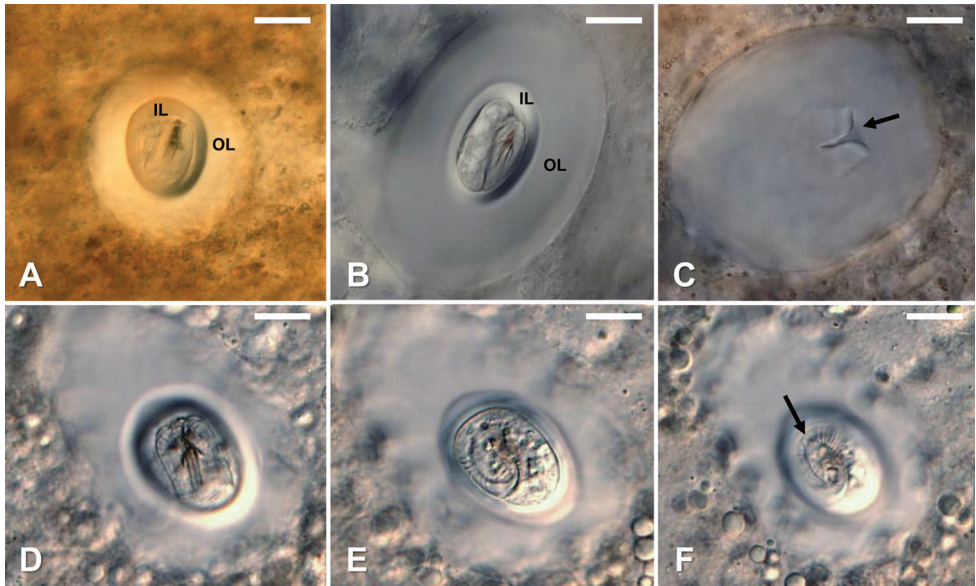


Figure 6. *Gordius terrestris* sp. nov., cysts, light photomicrographs **A–B** fully formed cysts in experimentally infected *Physa acuta* snails; note the folded larva surrounded by a clear cyst wall of unknown composition with a distinct inner layer (IL) and outer layer (OL) **C** remaining cyst wall after the folded larvae was extruded under coverslip pressure. Note the opening where the larvae emerged (arrow) **D–F** different focal planes showing the distinct larvae folding pattern; note the location of the terminal spine (arrow) in F and that the larva folds twice within the fully formed cyst. Scale bars: 20 μm (**A–F**).

most similar to *G. helveticus*. However, *G. helveticus* lacks well-defined areoles and therefore can be easily distinguished from *G. terrestris* sp. nov. (Schmidt-Rhaesa 2010).

The general morphology of the egg string, larvae, and larval folding pattern within the cysts of *G. terrestris* sp. nov. conform to previous descriptions of these non-adult stages for the genus *Gordius*. However, these non-adult stages are morphologically distinct from egg strings, larvae, and cysts of other gordiid genera such as *Chordodes*, *Neochordodes* and *Paragordius* (Szymgiel et al. 2014; Swantesson-Franz et al. 2018). Although the larval morphology conformed to the typical *Gordius* larval type, the three pairs of left, right, and dorsal spines on the distal end of the proboscis differed from the only other SEM imaged proboscis of an undescribed species of *Gordius* cf. *robustus* collected from streams in New Mexico (clade 3 in Hanelt et al. 2015). Szymgiel et al. (2014) reported that the right and left lateral sides of the proboscis of the New Mexico *G.* cf. *robustus* contained four pairs of spines; whereas the dorsal side contained three pairs of spines, all arranged in tandem. Finally, the egg morphology of *G. terrestris* sp. nov. was unlike egg descriptions for any other hairworm species (Schmidt-Rhaesa 1997a; Adrianov et al. 1998; Marchiori et al. 2009; Szymgiel et al. 2014; Bolek et al. 2015). Eggs of *G. terrestris* sp. nov. contained an outer shell separated by distinct space from a thick inner membrane. Our evaluation of eggs of three aquatic species of Gordiids (*G. difficilis*, *N. occidentalis*, and *P. obamai*) indicate that their eggs are elliptical in shape, with a distinct shell and a thin inner membrane surrounding the developing larva (Fig. 7).

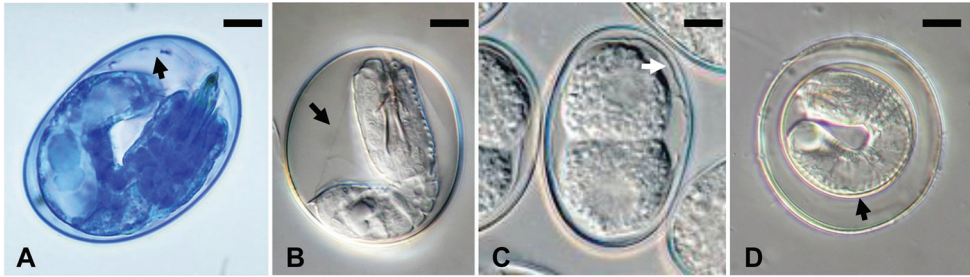


Figure 7. Eggs of aquatic and terrestrial hairworms, light photomicrographs **A** egg of *Gordius difficilis* stained with Nile Blue; note the thin inner membrane (arrow) surrounding the larva **B** egg of *Neochordodes occidentalis* showing a thin inner membrane (arrow) surrounding the larva **C** egg of *Paragordius obamai* showing a developing larva surrounded by a thin inner membrane (arrow) **D** egg of *Gordius terrestris* sp. nov. showing a distinct thick inner membrane (arrow) surrounding the larva. Scale bars: 6 μm (**A**); 8 μm (**B, C**); 11 μm (**D**).

Discussion

Gordius terrestris sp. nov. represents the first hairworm species consistently collected from a terrestrial habitat. Hundreds of adult free-living worms appeared after bouts of heavy rain on streets, sidewalks, and lawns during the winter season, where male and female worms were observed mating and some females were observed depositing egg strings (unpublished data). It is currently unclear what definitive host is used in the life cycle of *G. terrestris* sp. nov. However, over a two-year sampling period, no arthropod hosts were observed in the areas when adult worms appeared. More intriguing, free-living adult worms would disappear from these locations within days after the rains subsided.

Currently, there is only one other report of a European gordiid depositing egg strings in a terrestrial habitat. Schmidt-Rhaesa (2013) reported female *Gordius aquaticus* laying eggs under moist rotting leaves directly adjacent to water; whereas males of this species were observed in shallow forest streams and ponds. In contrast to the *G. aquaticus* observations, all collections of adult *G. terrestris* sp. nov. in this study and our previous collections of this species from Oklahoma, Texas, and Louisiana in Hanelt et al. (2015) and Harkins et al. (2016) were from terrestrial habitats. Finally, field surveys by Harkins et al. (2016) for hairworm cysts in aquatic paratenic hosts from 46 streams in Payne Co. Oklahoma, including the City of Stillwater, indicate that *Gordius* type cysts accounted for 1.7 % (31/1,749) of the total cysts collected, compared to 98.3% of cysts being represented by aquatic hairworm species in the genera *Paragordius*, *Chordodes*, and/or *Neochordodes* where they commonly mate. This is particularly significant since adults of *G. terrestris* sp. nov. is the most commonly encountered gordiid on lawns and sidewalks by the public in Oklahoma and Texas (MGB unpublished data) suggesting that *G. terrestris* sp. nov. is commonly encountered in terrestrial habitats and nonadult stages are rarely found in aquatic habitats.

One significant observation is the unique egg morphology of *G. terrestris* sp. nov. with a thick inner membrane surrounding the developing larval stage. Although few detailed hairworm egg descriptions or egg photographs exist in the literature, our evaluation of eggs for three aquatic gordiid species, clearly indicate that in aquatic Gordiids the developing larval stage is surrounded by a thin inner membrane (Schmidt-Rhaesa 1997b; Bolek and Coggins 2002; Bolek et al. 2010, 2013a, 2015; Schmidt-Rhaesa 2013). Additionally, our unpublished observations on the egg morphology of three undescribed *Gordius* species collected from aquatic habitats in Nebraska, New Mexico, and California (clades 2, 3, and 4 in Hanelt et al. 2015) also indicate that the eggs of these aquatic species lack the unique egg morphology of *G. terrestris* sp. nov. Considering the terrestrial habitat free-living adult *G. terrestris* sp. nov. occur in, we hypothesize that this unique egg morphology may be an adaptation for terrestrial habitats. In the future, we plan to publish our detailed observations on mating and oviposition by this species in terrestrial environments and the occurrence of cysts of *G. terrestris* sp. nov. in terrestrial paratenic hosts.

Acknowledgements

This work was supported by the National Science Foundation, award numbers DEB-0949951 to Matthew G. Bolek and DEB-0950066 to Ben Hanelt and Andreas Schmidt-Rhaesa and Oklahoma State Women's Faculty Council Student Research Award to Christina Anaya. We thank Brent Johnson and Lisa Whitworth of the OSU microscopy facility for their invaluable help with SEM work during this study and undergraduate students who assisted us in the laboratory including Lila Trainor, Kenneth Rogers, Ayrianna Swanson, Madison Houghton, Claire Gallagher, and Jordyn Taylor. Finally, we would like to thank the citizen scientists who collected hairworms and sent them to us. The authors have declared that no competing interests exist.

References

- Adrianov AV, Malakhov VV, Spiridonov SE (1998) Fine structure of the larva of *Gordius* sp. (Nematomorpha). *Doklady Akademii Nauk* 361: 558–561.
- Blair D (1983) Larval horsehair worms (Nematomorpha) from the tissues of native freshwater fish in New Zealand. *New Zealand Journal of Zoology* 10: 341–344. <https://doi.org/10.1080/03014223.1983.10423928>
- Bolek MG, Coggins JR (2002) Seasonal occurrence, morphology, and observations on the life history of *Gordius difficilis* (Nematomorpha: Gordioidea) from southeastern Wisconsin, United States. *Journal of Parasitology* 88: 287–294. <https://doi.org/10.2307/3285575>
- Bolek MG, Schmidt-Rhaesa A, Hanelt B, Richardson DJ (2010) Redescription of the African *Chordodes albibarbatulus* Montgomery, 1898, and description of *Chordodes janovyi* n.

- sp. (Gordiida, Nematomorpha) and its non-adult stages from Cameroon, Africa. *Zootaxa* 2631: 36–54. <https://doi.org/10.11646/zootaxa.2631.1.3>
- Bolek MG, Szmygiel C, Kubat A, Schmidt-Rhaesa A, Hanelt B (2013a) Novel techniques for biodiversity studies of gordiids and description of a new species of *Chordodes* (Gordiida, Nematomorpha) from Kenya, Africa. *Zootaxa* 3717: 23–38. <https://doi.org/10.11646/zootaxa.3717.1.2>
- Bolek MG, Rogers E, Szmygiel C, Shannon RP, Doerfert-Schrader WE, Schmidt-Rhaesa A, Hanelt B (2013b) Survival of larval and cyst stages of gordiids (Nematomorpha) after exposure to freezing. *Journal of Parasitology* 99: 397–402. <https://doi.org/10.1645/12-62.1>
- Bolek MG, Schmidt-Rhaesa A, De Villalobos LC, Hanelt B (2015) Phylum Nematomorpha. In: Thorp J, Rogers DC (Eds) Volume I: Ecology and General Biology: Thorp and Covich's Freshwater Invertebrates (4th edn). Academic Press, San Diego, 303–326. <https://doi.org/10.1016/B978-0-12-385026-3.00015-2>
- Carvalho JCM (1942) Studies on some Gordiacea of North and South America. *Journal of Parasitology* 28: 213–222. <https://doi.org/10.2307/3272775>
- Chiu MC, Huang CG, Wu WJ, Shiao SF (2017) A new orthopteran-parasitizing horsehair worm, *Acutogordius taiwanensis* sp. nov., with a redescription of *Chordodes formosanus* and novel host records from Taiwan (Nematomorpha, Gordiida). *ZooKeys* 683: 1–23. <https://doi.org/10.3897/zookeys.160.2290>
- Hanelt B, Janovy Jr J (2002) Morphometric analysis of nonadult characters of common species of American gordiids (Nematomorpha: Gordioidea). *Journal of Parasitology* 88: 557–562. <https://doi.org/10.2307/3285448>
- Hanelt B, Janovy Jr J (2003) Spanning the gap: experimental determination of paratenic host specificity of horsehair worms (Nematomorpha: Gordiida). *Invertebrate Biology* 122: 12–18. <https://doi.org/10.1111/j.1744-7410.2003.tb00068.x>
- Hanelt B, Thomas F, Schmidt-Rhaesa A (2005) Biology of the phylum Nematomorpha. *Advances in Parasitology* 59: 243–305. [https://doi.org/10.1016/S0065-308X\(05\)59004-3](https://doi.org/10.1016/S0065-308X(05)59004-3)
- Hanelt B, Bolek MG, Schmidt-Rhaesa A (2012) Going solo: discovery of the first parthenogenetic gordiid (Nematomorpha: Gordiida). *PLoS ONE* 7(4): e34472. <https://doi.org/10.1371/journal.pone.0034472>
- Hanelt B, Schmidt-Rhaesa A, Bolek MG (2015) Cryptic species of hairworm parasites revealed by molecular data and crowdsourcing of specimen collections. *Molecular Phylogenetics and Evolution* 82: 211–218. <https://doi.org/10.1371/journal.pone.0034472>
- Harkins C, Shannon R, Papeş M, Schmidt-Rhaesa A, Hanelt B, Bolek MG (2016) Using Gordiid cysts to discover the hidden diversity, potential distribution, and new species of Gordiids (Phylum Nematomorpha). *Zootaxa* 4088: 515–530. <https://doi.org/10.11646/zootaxa.4088.4.3>
- Leidy J (1851) On the Gordiacea. *Proceedings of the Academy of Natural Sciences of Philadelphia* 5: 262–275.
- Marchiori NC, Pereira Jr J, Castro AS (2009) Morphology of larval *Gordius dimorphus* (Nematomorpha: Gordiida). *Journal of Parasitology* 95: 1218–1220. <https://doi.org/10.1645/GE-2014.1>
- May HG (1919) Contributions to the life histories of *Gordius robustus* Leidy and *Paragordius varius* (Leidy). *Illinois Biological Monographs* 5: 1–119. <https://doi.org/10.5962/bhl.title.16768>
- Poinar Jr GO, Brockerhoff AM (2001) *Nectonema zealandica* n. sp. (Nematomorpha: Nectonematoidea) parasitizing the purple rock crab *Hemigrapsus edwardsi* (Brachyura: Decapoda)

- in New Zealand, with notes on the prevalence of infection and host defence reactions. *Systematic Parasitology* 50: 149–157. <https://doi.org/10.1023/A:1011961029290>
- Poulin R (1998) Book Review: Nematomorpha. *Journal of Parasitology* 84: 1–35. <https://doi.org/10.2307/3284525>
- Redlich A (1980) Description of *Gordius attoni* sp. nov. (Nematomorpha, Gordiidae) from Northern Canada. *Canadian Journal of Zoology* 58: 382–385. <https://doi.org/10.1139/z80-049>
- Schmidt-Rhaesa A (1997a) Ultrastructural observations of the male reproductive system and spermatozoa of *Gordius aquaticus* L. 1758 (Nematomorpha). *Invertebrate Reproduction and Development* 32: 31–40. <https://doi.org/10.1080/07924259.1997.9672602>
- Schmidt-Rhaesa A (1997b) Nematomorpha. In: Schwoerbel J, Zwick P (Eds) *Süßwasserfauna Mitteleuropas*. Gustav Fischer Verlag, Stuttgart, 124 pp.
- Schmidt-Rhaesa A (2010) Considerations on the genus *Gordius* (Nematomorpha, horsehair worms), with the description of seven new species. *Zootaxa* 2533: 1–35. <https://doi.org/10.11646/zootaxa.2533.1.1>
- Schmidt-Rhaesa A (2013) Nematomorpha. In: Schmidt-Rhaesa A (Ed.) *Handbook of Zoology. Gastrotricha, Cycloneuralia and Gnathifera. Nematomorpha, Priapulida, Kinorhyncha and Loricifera* (Vol. 1). De Gruyter, Berlin, 29–145. <https://doi.org/10.1515/9783110272536>
- Schmidt-Rhaesa A, Hanelt B, Reeves WK (2003) Redescription and compilation of Nearctic freshwater Nematomorpha (Gordiida), with the description of two new species. *Proceedings of the Academy of Philadelphia* 153: 77–117. [https://doi.org/10.1635/0097-3157\(2003\)153\[0077:RACONF\]2.0.CO;2](https://doi.org/10.1635/0097-3157(2003)153[0077:RACONF]2.0.CO;2)
- Schmidt-Rhaesa A, Prous M (2010) Records of horsehair worms (Nematomorpha) in Estonia, with description of three new species from the genus *Gordius*. *Estonia Journal of Ecology* 59: 39–51. <https://doi.org/10.3176/eco.2010.1.03>
- Schneider CA, Rasband WS, Eliceiri KW (2012) NIH Image to ImageJ: 25 years of image analysis. *Nature Methods* 9: 671–675. <https://doi.org/10.1038/nmeth.2089>
- Smith DG (1994) A reevaluation of *Gordius aquaticus difficilis* Montgomery, 1898 (Nematomorpha, Gordioidea, Gordiidae). *Proceedings of the Academy of Natural Sciences of Philadelphia* 145: 29–34.
- Swantesson-Franz RJ, Marquez DA, Goldstein CI, Schmidt-Rhaesa A, Bolek MG, Hanelt B (2018) New hairworm (Nematomorpha, Gordiid) species described from the Arizona Madrean Sky Islands. *ZooKeys* 733: 131–145. <https://doi.org/10.3897/zookeys.733.22798>
- Szmygiel C, Schmidt-Rhaesa A, Hanelt B, Bolek MG (2014) Comparative descriptions of non-adult stages of four genera of Gordiids (Phylum: Nematomorpha). *Zootaxa* 3768: 101–118. <https://doi.org/10.11646/zootaxa.3768.2.1>
- Townsend JI (1970) Records of gordian worms (Nematomorpha) from New Zealand Carabidae. *New Zealand Entomology* 4: 98–99. <https://doi.org/10.1645/GE-2929.1>
- Wethington AR, Lydeard C (2007) A molecular phylogeny of Physidae (Gastropoda: Basommatophora) based on mitochondrial DNA sequences. *Journal of Molluscan Studies* 73: 241–257. <https://doi.org/10.1093/mollus/eym021>
- Yadav AK, Tobias ZJC, Schmidt-Rhasesa A (2018) *Gordionus maori* (Nematomorpha: Gordiida), a new species of horsehair worm from New Zealand. *New Zealand Journal of Zoology* 45: 29–42. <https://doi.org/10.1080/03014223.2017.1329155>

Lithobius (Ezembius) hualongensis sp. nov. and *Lithobius (Ezembius) sui* sp. nov. (Lithobiomorpha, Lithobiidae), two new species of centipede from northwest China

Penghai Qiao^{1,2}, Wen Qin², Huiqin Ma³, Gonghua Lin⁴, Tongzuo Zhang²

1 Institute of Laboratory Animal Science, Guizhou University of Traditional Chinese Medicine, Guiyang, 550000, China **2** Qinghai Provincial Key Laboratory of Animal Ecological Genomics, Northwest Institute of Plateau Biology, Chinese Academy of Sciences, Xining 810008. No.23 Xinning Road, Chengxi District, Xining, Qinghai, China **3** Scientific Research Office, Hengshui University, Hengshui, 353000, China **4** School of Life Sciences, Jinggangshan University, Jian, 343009, Jiangxi, China

Corresponding author: Tongzuo Zhang (zhangtz@nwipb.cas.cn)

Academic editor: Marzio Zapparoli | Received 13 August 2019 | Accepted 4 October 2019 | Published 25 November 2019

<http://zoobank.org/61919583-6000-46DB-91CA-2CA664581543>

Citation: Qiao P, Qin W, Ma H, Lin G, Zhang T (2019) *Lithobius (Ezembius) hualongensis* sp. nov. and *Lithobius (Ezembius) sui* sp. nov. (Lithobiomorpha, Lithobiidae), two new species of centipede from northwest China. ZooKeys 892: 77–92. <https://doi.org/10.3897/zookeys.892.39033>

Abstract

Lithobius (Ezembius) hualongensis sp. nov. and *Lithobius (Ezembius) sui* sp. nov. (Lithobiomorpha, Lithobiidae) recently discovered from the Qinghai-Tibet Plateau, China are described. Morphologically, the two new species are very similar but can be distinguished by the number of coxosternal teeth: *L. (E.) hualongensis* sp. nov. has 2 + 2 while *L. (E.) sui* sp. nov. has 3 + 3. The two new species resemble *L. (E.) multispinipes* Pei et al., 2016, from the Xinjiang Autonomous Region, but can be readily distinguished by having the Tömösváry's organ slightly larger than the adjoining ocelli rather than smaller, 3 + 3 spurs on female gonopods versus 2 + 2, and the simple terminal claw of female gonopods with a small triangular protuberance on the basal ventral side versus simple, without a small triangular protuberance on the basal ventral side. We also compare the main morphological characters of the two new species with the other *Lithobius (Ezembius)* species known in Qinghai Province. A key to the Chinese species of *Ezembius* is presented.

Keywords

myriapod, Qinghai-Tibet Plateau, stone centipede, taxonomy

Introduction

The myriapod fauna of China is still poorly known and this is especially the case with centipedes of the order Lithobiomorpha. Only about 84 species/subspecies of lithobiomorphs are known from the country (Ma et al. 2014a, b, 2015, 2018; Pei et al. 2014, 2015, 2016, 2018; Qin et al. 2014; Qiao et al. 2018a, b, 2019a, b). Qinghai province is among the very poorly studied regions of China with only 11 species at present registered from its territory (Ma et al. 2014b, Qiao et al. 2018a, b, 2019a, b). Altogether, 26 species of *Lithobius* (*Ezembius*) have been recorded from China (Zhang 1996; Pei et al. 2018, Qiao et al. 2018b, 2019a, b). Herein we describe *Lithobius* (*Ezembius*) *hualongensis* sp. nov. found in Hualong County, Qinghai and *Lithobius* (*Ezembius*) *sui* sp. nov. collected from Minghe County, Qinghai.

The centipede subgenus *Ezembius* was erected by Chamberlin (1919) as a genus to receive *Lithobius stejnegeri* Bollman, 1893, *L. ostiacorum* Stuxberg, 1876, *L. princeps* Stuxberg, 1876, *L. sulcipes* Stuxberg, 1876 and *L. scrobiculatus* Stuxberg, 1876 and then was formally proposed as new and described in 1923 (Chamberlin 1923). It accommodates a group of 58 species/subspecies known mostly from Asia, but also western North America and spans a wide range of habitats, from the arctic and sub-arctic to tropical and sub-tropical forests, to steppe and overgrazed stony areas of central Asia, to Himalayan montane forests, from the sea shore up to 5500 m (Himalayas) (Zapparoli and Edgecombe 2011). Most of species are not widely distributed (Bonato et al. 2016), except *Lithobius* (*Ezembius*) *giganteus* Sselivanoff, 1881 distributed in Mongolia, eastern Kirgizia Buryat and Soviet Central Asia (Eason 1986) and *Lithobius* (*Ezembius*) *sibiricus* Gerstfeldt, 1858 distributed in Asian Russia in Western, Central and Eastern Siberia, the Russian Far East and northern Mongolia (Eason 1976).

Ezembius is characterized by antennae with ca 20 articles; ocelli 1 + 4 to 1 + 20; forcipular coxosternal teeth usually 2 + 2, sometimes 2 + 3, 3 + 2 or 3 + 3; prodonts generally setiform but sometimes stout; tergites generally without posterior triangular projections, occasionally with; tarsal articulation of legs 1–13 distinct; female gonopods with uni-, bi- or tridentate claw, 2 + 2 or 3 + 3, rarely 4 + 4, spurs (Zapparoli and Edgecombe 2011). The distinction between *Ezembius* and *Monotarsobius*, depends on the size and state of the anterior tarsal articulations (Eason 1992): *Monotarsobius* has smaller body size never more than 11 mm long and fused tarsal articulation (Zapparoli and Edgecombe 2011).

Materials and methods

All specimens were hand-collected under leaf litter or stones. The material was examined with the aid of a Motic-C microscope of which the measuring accuracy is +/- 0.01 mm. The color description is based on specimens in 75% ethanol, and body length is measured from the anterior margin of the cephalic plate to the posterior end of the postpedal tergite. Type specimens are preserved in 75% ethanol and deposited

in Northwest Institute of Plateau Biology, Chinese Academy of Sciences. The terminology of the external anatomy follows Bonato et al. (2010). The following abbreviations are used in the text and the tables: **a** anterior; **C** coxa; **D** dorsal; **F** femur; **m** median; **p** posterior; **P** prefemur; **S**, **SS** sternite, sternites; **T**, **TT** tergite, tergites; **Ti** tibia; **To** Tömösváry's organ; **Tr** trochanter; **V** ventral; **HL** Hualong County; **MHA** Minhe County.

Taxonomic accounts

Order Lithobiomorpha Pocock, 1895

Family Lithobiidae Newport, 1844

Subfamily Lithobiinae Newport, 1844

Genus *Lithobius* Leach, 1814

Subgenus *Ezembius* Chamberlin, 1919

***Lithobius (Ezembius) hualongensis* sp. nov.**

<http://zoobank.org/B145889E-4CEC-42E6-8C14-579C9B0616A0>

Fig. 1A–F; Tables 1, 2

Type materials. *Holotype*: ♂ (HL9), Hualong Hui Autonomous County, Qinghai Province, 36.18848333N, 102.2971333E, 3185 m, a.s.l., 14 April 2012, leg. Lin Gong-Hua, Li Wei-Ping. *Paratypes*: 1 ♀ (HL7), 2 ♂♂ (HL1, HL4), all from the same locality.

Diagnosis. A *Lithobius (Ezembius)* species with body length 12.31–16.15 mm, antennae of 20 + 20 articles; 8–11 ocelli on each side, arranged in 3 irregular rows, terminal two ocelli comparatively large; Tömösváry's organ distinctly larger than the adjoining ocelli; 2 + 2 coxosternal teeth; prodonts posterolateral and ventral to the lateral-most tooth; posterior angles of all tergites without triangular projections; 4–7 coxal pores oval to round, arranged in one row; female gonopods with 3 + 3 moderately large, coniform spurs; terminal claw of the third article simple, with a very small triangular protuberance on basal ventral side; male gonopods short and small, with one long setae on the terminal segment.

Description. Male (Fig. 1A). Body length 12.31 mm, cephalic plate 1.15 mm long, 0.92 mm broad.

Coloration. Body and antennae reddish brown. Pleural region pale grey. Sternites yellow-brown. Distal part of forcipules red-brown, with basal and proximal parts of forcipules and forcipular coxosternite yellow-brown. Legs 1–15 pale yellow-brown.

Antennae composed of 20 + 20 articles extending back to anterior part of T3, basal article about the same width as length, second article longer than wide, third article slightly longer than wide, with following articles tapering, distal-most article 2.7 times as long as wide; abundant setae on antennal surface, gradual increase in density of setae to about 4th article, then more or less constant.

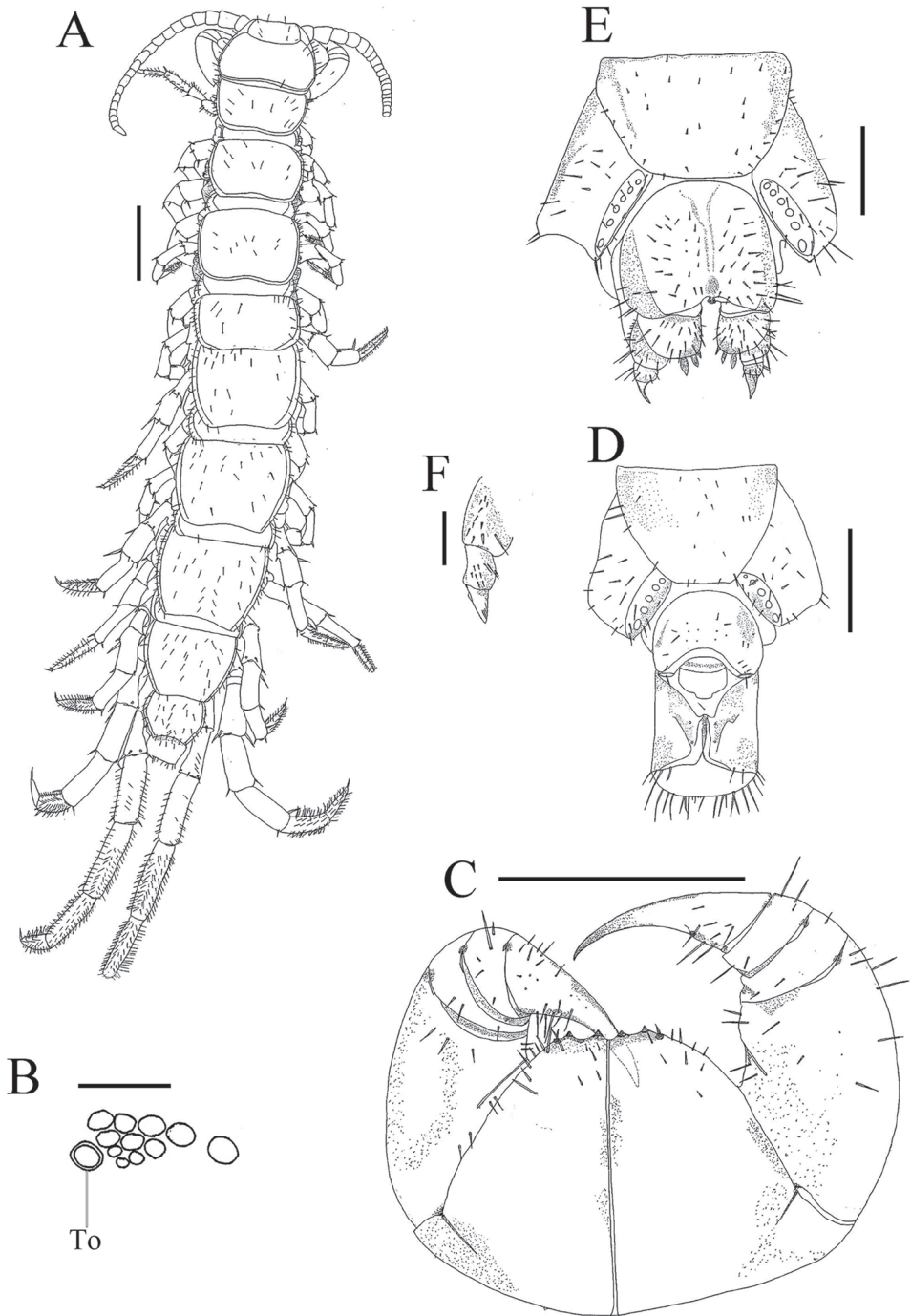


Figure 1. *Lithobius (Ezembius) hualongensis* sp. nov. **A, C, D** holotype, male: **A** habitus, dorsal view **C** forcipular coxosternite, ventral view **D** male posterior segments and gonopods, ventral view **B, E, F** paratype, female: **B** ocelli and Tömösváry's organ (**To**), lateral view **E** female gonopods, dorsal lateral view **F** female posterior segments and gonopods, ventral view. Scale bars: 1 mm (**A, C**); 500 μ m (**D, F**); 250 μ m (**B, E**).

Cephalic plate smooth, cordiform. Frontal marginal ridge of head with shallow anterior median furrow. Lateral marginal ridge discontinuous. Posterior margin continuous, convex (Fig. 1A).

On each side of head, 1 + 3, 3, 1 oval to rounded ocelli arranged in three irregular rows; posterior ocellus large; ocelli adjacent to the Tömösváry organ slightly smaller. Seriate ocelli domed, translucent, usually darkly pigmented. Tömösváry organ at anterolateral margin of the cephalic plate, larger than the adjacent ocelli.

Coxosternite subtrapezoidal (Fig. 1C) with narrow dental straight dental margin, anterior margin narrow, lateral margins of the coxosternite longer than medial margins. Median diastema shallow; anterior margin with 2 + 2 small blunt teeth that are encircled by a narrow rim. Porodont thick and strong, just posterolateral and ventral from the lateral tooth, bulged at base (Fig. 1C). Scattered short and long setae on the ventral side of coxosternite, longer setae near the porodont.

All tergites with numerous minute setae scattered on surface, several setae on anterior and posterior angles of each tergite and lateral borders, dorsum slightly convex; T1 slightly narrower posterolaterally than anterolaterally, generally trapezoidal, slightly narrower than the cephalic plate and T3, cephalic plate slightly about the same size as T3. Lateral marginal ridges of all tergites continuous. Posterior marginal ridges of TT 1, 3 and 5 concave, continuous, posterior marginal ridges of TT 7, 8, 10, 12 and 14 slightly concave, discontinuous. Posterior angles of all tergites rounded, without triangular projections.

Sternites smooth, posterior part of sternites narrower than anterior, generally trapezoidal. Sternites with 8 short to long setae on anterior corners and anterior lateral borders, 2 setae on posterior lateral borders.

Legs slender, tarsal articulation well defined on legs 1–15. All legs with fairly long curved claws; pretarsus of legs 1–13 with a slightly curved, long, principal claw and anterior and posterior accessory spines, anterior accessory spines slightly longer and slender, ca 0.56 the length of principal claw, posterior one stouter, ca 0.43 the length of principal claw, forming slightly larger angles with tarsal claws; leg 14 with only posterior spines; leg 15 lacking accessory spines. Dense glandular pore on surface of femur, tibia and tarsi of legs 14 and 15. Long setae sparsely scattered over surface of prefemur, femur, tibia, and tarsi of legs 14–15, more setae on the tarsal surface. 6–7 thicker setae arranged in one row on the ventral surface of tarsus 1 of legs 1–13, 6–7 pairs of thicker setae arranged in two rows on the ventral surface of tarsus 2 of legs 1–13. Legs 14 and 15 thicker and stronger than the anterior pairs. 15th leg 40.6% of body length, tarsus 1 3.3 times longer than wide, tarsus 2 44.4% length of tarsus on leg 15. No modification on legs 14 and 15 in males. Leg plectrotaxy as in Table 1.

Coxal pores 4655 round or slightly oval, variable in size, arranged in a row. Coxal pore field set in a relatively shallow groove, the coxal pore-field fringe with prominence. Prominence with short to moderately long setae sparsely scattered over the surface.

Male posterior segment. Male S15 subtrapeziform, posterior margin narrower than anterior, sparsely covered with short to long setae on ventral side of S15 and

Table 1. *Lithobius (Ezembius) hualongensis* sp. nov.: plectrotaxy of legs. Letters in brackets indicate spines on one leg of pair, or in one specimen.

Legs	Ventral					Dorsal				
	C	Tr	P	F	Ti	C	Tr	P	F	Ti
1	–	–	mp	amp	am	–	–	mp	ap	a
2–4	–	–	(a)mp	amp	am	–	–	(a)mp	ap	ap
5	–	–	amp	amp	am	–	–	(a)mp	ap	ap
6–11	–	–	amp	amp	am	–	–	amp	ap	ap
12	–	m	amp	amp	am	a	–	amp	ap	ap
13	–	m	amp	amp	am	a	–	amp	ap	ap
14	–	m	amp	amp	am	a	–	amp	p	p
15	–	m	amp	amp	a	a	–	amp	p	–

lateral and posterior borders (Fig. 1D); sternite of genital segment obviously smaller than the female, sclerotized; posterior margin deeply concave between the gonopods, without medial bulge. Long setae scattered on the ventral surface of the genital segment. Gonopods short, appearing as a small hemispherical bulge, with one long setae, apically slightly sclerotized (Fig. 1D).

Female posterior segment. Female S15 anterior margin broader than posterior, generally trapezoidal, posteromedially straight, S15 with short to long setae on the ventral surface and lateral and posterior borders. Posterior margin of genital sternite deeply concave between condyles of gonopods, except for a small, median rhomboid bulge. Short to long setae sparsely scattered on ventral surface of genital segment. Gonopods: first article fairly broad, bearing 17–20 short to moderately long setae, arranged in four irregular rows; with 3 + 3, moderately long and slender spurs, inner spur smaller than the outer (Fig. 1E); second article with 6–7 long setae, arranged in two irregular rows, with 10 short to long dorsal lateral setae, stouter than the general setae (Fig. 1F); third article with 6 long setae arranged in one irregular row, and 7 short setae on dorsal lateral side (Fig. 1F); third article terminal claw simple and sharp, having a very small triangular protuberance on ventral side (Fig. 1E).

Variations. Body length 12.31–16.15 mm; ocelli 1 + 3, 3, 1 or 1 + 4, 3, 3; coxal pores 6666 and 6777 in female and 4654 and 4655 in male.

Remarks. Morphologically, the new species can be easily distinguished from the seven species in the subgenus from Qinghai Province, *L. (E.) asulcutus*, *L. (E.) raribirsutipes*, *L. (E.) femorisulcutus*, *L. (E.) longibasitarsus*, *L. (E.) datongensis*, *L. (E.) maqinensis* and *L. (E.) dulanensis*, by the 3 + 3 coniform spurs on female gonopods contrary to 2 + 2 coniform spurs (Table 2).

Etymology. The new species is named from the type locality.

Habitat. The four specimens here examined (3 ♂♂, 1 ♀) were collected under granular gravel on the alpine meadows composed mainly of Poaceae, Cyperaceae, Fabaceae, Polygonaceae, Chenopodiaceae, Asteraceae, Rosaceae, Liliaceae and Cucurbitaceae. The region is located on the upper reaches of the Yellow River Valley and features an arid climate, with mean annual precipitation 451.2 mm and average annual temperature 2.8 °C (<http://data.cma.cn/data/weatherBk.html>).

***Lithobius (Ezembius) sui* sp. nov.**

<http://zoobank.org/71D02371-BD0E-43CA-8986-5775CC49405C>

Fig. 2A–G; Tables 2, 3

Type materials. *Holotype*: ♀ (MHA8), Minhe County, Qinghai Province, 36.12076N, 102.7809E, 2280 m, a.s.l., 24 October 2010, leg. Lin Gong-Hua. *Paratypes*: 1 ♂ (MHA6), 2 ♀♀ (MHA1, MHA5), all from the same locality.

Diagnosis. A *Lithobius (Ezembius)* species with body length 12.15–18.85 mm, antennae of 20 + 20 articles; 9–10 ocelli on each side, arranged in 3 irregular rows, terminal two ocelli comparatively large; Tömösváry's organ distinctly larger than the adjoining ocelli; 3 + 3 coxosternal teeth; porodonts posterolateral and ventral to the lateral-most tooth; posterior angles of all tergites without triangular projections; 4–8 coxal pores oval to round, arranged in one row; female gonopods with 3 + 3 moderately large, coniform spurs; terminal claw of the third article simple, with a very small triangular protuberance on basal ventral side; male gonopods short and small, with two long setae on the terminal segment.

Description. Female (Fig. 2A). Body length 12.15 mm, cephalic plate 1.54 mm long, 1.69 mm broad.

Coloration. Body yellow-brown, cephalic plate and antennae light yellow-brown with reddish hue. Pleural region pale grey. Sternites yellow-brown. Distal part of forcipules red-brown, with basal and proximal parts of forcipules and forcipular coxosternite yellow-brown. Legs 1–15 light yellow-brown.

Antennae composed of 20 + 20 articles extending back to posterior part of T3, basal article about the same width as length, second article slightly longer than wide, third article slightly wider than long, with following articles tapering, distal-most article 2.9 times as long as wide; abundant setae on antennal surface, gradual increase in density of setae basally to distally to about fourth articles.

Cephalic plate smooth, convex. Frontal marginal ridge of head with shallow anterior median furrow. Lateral marginal ridge discontinuous. Posterior margin continuous, slightly convex (Fig. 2A).

On each side of head, 1 + 4, 4, 1 oval to rounded ocelli (Fig. 2B), arranged in three irregular rows; posterior ocellus large; ocelli adjacent to the Tömösváry organ slightly small. Seriate ocelli domed, translucent, usually darkly pigmented. Tömösváry organ at anterolateral margin of the cephalic plate, larger than the adjacent ocelli (Fig. 2B-To).

Coxosternite subtrapezoidal (Fig. 2D), anterior margin narrow, lateral margins of the coxosternite longer than medial margins. Median diastema moderately shallow, V-shaped; anterior margin with 3 + 3 subtriangular blunt teeth, inner tooth smaller. Porodont thick and strong, just posterolateral and ventral from the lateral tooth, bulged at base (Fig. 2D). Scattered short setae on the ventral side of coxosternite, longer setae near the porodont.

All tergites with numerous minute setae scattered on surface, several setae on anterior and posterior angles of each tergite and lateral borders, dorsum slightly convex; T1 narrower posterolaterally than anterolaterally, generally trapezoidal, narrower than the

Table 2. Main morphological characters of Chinese species of subgenus *Lithobius* (*Ezembius*) Chamberlin, 1919 from Qinghai Province.

Characters	<i>asulcutus</i>	<i>ravilirsutipes</i>	<i>femorissulcutus</i>	<i>longibasitarsus</i>	<i>diatogensis</i>	<i>maqimensis</i>	<i>dulanensis</i>	<i>hualongensis</i> sp. nov.	<i>sui</i> sp. nov.
Sources	Zhang 1996	Zhang 1996	Zhang 1996	Qiao et al. 2018b	Qiao et al. 2018b	Qiao et al. 2019a	Qiao et al. 2019b	this paper	this paper
Body length (mm)	13–15	11–12	15–18	17–18	12.3–14.2	13.1–14.6	about 20.5	12.31–16.15	12.15–18.85
Number of antennal articles	20 + 20	20 + 20	20 + 20	20 + 20	20 + 20	20 + 20	20–21	20 + 20	20 + 20
Number, arrangement of ocelli	10, in 3 rows	11, in 3 rows	10–14, in 3 rows	10–14, in 3 rows	9–10 ocelli, in 3 broken rows	10–12, in 3 rows	11, in 3 rows	8–11, in 3 rows	9–10, in 3 rows
Posterior ocellus	round, comparatively large	oval to round, large	comparatively large	posterior ocellus is biggest	slightly larger than posterosuperior ocellus	posterior ocellus is biggest	posterior ocellus and posterosuperior ocellus comparatively large	terminal two ocelli comparatively large	terminal two ocelli comparatively large
Seriate ocelli	ones near ventral margin moderately small	ones near ventral margin moderately small	ones near ventral margin moderately small	ones near ventral margin moderately small	ones near ventral margin moderately small	ones near ventral margin moderately small	second row smaller than first, third smallest	ones near ventral margin moderately small	ones near ventral margin moderately small
Tömösváry's organ	round, smaller than adjoining ocelli	rounded, slightly, smaller than adjoining ocelli	slightly larger than adjoining ocelli	slightly smaller than adjoining ocelli	larger than adjoining ocelli	almost same size as adjacent ocelli	oval and slightly smaller than adjoining ocelli	obviously larger than adjoining ocelli	obviously larger than adjoining ocelli
Number and shape of coxosternal teeth	2 + 2 subtriangular teeth	2 + 2, subtriangular teeth	2 + 2	2 + 2 or 3 + 2	2 + 2	2 + 2, small coniform teeth	2 + 2, coniform, moderately robust teeth	2 + 2, small coniform teeth	3 + 3, inner tooth smaller than outer tooth
Porodont	long and slender, lying posterolateral to lateral-most teeth	long and slender, lying posterolateral to lateral-most teeth	long and strong, lying posterolateral to lateral-most teeth	thick and strong separated from lateral tooth ventrolaterally	setiform, separated from lateral tooth laterally	setiform, lying posterolateral to lateral-most tooth	long and strong, lying posterolateral to lateral-most tooth	thick and long, lying posterolateral to lateral-most tooth	thick and long, lying posterolateral to lateral-most tooth
Tergites	smooth	smooth	smooth	smooth	smooth	smooth	smooth	with numerous minute setae scattered on surface	with numerous minute setae scattered on surface
Number of coxal pores	4–7, 4544, 4554, 5665, 5766	not reported	5544, 5554, 5555, 5564	4–6	4–7	4–6	5–7, 5667, 5666	6666 and 6777 in female and 4654 and 4655 in male	5664, 5665, 7775 and 8875 in female and 6886 and 7665 in male.
Shape of coxal pores	not reported	not reported	round	circular	round	round	circular to ovate	round or slightly ovate	round or slightly ovate
Tarsus 1–tarsus 2 articulation on legs 1–13	not well defined	well defined	well defined	well defined	well defined	not well defined	not well defined	well defined	well defined

Characters	<i>asulcutus</i>	<i>ravilirsutipes</i>	<i>femorisulcutus</i>	<i>longibasitarsus</i>	<i>datongensis</i>	<i>maqimensis</i>	<i>dulanensis</i>	<i>hualongensis</i> sp. nov.	<i>sui</i> sp. nov.
Male 14 th leg	slightly thicker and stronger than other legs	markedly thicker and stronger than 1-13 legs	slightly thick and strong than 1-13 legs	moderately thick and strong than 1-13 legs	moderately thick and strong than 1-13 legs	moderately thick and strong than 1-13 legs	slightly thick and strong than 1-13 legs	slightly thick and strong than 1-13 legs	slightly thick and strong than 1-13 legs
Male 15 th leg	slightly thicker and stronger than other legs	markedly thicker and stronger than 1-13 legs	slightly thick and strong than 1-13 legs	moderately thick and strong than 1-13 legs	moderately thick and strong than 1-13 legs	moderately thick and strong than 1-13 legs	slightly thick and strong than 1-13 legs	slightly thick and strong than 1-13 legs	slightly thick and strong than 1-13 legs
Dorsal sulci on male 15 th legs	absent	two distinct, dorsal sulci on femur	distinct, dorsal sulcus on tibia and tarsus 1	absent	absent	absent	absent	absent	absent
DaC spine	on 12 th -15 th legs	on 12 th -15 th legs	on 11 th -15 th legs	on 12 th -15 th legs	on 12 th -15 th legs	on 11 th -15 th legs	on 11 th -15 th legs	on 12 th -15 th legs	on 12 th -15 th legs
14 th accessory spur	present	present	present	present	present	anterior accessory spur absent, posterior accessory spur present	anterior accessory spur absent, posterior accessory spur present	anterior accessory spur absent, posterior accessory spur present	anterior accessory spur absent, posterior accessory spur present
15 th accessory spur	absent	absent	present	present	present	absent	absent	absent	anterior accessory spur absent, posterior accessory spur present
Number and shape of spurs on female gonopods	2 + 2 coniform spurs	2 + 2 conical spurs	2 + 2 conical spurs	2 + 2 conical spurs	2 + 2 conical spurs	2 + 2 conical spurs	2 + 2 conical spurs	3 + 3 coniform spurs, inner spur moderately smaller than outer one	3 + 3 coniform spurs, inner spur moderately smaller than outer one
Dorsal side of second article of female gonopods	not reported	not reported	not reported	four short setae and three long setae on dorsolateral ridge	five long curved spines on dorsolateral side	not reported	with six dorsolateral setae	with 10 short dorsal lateral setae, stouter than general setae	with 10 short dorsal lateral setae, stouter than general setae
Apical claw of female gonopods (and lateral denticles)	simple	simple, having small sharp teeth on the inner side	simple	simple, having small triangular protuberance on ventral side	simple, bearing very small triangular protuberance on ventral side	simple, having very small triangular protuberance on ventral side	simple	simple, having very small triangular protuberance on ventral side	simple, having very small triangular protuberance on ventral side
Male gonopods	short and small bulge, with two long setae	with small bulge, with 3 long setae	not reported	single small semicircular article with 3-5 setae on its surface	hemispherical, with three setae	small, oblique apically, with 2 setae	small, one-segmented, with two long setae	short and small bulge, having long setae, apically slightly sclerotized	short and small, with two long setae on terminal segment

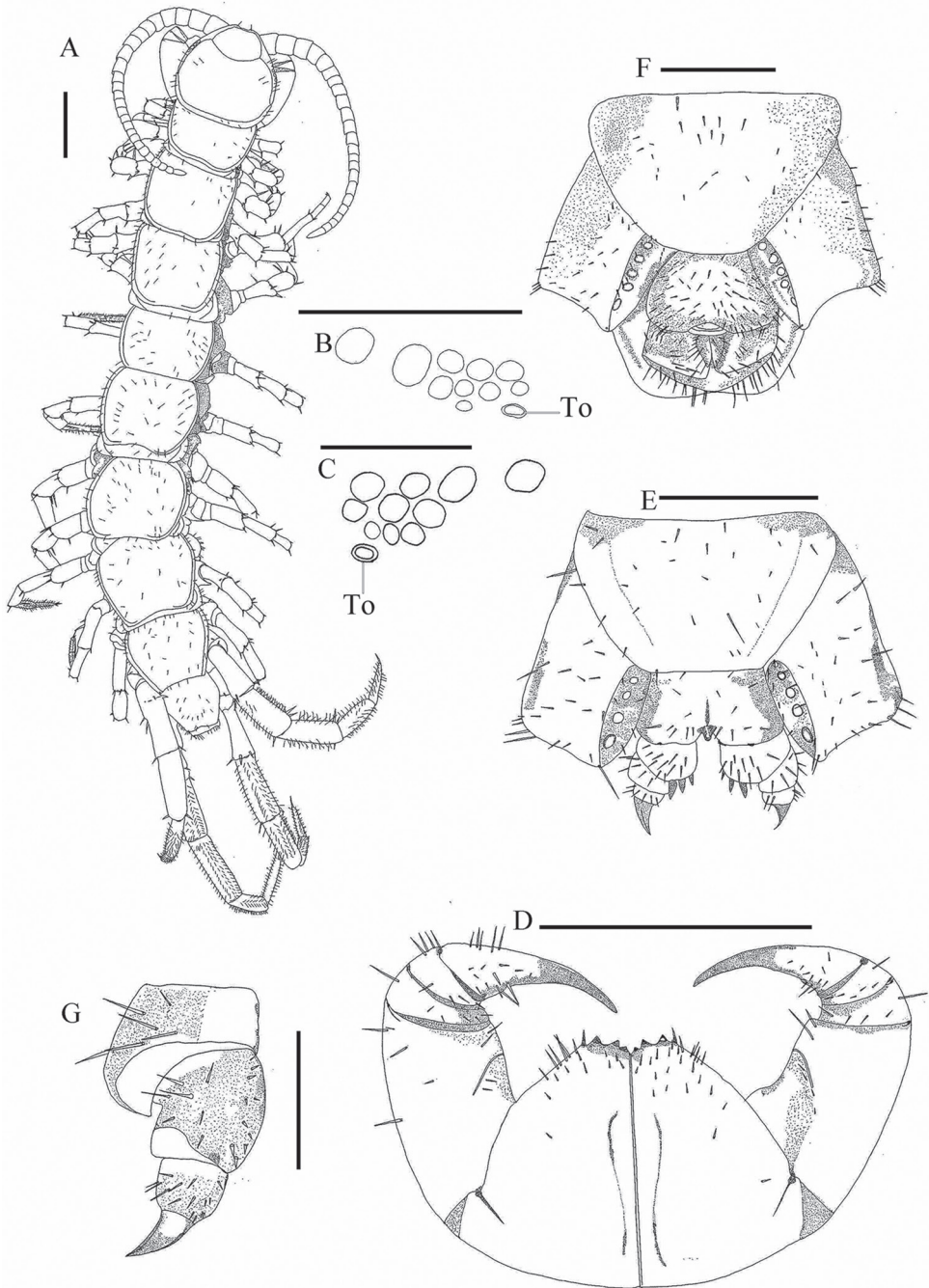


Figure 2. *Lithobius (Ezembius) sui* sp. nov. **A, B, D, E, G** holotype, female: **A** habitus, dorsal view **B** ocelli and Tömösváry's organ (**To**), lateral view **D** forcipular coxosternite, ventral view **E** female posterior segments and gonopods, ventral view **G** female gonopods, dorsal lateral view **C, F** paratype, male: **C** ocelli and Tömösváry's organ (**To**), lateral view **F** posterior segments and gonopods, ventral view. Scale bars: 1 mm (**A, D**); 500 µm (**E, F**); 250 µm (**B, C, G**).

cephalic plate and T3, cephalic plate slightly wider than T3. Lateral marginal ridges of all tergites continuous. Posterior marginal ridges of TT 1 and 3 slightly concave, continuous, posterior marginal ridges of TT 5, 7, 8, 10, 12 and 14 concave, discontinuous. Posterior angles of all tergites rounded, without triangular projections.

Sternites smooth, posterior part of sternites narrower than anterior, generally trapezoidal. Sternites with 2–7 short to long setae on anterior corners and anterior lateral borders, the same with posterior lateral and posterior angles.

Legs slender, tarsal articulation well defined on legs 1–15. All legs with fairly long curved claws; pretarsus of legs 1–13 with a slightly curved, long, principal claw and anterior and posterior accessory spines, anterior accessory spines slightly longer and slender, ca 0.50 the length of principal claw, posterior one stouter, ca 0.33 the length of principal claw, forming slightly larger angles with tarsal claws; legs 14 and 15 with only posterior spines. Dense glandular pore on surface of femur, tibia and tarsi of legs 14 and 15. Long setae sparsely scattered over surface of prefemur, femur, tibia, and tarsi of legs 14–15, more setae on the tarsal surface. 7–9 thicker setae arranged in one row on the ventral surface of tarsus 1 of legs 1–13, 7–8 pairs of thicker setae arranged in two rows on the ventral surface of tarsus 2 of legs 1–13. Legs 14 and 15 thicker and stronger than the anterior pairs. 15th leg 39.24% of body length, tarsus 1 3.8 times longer than wide, tarsus 2 44.4% length of tarsus on leg 15. Leg plectrotaxy as in Table 3.

Coxal pores 4–8 round or slightly oval, variable in size, arranged in a row. Coxal pore field set in a relatively shallow groove, the coxal pore-field fringe with prominence. Prominence with short to moderately long setae sparsely scattered over the surface.

Female posterior segment. Female S15 anterior margin broader than posterior, generally trapezoidal, posteromedially straight, S15 with short to long setae on the ventral surface and lateral and posterior borders. Posterior margin of genital sternite deeply concave between condyles of gonopods, except for a small, median rhomboid bulge. Short to long setae sparsely scattered on ventral surface of genital segment. Gonopods: first article fairly broad, bearing 9–11 short to moderately long setae, arranged in three irregular rows; with 3 + 3, moderately long and slender, bullet-shape spurs, inner spur smaller than the outer (Fig. 2E); second article with 6–7 long setae, arranged in two irregular rows, with 10 short dorsal lateral setae, stouter than the general setae (Fig. 2G); third article with 6 long setae arranged in one irregular row, and 7 short setae on dorsal lateral side (Fig. 2G); third article terminal claw simple and sharp, having a very small triangular protuberance on ventral side (Fig. 2E).

Male posterior segment. Male S15 subtrapeziform, posterior margin narrower than anterior, sparsely covered with short to long setae on ventral side of S15 and lateral and posterior borders (Fig. 2F); sternite of genital segment sclerotized; posterior margin deeply concave between the gonopods, without medial bulge. Long setae scattered on the ventral surface of the genital segment. Gonopods short, appearing as a small hemispherical bulge, with two long setae, apically slightly sclerotized (Fig. 2F). No modification on legs 14 and 15 in males.

Table 3. *Lithobius (Ezembius) sui* sp. nov.: plectrotaxy of legs. Letters in brackets indicate spines on one leg of pair, or in one specimen.

Legs	Ventral					Dorsal				
	C	Tr	P	F	Ti	C	Tr	P	F	Ti
1	–	–	mp	amp	am	–	–	(a)mp	ap	a
2–4	–	–	mp	amp	am	–	–	(a)mp	ap	ap
5–7	–	–	mp	amp	am	–	–	amp	ap	ap
8–11	–	–	amp	amp	am	–	–	amp	ap	ap
12	–	m	amp	amp	am	a	–	amp	ap	ap
13	–	m	amp	amp	am	a	–	amp	(a)p	ap
14	–	m	amp	amp	am	a	–	amp	p	p
15	–	m	amp	amp	a	a	–	amp	p	–

Variations. Body length 12.15–18.85 mm; ocelli 1 + 4, 4, 1, 1 + 4, 3, 2 or 1 + 4, 3, 1; coxal pores 5664, 5665, 7775 or 8875 in female and 6886, 7665 in male.

Remarks. The two new species are very similar in morphology, especially in both having numerous minute setae scattered on surface of all tergites, but can be distinguished by the number of coxosternal teeth: *L. (E.) hualongensis* sp. nov. has 2 + 2 while *L. (E.) sui* sp. nov. has 3 + 3.

Etymology. The specific name is a patronym in honor of the zoologist Dr Jianping Su, Academician at the Chinese Academy of Sciences.

Habitat. The four specimens here examined (1 ♂, 3 ♀♀) were collected under granular gravel on the alpine meadows composed mainly of Gramineae, Cyperaceae, Leguminosae, Polygonaceae, Chenopodiaceae, Compositae, Rosaceae, Liliaceae and Cucurbitaceae. This region adjacent to Hualong County in the west features plateau continental, with mean annual precipitation 338.1 mm and average annual temperature 8.3 °C (<http://data.cma.cn/data/weatherBk.html>).

Key to the Chinese species of *Lithobius (Ezembius)*

- 1 Posterior angles of tergites with triangular projections ... *L. (E.) sulcipes* Attems, 1927
- Posterior angles of tergites rounded, without projections..... 2
- 2 At most four ocelli on each side of cephalic plate *L. (E.) parvicornis* (Porat, 1893)
- At least five ocelli on each side of cephalic plate 3
- 3 Cephalic plate with scattered, rough puncta and tergite with distinct puncta *L. (E.) rhysus* Attems, 1934
- Cephalic plate and tergite without any puncta 4
- 4 All ocelli subequal in size.... *L. (E.) sulcifemoralis* Takakuwa & Takashima, 1949
- All ocelli not subequal in size 5
- 5 Terminal two ocelli comparatively large 6
- Terminal one ocellus comparatively large 13
- 6 Ocelli arranged in two rows *L. (E.) laevidentata* Pei, Ma, Hou, Zhu & Gai, 2015
- Ocelli arranged in three rows 7

7	3 + 3 coxosternal teeth	8
–	2 + 2 coxosternal teeth	9
8	First article of female gonopods with 3 + 3 spurs.....	<i>L. (E.) sui sp. nov.</i>
–	First article of female gonopods with 2 + 2 spurs.....	<i>L. (E.) multispinipes</i> Pei, Lu, Liu, Hou, Ma & Zapparoli, 2016
9	Tömösváry's organ larger than adjoining ocellus.....	10
–	Tömösváry's organ smaller than adjoining ocellus	11
10	First article of female gonopods with 3 + 3 spurs ...	<i>L. (E.) hualongensis sp. nov.</i>
–	First article of female gonopods with 2 + 2 spurs.....	<i>L. (E.) bilineatus</i> Pei, Ma, Zhu & Gai, 2014
11	Apical claw of female gonopods simple, without inner small subtriangular teeth.	<i>L. (E.) tetraspinus</i> Pei, Lu, Liu, Hou & Ma, 2018
–	Apical claw of female gonopods simple, with inner small subtriangular teeth	12
12	Number of antennal articles 23 + 23	<i>L. (E.) anabilineatus</i> Ma, Pei, Hou, Zhu & Gai, 2015
–	Number of antennal articles 20 + 20–21 + 21	<i>L. (E.) dulensis</i> Qiao, Ma, Pei, Zhang & Su, 2019
13	Only five ocelli on each side of cephalic plate.....	<i>L. (E.) chekianus</i> Chamberlin & Wang, 1952
–	At least six ocelli on each side of cephalic plate.....	14
14	Tömösváry's organ smaller than adjoining ocellus.	15
–	Tömösváry's organ larger or subequal in size as adjoining ocellus	21
15	First article of female gonopods with 3 + 3 or 4 + 4 spurs	16
–	First article of female gonopods with 2 + 2 spurs.....	17
16	Apical claw of female gonopods simple, with inner small subtriangular teeth	<i>L. (E.) bidens</i> Takakuwa, 1939
–	Apical claw of female gonopods simple, without inner small subtriangular teeth.	<i>L. (E.) insolitus</i> Eason, 1993
17	Terminal claw of female gonopods bipartite	<i>L. (E.) anasulcifemoralis</i> Ma, Pei, Wu & Gai, 2013
–	Terminal claw of female gonopods simple	18
18	Terminal claw of female gonopods simple, with inner small triangular teeth.....	19
–	Terminal claw of female gonopods simple, without inner small triangular teeth....	20
19	Body length 11–12 mm, 15 th accessory spur absent	<i>L. (E.) rarihirsutipes</i> Zhang, 1996
–	Body length 17–18 mm, 15 th accessory spur present	<i>L. (E.) longibasitarsus</i> Qiao, Qin, Ma, Zhang, Su & Lin, 2018
20	DaC spine on 12 th –15 th legs	<i>L. (E.) asulcutus</i> Zhang, 1996
–	DaC spine absent.....	<i>L. (E.) giganteus</i> Sseliwanoff, 1881
21	Six ocelli on each side of cephalic plate	<i>L. (E.) gantoensis</i> Takakuwa & Takashima, 1949
–	At least seven ocelli on each side of cephalic plate	22
22	Ocelli arranged in two rows	<i>L. (E.) irregularis</i> Takakuwa & Takashima, 1949
–	Ocelli arranged in three rows	23

23	First article of female gonopods with 3 + 3 spurs.....	24
–	First article of female gonopods with 2 + 2 spurs.....	25
24	DaC spine on 14 th –15 th legs	<i>L. (E.) lineatus</i> Takakuwa, 1939
–	DaC spine on 12 th –15 th legs	<i>L. (E.) mandschreiensis</i> Takakuwa, 1940
25	Terminal claw of female gonopods tridentate	
	<i>L. (E.) zhui</i> Pei, Ma, Shi, Wu & Gai, 2011
–	Terminal claw of female gonopods simple	26
26	Terminal claw of female gonopods simple, without inner small triangular teeth..	
	<i>L. (E.) femorisulcutus</i> Zhang, 1996
–	Terminal claw of female gonopods simple, with inner small triangular teeth.....	27
27	Tarsal articulation on legs 1–13 well defined, 14 th accessory spur present	
	<i>L. (E.) datongensis</i> Qiao, Qin, Ma, Zhang, Su & Lin, 2018
–	Tarsal articulation on legs 1–13 not well defined, only 14 th posterior accessory spur present	<i>L. (E.) maqinensis</i> Qiao, Qin, Ma & Zhang, 2019

Acknowledgements

We are grateful to Dr Gregory D. Edgecombe, London, U. K., Dr Ivan H. Tuf, Olomouc, Czech Republic, Dr Pavel Stoev, Sofia, Bulgaria and Dr Marzio Zapparoli, Viterbo, Italy for their hospitality and everlasting help during our research, respectively. We thank Dr Rowland M. Shelley, North Carolina, USA, and Dr His-Te Shih, Tai-chung, China, for providing us with invaluable literature.

Funding

This work was financially supported by the the Strategic Priority Research Program of the Chinese Academy of Sciences [XDA23060602, XDA2002030302]; National Key R&D Program of China [2017YFC0506405]; and Qinghai Key R&D and Transformation Program [2019-SF-150].

References

- Attems C (1927) Neue Chilopoden. Zoologischer Anzeiger 72: 291–305.
- Attems C (1934) Einige neue Geophiliden und Lithobiiden des Hamburger Museums. Zoologischer Anzeiger 107: 310–317.
- Bonato L, Edgecombe GD, Lewis JGE, Minelli A, Pereira LA, Shelley RM, Zapparoli M (2010) A common terminology for the external anatomy of centipedes (Chilopoda). ZooKeys 69: 17–51. <https://doi.org/10.3897/zookeys.69.737>
- Bonato L, Chagas Junior A, Edgecombe GD, Lewis JGE, Minelli A, Pereira LA, Shelley RM, Stoev P, Zapparoli M (2016) ChiloBase 2.0 – A World Catalogue of Centipedes (Chilopoda). <http://chilobase.biologia.unipd.it> [Accessed 01 January 2019]

- Chamberlin RV (1919) The Chilopoda collected by the Canadian Arctic Expedition, 1913–1918. Report of the Canadian Arctic Expedition, 1913–1918 (Volume III). Insects. Part H: Spiders, Mites and Myriapods, 15–22.
- Chamberlin RV (1923) Chilopoda. In: US Bureau of Biological Survey (Ed.) A Biological Survey of the Pribilof Islands. North American Fauna Vol. 46, 240–244.
- Chamberlin RV, Wang YX (1952) Some records and descriptions of Chilopods from Japan and other oriental areas. Proceeding of the Biological Society of Washington 65: 177–188.
- Eason EH (1976) The type specimens and identity of the Siberian species described in the genus *Lithobius* by Anton Stuxberg in 1876 (Chilopoda: Lithobiomorpha). Zoological Journal of the Linnean Society 58(2): 91–127. <https://doi.org/10.1111/j.1096-3642.1976.tb00822.x>
- Eason EH (1986) On the synonymy of *Lithobius giganteus* Seliwanoff, 1881 and the taxonomic status of *Porobius* Attems, 1926 (Chilopoda). Annalen des Naturhistorischen Museums in Wien, Serie B (87): 181–192.
- Eason EH (1992) On the taxonomy and geographical distribution of the Lithobiomorpha. Berichte Des NaturwissenschaftlichMedizinischen Vereins in Innsbruck Supplement 10: 1–9.
- Eason EH (1993) Descriptions of four new species of *Lithobius* from the Oriental region and a redescription of *Australobius palnis* (Eason, 1973) from Sri Lanka (Chilopoda: Lithobiomorpha). Bollettino del museo civico di storia naturale di Verona 17: 181–199.
- Ma H, Lu Y, Liu H, Hou X, Pei S (2018) *Hessebius luculentus*, a new species of the genus *Hessebius* Verhoeff, 1941 from China (Lithobiomorpha, Lithobiidae). ZooKeys 741: 193–202. <https://doi.org/10.3897/zookeys.741.20061>
- Ma H, Pei S, Hou X, Zhu T (2014a) *Lithobius (Monotarsobius) zhangii* sp. nov., a new species from Eastern China (Chilopoda, Lithobiomorpha, Lithobiidae). ZooKeys 459: 1–10. <https://doi.org/10.3897/zookeys.459.8169>
- Ma H, Pei S, Hou X, Zhu T, Gai Y (2015) *Lithobius (Ezembius) anabilineatus* sp. nov., a new species (Lithobiomorpha: Lithobiidae) from Eastern China. Oriental Insects 49(3–4): 256–263. <https://doi.org/10.1080/00305316.2015.1081647>
- Ma H, Pei S, Hou X, Zhu T, Wu D, Gai Y (2014b) An annotated checklist of Lithobiomorpha of China. Zootaxa 3847(3): 333–358. <https://doi.org/10.11646/zootaxa.3847.3.2>
- Ma H, Pei S, Wu D, Gai Y (2013) A new lithobiid centipede of *Lithobius (Ezembius)* (Lithobiomorpha) from China. Oriental Insects 1: 1–6. <https://doi.org/10.1080/00305316.2012.753763>
- Pei S, Lu Y, Liu H, Hou X, Ma H, Zapparoli M (2016) *Lithobius (Ezembius) multispinipes* n. sp., a new species of centipede from Northwest China (Lithobiomorpha: Lithobiidae). Zootaxa 4169(2): 390–400. <https://doi.org/10.11646/zootaxa.4169.2.12>
- Pei S, Lu Y, Liu H, Hou X, Ma H (2018) *Lithobius (Ezembius) tetraspinus*, a new species of centipede from northwest China (Lithobiomorpha, Lithobiidae). ZooKeys 741: 203–217. <https://doi.org/10.3897/zookeys.741.19980>
- Pei S, Ma H, Hou X, Zhu T, Gai Y (2015) *Lithobius (Ezembius) laevidentata* sp. nov., a new species (Chilopoda: Lithobiomorpha: Lithobiidae) from the Northwest region of China. Biologia 70(8): 1113–1117.
- Pei S, Ma H, Shi B, Wu D, Gai Y (2011) A new centipede species of *Lithobius* Leach (Lithobiomorpha: Lithobiidae) from China. Oriental Insects 45(1): 108–114. <https://doi.org/10.1080/00305316.2011.590642>

- Pei S, Ma H, Zhu T, Gai Y (2014) A new species of *Lithobius* (*Ezembius*) Chamberlin (Lithobiomorpha: Lithobiidae) from China. *Oriental Insects* 48(1–2): 102–107. <https://doi.org/10.1080/00305316.2014.959787>
- Qin W, Lin G, Zhao X, Li B, Xie J, Ma H, Su J, Zhang T (2014) A new species of *Australobius* (Lithobiomorpha: Lithobiidae) from the Qinghai-Tibet Plateau, China. *Biologia* (11): 1601–1605. <https://doi.org/10.2478/s11756-014-0459-4>
- Qiao P, Qin W, Ma H, Su J, Zhang T (2018a) Two new species of the genus *Hessebius* Verhoeff, 1941 from China (Lithobiomorpha, Lithobiidae). *ZooKeys* 735: 65–82. <https://doi.org/10.3897/zookeys.735.22237>
- Qiao P, Qin W, Ma H, Zhang T, Su J, Lin G (2018b) Two new species of *Lithobius* on Qinghai-Tibetan plateau identified from morphology and COI sequences (Lithobiomorpha: Lithobiidae). *ZooKeys* 785: 11–28. <https://doi.org/10.3897/zookeys.785.28580>
- Qiao P, Qin W, Ma H, Zhang T (2019a) Two new species of lithobiid centipedes and the first record of *Lamyctes africanus* Porath (Chilopoda: Lithobiomorpha) in China. *Journal of Natural History* 53(15–16): 897–921. <https://doi.org/10.1080/00222933.2019.1606355>
- Qiao P, Ma H, Pei S, Zhang T, Su J (2019b) *Lithobius* (*Ezembius*) *polyommatus* sp. nov. and *Lithobius* (*Ezembius*) *dulanensis* sp. nov. (Lithobiomorpha: Lithobiidae), two new species from Qinghai-Tibet Plateau, China. *Biologia* 74(5): 455–462. <https://doi.org/10.2478/s11756-018-00173-z>
- Takakuwa Y (1939) *Bothropolys*-Arten aus Japan. *Transactions of the Natural History Society of Formosa* 29(188): 103–110.
- Takakuwa Y (1940) Class Chilopoda, Epimorpha, Lithobiomorpha. *Fauna Nipponica* (Vol. 9) Fas. 8 No. (3). Sanseido Book Store, Tokyo, 104 pp.
- Takakuwa Y, Takashima H (1949) Myriapods collected in Shansi, North China. *Acta Arachnologica* 11(3–4): 51–69. <https://doi.org/10.2476/asjaa.11.51>
- Zapparoli M, Edgecombe GD (2011) Lithobiomorpha. In: Minelli A (Ed.) *Treatise on Zoology – Anatomy, Taxonomy, Biology – The Myriapoda* (Vol. 1). Jorandaan Luchtmans, Brill, 538pp.
- Zhang CZ (1996) Chilopoda: Lithobiomorpha. In: Wu SG, Feng ZJ (Eds) *The Biology and Human Physiology in the Hoh Xil Region. The Series of the Comprehensive Scientific Expedition to the Hoh Xil Region*, Science Press, Beijing, 357 pp. [In Chinese with English summary]

Under an integrative taxonomic approach: the description of a new species of the genus *Loxosceles* (Araneae, Sicariidae) from Mexico City

Alejandro Valdez-Mondragón^{1,3}, Claudia I. Navarro-Rodríguez^{2,4},
Karen P. Solís-Catalán^{2,4}, Mayra R. Cortez-Roldán², Alma R. Juárez-Sánchez²

1 CONACYT Research Fellow. Laboratory of Arachnology (LATLAX), Laboratorio Regional de Biodiversidad y Cultivo de Tejidos Vegetales (LBCTV), Instituto de Biología, Universidad Nacional Autónoma de México (UNAM), sede Tlaxcala, Ex-Fábrica San Manuel, San Miguel Contla, C. P. 90640 Santa Cruz Tlaxcala, Tlaxcala, Mexico **2** Laboratory of Arachnology (LATLAX), Laboratorio Regional de Biodiversidad y Cultivo de Tejidos Vegetales (LBCTV), Instituto de Biología, Universidad Nacional Autónoma de México (UNAM), sede Tlaxcala, Mexico **3** Colección Nacional de Arácnidos (CNAN), Departamento de Zoología, Instituto de Biología, Universidad Nacional Autónoma de México, (UNAM), Ciudad Universitaria, Apartado Postal 04510, Coyoacán, Mexico City, Mexico **4** Posgrado en Ciencias Biológicas, Centro Tlaxcala de Biología de la Conducta (CTBC), Universidad Autónoma de Tlaxcala (UATx), Carretera Federal Tlaxcala-Puebla, Km. 1.5, C. P. 90062, Tlaxcala, Tlaxcala, Mexico

Corresponding author: *Alejandro Valdez-Mondragón* (lat_mactans@yahoo.com.mx)

Academic editor: *A. Pérez-González* | Received 30 August 2019 | Accepted 4 October 2019 | Published 27 November 2019

<http://zoobank.org/E176337C-6F78-4462-8FD0-ACB727C043E4>

Citation: Valdez-Mondragón A, Navarro-Rodríguez CI, Solís-Catalán KP, Cortez-Roldán MR, Juárez-Sánchez AR (2019) Under an integrative taxonomic approach: the description of a new species of the genus *Loxosceles* (Araneae, Sicariidae) from Mexico City. ZooKeys 892: 93–133. <https://doi.org/10.3897/zookeys.892.39558>

Abstract

A new species of the spider genus *Loxosceles* Heineken & Lowe, 1832, *Loxosceles tenochtitlan* Valdez-Mondragón & Navarro-Rodríguez, **sp. nov.**, is described based on adult male and female specimens from the states of Mexico City, Estado de Mexico and Tlaxcala. Integrative taxonomy including traditional morphology, geometric and lineal morphology, and molecules (DNA barcodes of cytochrome *c* oxidase subunit 1 (CO1) and internal transcribed spacer 2 (ITS2)), were used as evidence to delimit the new species. Four methods were used for molecular analyses and species delimitation: 1) corrected *p*-distances under neighbor joining (NJ), 2) automatic barcode gap discovery (ABGD), 3) general mixed yule coalescent model (GMYC), and 4) poisson tree processes (bPTP). All molecular methods, traditional, geometric and lineal morphology were consistent in delimiting and recognizing the new species. *Loxosceles tenochtitlan* **sp. nov.** is closely related to *L. misteca* based on molecular data. Although both species are morphologically similar, the average *p*-distance from CO1 data was 13.8% and 4.2% for ITS2 data. The molecular species

delimitation methods recovered well-supported monophyletic clusters for samples of *L. tenochtitlan* **sp. nov.** from Mexico City + Tlaxcala and for samples of *L. misteca* from Guerrero. *Loxosceles tenochtitlan* **sp. nov.** is considered a unique species for three reasons: (1) it can be distinguished by morphological characters (genitalic and somatic); (2) the four different molecular species delimitation methods were congruent to separate both species; and (3) there is variation in leg I length of males between both species, with the males of *L. misteca* having longer legs than males of *L. tenochtitlan* **sp. nov.**, also morphometrically, the shape of tibiae of the palp between males of both species is different.

Keywords

DNA barcodes, ecological niche modeling, *Loxosceles tenochtitlan* sp. nov., species delimitation, taxonomy

Introduction

The spider family Sicariidae Keyserling, 1880 comprises three genera: *Hexophthalma* Karsch, 1879 with eight species from Africa, *Sicarius* Walckenaer, 1847 with 21 species distributed in Central and South America, and *Loxosceles* Heineken & Lowe, 1832, with 139 described species worldwide (Magalhães et al. 2017; WSC 2019). Spiders of the genus *Loxosceles* are better known in North America as “violin spiders”, “recluse spiders”, or “brown recluse spiders”. They are well known by the medical community and general public as their bites can cause dermonecrotic lesions due to the action of Sphingomyelinase D, an enzyme in their venom that destroys endothelial cells lining the blood vessels (Sandidge and Hopwood 2005; Vetter 2008, 2015; Ramos-Rodríguez and Méndez 2008; Manríquez and Silva 2009; Swanson and Vetter 2009).

Gertsch (1958, 1967) and Gertsch and Ennik (1983) proposed that the species of *Loxosceles* belong in eight species groups: *reclusa*, *laeta*, *amazonica*, *gaucho*, *spadicea*, *rufescens*, *vonwredei*, and *spinulosa*. However, Duncan et al. (2010) and Fukushima et al. (2017), using molecular data, synonymized the species group *amazonica* with the species group *rufescens*; therefore, the genus is currently composed of seven species groups. The *reclusa* group has the highest diversity, with more than 50 species from North America, the majority from Mexico (Gertsch and Ennik 1983).

Mexico has the highest diversity of *Loxosceles* worldwide, with 39 species, 37 native (not including the new species described here), and two introduced species: *Loxosceles reclusa* Gertsch & Mulaik, 1940 and *Loxosceles rufescens* (Dufour, 1820) (Gertsch 1958, 1973; Gertsch and Ennik 1983; Valdez-Mondragón et al. 2018b, WSC 2019). Species diversity is greater in the north, decreasing to the south (Valdez-Mondragón et al. 2018b: figs 73–76). The states with the greatest diversity are Baja California Sur, Baja California and Sonora, with five species each (Valdez-Mondragón et al. 2018a, b). *Loxosceles boneti* Gertsch, 1958 is the most common species in Mexico, primarily found in the central region of the country (Valdez-Mondragón et al. 2018b). The preferred habitats of *Loxosceles* in Mexico are mainly dry and tropical forests, including tropical deciduous forests, and deserts; however, some species, such as *L. chinateca* and *L. yucatanana*, are distributed in tropical rain forests. Additionally, some species have

been recorded from caves, a preferred microhabitat of Mexican species (e.g., *L. misteca*, *L. boneti*, *L. chinateca*, *L. tehuana*, *L. tenango*, and *L. yucatanana*) (Valdez-Mondragón et al. 2018b). The first species described from Mexico was *Loxosceles yucatanana* Chamberlin & Ivie, 1938 from the Yucatan Peninsula, and the most recently described was *Loxosceles malintzi* Valdez-Mondragón, Cortez-Roldán, Juárez-Sánchez & Solís-Catalán, 2018 from the central region of Mexico (Valdez-Mondragón et al. 2018b). To date, the taxonomy of the species has been based only on traditional morphology, using genitalic characters, male palps and seminal receptacles in females.

Modern taxonomy uses multiple lines of evidence for species recognition, identification, diagnosis and delimitation. Several recently developed molecular delimitation methods have highlighted the extensive inconsistency in classical morphological taxonomy (Ortiz and Francke 2016). Molecular methods have provided a new way to resolve species delimitation problems by using the infra-specific genealogical information in DNA markers which provides objective implementation of modern species concepts (e.g., biological, phylogenetic, genotypic cluster). The appropriate way to species delimitation research is to analyze the data with a wide variety of methods and different lines of evidence to delimit lineages that are consistent across the results, understanding the behavior of the molecular species delimitation methods and contributing in this way to integrative taxonomy (Carstens et al. 2013, Luo et al. 2018).

Currently, there are two separate tasks to which DNA barcodes are being applied in modern systematics. The first is distinguishing between species (equivalent to species identification or species diagnosis), and the second is the use of DNA data to discover new species (equivalent to species delimitation and species description) (DeSalle et al. 2005). For some groups of organisms, including some groups of spiders, morphology alone cannot determine species boundaries, and identifying morphologically inseparable cryptic or sibling species requires a new set of taxonomic tools, including the analysis of molecular data (Jarman and Elliott 2000; Witt and Hebert 2000; Proudlove and Wood 2003; Hebert et al. 2003, 2004; Bickford et al. 2007; Hamilton et al. 2011, 2014, 2016; Ortiz and Francke 2016). The spider genus *Loxosceles* is no exception. Recent studies based on molecular evidence have suggested that the known diversity within the genus could be highly underestimated (Binford et al. 2008; Duncan et al. 2010; Planas and Ribera 2014, 2015; Tahami et al. 2017). One important factor leading to the underestimation is widespread intraspecific variation in sexual structures, mainly in the seminal receptacles of females, something noted previously by Brignoli (1968) and Gertsch and Ennik (1983) and recently by Valdez-Mondragón et al. (2018b) in the case of the species from Mexico.

The primary aim of this study is to use an integrative taxonomic approach for the delimitation and description of a new species of *Loxosceles* from Mexico City. We analyzed DNA barcodes and used traditional morphology, ultra-morphology, geometric and linear morphometrics, biogeography, and ecological niche modeling for species delimitation. This is the first-time multiple lines of evidence have been used in the taxonomy of the genus.

Materials and methods

Biological material

The specimens of the new species were collected and deposited in 80% ethanol and labeled with their complete field data. The type specimens and additional examined material are deposited with their collection codes in the Laboratory of Arachnology (**LAT-LAX**), Laboratorio Regional de Biodiversidad y Cultivo de Tejidos Vegetales (**LBCTV**), Institute of Biology, Universidad Nacional Autónoma de México (**IBUNAM**), Tlaxcala City. The male holotype of *Loxosceles misteca* Gertsch, 1958 was examined and is deposited at the American Museum of Natural History (**AMNH**). The descriptions and observations of the specimens were done using a Zeiss Discovery V8 stereoscope. A Zeiss Axiocam 506 color camera attached to a Zeiss AXIO Zoom V16 stereoscope was used to photograph the different structures of specimens. The female seminal receptacles and male palps were dissected in ethanol (80%) and cleaned in potassium hydroxide (KOH-10%) for 5 to 10 min. Habitus, seminal receptacles and palps were submerged in 96% gel alcohol and covered with a thin layer of liquid ethanol (80%) to minimize diffraction during photography (Valdez-Mondragón and Francke 2015). For the photomicrographs, the morphological structures were dissected and cleaned with an ultrasonic cleaner at 20–40 kHz; subsequently, they were critical-point dried, and examined at low vacuum in a Hitachi S-2460N Scanning Electron Microscope (**SEM**). The descriptions follow Valdez-Mondragón et al. (2018b). All measurements in the descriptions are in millimeters (mm). Scale measurements on photomicrographs are in micrometers (μm). The distribution map was made using QGIS v. 2.18. Expeditions for collecting additional material deposited at LATLAX of different species were carried out in Puebla (March and June 2017), Tlaxcala (April 2017), Hidalgo (May 2017), Oaxaca (June 2017), Guerrero (September 2017), and Oaxaca (March 2018). Abbreviations:

AME	anterior median eyes;	PLS	posterior lateral spinnerets;
PLE	posterior lateral eyes;	PME	posterior median eyes.

Taxon sampling

The molecular analyses presented here are based on a total of 52 individuals from 11 species of *Loxosceles*, including the new species described here and two outgroups: *Loxosceles rufescens* (Dufour, 1820) and *Scytodes thoracica* (Latreille, 1802) (Table 1). Three different partitions were used (CO1: 656 bp, ITS: 435 bp, and CO1+ITS2: 1091 bp).

DNA extraction, amplification and sequencing

Specimens for DNA extraction were preserved in ethanol (96%) and kept at $-20\text{ }^{\circ}\text{C}$. DNA was isolated from legs, prosoma or complete specimens in the case of im-

Table 1. Specimens sequenced for each species, DNA voucher numbers, localities, and GenBank accession numbers.

Species	DNA voucher LATLAX	Locality	GenBank accession number	
			COI	ITS2
<i>L. misteca</i>	Ara0082	Mexico: Guerrero	MK936272	MK957212
	Ara0089	Mexico: Guerrero	MK936273	MK957215
	Ara0090	Mexico: Guerrero	MK936274	MK957214
	Ara0084	Mexico: Guerrero	MK936275	MK957213
	Ara0236	Mexico: Guerrero	MK936276	–
	Ara0237	Mexico: Guerrero	MK936277	–
<i>L. tenochtitlan</i> sp. nov.	Ara0146	Mexico: Mexico City	MK936278	MK957209
	Ara0161	Mexico: Mexico City	MK936279	–
	Ara0173	Mexico: Tlaxcala	MK936280	MK957210
	Ara0164	Mexico: Tlaxcala	MK936281	MK957211
<i>L. malintzi</i>	Ara0100	Mexico: Guerrero	MK936282	MK957220
	Ara0001	Mexico: Puebla	MK936283	MK957218
	Ara0002	Mexico: Puebla	MK936284	–
	Ara0025	Mexico: Puebla	MK936285	MK957219
	Ara0072	Mexico: Puebla	MK936286	MK957222
	Ara0074	Mexico: Puebla	MK936287	MK957223
	Ara0101	Mexico: Guerrero	MK936288	–
	Ara0004	Mexico: Puebla	MK936289	MK957221
	Ara0191	Mexico: Hidalgo	MK936290	–
<i>L. tenango</i>	Ara0192	Mexico: Hidalgo	MK936291	MK957201
	Ara0045	Mexico: Hidalgo	–	MK957195
	Ara0189	Mexico: Hidalgo	–	MK957196
	Ara0190	Mexico: Hidalgo	–	MK957197
	Ara0193	Mexico: Hidalgo	–	MK957198
	Ara0188	Mexico: Hidalgo	–	MK957200
	Ara0186	Mexico: Hidalgo	MK936292	MK957194
	Ara0048	Mexico: Hidalgo	MK936293	–
	Ara0046	Mexico: Hidalgo	–	MK957192
<i>Loxosceles</i> sp. 1	Ara0047	Mexico: Hidalgo	–	MK957193
	Ara0183	Mexico: Hidalgo	–	MK957199
	Ara0175	Mexico: Hidalgo	MK936294	MK957208
	Ara0181	Mexico: Hidalgo	MK936295	MK957206
	Ara0182	Mexico: Hidalgo	MK936296	MK957207
	Ara0174	Mexico: Hidalgo	–	MK957202
	Ara0176	Mexico: Hidalgo	–	MK957203
	Ara0177	Mexico: Hidalgo	–	MK957204
	Ara0178	Mexico: Hidalgo	–	MK957205
<i>L. nahuana</i>	Ara0076	Mexico: Hidalgo	MK936297	MK957216
	Ara0077	Mexico: Hidalgo	MK936298	–
	Ara0079	Mexico: Hidalgo	MK936299	MK957217
<i>L. zapoteca</i>	Ara0094	Mexico: Guerrero	MK936300	MK957224
	Ara0220	Mexico: Guerrero	MK936301	–
	Ara0227	Mexico: Guerrero	MK936302	–
<i>L. colima</i>	Ara0115	Mexico: Colima	MK936303	MK957224
<i>Loxosceles</i> sp. 2	Ara0194	Mexico: Guerrero	MK936304	–
	Ara0198	Mexico: Guerrero	MK936305	–
	Ara0199	Mexico: Guerrero	MK936306	–
	Ara0205	Mexico: Guerrero	MK936307	–
	Ara0209	Mexico: Guerrero	MK936308	–
	Ara0210	Mexico: Guerrero	MK936309	–
	Ara0204	Mexico: Guerrero	MK936310	–
	GenBank	Greece: Peloponnese	–	KR864735
<i>L. rufescens</i>	GenBank	Turkey: Antalya	KR864739	
<i>Scytodes thoracica</i>	GenBank			

Table 2. Primers used for PCR.

Gene	Primer name	Primer sequence (5'–3')	Reference
CO1	LCO	GGT CAA CAA ATC ATA AAG ATA TTG G	Folmer et al. (1994)
	HCO	TAA ACT TCA GGG TGA CCA AAA AAT CA	
	LCO-JJ	CHA CWA AYC ATA AAG ATA TYG G	Astrin and Stueben (2008)
	HCO-JJ	AWA CTT CVG GRT GCV CAA ARA ATC A	
ITS2	5.8S	CAC GGG TCG ATG AAG AAC GC	Ji et al. (2003),
	CAS28sB1d	TTC TTT TCC TCC SCT TAY TRA TAT GCT TAA	Planas and Ribera (2014)

matures. DNA extractions were done using a Qiagen DNeasy Tissue Kit following the protocol of Valdez-Mondragón and Francke (2015). DNA fragments included approximately 650 bp of the cytochrome *c* oxidase subunit 1 (CO1) mitochondrial gene, and 435 bp of the Internal Transcribed Spacer 2 (ITS2) nuclear gene. The fragments were amplified using the primers in Table 2. Amplifications were carried out in a Veriti Applied-Biosystems 96 Well Thermal Cycler, in a total volume of 25 μ L: 3 μ L DNA, 8.7 μ L H₂O, 12.5 μ L Multiplex PCR Kit of QIAGEN, 0.4 μ L of each molecular marker (forward and reverse). The PCR program for CO1 was as follows: initial step 1 min at 95 °C; amplification 35 cycles of 30 sec at 95 °C (denaturation), 30 sec at 48 °C (annealing), 1 min at 72 °C (elongation), and final elongation 5 min at 72 °C. PCR program for ITS2 was as follows: initial step 3 min at 94 °C; amplification 40 cycles of 30 sec at 94 °C (denaturation), 1 min at 53 °C (annealing), 1 min at 72 °C (elongation), and final elongation 5 min at 72 °C. PCR products were checked to analyze length and purity on 1% agarose gels with a marker of 100 bp and purified directly using the QIAquick PCR Purification kit of QIAGEN. DNA extraction and amplification were performed at the Molecular Laboratory at the Laboratorio Regional de Biodiversidad y Cultivo de Tejidos Vegetales (LBCTV), Institute of Biology, Universidad Nacional Autónoma de México (UNAM), Tlaxcala City. Sequencing was performed at the Molecular Laboratory at the Institute of Biology, UNAM, Mexico City. Sequencing of both strands (5'–3' and 3'–5') of PCR products were performed in a Sequencer Genetic Analyzer RUO Applied Biosystems Hitachi model 3750xL. Sequence data of CO1 and ITS2 are deposited in GenBank with accession numbers: MK936272–MK936310 for CO1 and MK957192–MK957225 for ITS2 (Table 1).

DNA sequence alignment and editing

Sequences were edited with the programs BioEdit v. 7.0.5.3 (Hall 1999) and Geneious v. 10.2.3 (Kearse et al. 2012). Sequences were aligned online using the default gap opening penalty of 1.53 in MAFFT (Multiple sequence alignment based on Fast Fourier Transform) v. 7 (Katoh and Toh 2008) using the following alignment strategy: Auto (FFT-NS-2, FFTNS-i or L-INS-i; depending on data size). These aligned matrices were subsequently used in analyses.

Molecular analyses, species delimitation and haplotypes networks

For molecular species delimitation four methods were used for analyzing the concatenated CO1+ITS2 matrix (1091 characters): 1) *p*-distances under neighbor joining (NJ) using MEGA v. 7.0, 2) automatic barcode gap discovery (ABGD) online version (Puillandre et al. 2012) using both uncorrected and K2P distance matrices. 3) general mixed yule coalescent model (GMYC) (Pons et al. 2006) using GMYC web server (<https://species.h-its.org/gmyc/>), and 4) Bayesian Poisson tree process (bPTP) (Zhang et al. 2013, Kapli et al. 2017) using web server (<https://species.h-its.org/ptp/>). The models of sequence evolution were selected using the Akaike information criterion (AIC) in jModelTest v. 2.1.10 (Posada and Buckley 2004). The models selected for CO1 for each partition block were: GTR+G+I (1st and 2nd codon positions) and GTR+G (3rd position). The model selected for ITS2 was GTR+G. The bootstrap values in the NJ analysis were calculated with the following commands: Number of replicates = 1000, Bootstrap support values = 1000 (significant values $\geq 50\%$), Substitution type = nucleotide, Model = Kimura 2-parameter, Substitution to Include = d: transitions + transversions, Rates among Sites = Gamma distributed (G), missing data treatment = pairwise deletion, select codon position = 1st+2nd+3rd+Noncoding Sites. The approaches for DNA barcoding tree-based delimitation explicitly use the phylogenetic species concept. A starting tree is input with Maximum Likelihood (ML) using MEGA v. 7.0, and Bayesian inference (BI) using MrBayes v. 3.1.2 (Ronquist and Huelsenbeck 2003) were implemented, and the analysis recognizes monophyletic cluster by searching differential intra- and inter-specific branching patterns (Ortiz and Francke 2016). The ML analysis was calculated with the parameters for CO1 and ITS2: Number of replicates = 1000, Bootstrap support values = 1000 (significant values $\geq 50\%$), Models of sequence evolution selected using jModelTest = GTR, Rates among sites = G+I, No. of discrete Gamma Categories = 6, Gaps Data Treatment = Complete deletion, Select Codon Position = 1st+2nd+3rd+Noncoding Sites, ML Heuristic Method = Subtree-Pruning-Regrafting – Extensive (SPR level 5), Initial Tree for ML = Make initial tree automatically (Default – NJ/BioNJ). The BI analyses were run with four parallel Markov chains with the following parameters: MCMC (Markov Chain Monte Carlo) generations = 20000000, sampling frequency = 1000, print frequency = 1000, number of runs = 2, number of chains = 4, MCMC burnin = 2500, sumt burnin = 2500, sump burnin = 2500, Models of sequence evolution selected using jModelTest = GTR, Rates among sites = G+I, Select Codon Position = 1st, 2nd, and 3rd. TRACER v. 1.6 (Rambaut and Drummond 2003–2009) was used to analyze the parameters and the effective sample size (ESS) of the MCMC to ensure the runs converged. FigTree v. 1.4.3 was used to visualize the topology of the tree with the posterior probability values (PP) at nodes. The ABGD species delimitation method uses recursive partitioning with a range of prior intraspecific divergence and relative gap widths, estimating the threshold between intra- and interspecific genetic variation, generating species-level groupings (Ortiz and Francke 2016). ABGD analyses were conducted using both uncorrected and K2P distance matrices with default options: Pmin = 0.001, Pmax = 0.1, Steps = 10,

Relative gap width (X) = 1, Nb bins = 20. The GMYC species delimitation method applies single (Pons et al. 2006) or multiple (Monaghan et al. 2009) time thresholds to delimit species in a Maximum Likelihood context, using ultrametric trees (Ortiz and Francke 2016). Phylogenetic analyses were run in BEAST v. 2.6.0 (Drummond et al. 2012) using a coalescent (constant population) tree prior. Independent lognormal relaxed clock was applied to each partition, for analyses of 20×10^6 generations were run. Convergence was assessed with TRACER v. 1.6 (Rambaut and Drummond 2014). TREEANNOTATOR v. 2.6.0 (BEAST package) was used to build maximum clade credibility trees, after discarding the first 25% of generations by burn-in. Following gene tree inference, GMYC was implemented in the web interface for single and multiple threshold GMYC (<https://species.h-its.org/gmyc/>) the backend of this web server runs the original R implementation of the GMYC model authored by Fujisawa and Barraclough (2013). A single threshold was used for the concatenated matrix. The PTP species delimitation method (Zhang et al. 2013) is similar to GMYC, but uses substitution calibrated (not ultrametric) trees to avoid the potential flaws in constructing time calibrated phylogenies (Zhang et al. 2013, Ortiz and Francke 2016). We employed the Bayesian variant of the method (bPTP) on the online version (<https://species.h-its.org/ptp/>). It was run on the Bayesian gene trees with default options: rooted tree, MCMC generations = 100000, Thinning = 100, Burnin = 0.1, Seed = 123. Haplotypes network for CO1 was constructed to visualize the mutations among haplotypes of species using the TCS algorithm (Clement et al. 2000) in PopArt v. 1.7 (Leigh and Bryant 2015).

Geometric and linear morphometry and sexual dimorphism

For the morphometric studies, tibiae of adult males in retrolateral views of *L. tenochtitlan* sp. nov. ($N = 12$) and *L. misteca* ($N = 9$) were analyzed using Make Fan 8 v. 1.0 software (Sheets and Zelditch 2014), performing brand and semi-brand protocols. Using TPsUtil v. 1.76 software (Rohlf 2015) the file was formatted (.tps) to perform the digitalization of the landmarks and semi-landmarks of the contours in the tpsDig v. 2.31 software (Rohlf 2015). In the CordGen8 v. 1.0 software (Sheets and Zelditch 2014), a “Procrustes” alignment was made for the brands and with the Semi Land option included in the CordGen8 v. 1.0 software (Sheets and Zelditch 2014). Posteriorly, the alignment of the semi-landmarks was carried out. To analyze the formation of groups in relation to the tibia shape, an analysis of canonical variables (CVA) was performed with the CVA Gen 8 v. 1.0 software. To analyze sexual dimorphism and variation in the new species, a T-test was performed to evaluate if the females and males have significant statistical differences in: 1) leg I length, 2) carapace length, and 3) carapace width. Also, leg I length was used to test if differences exist between the new species and *Loxosceles misteca* Gertsch, 1958; species that appears to be closely related to *L. tenochtitlan* sp. nov. morphologically. Forty specimens of *Loxosceles tenochtitlan* sp. nov. (24 females and 16 males) and 22 specimens of *L. misteca* (11 females and 11 males) were measured (Table 5). The statistical analysis was carried out and graphics were made with R studio v.1.1.463 software.

Ecological niche modeling (ENM)

For georeferencing and corroboration of localities, two programs were used: GeoLocate online version (<http://www.museum.tulane.edu/geolocate/>) and Google Earth v. 7.1.5.1557. The geographic coordinates were transformed from NAD83 to WGS84 online on INEGI: Transformation of coordinates TRANINV (INEGI 2019). Geographical coordinates are given in degrees. ENM data were generated using Maxent v. 3.3 (Maximum Entropy Algorithm) (Phillips et al. 2004) which estimates the probability of the presence of a lineage by looking for the distribution of maximum entropy (as uniform as possible) based on both quantitative and qualitative environmental variables. The AUC (Area Under the Curve) variable measures the ability of models to discriminate true and false positives for ENM using the following scale: excellent (AUC > 0.90), good (0.80 > AUC < 0.90), acceptable (0.70 > AUC < 0.80) (Phillips et al. 2006; Phillips and Dudík 2008; Illoldi-Rangel and Escalante 2008). ENM was conducted using 19 climatic variables: 17 from WorldClim v.1.0. (<http://www.worldclim.org/>) (BIO1-BIO19) (Fick and Hijmans 2017) and two from CONABIO (<http://www.conabio.gob.mx/informacion/gis/>) (CON01: vegetation type, and CON02: level curves for the Mexican Republic) (CONABIO, 2015). The climatic variables were previously processed in QGIS v. 2.18 “Las Palmas” to be read in MaxEnt. The ENM prediction and distribution maps were made using QGIS. Maps were edited using Adobe Photoshop CS6.

Taxonomy

Family Sicariidae Keyserling, 1880

Genus *Loxosceles* Heineken & Lowe, 1832

Type species. *Loxosceles rufescens* (Dufour, 1820).

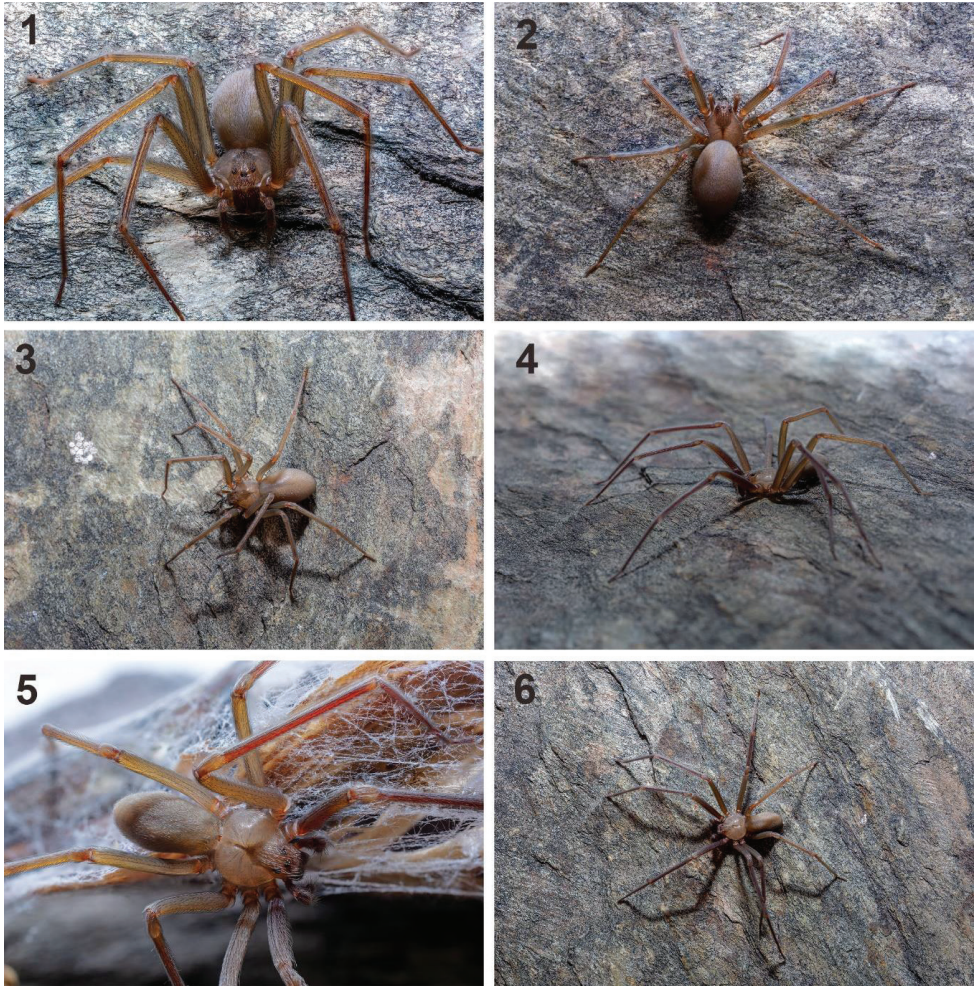
Loxosceles tenochtitlan Valdez-Mondragón & Navarro-Rodríguez, sp. nov.

<http://zoobank.org/C87C7B99-E4A7-41CC-8F79-4229A05BBDB9>

Figs 1–9, 13–17, 19–28, 32–37, 48–61

Type material. MEXICO: *Mexico City*: male holotype (LATLAX-T001) from Street Cruz Verde No. 132 (lat 19.2921, lon -99.174203; 2281 m), Tlalpan, 10-XII-2017, M. Sánchez-Vilchis leg. (inside house). Paratypes: 1 female (LATLAX-T002), 2 males (LATLAX-T003), 4 females (LATLAX-0004), same data as holotype.

Other material examined. MEXICO: *Mexico City*: 5 females, 1 immature (LATLAX-Ara 0539), same data as holotype. 3 males, 8 immatures (LATLAX-Ara 0540), same data as holotype. 1 male (LATLAX-Ara 0542), 19-I-2019, A. Valdez leg., same



Figures 1–6. Live specimens of *Loxosceles tenochtitlan* sp. nov. from Street Juárez Norte #214, Huamantla, Municipality Huamantla, Tlaxcala, Mexico **1–3** females **4–6** males. Photographs by Jared Lacayo-Ramírez (2019).

locality as holotype. 1 female, 1 immature (LATLAX-Ara0156) from Street Tepocatl #61, Pedregal de Santo Domingo (19.330101, -99.147210; 2256 m), Coyoacán, 02-VII-2017, R. Cansino López leg. 1 male (LATLAX-Ara1087) from Pedregal de Santo Domingo, (19.328704, -99.164989, 2273 m) Coyoacán, 21-VII-2017 R. Cansiano López leg. 1 male, 1 female, 1 immature (LATLAX-Ara 0193) Los Reyes Copilco, Fracc. Areada Dpto. 102-A (19.336984, -99.182979, 2272 m), Coyoacán, IX-2017, D. Guerrero leg. 1 female, 1 immature (LATLAX-Ara196) Los Reyes Copilco, Fracc. Areada Dpto. 102-A (19.336984, -99.182979, 2272 m), Coyoacán, XII-2017, D. Guerrero leg. 1 immature (LATLAX-Ara 0482) from Street Toriello Guerra, Cuitlahuac S/N (19.297228, -99.174510, 2269 m) Tlalpan, II-2018, D. Barrales leg. 1

male 1 immature (LATLAX-Ara 0487) from Street Toriello Guerra, Cuitlahuac S/N (19.297228, -99.174510, 2269 m) Tlalpan, II-2018, D. Barrales leg. 1 female (LATLAX-Ara 0507) from Street Tepocatl #61, Pedregal de Santo Domingo (19.330101, -99.147210; 2256 m), Coyoacán 09-VIII-2018, R. Cansino López leg. *Estado de Mexico*: 1 female (LATLAX-Ara 0529) from Street Juárez #23, San Mateo Ixtacalco (19.702460, -19.187150, 2355 m), Municipality Cuautitlán Izcalli 05-III-2019, M. Cortez. *Tlaxcala*: 1 male, 3 females, 15 immatures (LATLAX-Ara0132) from Street Reforma #5, Santiago Tlacoachcalco (19.26939, -98.22303, 2245 m), Municipality of Tepeyanco, 06-VI-2017, M. Cortez, A. Juárez, J. Valerdi Cols. 1 female (LATLAX-Ara0188) from the Trinidad Tenexyecac (19.335588, -98.315688, 2241 m), Municipality of Ixtacuixtla of Mariano Matamoros, 02-III-2018, E. Briones leg. 2 males, 3 females, 10 immatures (LATLAX-Ara0500) from North Street Juárez #214, Huamantla downtown (19.3168, -97.92245, 2511 m), Municipality Huamantla, 15-V-2018, A. Valdez, I. Navarro, P. Solís, A. Cabrera, D. Montiel. Cols. 6 males, 5 females, 46 immatures (LATLAX-Ara0501) from Street North Juárez #214, Huamantla downtown (19.3168, -97.92245, 2511 m), Municipality Huamantla, 08-VI-2018, A. Valdez, I. Navarro, P. Solís, A. Cabrera, D. Montiel. Cols. 6 male, 2 females, 46 immatures (LATLAX-Ara0502) from Santiago Tlacoachcalco (19.26939, -98.22303, 2245 m), Municipality of Tepeyanco, 25-IV-2018, P. Solís, I. Navarro A. Juárez, J. Valerdi Cols.

Etymology. The species is a noun in apposition dedicated to Tenochtitlán (Nahuatl language) city, a large Mexica city-state in what is now Mexico City where the type locality is located. Tenochtitlán was built on an island in what was then Lake Texcoco in the Valley of Mexico, being the capital of the expanding Aztec Empire in the 15th century.

Diagnosis. The male of *Loxosceles tenochtitlan* sp. nov. morphologically resembles those of *Loxosceles misteca* Gertsch, 1958 (Figs 29–31, 38–47) from Guerrero; however, in the new species, the curvature of the basal-ventral part of the tibia of the male palp is less pronounced than in *L. misteca*, where it is prominent (Figs 23, 25, 42, 44, 48–55). Both species have a spatula-shaped embolus; in the new species, the embolus is slightly wider than that of *L. misteca* (Figs 23, 25, 26, 42, 44, 45, 48–55, 62–65). In dorsal view, the embolus basally is wider in *L. tenochtitlan* sp. nov. than in *L. misteca* (Figs 26, 45). Leg I length of males of *L. tenochtitlan* sp. nov. is shorter than legs I of *L. misteca* (Fig. 81). The seminal receptacles of females of *L. tenochtitlan* sp. nov. and *L. misteca* are similar, however in the new species the distance between the base of the receptacles is larger than in *L. misteca* (Figs 56–61, 66–69), also, the genitalia of *L. tenochtitlan* sp. nov. has small accessory lobes receptacles on each side (Figs 56–61), which are absent on *L. misteca* (Figs 66–69).

Description. Male (holotype; LATLAX-T001): Specimen collected manually, preserved and observed in 80% ethanol. *Measurements:* Total length (prosoma + opisthosoma) 6.70. Carapace 3.20 long, 2.90 wide. Clypeus length 0.45. Diameter of AME 0.13, PME 0.17, PLE 0.20; AME-PME 0.20 Labium: length 0.79, width 0.58. Sternum: length 1.80, width 1.62. Leg lengths: I (total 18.55): femur 5.00 / patella 1.10 / tibia 5.90 / metatarsus 5.35 / tarsus 1.20; II (20.98): 5.60 / 1.12 / 6.75 / 6.20 /



Figures 7–13. Live female specimens of the *Loxosceles tenochtitlan* sp. nov. from Street Cruz Verde #132, Tlalpan, Mexico City, Mexico (type locality). Red arrows indicate specific places where the specimens were collected inside the house. Photographs by Martín Sánchez Vílchis (2019).

1.31; III (15.67): 4.40 / 1.10 / 4.45 / 4.60 / 1.12; IV (16.99): 4.75 / 1.02 / 4.92 / 5.10 / 1.20. Leg formula: 2-1-4-3.

Prosoma: Carapace orange, longer than wide, piriform, with small and numerous setae laterally, with defined pale brown violin-shaped pattern dorsally, darker toward ocular region, carapace without spots (Fig. 19). Fovea brown (Fig. 19). Six eyes in



Figures 14–18. Live specimens and urban microhabitat of *Loxosceles tenochtitlan* sp. nov. from Tlaxcala **14–17** specimens from Street Juárez Norte #214, Huamantla downtown, Municipality, Huamantla, Tlaxcala, Mexico **18** microhabitat where some specimens were collected from Street Reforma #5, Santiago Tlacoachcalco, Municipality Tepeyanco, Tlaxcala, Mexico. Red arrows indicate the specific places where specimens were collected. Photographs **14–17** by José A. Castilla-Vázquez (2018–2019). Photograph **18** by Alma R. Juárez-Sánchez (2018).

three groups, clypeus reddish orange. Sternum pale orange, longer than wide (Fig. 20). Labium reddish, longer than wide, trapezoidal, fused to the sternum (Fig. 20). Endites pale orange basally, reddish distally and white apically, longer than wide, rounded basally (Fig. 20).

Legs: Coxae pale orange (Fig. 20). Trochanters pale orange. Femora pale orange, reddish orange on femora I (Figs 19, 20). Patellae dark orange. Tibiae, metatarsi and tarsi reddish orange.

Chelicerae: Fused basally, chelated chelicerae laminae, reddish orange, stridulatory lines laterally. Fangs reddish orange, paler distally, with long and thin setae.

Opisthosoma: Pale yellow, darker posteriorly, oval, longer than both width and height (Figs 19, 20). Region of gonopore pale yellow (Fig. 20), surrounded by small setae. Colulus long, pale orange, conical. Spinnerets pale orange, anterior lateral spinnerets cylindrical, longest, posterior median spinnerets shortest, with long setae; posterior lateral spinnerets cylindrical, slightly curved and with some long setae. Tracheal opening near posterior margin of opisthosoma.

Palps: Trochanters orange, femora reddish brown, long and thin, patellae reddish brown; tibiae reddish orange, darker, oval, curved ventrally, almost straight dorsally, wider distally than ventrally (Figs 23–25). Tarsus oval, reddish brown, bulb oval, with short, wide and slightly curved embolus (Figs 26–28, 32–34, 35, 36). Canal along embolus (Figs 32–34, 37).

Female (paratype; LATLAX-T002): Specimen collected manually, preserved and observed in 80% ethanol. Measurements: Total length 10.40. Carapace 3.75 long, 3.25 wide. Clypeus length 0.55. Diameter of AME 0.16, PME 0.20, PLE 0.20; AME-PME 0.23 Labium: length 0.80, width 0.75. Sternum: length 2.05, width 1.75. Leg lengths: I (total 18.73): femur 5.10 / patella 1.20 / tibia 5.68 / metatarsus 5.50 / tarsus 1.25; II (19.79): 5.50 / 1.24 / 6.10 / 5.60 / 1.35; III (15.83): 4.50 / 1.25 / 4.50 / 4.50 / 1.08; IV (18.09): 5.10 / 1.20 / 5.18 / 5.37 / 1.24. Leg formula: 2-1-4-3.

Differs from the male as follows. **Prosoma:** Carapace paler orange, with darker brown violin-shaped pattern; ocular region dark brown (Fig. 21). Clypeus dark reddish orange. Sternum dark orange (Fig. 22). Labium and endites more reddish orange, endites flat basally (Fig. 22). **Legs:** Coxae dark orange (Figs 21, 22). Trochanters dark orange (Fig. 22). All femora pale orange (Figs 21, 22). Patellae dark orange. Tibiae, metatarsi, and tarsi pale reddish orange (Figs 21, 22).

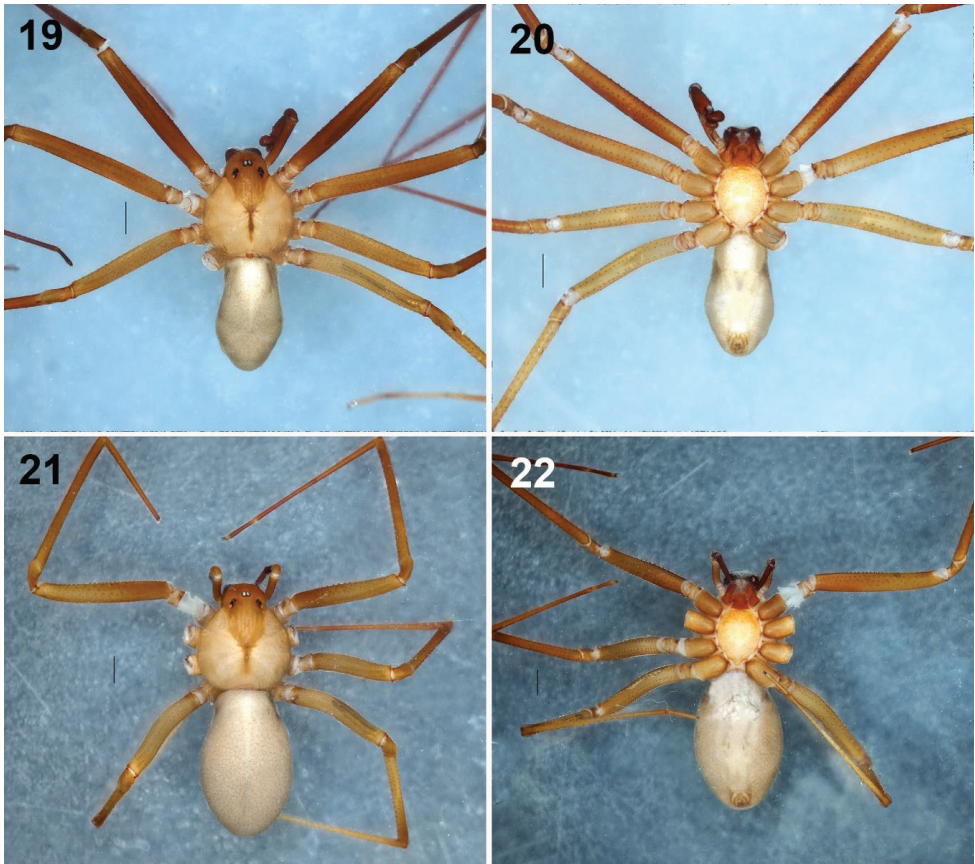
Chelicerae: Wider than in the male. Slightly dark reddish brown, with stridulatory lines laterally. Fangs dark reddish orange.

Opisthosoma: Opisthosoma pale yellow (Figs 21, 22). Spinnerets dark orange.

Palps: Trochanters pale orange, femora pale brown, paler ventrally; patellae pale brown, tibiae and tarsi reddish surrounded with several long and sparse setae. Tibiae cylindrical, tarsi conical.

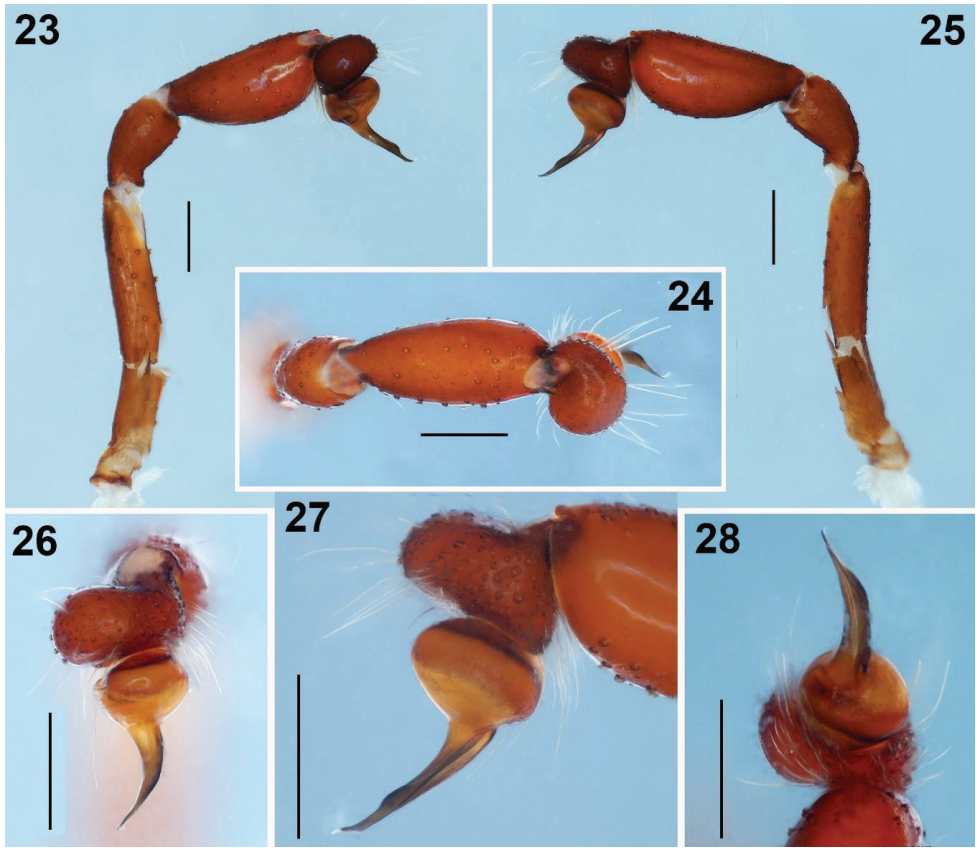
Genital area: Seminal receptacles asymmetric, S-shaped, curved basally and apically with rounded lobes (Fig. 56). Base of seminal receptacles wide and slightly sclerotized, round internally (Fig. 56). See variation section for more details (Figs 57–61).

Variation. MALES. *Mexico City:* Males from Coyoacán are light brown, legs slightly darker than the carapace, males from Tlalpan are light brown, legs slightly darker than the carapace. *Tlaxcala:* Males from Santiago Tlacoachcalco Municipality of Tepeyanco are light brown, legs slightly darker than the carapace and light brown, legs slightly darker than the carapace. Males from Huamantla are dark brown, legs



Figures 19–22. *Loxosceles tenochtitlan* sp. nov. **19–20** habitus of male holotype, dorsal and ventral views, respectively **21–22** habitus of female paratype, dorsal and ventral views, respectively. Scale bars: 1 mm.

slightly darker than the carapace. *Mexico City*: Coyoacán ($N = 3$): Tibia I 5.9–6.5 ($\bar{x} = 6.1$); carapace length (CL) 2.6–3.1 ($\bar{x} = 2.9$); carapace width (CW) 2.4–2.7 ($\bar{x} = 2.5$). Tlalpan ($N = 3$): Tibia I 6.0–7.6 ($\bar{x} = 5.8$); carapace length (CL) 2.2–3.2 ($\bar{x} = 2.8$); carapace width (CW) 2.5–2.7 ($\bar{x} = 2.6$). *Tlaxcala*: Santiago Tlacoachcalco Municipality of Tepeyanco ($N = 7$): Tibia I 3.8–6.6 ($\bar{x} = 5.0$); carapace length (CL) 2.5–4.2 ($\bar{x} = 3.1$); carapace width (CW) 2.2–3.2 ($\bar{x} = 2.7$). Huamantla ($N = 3$): Tibia I 5.0–6.5 ($\bar{x} = 5.8$); carapace length (CL) 3.2–3.3 ($\bar{x} = 3.2$); carapace width (CW) 2.7–2.9 ($\bar{x} = 2.8$). FEMALES. *Mexico City*: Females from Coyoacán are dark brown, legs the same color as the carapace. Females from Tlalpan are dark brown, legs the same color as the carapace. *Estado de Mexico*: Female from San Mateo Ixtacalco, Municipality Cuautitlán Izcalli is dark brown, legs slightly darker than the carapace. *Tlaxcala*: Females from Santiago Tlacoachcalco, Municipality of Tepeyanco are light brown, legs slightly darker than the carapace. Females from Huamantla are dark brown, legs the same color as the carapace and light brown, legs the same color as the carapace and light brown. A female from the Trinidad Tenexyecac, Municipality of Ixtacuixtla is light brown, legs the same color



Figures 23–28. *Loxosceles tenochtitlan* sp. nov. Male Holotype **23–25** left palp, prolateral, dorsal and retrolateral views respectively **26–28** detail of the bulb and embolus, dorsal, retrolateral and apical views, respectively. Scale bars: 0.5 mm (**23–25**), 0.2 mm (**26–28**).

as the carapace. *Mexico City*: Coyoacán ($N = 3$): Tibia I 5.8–7.1 ($\bar{x} = 6.7$); carapace length (CL) 3.9–4.2 ($\bar{x} = 4.1$); carapace width (CW) 3.2–4.0 ($\bar{x} = 3.7$). Tlalpan ($N = 6$): Tibia I 4.6–6.3 ($\bar{x} = 5.2$); carapace length (CL) 1.7–4.0 ($\bar{x} = 3.2$); carapace width (CW) 1.8–3.3 ($\bar{x} = 2.6$). *Estado de Mexico*: San Mateo Ixtacalco, Municipality Cuauhtitlán Izcalli ($N = 1$) Tibia I 3.6; carapace length (CL) 2.5; carapace width (CW) 2.5. *Tlaxcala*: Santiago Tlacoachcalco Municipality of Tepeyanco ($N = 2$): Tibia I 4.5, 5.3; carapace length (CL) 3.2, 3.3; carapace width (CW) 2.5, 2.9. Huamantla ($N = 11$): Tibia I 4.1–6.7 ($\bar{x} = 5.1$); carapace length (CL) 1.7–4.0 ($\bar{x} = 3.3$); carapace width (CW) 1.8–3.5 ($\bar{x} = 2.7$). Trinidad Tenexyecac, Municipality of Ixtacuixtla ($N = 1$): Tibia I 5.4; carapace length (CL) 3.3; carapace width (CW) 2.5.

There is little variation in the shape of the male palps, even those of specimens from different populations (Figs 48–55). The shape of the embolus varies little; the specimens from Tlaxcala have the embolus slightly more curved than the specimens from Mexico City (Figs 52–55). Also, the specimens from Tlaxcala have a slightly

thinner palpal tibia than specimens from Mexico City (Figs 48–51). The seminal receptacles of females are asymmetrical, and although all they are all S-shaped with rounded or oval lobes apically, they are highly variable (Figs 56–61). The small accessory lobes of the receptacles on each side vary in width among specimens (Figs 56–61). The internal part of the bases of the seminal receptacles is round, wide and slightly sclerotized in all specimens, with the distance between them equal to their height (Figs 56–61).

Natural history. The specimens of *L. tenochtitlan* sp. nov. (Figs 1–9, 11–17) were collected in urban areas in houses and buildings (Figs 10, 18). The specimens from Mexico City were collected in houses, on doors, storage boxes, drawers, under chairs and tables (Figs 7–13). The specimens from Tlaxcala were collected in houses behind doors, behind decorative items on the wall, under beds, under chairs and tables, among wooden boards for construction, under wardrobes, and between ornamental artificial plants, and under stored items (Figs 14–18). Even the first record from Tlaxcala (Trinidad Tenexyecac) was a female specimen collected among construction debris close to a football/soccer field. Some specimens from Huamantla, Tlaxcala were collected inside an abandoned house, mainly under stored items, behind doors and under wardrobes; other specimens were collected outside of a house in spaces and cracks in a wall (Figs 14–17).

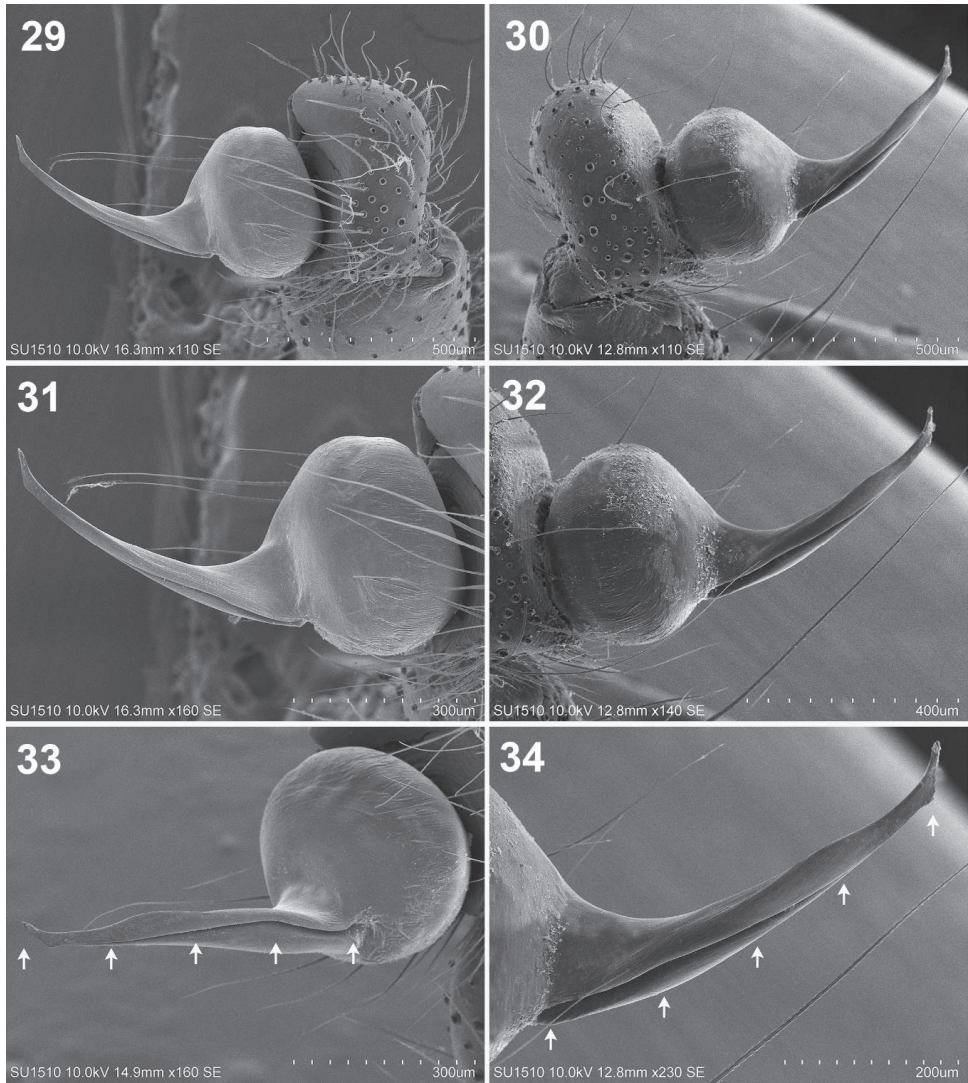
Distribution. MEXICO: Mexico City, Tlaxcala, Estado de Mexico (Figs 82–84).

Loxosceles misteca Gertsch, 1958

Figs 29–31, 38–41, 42–47, 62–69

Type material. MEXICO: *Guerrero*: male holotype (examined) (AMNH_IZC00327631) from Taxco, Municipality Taxco de Alarcón, Guerrero, Mexico, Date? 1946, Collected in the fall, Leo Isaacs leg.

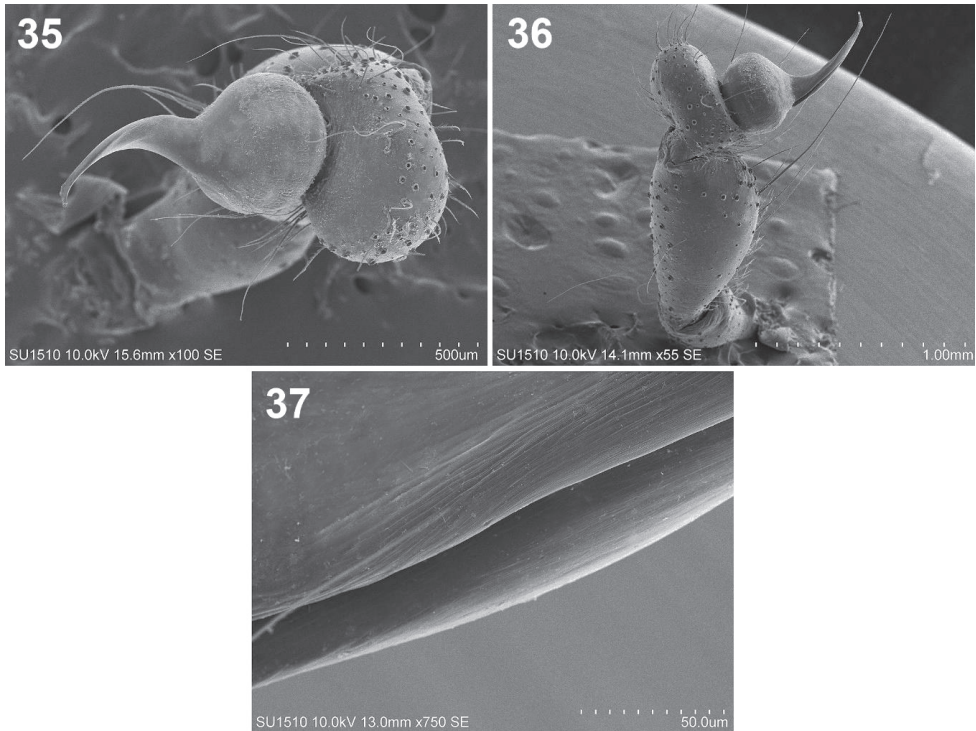
Material examined. MEXICO: *Guerrero*: 1 male, 1 female (CNAN-AR008985) from Cueva del Diablo, Acuitlapan (18.60106, -99.54318, 1581 m) Municipality Taxco de Alarcón, 04-VI-2010, O. Francke, D. Barrales, J. Cruz, A. Valdez Cols. 2 males (LATLAX-Ara 0158) from Cueva del Jardín Botánico, Parque Nacional Grutas de Cacahuamilpa (18.67038, -99.51134, 1145 m) Municipality Pilcaya, 15-IX-2017, A. Valdez, P. Solís, I. Navarro, J. Valerdi Cols. 2 males (LATLAX-Ara 0161) from Grutas del General Pacheco (18.66562, -99.50943, 1086 m) Municipality Pilcaya, 19-IX-2017, A. Valdez, P. Solís, I. Navarro, J. Valerdi Cols. 6 females (LATLAX-Ara 0162) from Cueva Agustín Lorenzo, Mexcaltepec (18.431, -99.55013, 922 m) Municipality Taxco de Alarcón, 20-IX-2017, A. Valdez, P. Solís, I. Navarro, J. Valerdi Cols. 3 males, 5 females (LATLAX-Ara 0526) from Jardín Botánico, Parque Nacional Grutas de Cacahuamilpa (18.67038, -99.51134, 1145 m) Municipality Pilcaya, 15-X-2019, A. Valdez, P. Solís, I. Navarro, A. Juaréz, A. Cabrera Cols. *Morelos*. 1 male (CNAN-Ar009069) from Lomas de Cortés, Municipality Cuernavaca, 11-II-2013, P. Bernard leg. 1 male (CNAN-Ar009070) from Tlaltenango (18.946414, -99.24392, 1660 m)



Figures 29–34. 29–31 *Loxosceles misteca* Gertsch. Male 29 left palp, retrolateral view, detail of tarsus, bulb and embolus 30 detail of bulb and embolus, retrolateral view 31 detail of the embolus 32–34 *Loxosceles tenochtitlan* sp. nov. Male paratype 32 right palp, retrolateral view, detail of tarsus, bulb and embolus 33 detail of bulb and embolus, retrolateral view 34 detail of the embolus. Arrows indicate the canal along the embolus.

Municipality Cuernavaca, III-2013. R. Rosas leg. 1 male (CNAN-Ar009071) from Boulevard Cuahutémoc #33, Lomas de Cortés (18.951125, -99.22408, 1640) Municipality Cuernavaca, 24-II-2012.

Diagnosis. *Loxosceles misteca* Gertsch, 1958 resembles *L. tenochtitlan* sp. nov. (Figs 23–28, 42–47); however, in *L. misteca*, the curvature of the basal-ventral part of the tibia of the male palp is more pronounced than in the new species (Figs 23,

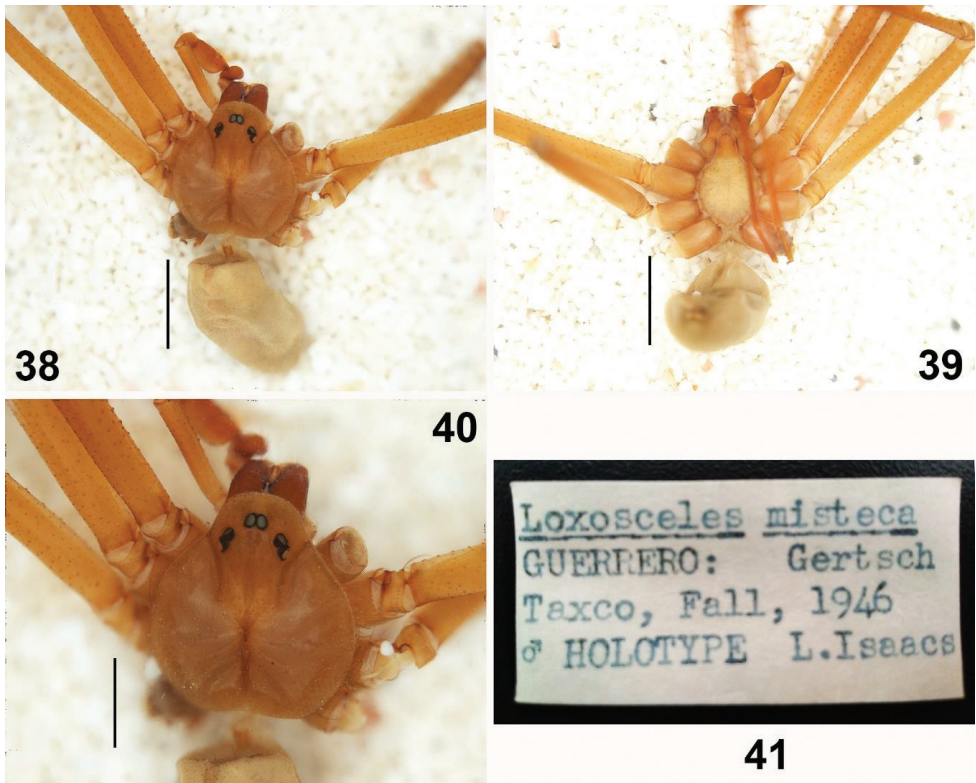


Figures 35–37. *Loxosceles tenochtitlan* sp. nov. Male paratype **35** right palp, tarsus, bulb and embolus, dorsal view **36** right palp, retrolateral view **37** detail of the canal along the embolus.

25, 42, 44, 48–55, 62–65, 76–77). Both species have a spatula-shaped embolus; in *L. misteca*, the embolus is slightly thinner than that of the new species (Figs 23, 25, 42, 44, 48–55, 62–65, 76–77). Leg I length of males of *L. misteca* is longer than legs I of *L. tenochtitlan* sp. nov. (Fig. 81). The seminal receptacles of the females of *L. misteca* and *L. tenochtitlan* sp. nov. are similar, however in *L. misteca* the distance between the base of the receptacles is shorter than in the new species (Figs 56–61, 66–69), also, the genitalia of *L. misteca* does not have small accessory lobes receptacles on each side, which are present in *L. tenochtitlan* sp. nov. (Figs 56–61, 66–69).

Molecular analyses and species delimitation

The analyzed matrices include 52 individuals of 11 species of *Loxosceles*, 39 individuals for the CO1 data set and 34 individuals for ITS2 (Table 1, Figs 70, 71). Specimens used in this study, GenBank accession numbers and localities of the specimens are listed in Table 1. Analyses of the concatenated matrix indicated that the four different methods used to delimit species with molecular data (CO1+ITS2) were consistent with morphology, recovering ten species (Fig. 72). Only the ABGD species delimitation



Figures 38–41. Male holotype (examined) of *Loxosceles misteca* Gertsch, 1958 (AMNH_IZC00327631), from Taxco, Municipality Taxco de Alarcón, Guerrero, Mexico; Date? 1946, collected in the fall, Leo Isaacs leg. **38, 39** habitus of male holotype, dorsal and ventral views, respectively **40** carapace **41** label of the holotype. Scale bars: 1 mm (**38–40**).

tation method under recursive partitions (RP) recovered 12 species (Fig. 72). Even, *Loxosceles malintzi*, the last species described from Mexico by Valdez-Mondragón et al. (2018) by only morphological characters, was recovered with molecular data under the different species delimitation methods (Fig. 70–72). The average genetic *p*-distance among analyzed species was of 17% for CO1 and 7.6% for ITS2 (Figs 70, 71). Corrected *p*-distances from the CO1 data recovered ten species of *Loxosceles* (Fig. 70), whereas nine species were recovered with ITS2 (Fig. 71) both with high statistical support. Based on molecular evidence, *L. tenochtitlan* sp. nov. is closely related to *L. misteca* (Figs 70–72), the average *p*-distances between both species for CO1 was 13.8% (Table 3) and 4.2% for ITS2 (Table 4). The haplotype network analysis with CO1 data is concordant with the results of the different species delimitation analyses (Fig. 73). There were more than ten mutations between haplotypes of CO1 for all the species (Fig. 73). Regarding *L. tenochtitlan* sp. nov. and *L. misteca*, the haplotype network was concordant with the delimitation of both species, showed 49 mutations between haplotypes under CO1 (Fig. 73).

Table 3. Genetic *p*-distance matrix from the CO1 data between *Loxosceles tenochtitlan* sp. nov. and *Loxosceles misteca*. Average *p*-distance = 13.8%.

Species	1	2	3	4	5	6	7	8	9
1. Ara0082- <i>L. misteca</i> Gro									
2. Ara0089- <i>L. misteca</i> Gro	0.007								
3. Ara0090- <i>L. misteca</i> Gro	0.010	0.003							
4. Ara0084- <i>L. misteca</i> Gro	0.017	0.020	0.024						
5. Ara0236- <i>L. misteca</i> Gro	0.009	0.012	0.014	0.019					
6. Ara0237- <i>L. misteca</i> Gro	0.009	0.012	0.014	0.021	0.000				
7. Ara0146- <i>L. tenochtitlan</i> CDMX	0.150	0.153	0.153	0.166	0.155	0.157			
8. Ara0161- <i>L. tenochtitlan</i> CDMX	0.133	0.131	0.131	0.150	0.134	0.137	0.014		
9. Ara0173- <i>L. tenochtitlan</i> Tlax	0.122	0.126	0.126	0.136	0.124	0.126	0.019	0.006	
10. Ara0164- <i>L. tenochtitlan</i> Tlax	0.131	0.135	0.136	0.145	0.129	0.131	0.023	0.012	0.008

Table 4. Genetic *p*-distance matrix from the ITS2 data between *Loxosceles tenochtitlan* sp. nov. and *Loxosceles misteca*. Average *p*-distance = 4.2%.

Species	1	2	3	4	5	6
1. Ara0146- <i>L. tenochtitlan</i> CDMX						
2. Ara0173- <i>L. tenochtitlan</i> Tlax	0.000					
3. Ara0164- <i>L. tenochtitlan</i> Tlax	0.021	0.019				
4. Ara0082- <i>L. misteca</i> Gro	0.036	0.037	0.062			
5. Ara0084- <i>L. misteca</i> Gro	0.030	0.031	0.059	0.005		
6. Ara0090- <i>L. misteca</i> Gro	0.026	0.026	0.066	0.020	0.014	
7. Ara0089- <i>L. misteca</i> Gro	0.036	0.036	0.055	0.007	0.003	0.003

Geometric and linear morphometry and sexual dimorphism

The analysis of canonical variables CVA shows a significant difference ($\chi^2 = 10.2555$, $df = 2$, $p = 0.00593003$, $\lambda = 0.5988$) between both species, which indicates the formation of two groups according to the tibiae shape of the palps of the males (Fig. 74). The differences on the tibiae can be observed in the deformation rack, where a deformation is shown mainly in the ventral-basal and the dorsal-apical parts (Fig. 75). In this way, the tibiae of *L. tenochtitlan* sp. nov. is thinner in ventral-basal part (Fig. 77), whereas in *L. misteca* the ventral-basal part is wider and slightly less curved in the dorsal-apical part (Fig. 76). To analyze sexual dimorphism and variation in the new species, a T-test showed that between the males and females of *L. tenochtitlan* sp. nov., there are no statistically significant differences in leg I length ($t = -1.3106$, $p = 0.1981$, $df = 37$, $\alpha = 0.05$), carapace length ($t = 1.498$, $p = 0.142$, $df = 38$, $\alpha = 0.05$), and carapace width ($t = 0.6955$, $p = 0.4912$, $df = 36$, $\alpha = 0.05$) (Figs 78–80). Therefore, there is no secondary sexual dimorphism between males and females of the new species (Table 5, Figs 78–81). However, a T-test showed that there is secondary sexual dimorphism between males and females of *L. misteca* in leg I length ($t = 3.1086$, $p = 0.0038$, $df = 21$, $\alpha = 0.05$) (Fig. 81). A T-test indicated that there

are statistically significant differences between the new species and *L. misteca* in leg I length of males ($t = 3.6174$, $p = 0.00331$, $df = 13$, $\alpha = 0.05$) with the longest legs occurring in *L. misteca* (Table 5, Fig. 81). There was no statistical support for significant differences in leg I length between females of each species ($t = 0.274$, $p = 0.787$, $df = 17$, $\alpha = 0.05$) (Table 5, Fig. 81).

Ecological niche modeling (ENM)

To analyze the potential distribution of *L. tenochtitlan* sp. nov., ENM was performed for the new species, with a total of 34 records from Mexico City, Estado de Mexico and Tlaxcala (Figs 82–84). The highest contribution to the model came from Vegetation Type (CON01) with 42% and Mean Temperature of Wettest Quarter (BIO10) with 28.5% (Table 6). Additionally, the Area Under the Curve (AUC) demonstrated good performance AUC= 0.993.

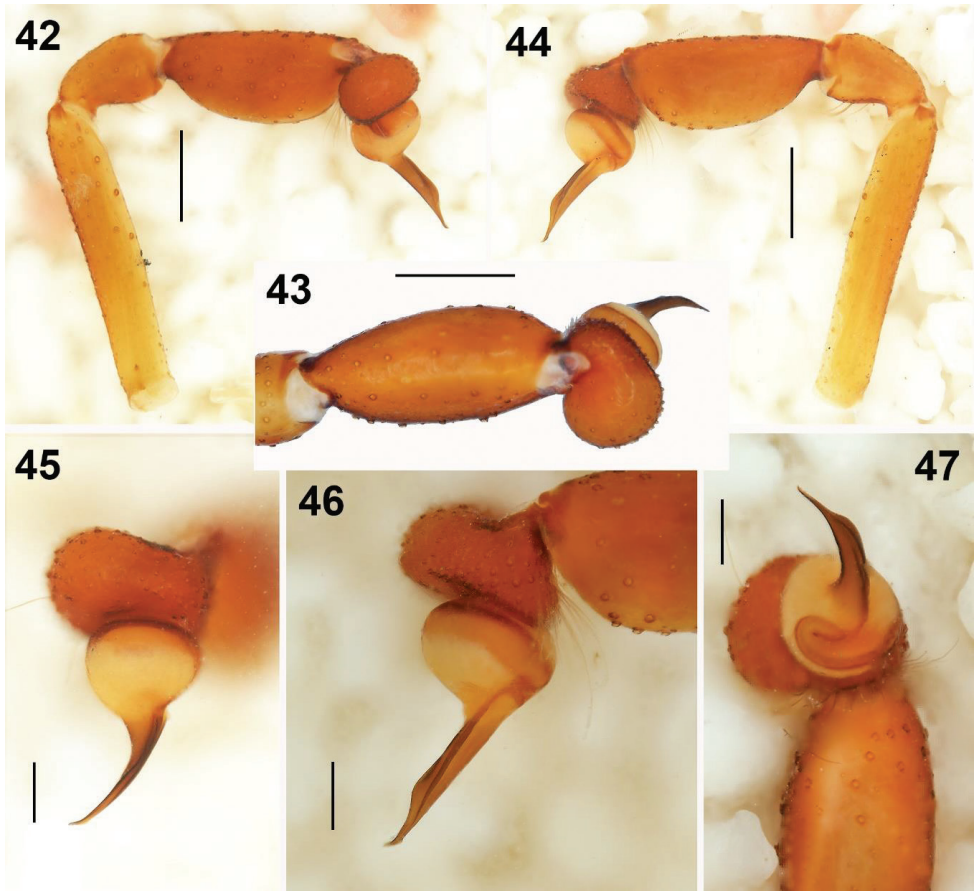
Following the biogeographic scheme for Mexico proposed by Morrone (2004, 2005), the highest probability of the presence of *L. tenochtitlan* sp. nov. (0.75–1.0) was markedly toward the biogeographical province of the Transmexican Volcanic Belt (TVB), with a potential distribution including Mexico City, north of Estado de Mexico, west of Puebla, most of Tlaxcala, and a small portion of Hidalgo and Queretaro (Fig. 84).

Table 5. Average of linear measurements of *Loxosceles tenochtitlan* sp. nov. and *Loxosceles misteca*. *N* = number of individuals. LL1 = Length of leg I. Cl = Carapace length. Cw = Carapace width. Sl = Sternum length. Sw = Sternum width. ♂ = males. ♀ = females. Numbers in parentheses represent minimum and maximum measurements.

Species	<i>N</i>	LL1	Cl	Cw	Sl	Sw
<i>Loxosceles tenochtitlan</i> sp. nov.	♂ 16	18.10	3.00	2.70	1.80	1.50
		(13.8–21.3)	(2.2–4.2)	(2.2–3.2)	(1.6–2.1)	(1.2–2.0)
	♀ 24	22.36	2.94	2.71	1.55	1.38
		(17.7–26.5)	(1.8–3.9)	(2.2–3.1)	(1.3–2.1)	(1.2–1.9)
<i>Loxosceles misteca</i>	♂ 11	23.75	3.05	2.73	1.59	1.42
		(18–31.9)	(2.5–3.4)	(2.5–3.0)	(1.2–1.9)	(1.1–1.5)
	♀ 11	18.47	3.08	2.67	1.59	1.31
		(14.1–18.9)	(2.5–3.3)	(2.3–3.0)	(1.4–1.9)	(1.1–1.7)

Table 6. Percent contribution of the climatic variables for the distribution model for *Loxosceles tenochtitlan* sp. nov. using the Maxent algorithm.

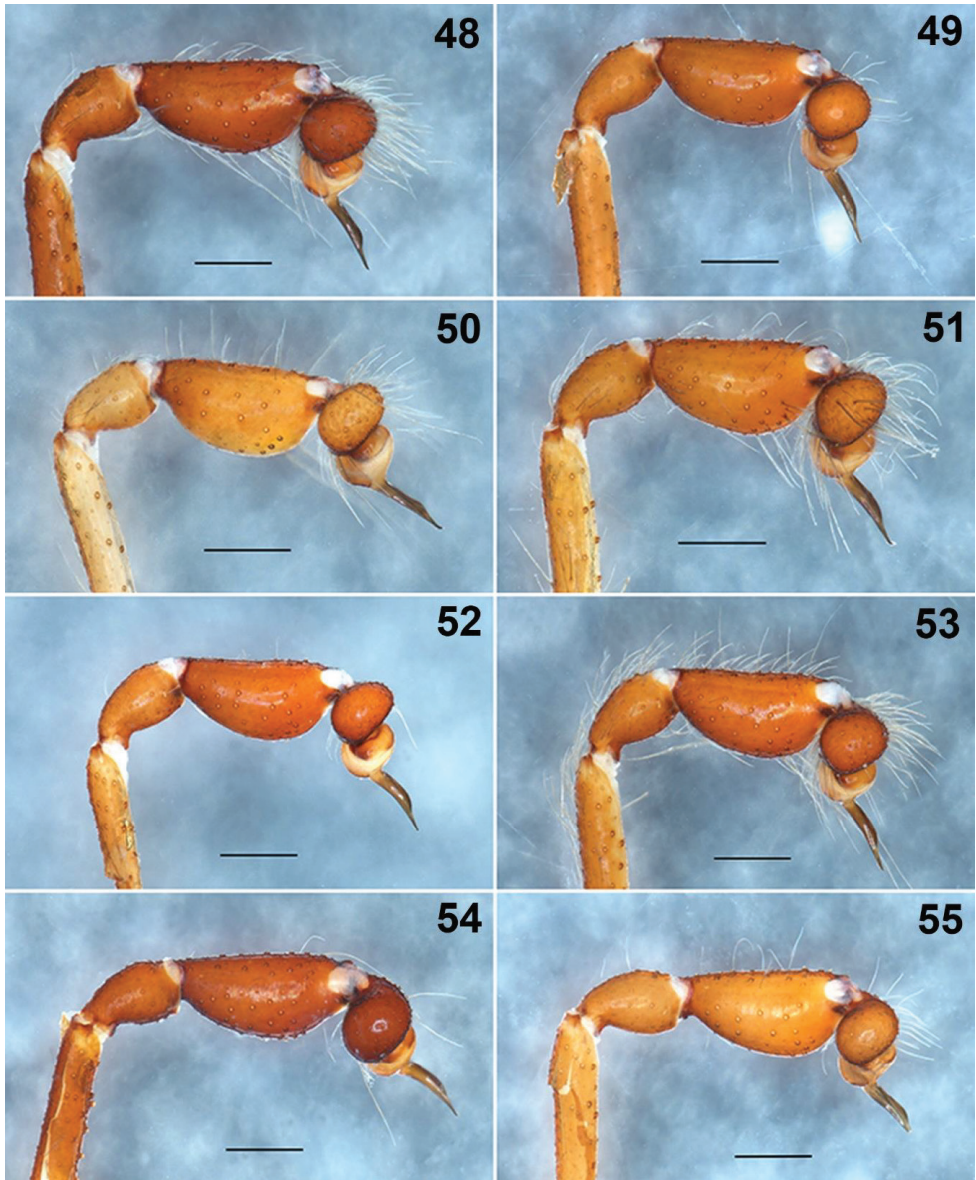
Variables	Contribution (%)
Vegetation type (CON01)	42
Mean Temperature of Wettest Quarter (BIO10)	28.5
Max Temperature of Warmest Month (BIO05)	7.2
Temperature Seasonality (BIO04)	5.3



Figures 42–47. Male holotype (examined) of *Loxosceles misteca* Gertsch, 1958 (AMNH_IZC 00327631), from Taxco, Municipality Taxco de Alarcón, Guerrero, Mexico; 1946, collected in the fall, Leo Isaacs leg. **42–44** left palp, prolateral, dorsal and retrolateral views respectively **45–47** detail of the bulb and embolus, dorsal, retrolateral and apical views, respectively. Scale bars: 0.5 mm (**42–44**), 0.2 mm (**45–47**).

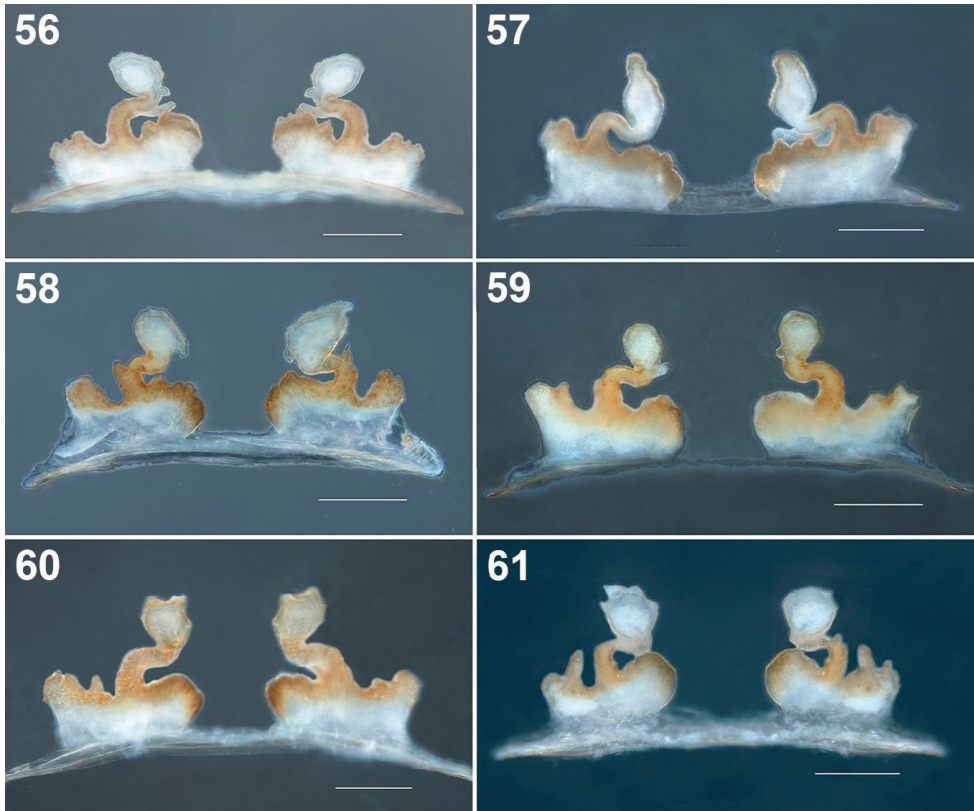
Discussion

The first record of *Loxosceles* from Mexico City was by Gertsch (1958), who reported a female of *Loxosceles nahuana* Gertsch, 1958, a native species from Zimapán, Hidalgo; however, this record is a misidentification because posteriorly Gertsch and Ennik (1983) did not consider this record in their taxonomic revision of *Loxosceles* from North America. Hoffmann (1976) includes the same record of *L. nahuana* in her preliminary list of Mexican spiders, but she did not mention other species. Francke et al. (2009), Durán-Barrón and Pérez-Ortíz (2016) and Durán-Barrón and Ayala-Islas (2007) reported two species from Mexico City, *L. misteca* and one unidentified species of *Loxosceles*, comprising a single female, two males and two immature specimens. Surprisingly, the authors never identified it to species level. Unfortunately, we



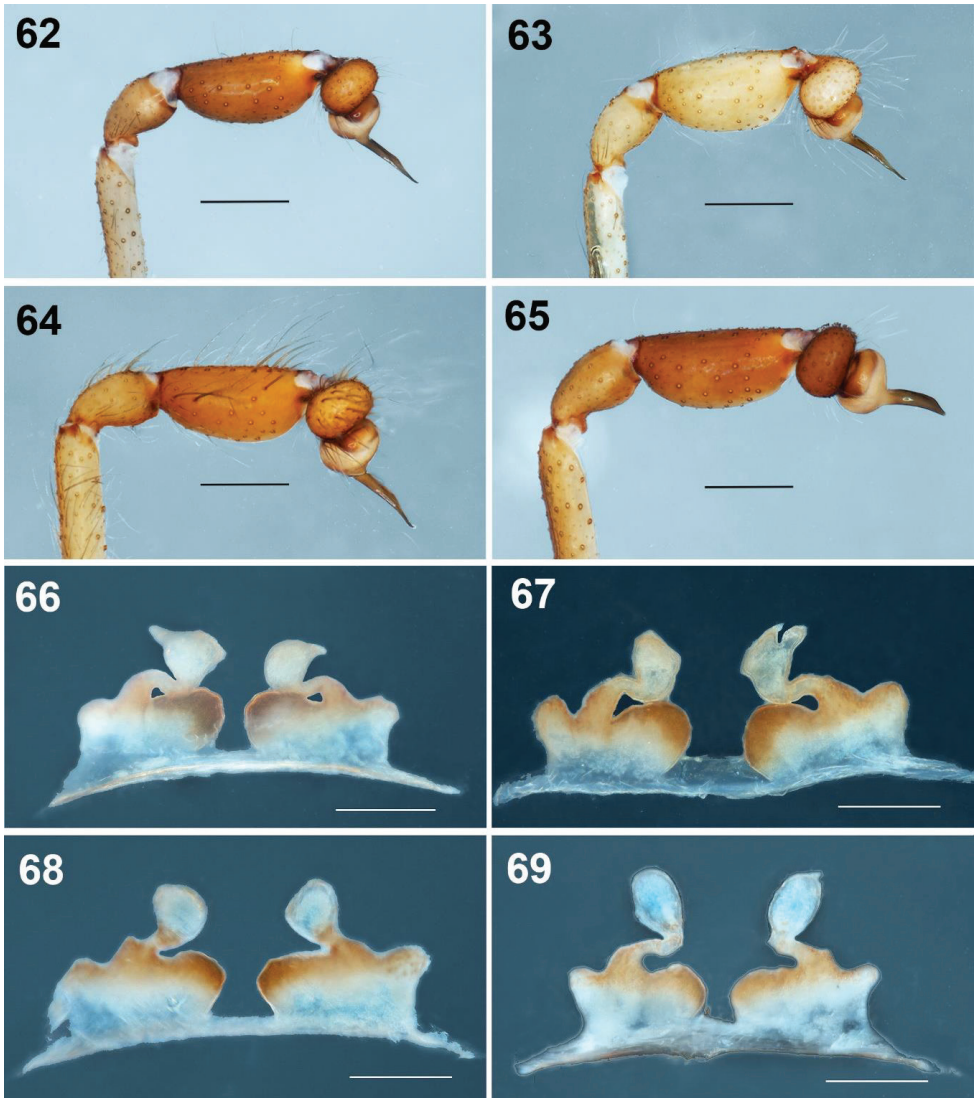
Figures 48–55. *Loxosceles tenochtitlan* sp. nov. Variation of the male palps, left palps, prolatral views **48** turiello Guerra, Street Cuitlahuac S/N, Tlalpan, Mexico City **49** Cruz Verde #132, Tlalpan, Mexico City (type locality) **50** Street Tepocat #61, Pedregal de Santo Domingo, Coyoacán, Mexico City **51** Los Reyes Copilco, Frac. Areada Dpto. 102-A, Coyoacán, Mexico City **52, 53** Street Reforma #5, Santiago Tlacochcalco, Municipality of Tepeyanco, Tlaxcala **54, 55** Street Juárez Norte #214, Huamantla, Municipality Huamantla, Tlaxcala, Mexico. Scale bars: 0.5 mm.

did not have access to those collections; therefore, we do not know whether there are two species or only one from Mexico City. In this way, *L. nabuana* is a valid and different species as the species delimitation methods and different topologies showed



Figures 56–61. *Loxosceles tenochtitlan* sp. nov. Variation of the seminal receptacles of the females, dorsal views **56** Street Cruz Verde #132, Tlalpan, Mexico City (type locality) (female paratype) **57** Los Reyes Copilco, Fracc. Areada Dpto. 102-A, Coyoacán, Mexico City **58** Street Juárez #23, San Mateo Ixtacalco, Municipality Cuautitlán Izcalli, Estado de Mexico **59** Street Reforma #5, Santiago Tlacoachcalco, Municipality of Tepeyanco, Tlaxcala **60, 61** Street Juárez Norte #214, Huamantla, Municipality of Huamantla, Tlaxcala, Mexico.

(Figs 70–72), even this species is not closely related with the new species described herein neither with *L. misteca* (Figs 70–72). In the present work, all the specimens reviewed belong to *Loxosceles tenochtitlan* sp. nov., therefore we can assume that the previous records of *L. misteca* belong to the new species described herein, and that *L. misteca* is not found in Mexico City or the rest of the states where the new species has been recorded (Estado de Mexico and Tlaxcala). Recently, Valdez-Mondragón et al. (2018a, b) mentioned that *L. misteca* from Mexico City and Tlaxcala was an introduced species, however this was an incorrect interpretation. *Loxosceles misteca* is a species from Guerrero and Morelos, whereas the records of *L. misteca* from Mexico City and Tlaxcala belong to *L. tenochtitlan* sp. nov., a native species of the region (Fig. 82–84). Only two introduced species have been recorded in Mexico, *Loxosceles reclusa* Gertsch & Mulaik, 1940 from the south-central United States and *Loxosceles rufescens* (Dufour, 1820), a widely distributed species throughout the Mediterranean Basin



Figures 62–69. *Loxosceles misteca* Gertsch, 1958 **62–65** variation of the male palps, left palps, pro-lateral views **62** Grutas General Carlos Pacheco, Municipality Pilcaya, Guerrero **63** Cueva del Diablo Acuitlalpan, Municipality Taxco, Guerrero **64** boulevard Cuauhtémoc #99, Colonia Lomas de Cortes, Municipality Cuernavaca, Morelos **65** Grutas de Cacahuamilpa National Park, Municipality Pilcaya, Guerrero **66–69** variation of the seminal receptacles of the females, dorsal views **66, 67** Agustin Lorenzo Cave, Mexcaltepec, Municipality Taxco de Alarcón, Guerrero **68, 69** Botanical Garden Cave, Grutas de Cacahuamilpa National Park, Municipality Pilcaya, Guerrero.

and the Middle East (Gertsch 1958, 1973; Gertsch and Ennik 1983; Nentwig et al. 2017; Tahami et al. 2017; Valdez-Mondragón et al. 2018a, b; WSC 2019).

As was mentioned previously, recent taxonomic studies based on molecular analyses using mitochondrial markers have suggested that the known diversity within the

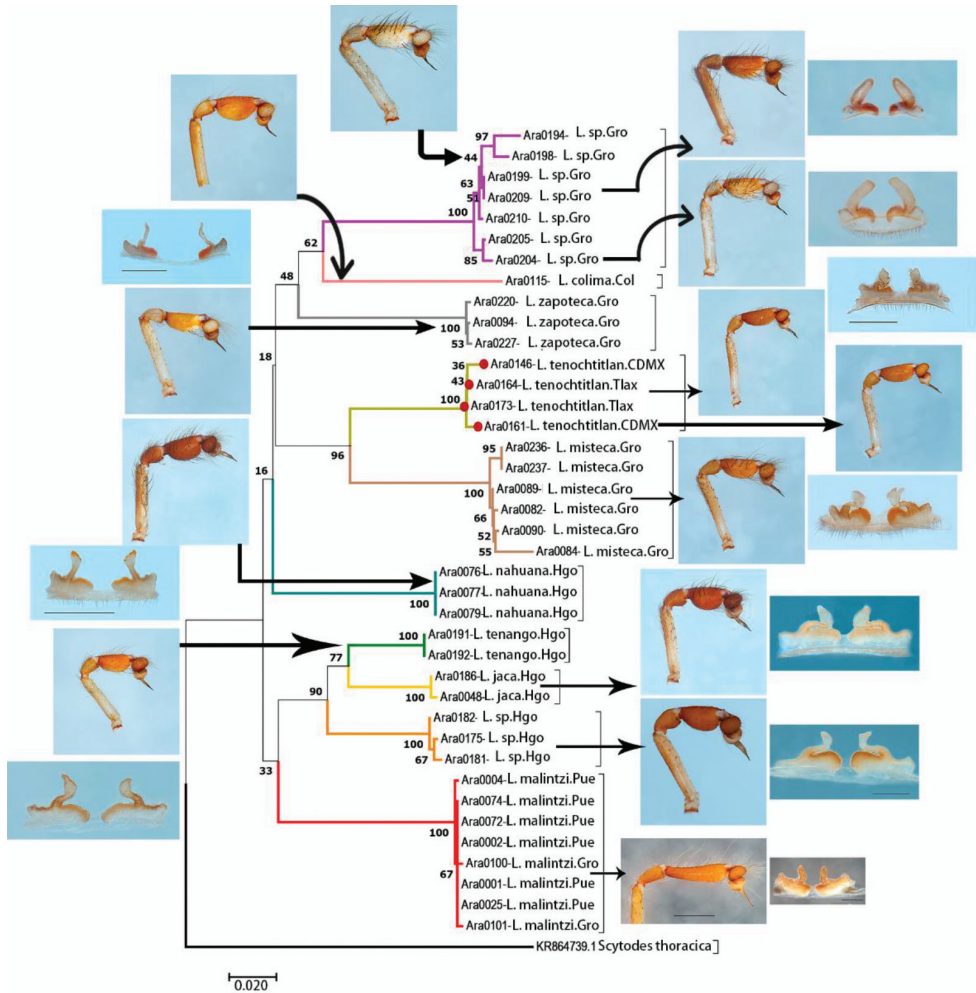


Figure 70. Neighbor-joining (NJ) tree constructed from COI data of ten species of *Loxosceles* from Mexico. Colors of branches indicate different species. Numbers on nodes are bootstrap support values. Red circles represent *Loxosceles tenochtitlan* sp. nov.

genus *Loxosceles* could be greatly underestimated (Binford et al. 2008; Duncan et al. 2010; Planas and Ribera 2014, 2015; Tahami et al. 2017). Additionally, it has been decades since a revision of the North American species has been conducted, and given the intraspecific variation in sexual structures, primarily in the seminal receptacles in the females (Brignoli 1968, Gertsch and Ennik 1983) this can be very difficult. Despite this, the male palps remain a good character for species identification because there is little morphological variation in comparison with seminal receptacles as was showed by Valdez-Mondragón et al. (2018b) recently in the description of *Loxosceles malintzi*.

Although DNA barcodes are being applied in modern systematics as a useful tool to resolve species delimitation problems, modern taxonomy includes many different

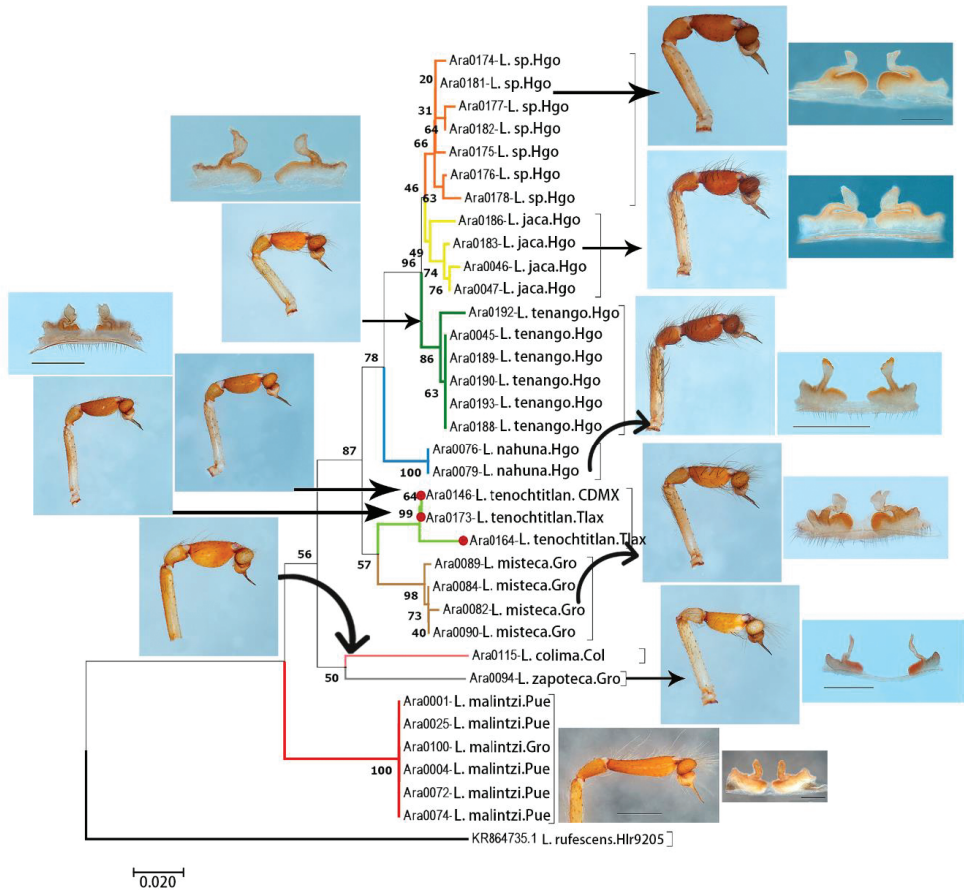


Figure 71. Neighbor-joining (NJ) tree of ITS2 data of nine species of *Loxosceles* from Mexico. Colors of branches indicate different species. Numbers at nodes represent bootstrap support values. Red circles represent *Loxosceles tenochtitlan* sp. nov.

sources of evidence, such as traditional morphology, ecology, reproduction, and biogeography. Traditional morphology alone cannot determine species boundaries in some cases, and the genus *Loxosceles* is no exception. Identifying morphologically inseparable cryptic or sibling species requires a new set of taxonomic tools, including DNA and additional sources of evidence (integrative taxonomy) (Jarman and Elliott 2000; Witt and Hebert 2000; DeSalle et al. 2005; Hebert et al. 2003, 2004; Bickford et al. 2007; Hamilton et al. 2011, 2014, 2016; Ortiz and Francke 2016). The researchers should apply different range of species delimitation method at the same time to their data and place their truth in delimitation that are congruent across methods (Carstens et al. 2013). Using several species delimitation methods, incongruence across the different results is evidence of either a difference in the power to detect cryptic lineages across one or more of the approaches used to delimit species and could indicate that assump-

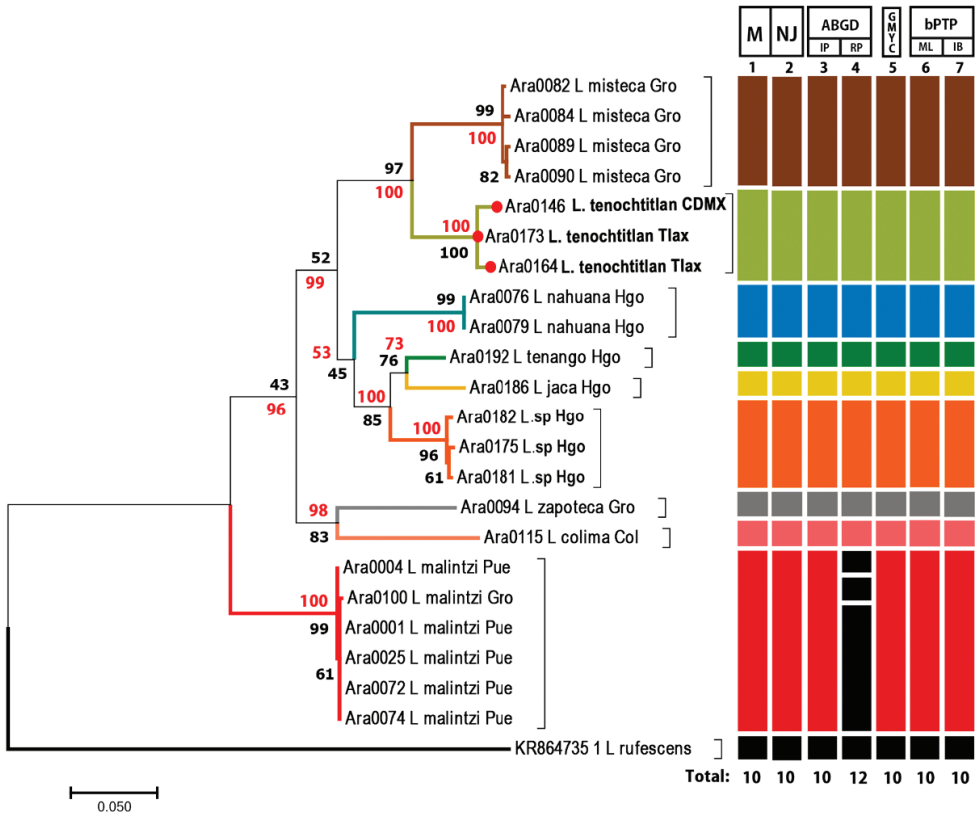


Figure 72. Maximum likelihood tree inferred from the concatenated matrix (CO1 + ITS2) of *Loxosceles* species from Mexico. Colors of branches and bars indicate different species. Numbers above bars at right represent the delimitation methods: 1: morphology (M). 2: neighbor-joining (NJ). 3: ABGD with initial partitions (IP). 4: ABGD with recursive partitions (RP). 5: GMYC. 6: bPTP with ML. 7: bPTP with IB. Numbers below bars represent species recovered for each delimitation method. Red numbers correspond to Bayesian posterior probabilities, and black numbers are bootstrap support values from the ML analysis.

tions of one or more of the methods have been violated, in this cases the assumptions for species delimitations should be conservative (Carstens et al. 2013). In this work, the four different molecular species delimitation methods were congruent and consistent to separate *L. tenochtitlan* sp. nov and *L. misteca* (Fig. 72).

Although morphologically *L. tenochtitlan* sp. nov is quite similar to *L. misteca* in the seminal receptacles of the females and the male palps, there are some subtle morphological differences that allow diagnosis of the new species as was mentioned in the description section. Multiple lines of robust evidence are able to clearly separate it as a new species. These methods are genetic differences, geometric and linear morphometry and different biogeographical distribution patterns. Strictly, cryptic species are those that cannot be differentiated based on their morphology or external appearance and are reproductively isolated. The present genetic divergence indicates

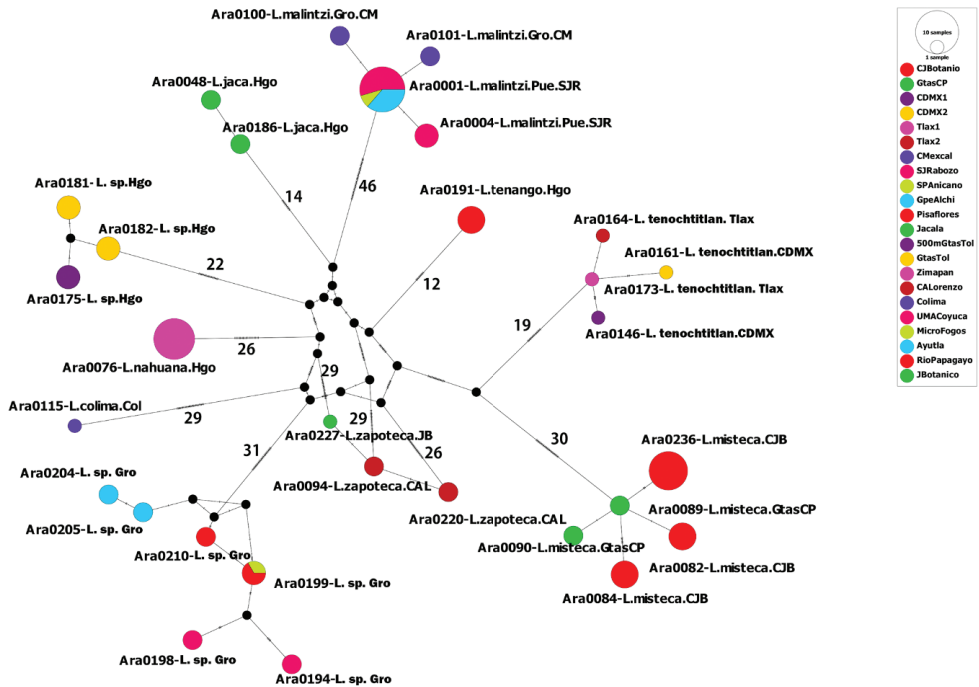
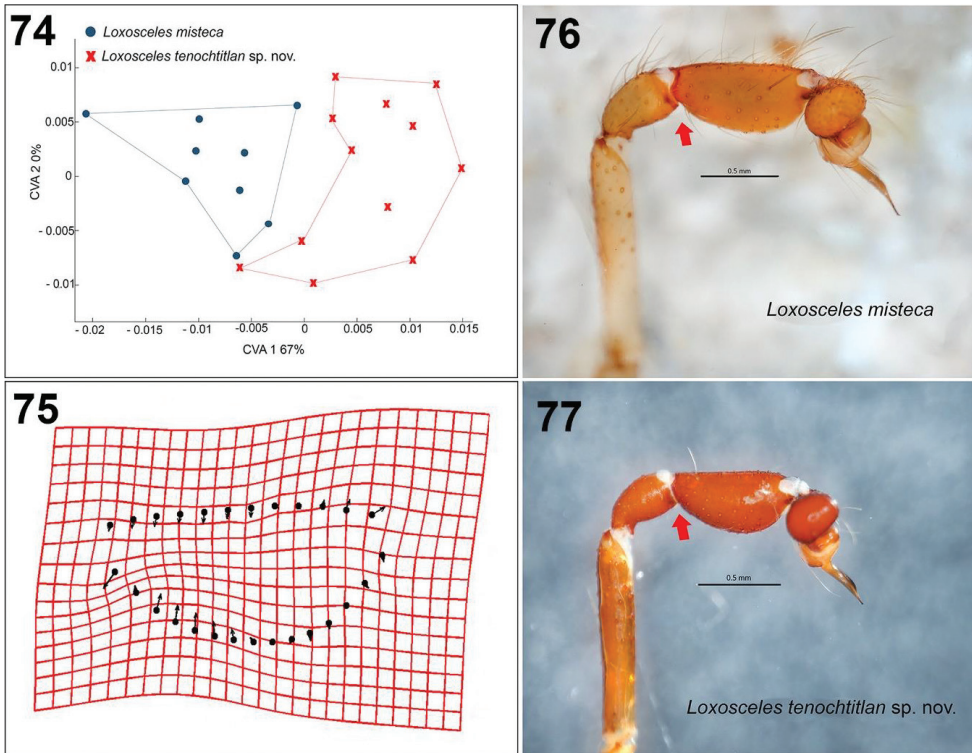


Figure 73. Haplotype network from the CO1 data obtained with TCS using PopArt. Each circle represents the haplotypes found in ten species of *Loxosceles* from Mexico. Numbers on branches indicate the number of mutations between haplotypes.

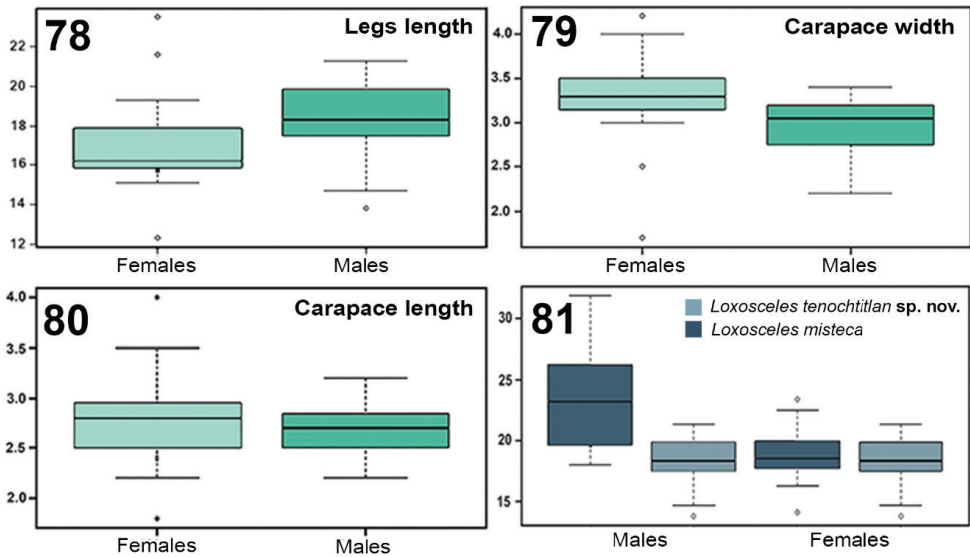
the two species are independent lineages (Bickford et al. 2007; Hebert et al. 2004; Struck and Cerca 2019).

The species separation based on corrected genetic distances indicates that CO1 performed better for species delimitation than ITS2 (Figs 70, 71). This result confirms the utility of DNA barcoding as a fast and reliable tool for the identification and species delimitation of the *Loxosceles* from the *reclusa* group of North America. Similar results have also been found in other molecular studies of *Loxosceles*. Planas and Ribera (2014, 2015) found genetic distances between species from the Canary Islands to be > 12% using CO1, whereas Tahami et al. (2017) found genetic distances between species from the Middle East ranged for CO1 from 17.5 to 20.6%. Additionally, CO1 haplotypes network also corroborated the distinctiveness of the different species (Fig. 73). The approaches for analyzing DNA barcode data, using *p*-distances for CO1 and ITS2 and tree-based delimitation with ML and BI (CO1+ITS2), recovered a monophyletic cluster with high support values for the samples of *L. tenochtitlan* sp. nov from Mexico City + Tlaxcala (Figs 70–72), as well as another monophyletic cluster of the samples of *L. misteca* from Guerrero, where some samples were collected near the type locality of the species as well as localities previously reported by Gertsch (1958) and Gertsch and Ennik (1983) (Figs 41, 62–69).



Figures 74–77. Geometric morphometry of the tibia shape on retrolateral view of the palps of males of *L. tenochtitlan* sp. nov. ($N = 12$) and *L. misteca* ($N = 9$) **74** CVA plot showing a significant difference ($\chi^2 = 10.2555$, $df = 2$, $p = 0.00593003$, $\lambda = 0.5988$) between both species in the tibiae shape **75** deformation grid, the vectors indicate the direction of change in the tibia with respect to the average shape of the 21 individuals analyzed of both species **76,77** palps of the males of *L. misteca* and *L. tenochtitlan* sp. nov. respectively, retrolateral views (red arrows indicate the change in the shape of the tibiae of the species analyzed).

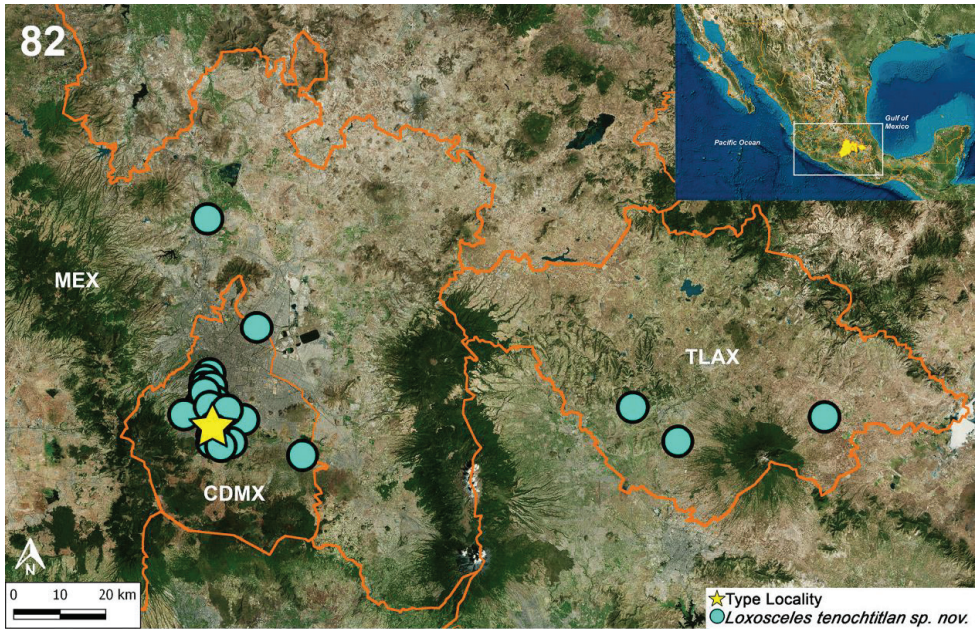
Sexual characters in spiders are robust and important morphological characters that are still used to separate species and to provide a diagnosis. This means that genitalia evolve, on average, more rapidly than non-genital morphological traits (Huber, 2003; Huber and Dimitrov 2014). Also, the somatic characters are useful as additional evidence to separate species in some groups of spiders; coloration, color pattern, body proportions, and even extreme size differences are useful traits for species separation (Huber et al. 2005; Huber and Dimitrov 2014). As additional evidence for the separation between *L. tenochtitlan* sp. nov. and *L. misteca*, geometric and linear morphometric variation was statistically significant for tibia shape of the palp of males and leg I length between males of both species, where the males of *L. misteca* have longer legs than the males of the new species (Table 5, Fig. 81). We do not know whether these differences in leg lengths between males of both species correspond to the microhabitat of each species or why this morphological difference only occurs in males. *Loxosceles*



Figures 78–81. Sexual dimorphism of *Loxosceles tenochtitlan* sp. nov. (T test) **78** box plots showing the variation of leg length 1 between males and females ($t = -1.3106$, $p = 0.1981$, $df = 37$, $\alpha = 0.05$) **79, 80** box plots showing variation of carapace length (**79**) and width (**80**) between males and females (length: $t = 1.498$, $p = 0.142$, $df = 38$, $\alpha = 0.05$; width: $t = 0.6955$, $p = 0.4912$, $df = 36$, $\alpha = 0.05$) **81** linear morphometric variation of leg I length between males and females of *L. tenochtitlan* and *L. misteca* (T test) (males: $t = 3.6174$, $p = 0.00331$, $df = 13$, $\alpha = 0.05$; females: $t = 0.274$, $p = 0.787$, $df = 17$, $\alpha = 0.05$).

tenochtitlan sp. nov. only has been collected in urban areas (Figs 7–18), whereas *L. misteca* are common in caves and have been collected from caves in Guerrero and Estado de Mexico. Some studies have demonstrated how microhabitat plays an important role in driving spider diversification. Eberle et al. (2018) analyzed diversification in pholcids based on the framework of the largest molecular phylogeny of the spider family Pholcidae to date, analyzed their diversification and found that diversity may be caused by microhabitat changes. Planas and Ribera (2014) and Souza and Ferreira (2018) mentioned that *Loxosceles* are generally considered troglophiles because of their abundance in caves. In other animals, long legs are considered a hallmark of troglomorphism. Further research of North American species of *Loxosceles* is required to address a correlation between leg length and microhabitat.

ENM is a powerful approach to understand how abiotic factors (e.g., temperature, precipitation, and seasonality) impact the geographic limits of the species (Graham et al. 2004a; Wiens and Graham 2005). The integration of genetic and ecological approaches in the study of mechanisms driving geographic distributions of organisms is becoming more common (Hugall et al. 2002; Johnson and Cicero 2002; Graham et al. 2004; Lapointe and Rissler 2005; Rissler and Apodaca 2007; Raxworthy et al. 2007). In the ENM, following the biogeographical provinces proposed by Morrone



83

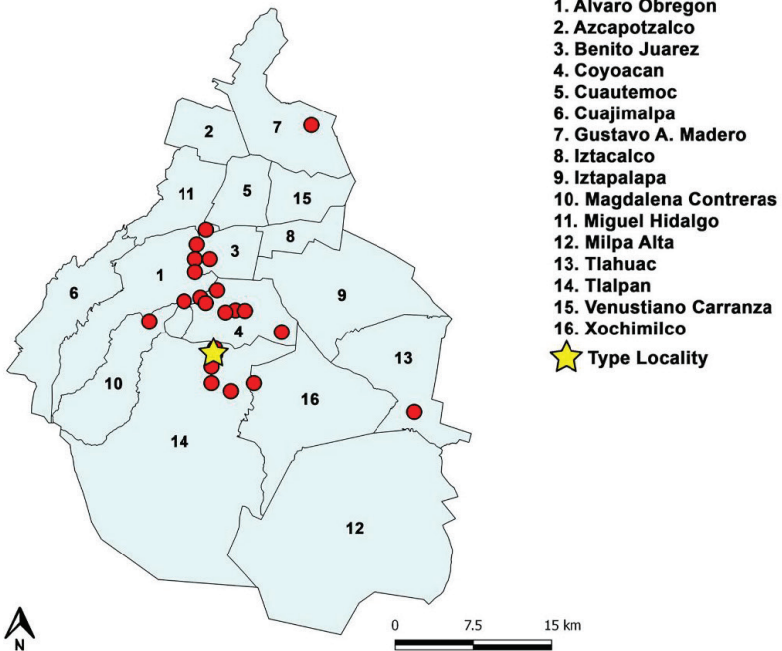
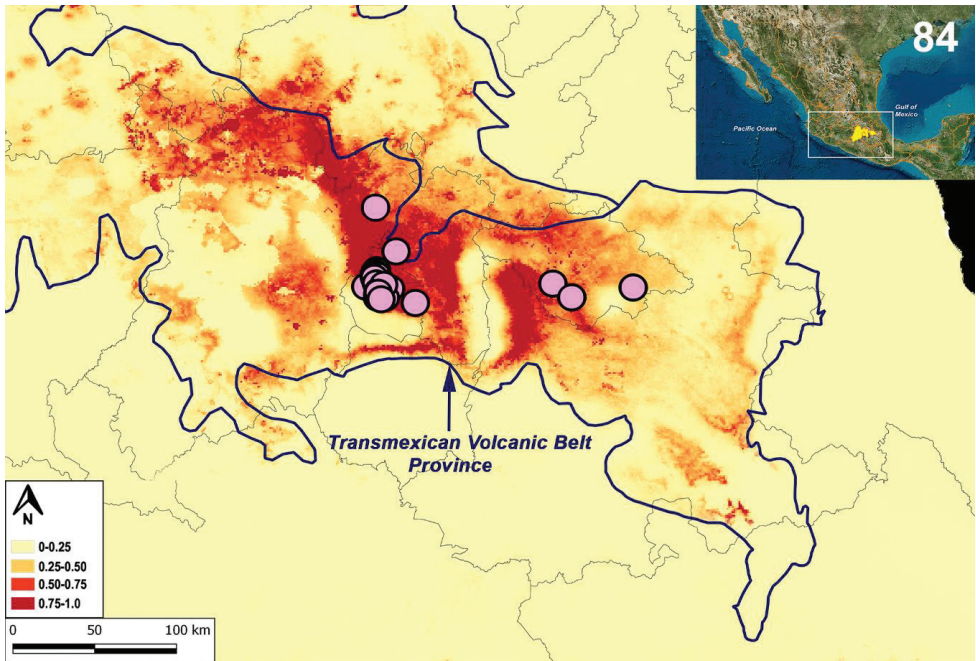


Figure 82–83. **82** Distribution records of *Loxosceles tenochtitlan* sp. nov. from Mexico City (CDMX), Estado de Mexico (MEX), and Tlaxcala (TLAX) **83** known records of *L. tenochtitlan* sp. nov. from Mexico City, including the type locality (star).



Figures 84. Ecological niche modeling (ENM) under Maxent algorithm for *Loxosceles tenochtitlan* sp. nov. Colors represent different ranges of probabilities of presence (high probability: 0.75–1.0). Circles represent known records of the new species. Blue lines represent biogeographical provinces proposed by Morrone (2004, 2005).

(2004, 2005), vegetation type plays an important role in the ecological niche of the species (Fig. 84). ENM showed that the highest probability of presence (0.75–1.0) for *L. tenochtitlan* sp. nov. is strongly limited towards the Transmexican Volcanic Belt (TVB) (Fig. 84), characterized by high mountains and a temperate climate, with pine, oak or oak-pine forest. Although ENM calculated a potential distribution to the south of states of Puebla, south and north of the Estado de Mexico, and small regions of the states of Michoacan, Guanajuato and Queretaro, this can be explained as an over-prediction, and other species of *Loxosceles* might occur there (Fig. 84) (Valdez-Mondragón et al. 2018: figs 75–77). Although *L. tenochtitlan* sp. nov. is distributed widely in urban areas of Mexico City, Estado de Mexico and Tlaxcala, this species can be considered a native of this region and the urbanization process has not affected its establishment in such areas. However, the species has never been collected in natural areas in the state (Valdez-Mondragón et al. 2018a, b). In 2017, four collectors collected around 40 specimens of *L. tenochtitlan* sp. nov. in two hours from a house in the state of Tlaxcala, Mexico (Valdez-Mondragón et al. 2018a, b). As has been demonstrated for other species of the genus as *Loxosceles reclusa* from the United States, the partial synanthropy of some species of the brown recluse spiders is not the dominant influence on distributional patterns (Saupe et al. 2011). Although the species may be able to expand beyond their distribution with the aid of the anthropogenic activities, the species analyzed

herein does not have widespread distribution due to historical or biological barriers or their limited dispersion potential, where the vegetation type plays an important role to delimitation of their distribution (Table 6, Fig. 84).

Despite the similarity between *L. tenochtitlan* sp. nov. and *L. misteca*, we consider them different species for three main reasons: (1) they can be distinguished by morphological characters (genitalic and somatic); and the new species can be diagnosed morphologically; (2) molecular data from multiple genes analyzed with multiple methods consistently separate them (congruence among methods); and (3) statistically significant geometric and linear morphometric variation in tibiae shape of the palp of the male and leg I length of males respectively.

Acknowledgments

The first author thanks the program “Cátedras CONACyT”, Consejo Nacional de Ciencia y Tecnología (CONACyT), Mexico; for scientific support for the project No. 59: “Laboratorio Regional de Biodiversidad y Cultivo de Tejidos Vegetales (LBCTV) del Institute of Biology, Universidad Nacional Autónoma de México (IBUNAM), sede Tlaxcala”. The first author also thanks SEP-CONACyT for the financial support of the project of Basic Science (Ciencia Básica) 2016, No. 282834: Arañas de Importancia Médica: Taxonomía integrativa basada en evidencia molecular y morfológica para la delimitación de las especies mexicanas de arañas violinistas del género *Loxosceles* Heineken & Lowe (Araneae, Sicariidae)-Etapa 1. The second and third authors thank Posgrado en Ciencias Biológicas of Centro Tlaxcala de Biología de la Conducta (CTBC), Universidad Autónoma de Tlaxcala (UATx) for educational support, and CONACyT for scholarship support during the Master’s degree of Biological Science and to the Secretaría de Fomento Agropecuario del Estado de Tlaxcala (SEFOA) and the Government of the state of Tlaxcala for the facilities and support to conduct this research. We thank Dr. Oscar F. Francke, Curator of the Colección Nacional de Arácnidos (CNAN), IBUNAM, Mexico City, for the loan of the collection of *Loxosceles* specimens of the CNAN, Dr. Lazaro Guevara López for his suggestions and comments that improved the manuscript. We also thank the students of the CNAN and Laboratory of Arachnology (LATLAX), IBUNAM, Tlaxcala, for their donation of specimens, help in the field, and processing of the material in the laboratory, M. Sc. Berenit Mendoza Gárfias for the SEM photographs, Jared Lacayo-Ramírez for his helping photograph live specimens. A special thanks to the Biól. and friend Martin Sánchez Vilchis and his family for the disposition and the donation of the specimens collected in their house, which were selected as types of the species (¡gracias carnal!). We thank the family Juárez-Sánchez and José A. Castilla-Vázquez from Tlaxcala for allowing us to collect in their houses, Ignacio Beltrán for his help in the Grutas de Cacahuamilpa, Guerrero, Dr. Sarah Crews for the English language review of the manuscript, José C. Valerdi-Tlachi († may he rest in peace). The specimens were collected under Scientific Collector Permit FAUT-0309 from the Secretaría de Medio Ambiente y Recursos Naturales (SEMARNAT) to AVM.

References

- Astrin JJ, Stueben PE (2008) Phylogeny in cryptic weevils: molecules, morphology and new genera of western Palaearctic Cryptorhynchinae (Coleoptera: Curculionidae). *Invertebrate Systematics* 22(5): 503–522. <https://doi.org/10.1071/IS07057>
- Bickford D, Lohman DJ, Sodhi NS, Ng PKL, Meier R, Winker K, Ingram KK, Das I (2007) Cryptic species as a window on diversity and conservation. *Trends in Ecology and Evolution* 22(3): 148–155. <https://doi.org/10.1016/j.tree.2006.11.004>
- Binford GJ, Callahan MS, Bodner MR, Rynerson MR, Berea-Núñez P, Ellison CE, Duncan RP (2008) Phylogenetic relationships of *Loxosceles* and *Sicarius* spiders are consistent with Western Gondwanan vicariance. *Molecular Phylogenetics and Evolution* 49(2): 538–553. <https://doi.org/10.1016/j.ympev.2008.08.003>
- Brignoli P (1968) Note sugli Scytodidae d'Italia e Malta (Araneae). *Fragmenta Entomologica* 6: 121–166.
- Carstens BC, Pelletier TA, Reid NM, Satler J (2013) How to fail at species delimitation. *Molecular Ecology* 22(17): 4369–4383. <https://doi.org/10.1111/mec.12413>
- Clement M, Posada DCKA, Crandall KA (2000) TCS: a computer program to estimate gene genealogies. *Molecular Ecology* 9(10): 1657–1659. <https://doi.org/10.1046/j.1365-294x.2000.01020.x>
- CONABIO (2015) Comisión Nacional para el Conocimiento y Uso de la Biodiversidad. <http://www.conabio.gob.mx> [consulted on May 14, 2019]
- DeSalle R, Egan MG, Siddall M (2005) The unholy trinity: taxonomy, species delimitation and DNA barcoding. *Philosophical Transactions of the Royal Society, London, Ser. B* 360 (1462): 1905–1916. <https://doi.org/10.1098/rstb.2005.1722>
- Drummond AJ, Suchard MA, Xie D, Rambaut A (2012) Bayesian phylogenetics with BEAUti and the BEAST 1.7. *Molecular Biology and Evolution* 29(8): 1969–1973. <https://doi.org/10.1093/molbev/mss075>
- Duncan RP, Rynerson MR, Ribera C, Binford GJ (2010) Diversity of *Loxosceles* spiders in Northwestern Africa and molecular support for cryptic species in the *Loxosceles rufescens* lineage. *Molecular Phylogenetic and Evolution* 55(1): 234–248. <https://doi.org/10.1016/j.ympev.2009.11.026>
- Durán-Barrón CG, Ayala-Islas DE (2007) Presencia de arañas del género *Loxosceles* Heineken & Lowe, 1832 en la Ciudad de México. *Memorias de la 8a. reunión internacional de expertos en envenenamiento por animales ponzoñosos. Instituto de Biotecnología/Instituto de Neurobiología, UNAM, Querétaro, México.*
- Durán-Barrón CG, Pérez-Ortiz TM (2016) Arañas de importancia médica: la viuda negra y la araña violinista. En: *La biodiversidad en la Ciudad de México, vol 2. CONABIO/SEDEMA, México, 239–244.*
- Eberle J, Dimitrov D, Valdez-Mondragón A, Huber BA (2018) Microhabitat change drives diversification in pholcid spiders. *BMC Evolutionary Biology* 18: 141. <https://doi.org/10.1186/s12862-018-1244-8>
- Fick SE, Hijmans RJ (2017) Worldclim 2: New 1-km spatial resolution climate surfaces for global land areas. *International Journal of Climatology*. <https://doi.org/10.1002/joc.5086>

- Folmer M, Black W, Lutz R, Vrijenhoek R (1994) DNA primers for amplification of mitochondrial cytochrome c oxidase subunit I from diverse metazoan invertebrates. *Molecular Marine Biology and Biotechnology* 3: 294–299. [https://doi.org/10.1603/00222585\(2005\)042\[0756:MOBLIA\]2.0.CO;2](https://doi.org/10.1603/00222585(2005)042[0756:MOBLIA]2.0.CO;2)
- Francke O, Durán-Barrón CG, Pérez-Ortíz TM (2009) Diversidad de arañas (Arachnidae: Araneae) asociadas con viviendas de la Ciudad de México (Zona Metropolitana). *Revista Mexicana de Biodiversidad* 80: 55–69. <https://doi.org/10.22201/ib.20078706e.2009.001.584>
- Fujisawa T, Barraclough TG (2013) Delimiting species using single-locus data and the Generalized Mixed Yule Coalescent approach: a revised method and evaluation on simulated data sets. *Systematic Biology* 62(5): 707–724. <https://doi.org/10.1093/sysbio/syt033>
- Fukushima CS, Gonçalves de Andrade RM, Bertani R (2017) Two new Brazilian species of *Loxosceles* Heineken & Lowe, 1832 with remarks on *amazonica* and *rufescens* groups (Araneae, Sicariidae). *Zootaxa* 667: 67–94. <https://10.3897/zookeys.667.11369>
- Graham CH, Ron S, Santos J, Schneider C, Moritz C (2004a) Integrating phylogenetics and environmental niche models to explore speciation mechanisms in dendrobatid frogs. *Evolution* 58(8): 1781–1793. <https://doi.org/10.1554/03-274>
- Graham CH, Ferrier S, Huettman F, Moritz C, Peterson A (2004b) New developments in museum-based informatics and applications in biodiversity analysis. *Trends in Ecology and Evolution* 19(9): 497–503. <https://doi.org/10.1016/j.tree.2004.07.006>
- Gertsch WJ (1967) The spider genus *Loxosceles* in South America (Araneae, Scytodidae). *Bulletin of the American Museum of Natural History* 136: 117–174.
- Gertsch WJ (1958) The spider genus *Loxosceles* in North America, Central America, and the West Indies. *American Museum Novitates* 1907: 1–46.
- Gertsch WJ (1973) A report on cave spiders from Mexico and Central America. *Association for Mexican Cave Studies Bulletin* 5: 141–163.
- Gertsch WJ, Ennik F (1983) The spider genus *Loxosceles* in North America, Central America, and the West Indies (Araneae, Loxoscelidae). *Bulletin of the American Museum of Natural History* 175: 264–360.
- Hall TA (1999) “BioEdit: a user-friendly biological sequence alignment editor and analysis program for Windows 95/98/NT”. *Nucleic Acids Symposium Series* 41: 95–98.
- Hamilton CA, Formanowicz DR, Bond JE (2011) Species delimitation and phylogeography of *Aphonopelma hentzi* (Araneae, Mygalomorphae, Theraphosidae): cryptic diversity in North American tarantulas. *PLoS ONE* 6(10): e26207. <https://doi.org/10.1371/journal.pone.0026207>
- Hamilton CA, Hendrixson BE, Brewer MS, Bond JE (2014) An evaluation of sampling effects on multiple DNA barcoding methods leads to an integrative approach for delimiting species: A case study of the North American tarantula genus *Aphonopelma* (Araneae, Mygalomorphae, Theraphosidae). *Molecular Phylogenetics and Evolution* 71: 79–93. <https://doi.org/10.1016/j.ympev.2013.11.007>
- Hamilton CA, Hendrixson BE, Bond JE (2016) Taxonomic revision of the tarantula genus *Aphonopelma* Pocock, 1901 (Araneae, Mygalomorphae, Theraphosidae) within the United States. *Zookeys* 560: 1–340. <https://doi.org/10.3897/zookeys.560.6264>

- Hebert PDN, Cywinska A, Ball SL, Dewaard JR (2003) Biological identifications through DNA barcodes. *Proceedings Biological Sciences* 270(1512): 313–321. <https://doi.org/10.1098/rspb.2002.2218>
- Hebert PDN, Penton EH, Burns JM, Janzen DH, Hallwachs W (2004) Ten species in one: DNA barcoding reveals cryptic species in the Neotropical skipper butterfly *Astraptes fulgerator*. *Proceedings of the National Academy of Sciences of the United States of America* 101(41): 14812–14817. <https://doi.org/10.1073/pnas.0406166101>
- Hoffmann A (1976) Relación bibliográfica preliminar de las arañas de México (Arachnida: Araneae). Instituto de Biología, Universidad Nacional Autónoma de México, México D. F, 117 pp.
- Huber BA (2003) Rapid evolution and species-specificity of arthropod genitalia: fact or artifact? *Organisms Diversity & Evolution* 3(1): 63–71. <https://doi.org/10.1078/1439-6092-00059>
- Huber BA, Rheims CA, Brescovit AD (2005) Speciation without changes in genital shape: a case study on Brazilian pholcid spiders (Araneae: Pholcidae). *Zoologischer Anzeiger* 243(4): 273–279. <https://doi.org/10.1016/j.jcz.2004.12.001>
- Huber BA, Dimitrov D (2014) Slow genital and genetic but rapid non-genital and ecological differentiation in a pair of spider species (Araneae, Pholcidae). *Zoologischer Anzeiger* 253(5): 394–403. <https://doi.org/10.1016/j.jcz.2014.04.001>
- Hugall A, Moritz C, Moussalli A, Stanisic J (2002) Reconciling paleodistribution models and comparative phylogeography in the Wet Tropics rainforest land snail *Gnarosophia bellendenkerensis* (Brazier 1875). *PNAS* 99(9): 6112–6117. <https://doi.org/10.1073/pnas.092538699>
- Illoldi-Rangel P, Escalante T (2008) De los modelos de nicho ecológico a las áreas de distribución geográfica. *Biogeografía* 3: 7–12.
- INEGI (2019) Instituto Nacional de Estadística y Geografía. <http://www.inegi.org.mx/> [consultado el 22/05/2019]
- Jarman SN, Elliott NG (2000) DNA evidence for morphological and cryptic Cenozoic speciations in the Anaspididae 'living fossils' from the Triassic. *Journal of Evolutionary Biology* 13(4): 624–633. <https://doi.org/10.1046/j.1420-9101.2000.00207.x>
- Ya-Jie J, De-Xing Z, Li-Jun H (2003) Evolutionary conservation and versatility of a new set of primers for amplifying the ribosomal internal transcribed spacer regions in insects and other invertebrates. *Molecular Ecology Notes* 3(4): 581–585. <https://doi.org/10.1046/j.1471-8286.2003.00519.x>
- Johnson NK, Cicero C (2002) The role of ecologic diversification in sibling speciation of *Empidonax flycatchers* (Tyrannidae): Multigene evidence from mtDNA. *Molecular Ecology* 11(10): 2065–2081. <https://doi.org/10.1046/j.1365-294X.2002.01588.x>
- Katoh K, Toh H (2008) Recent developments in the MAFFT multiple sequence alignment program. *Briefings in Bioinformatics* 4(9): 286–298. <https://doi.org/10.1093/bib/bbn013> [MAFFT Version 6]
- Kapli P, Lutteropp S, Zhang J, Kobert K, Pavlidis P, Stamatakis A, Flouri T (2017) Multi-rate Poisson tree processes for single-locus species delimitation under maximum likelihood and Markov chain Monte Carlo. *Bioinformatics* 33(11): 1630–1638. <https://doi.org/10.1093/bioinformatics/btx025>

- Kearse M, Moir R, Wilson A, Stones-Havas S, Cheung M, Sturrock S, Buxton S, Cooper A, Markowitz S, Durán C, Thierer T, Ashton B, Meintjes P, Drummond A (2012) Geneious Basic: an integrated and extendable desktop software platform for the organization and analysis of sequence data. *Bioinformatics* 28(12): 1647–1649. <https://doi.org/10.1093/bioinformatics/bts199>
- Lapointe FJ, Rissler LJ (2005) Congruence, consensus, and the comparative phylogeography of co-distributed species in California. *The American Naturalist* 166(2): 290–299. <https://doi.org/10.1086/431283>
- Leigh JW, Bryant D (2015) PopArt: full-feature software for haplotype network construction. *Methods in Ecology and Evolution* 6(9): 1110–1116. <https://doi.org/10.1111/2041-210X.12410>
- Luo A, Ling C, Ho YM, Zhu CD (2018) Comparison of Methods for Molecular Species Delimitation Across a Range of Speciation Scenarios. *Systematic Biology* 67(5): 830–846. <https://doi.org/10.1093/sysbio/syy011>
- Magalhães ILF, Brescovit AD, Santos AJ (2017) Phylogeny of Sicariidae spiders (Araneae: Haplogynae), with a monograph on Neotropical Sicarius. *Zoological Journal of the Linnean Society* 179(4): 767–864. <https://doi.org/10.1111/zoj.12442>
- Manríquez JJ, Silva S (2009) *Loxoscelismo* cutáneo y cutáneo-visceral: Revisión sistemática. *Revista Chilena de Infectología* 26(5): 420–432. <https://doi.org/10.4067/S0716-10182009000600004>
- Monaghan MT, Wild R, Elliot M, Fujisawa T, Balke M, Inward DJ, Vogler AP (2009) Accelerated species inventory on Madagascar using coalescent-based models of species delineation. *Systematic Biology* 58(3): 298–311. <https://doi.org/10.1093/sysbio/syp027>
- Morrone JJ (2004) Panbiogeografía, componentes bióticos y zonas de transición. *Revista Brasileira de Entomologia* 48(2): 149–162. <https://doi.org/10.1590/S0085-56262004000200001>
- Morrone JJ (2005) Hacia una síntesis biogeográfica de México. *Revista Mexicana de Biodiversidad* 76(2): 207–252. <https://doi.org/10.22201/ib.20078706e.2005.002.303>
- Nentwig W, Pantini P, Vetter RS (2017) Distribution and medical aspects of *Loxosceles rufescens*, one of the most invasive spiders of the world (Araneae: Sicariidae). *Toxicon* 132: 19–28. <https://doi.org/10.1016/j.toxicon.2017.04.007>
- Ortiz D, Francke OF (2016) Two DNA barcodes and morphology for multi-method species delimitation in *Bonnetina* tarantulas (Araneae: Theraphosidae). *Molecular Phylogenetics and Evolution* 101: 176–193. <https://doi.org/10.1016/j.ympev.2016.05.003>
- Phillips SJ, Dudík M, Schapire RE (2004) A maximum entropy approach to species distribution modeling. In: *Proceedings of the twenty-first international conference on Machine learning*, Banff, Canada, ACM, 83 pp. <https://doi.org/10.1145/1015330.1015412>
- Phillips SJ, Anderson RP, Schapire RE (2006) Maximum entropy modeling of species geographic distributions. *Ecological Modelling* 190: 231–259. <https://doi.org/10.1016/j.ecolmodel.2005.03.026>
- Phillips SJ, Dudík M (2008) Modeling of species distributions with Maxent: new extensions and a comprehensive evaluation. *Ecography* 31(2): 161–175. <https://doi.org/10.1111/j.0906-7590.2008.5203.x>

- Planas E, Ribera C (2014) Uncovering overlooked island diversity: colonization and diversification of the medically important spider genus *Loxosceles* (Arachnida: Sicariidae) on the Canary Islands. *Journal of Biogeography* 41(7): 1255–1266. <https://doi.org/10.1111/jbi.12321>
- Planas E, Ribera C (2015) Description of six new species of *Loxosceles* (Araneae: Sicariidae) endemic to the Canary Islands and the utility of DNA barcoding for their fast and accurate identification. *Zoological Journal of the Linnean Society* 174(1): 47–73. <https://doi.org/10.1111/zoj.12226>
- Pons J, Barraclough TG, Gomez-Zurita J et al. (2006) Sequence based species delimitation for the DNA taxonomy of undescribed insects. *Systematic Biology* 55(4): 595–609. <https://doi.org/10.1080/10635150600852011>
- Posada D, Buckley TR (2004) Model selection and model averaging in phylogenetics: advantages of Akaike information criterion and Bayesian approaches over likelihood ratio tests. *Systematic biology* 53(5): 793–808. <https://doi.org/10.1080/10635150490522304>
- Proudlove G, Wood PJ (2003) The blind leading the blind: cryptic subterranean species and DNA taxonomy. *TRENDS in Ecology and Evolution* 18(6): 272–273. [https://doi.org/10.1016/S0169-5347\(03\)00095-8](https://doi.org/10.1016/S0169-5347(03)00095-8)
- Puillandre N, Lambert A, Brouillet S, Achaz G (2012) ABGD, Automatic Barcode Gap Discovery for primary species delimitation. *Molecular ecology* 21(8): 1864–1877. <https://doi.org/10.1111/j.1365-294X.2011.05239.x>
- Rambaut A, Drummond AJ (2014) TRACER, MCMC trace analysis tool version 1.5. University of Edinburgh (Edinburgh) and University of Auckland (Auckland).
- Ramos-Rodríguez HG, Méndez JD (2008) Necrotic Araneism. A review of the *Loxosceles* genus. I. General aspects, distribution and venom composition. *Advances in Environmental Biology* 2(1): 9–19.
- Raxworthy CJ, Ingra CM, Rabibisoa N, Pearson R (2007) Applications of Ecological Niche Modeling for species Delimitation: A review and empirical evaluation using day Geckos (*Phelsuma*) from Madagascar. *Systematic Biology* 56(6): 907–923. <https://doi.org/10.1080/10635150701775111>
- Rissler LJ, Apodaca JJ (2007) Adding More Ecology into Species Delimitation: Ecological Niche Models and Phylogeography Help Define Cryptic Species in the Black Salamander (*Aneides flavipunctatus*). *Systematic Biology* 56(6): 924–942. <https://doi.org/10.1080/10635150701703063>
- Rohlf FJ (2015) The tps series of software. *Hystrix* 26(1): 9–12. <https://doi.org/10.4404/hystrix-26.1-11264>
- Ronquist F, Huelsenbeck JP (2003) MrBayes 3: Bayesian phylogenetic inference under mixed models. *Bioinformatics* 19(12): 1572–1574. <https://doi.org/10.1093/bioinformatics/btg180>
- Sandidge JS, Hopwood JL (2005) Brown recluse spiders: a review of biology, life history and pest management. *Transactions of the Kansas Academy of Science* 108(3): 99–108. [https://doi.org/10.1660/0022-8443\(2005\)108\[0099:BRSARO\]2.0.CO;2](https://doi.org/10.1660/0022-8443(2005)108[0099:BRSARO]2.0.CO;2)
- Saupe EE, Papes M, Selden PA, Vetter RS (2011) Tracking a medically important spider: climate change, ecological niche modeling, and the brown recluse (*Loxosceles reclusa*). *PLoS ONE* 6(3): e17731. <https://doi.org/10.1371/journal.pone.0017731>

- Sheets HD, Zelditch ML (2014) IMP: TMorphGen8 compiled 3/5/14. Traditional Morphometrics Data Set Generator. In: CoordGen8, 6/3/2014. Dept. of Physics, Canisius College and Dept. of Geology, SUNY at Buffalo, Buffalo NY. http://www.filenetica.org/cursos/Morfometria/IMP_installers/index.php
- Souza MFVR, Ferreira RL (2018) A new highly troglomorphic *Loxosceles* (Araneae: Sicariidae) from Brazil. *Zootaxa* 4438(3): 575–587. <https://doi.org/10.11646/zootaxa.4438.3.9>
- Struck TH, Cerca J (2019) Cryptic species and their evolutionary significance. eLS. John Wiley & Sons, Ltd: Chichester. <https://doi.org/10.1002/9780470015902.a0028292>
- Swanson DL, Vetter RS (2009) Loxoscelism. *Clinics in Dermatology* 24: 213–221. <http://10.1016/j.clindermatol.2005.11.006>
- Tahami MS, Zamani A, Sadeghil S, Ribera C (2017) A new species of *Loxosceles* Heineken & Lowe, 1832 (Araneae: Sicariidae) from Iranian caves. *Zootaxa* 4318(2): 377–387. <https://doi.org/10.11646/zootaxa.4318.2.10>
- Valdez-Mondragón A, Francke OF (2015) Phylogeny of the spider genus *Ixchela* Huber, 2000 (Araneae: Pholcidae) based on morphological and molecular evidence (CO1 and 16S), with a hypothesized diversification in the Pleistocene. *Zoological Journal of the Linnean Society* 175: 20–58. <https://doi.org/10.1111/zoj.12265>
- Valdez-Mondragón A, Cortez-Roldán MR, Juárez-Sánchez AR, Solís-Catalán KP, Navarro-Rodríguez CI (2018a) Arañas de Importancia Médica: Arañas violinistas del género *Loxosceles* en México, ¿qué sabemos acerca de su distribución y biología hasta ahora? *Boletín de la Asociación Mexicana de Sistemática de Artrópodos (AMXSA)* 2(1): 14–24.
- Valdez-Mondragón A, Cortez-Roldán MR, Juárez-Sánchez AR, Solís-Catalán KP (2018b) A new species of *Loxosceles* Heineken & Lowe (Araneae, Sicariidae), with updated distribution records and biogeographical comments for the species from Mexico, including a new record of *Loxosceles rufescens* (Dufour). *ZooKeys* 802: 39–66. <https://doi.org/10.3897/zookeys.802.28445>
- Vetter RS (2008) Spiders of the genus *Loxosceles* (Araneae, Sicariidae): a review of biological, medical and psychological aspects regarding envenomations. *Journal of Arachnology* 36(1): 150–163. <https://doi.org/10.1636/RSt08-06.1>
- Vetter RS (2015) *The Brown Recluse Spider*. Cornell University Press/Comstock Publishing Associates, Ithaca/London, 186 pp.
- Wiens JJ, Graham CH (2005) Niche conservatism: Integrating evolution, ecology, and conservation biology. *Annual Review of Ecology, Evolution, and Systematics* 36: 519–539. <https://doi.org/10.1146/annurev.ecolsys.36.102803.095431>
- Witt JDS, Hebert PDN (2000) Cryptic species diversity and evolution in the amphipod genus *Hyaletta* within central glaciated North America: a molecular phylogenetic approach. *Canadian Journal of Fisheries and Aquatic Sciences* 57(4): 687–698. <https://doi.org/10.1139/f99-285>
- World Spider Catalog (2019) World Spider Catalog. Version 20.0. Natural History Museum Bern. <https://doi.org/10.24436/2> [accessed on July 7, 2019]
- Zhang J, Kapli P, Pavlidis P, Stamatakis A (2013) A general species delimitation method with applications to phylogenetic placements. *Bioinformatics* 29(22): 2869–2876. <https://doi.org/10.1093/bioinformatics/btt499>

Rhynchotermes armatus, a new mandibulate nasute termite (Isoptera, Termitidae, Syntermitinae) from Colombia

Rudolf H. Scheffrahn¹

¹ Fort Lauderdale Research and Education Center, Institute for Food and Agricultural Sciences, 3205 College Avenue, Davie, Florida 33314, USA

Corresponding author: *Rudolf H. Scheffrahn* (rhsc@ufl.edu)

Academic editor: *E. Canello* | Received 1 August 2019 | Accepted 15 October 2019 | Published 27 November 2019

<http://zoobank.org/B837DE29-F983-4518-98DE-1AFC2BB1AA23>

Citation: Scheffrahn RH (2019) *Rhynchotermes armatus*, a new mandibulate nasute termite (Isoptera, Termitidae, Syntermitinae) from Colombia. ZooKeys 892: 135–142. <https://doi.org/10.3897/zookeys.892.38743>

Abstract

Rhynchotermes armatus **sp. nov.** is described from soldiers and workers collected in the Magdalena River Valley of Colombia. Both castes of this new termite are superficially similar to *R. perarmatus* (Snyder) but the former are smaller, head capsules yellowish instead of reddish, and among additional characters, the soldier has narrower mandibles and marginal teeth.

Keywords

endemic, Magdalena Valley, taxonomy, vicariant divergence

Introduction

The genus *Rhynchotermes* Holmgren constitutes a peculiar group of neotropical termites ranging from Belize to Argentina. They feed openly on surface litter during crepuscular or nocturnal forays. They nest underground or in shallow epigeal nests. Soldiers are either monomorphic or weakly dimorphic and workers are monomorphic. A thorough revision of *Rhynchotermes* by Constantini and Canello (2016) included seven species: *R. amazonensis* Constantini & Canello, *R. bulbinasus* Scheffrahn, *R. diphyes* Mathews, *R. matraga* Constantini & Canello, *R. nasutissimus* (Silvestri), *R. perarmatus* (Snyder), and *R. piauy* Canello. I herein describe an eight species, *R. armatus* sp. nov., from Colombia.

Material and methods

Live specimens were preserved in 85% ethanol. External and internal worker morphology was depicted using two different methods. In the first method, soldiers and workers were suspended in Purell Instant Hand Sanitizer in a plastic Petri dish. This allowed for transparent posturing and support during photography using a Leica M205C stereomicroscope controlled by Leica Application Suite version 4.0 montage software. The worker enteric valve armature (EVA) was prepared for photography by removing the entire worker P2 section in ethanol. Food particles were expelled from the P2 tube by pressure manipulation. The tube was quickly submerged in a droplet of PVA medium (BioQuip Products Inc.) which eased muscle detachment by further manipulation. The remaining EVA cuticle was longitudinally cut, splayed open, and mounted on a microscope slide using the PVA medium. The EVA was photographed with a Leica CTR 5500 compound microscope with bright field optics using the same montage software.

Taxonomy

Rhynchotermes armatus Scheffrahn, sp. nov.

<http://zoobank.org/6BAF94E6-EA51-4A1B-B300-92151D9F98F4>

Figs 1–3

Rhynchotermes perarmatus: Pinzón and Castro 2018 [Colombia, Huila, El Agrado].

Material examined. Colombia: Pandi, Depto. Cundinamarca (4.13, -74.49; Elev. 930 m), 23JAN96, col. J. Krecek. Three colonies: CO879, **holotype** soldier (Fig. 1), one other soldier, 30 workers, and three larvae; CO880, eight soldiers and six workers; CO881, 17 soldiers and two workers (Fig. 3). All material is housed at the University of Florida Termite Collection in Davie, Florida, USA.

Description. The revised description of the genus *Rhynchotermes* by Constantini and Canello (2016) includes all characters found in *R. armatus*.

Imago. Unknown.

Soldier (Figs 1, 3; Table 1). Monomorphic. Head capsule, nasus, and mandible bases straw yellow; apical and marginal teeth yellow-brown. Head capsule dome shaped in lateral view. Nasus projecting well beyond mandibles; nearly cylindrical, tapering to rather large circular opening. Nasus hollow, thickness of outer wall even. Pilosity of head capsule limited to two faint setae near level of antennal fossae and one or two even shorter and fainter setae on vertex. Nasus without setae; curved slightly downward. Mandibles curved ~150–180° with greatest curvature beyond marginal teeth. Mandibles narrowing beyond marginal teeth. Apical teeth exceptionally narrow and sharp; marginal teeth extremely thin and angled ~60° toward labrum. Antennae very long, about twice the length of the nasus; 14 articles, 2<3>4=5. Pronotum slightly lighter than head; asymmetrically bilobed in dorsal view, posterior lobe larger; in lateral

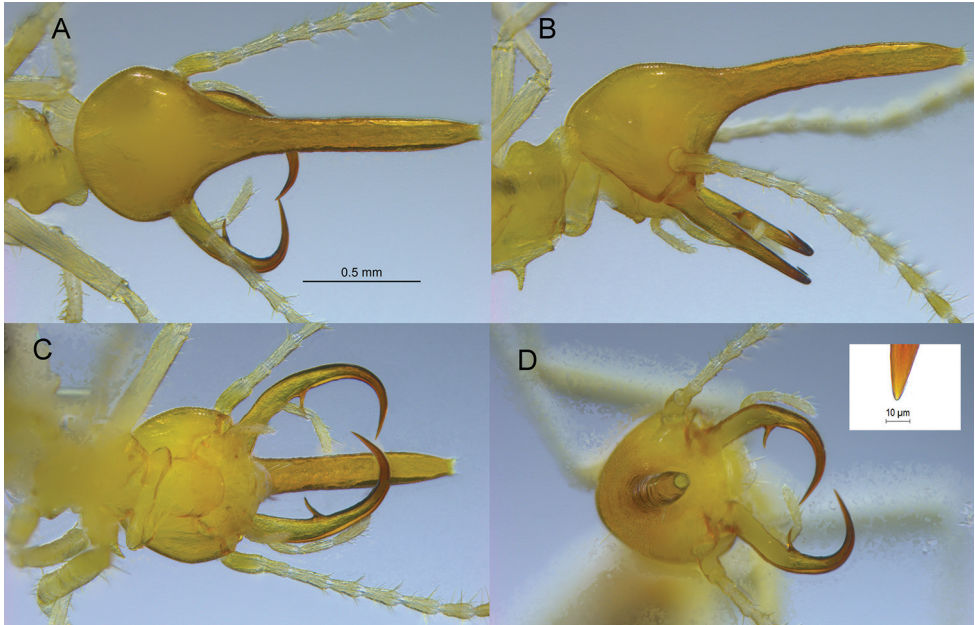


Figure 1. *Rhynchotermes armatus* sp. nov. soldier **A** dorsal **B** lateral **C** ventral and **D** anterior views (inset is tip of left apical tooth).

Table 1. Measurements (mm, $N = 12$) of *Rhynchotermes armatus* sp. nov. soldiers from three colonies.

Measurements	Max	Min	Mean
Head length with nasus	2.20	1.73	2.06
Head max. width	0.88	0.67	0.81
Pronotum width	0.56	0.37	0.52
Length of hind tibia	1.54	1.19	1.39
Max. length L mandible	1.05	0.61	0.89
No. antennal articles	14	14	14

view, margin of anterior lobe continuous with vertex, posterior lobe forming hump. Fore coxae with thorn-like process, slight downward curvature.

Worker (Fig. 2; Table 2). Monomorphic. Head capsule concolorous with soldier. Head capsule with eight-to-ten long, evenly spaced setae; postclypeus strongly inflated. In lateral view, posterior lobe of pronotum much longer and angled ca. 130° from plane of posterior lobe. Antennae with 14 articles. Forecoxa with elevated rise on anterior margin. Enteric valve weakly armed consisting of three rectangular cushions, each with 30–40 very small triangulate spines; cushions separated by wider cuticular lining interspersed with even smaller spines.

Comparison. Constantini and Canello (2016) divided *Rhynchotermes* soldiers into two morphogroups: those with mandibles larger than the head (*R. perarmatus* and *R. bulbinasus*) and those with mandibles shorter than the head (all remaining species). *Rhynchotermes armatus* falls into the former group and is closest *R. perarmatus*, each

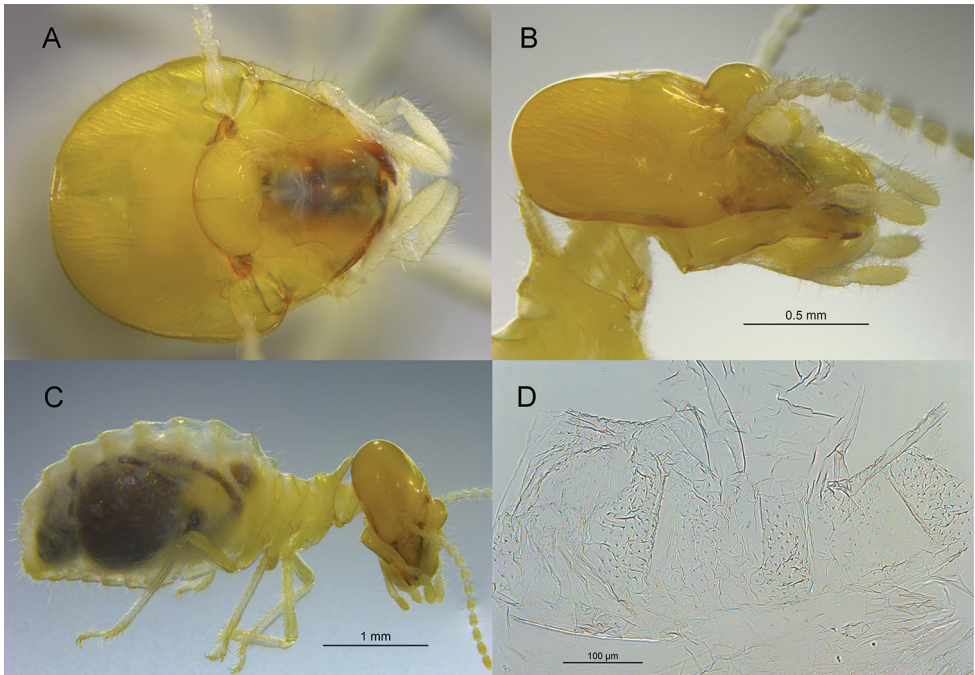


Figure 2. *Rhynchotermes armatus* sp. nov. worker **A** dorsal and **B** lateral views of head capsule **C** lateral view of habitus and **D** enteric valve armature cut longitudinally and laid flat.

Table 2. Measurements (mm, $N = 12$) of *Rhynchotermes armatus* sp. nov. workers from three colonies.

Measurements	Max	Min	Mean
Head length to condyles	1.00	0.61	0.79
Head width	1.25	1.09	1.17
Pronotum width	0.70	0.58	0.63
Length of hind tibia	1.37	1.16	1.26
No. antennal articles	14	14	14

having a tubular nasus and large mandibles. Snyder (1925a) reported a soldier head length of 2.5–2.6 mm for *R. perarmatus* and 3.0–3.2 mm for its junior synonym, *R. major* (Snyder 1925b) from Panama and Costa Rica, respectively. These measurements are from 1.14 to 1.85 times larger than *R. armatus*.

In addition to the head length, the *R. armatus* soldier is smaller in all measurements, has a yellowish head pigmentation versus reddish, and has narrower (thinner) mandibles, including the marginal teeth (Fig. 3A). The nasus of *R. armatus* has a greater curvature and the third antennal article is proportionately shorter (Fig. 3B). The workers of both species are concolorous with their respective soldiers. The *R. armatus* worker has a small and faint fontanelle (Fig. 2A) compared to the proportionately larger and more contrasting fontanelle and cranial suture of *R. perarmatus* (Fig. 3C). The *R. armatus* worker EVA has fewer spines on the three cushions and the inter-cushion areas than *R. perarmatus*. Also the *R. perarmatus* EVA has longitudinal folds covered with fine fringes anterior to the cushions (Fig. 3D) which are lacking in *R. armatus*.

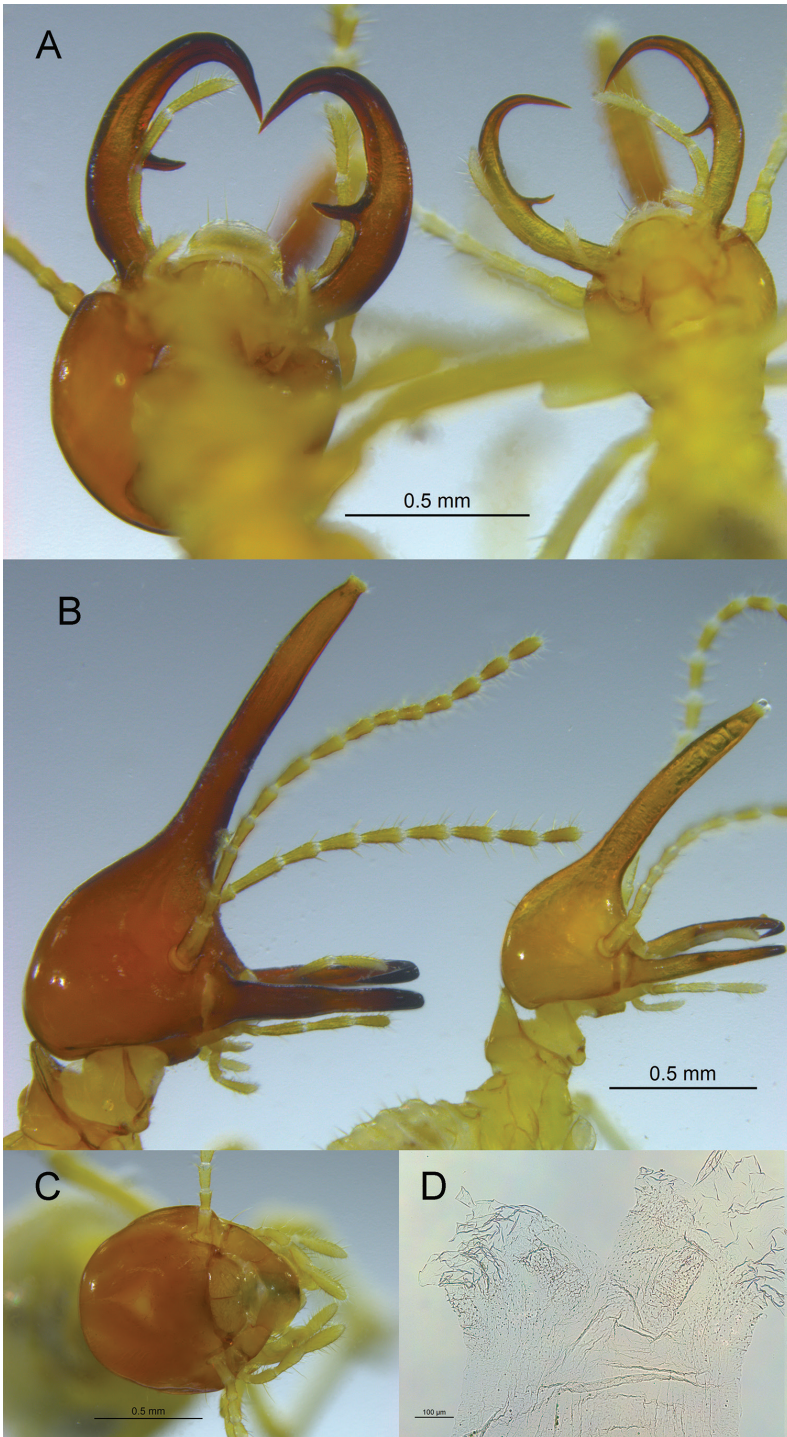


Figure 3. **A** Ventral view of soldiers of *Rhynchotermes perarmatus* from Panama (left PN153) and *R. armatus* sp. nov. from Colombia (right, CO881) **B** same as **A**, but lateral view **C** *R. perarmatus* worker and **D** worker enteric valve armature (PN153).

The next closest species, *R. bulbinasus*, differs from the other two in having a median inflation of the nasus. The apical teeth of *R. armatus* are extremely sharp (point ca. 1.5 µm wide, Fig. 1D inset), probably only comparable with those of *Silvestritermes gnomus* (Constantino) (<https://www.termediversity.org/sandsi-sinocapri?lightbox=dataItem-jy00jfyf>).

Etymology. The species name is a truncated derivative of its closest congener, *R. perarmatus*. Although Snyder (1925a) did not provide an etymology for *R. perarmatus*, he gave an apt analogy for the gestalt of all *Rhynchotermes* soldiers: “It is a thoroughly armed species and runs about audaciously with its nasus or beak elevated at an angle of 45°, reminding one of an anti-aircraft gun”.

Key addition

A new couplet (3) for the *Rhynchotermes* key by Constantini and Canello (2016) is offered below to accommodate *R. armatus*:

- | | | |
|---|---|-----------------------------|
| 1 | Mandibles larger than head, clearly visible from dorsal view when closed; apical region of each mandible extending well beyond the opposite mandible when closed (fig. 6B) | 2 |
| – | Mandibles shorter than head capsule, barely or not visible from dorsal view when closed; apical region of each mandible aligns to the proximal region of the opposite mandible when closed (fig. 6A)..... | 4* |
| 2 | Proximal region of frontal tube constricted; apical region bulbous (figs 3C, 4C)..... | <i>R. bulbinasus</i> |
| – | Frontal tube elongate, subcylindrical (figs 3H, 4H) | 3 |
| 3 | Length of head with nasus ≤ 2.20 mm, head yellowish | <i>R. armatus</i> |
| – | Length of head with nasus ≥ 2.5 mm, head reddish brown | <i>R. perarmatus</i> |

Discussion

The long-mandible clade (*R. perarmatus*, *R. bulbinasus*, and *R. armatus*) are restricted to Central America and northern Colombia (localities herein; Constantini and Canello 2016) with one unconfirmed report of *R. perarmatus* from Ecuador (Snyder 1949). All remaining *Rhynchotermes* species have an Amazonian or austral distribution (Constantini and Canello 2016).

The Magdalena River Valley lies between the central and eastern ranges of the Colombian Andes and is host to various endemic faunas including birds (Cracraft 1985), fishes (Anderson and Maldonado-Ocampo 2011), frogs (Ospina-Sarria et al. 2015), lizards (Velasco and Hurtado-Gómez 2014), and insects (Huertas et al. 2009; Padilla-Gil 2015). *Rhynchotermes armatus* is apparently another endemic species from the Magdalena River Valley. It is plausible that *R. armatus* and *R. bulbinasus* evolved

* Couplet 4 replaces 3 in original key so a digit is added to all ensuing couplets.

from an ancestor of *R. perarmatus* following the gradual land bridge closure joining Central and South America during the Miocene (Woodburne 2010). This timeframe coincides with the orogenic rise of the Eastern Cordillera of Colombia (Gregory-Wodzicki 2000) which may have led to the vicariant divergence and allopatric speciation across elevational gradients leading to one or both Colombian species. This scenario was reported for *Rheobates* frogs of the same region (Muñoz Ortiz et al. 2015). Additional undescribed termites known only from this valley include a new genus of Apicotermatinae, a new species of *Rugitermes*, and a new *Obtusitermes* (Scheffrahn and Pinzón, unpublished). No doubt further exploration will yield more new taxa.

Acknowledgments

My thanks to Jan Krecke for his tenacious collecting efforts and John Warner for measurements.

References

- Anderson EP, Maldonado Ocampo JA (2011) A regional perspective on the diversity and conservation of tropical Andean fishes. *Conservation Biology* 25(1): 30–39. <https://doi.org/10.1111/j.1523-1739.2010.01568.x>
- Cracraft J (1985) Historical Biogeography and Patterns of Differentiation Within the South American Avifauna: Areas of Endemism. *Ornithological Monographs* 36, Neotropical Ornithology, American Ornithological Society 49–84. <https://doi.org/10.2307/40168278>
- Constantini JP, Canello EM (2016) A taxonomic revision of the Neotropical termite genus *Rhynchotermes* (Isoptera Termitidae Syntermitinae). *Zootaxa* 4109: 501–522. <https://doi.org/10.11646/zootaxa.4109.5.1>
- Gregory-Wodzicki KM (2000) Uplift history of the Central and Northern Andes: a review. *Geological Society of America Bulletin* 112(7): 1091–1105. [https://doi.org/10.1130/0016-7606\(2000\)112<1091:UHOTCA>2.3.CO;2](https://doi.org/10.1130/0016-7606(2000)112<1091:UHOTCA>2.3.CO;2)
- Huertas B, Ríos C, Le Crom JF (2009) A new species of *Splendeptychia* from the Magdalena Valley in Colombia (Lepidoptera: Nymphalidae: Satyrinae). *Zootaxa* 2014(1): 51–58. <https://doi.org/10.11646/zootaxa.2014.1.5>
- Muñoz Ortiz A, Velásquez Álvarez ÁA, Guarnizo CE, Crawford AJ (2015) Of peaks and valleys: testing the roles of orogeny and habitat heterogeneity in driving allopatry in mid-elevation frogs (Aromobatidae: Rheobates) of the northern Andes. *Journal of Biogeography* 42(1): 193–205. <https://doi.org/10.1111/jbi.12409>
- Ospina-Sarria JJ, Angarita-Sierra T, Pedroza-Banda R (2015) A new species of *Craugastor* (Anura: Craugastoridae) from the Magdalena River Valley Colombia with evaluation of the characters used to identify species of the *Craugastor fitzingeri* group. *South American Journal of Herpetology* 10(3): 165–178. <https://doi.org/10.2994/SAJH-D-14-00014.1>

- Padilla-Gil DN (2015) Ten new species of *Rhagovelia* in the *angustipes* complex (Hemiptera: Heteroptera: Veliidae) from Colombia with a key to the Colombian species. *Zootaxa* 4059(1): 71–95. <https://doi.org/10.11646/zootaxa.4059.1.4>
- Pinzón OP, Castro JD (2018) New records of termites (Blattodea: Termitidae: Syntermitinae) from Colombia. *Journal of Threatened Taxa* 10(9): 12218–12225. <https://doi.org/10.11609/jott.3909.10.9.12218-12225>
- Snyder TE (1925a) New termites and hitherto unknown castes from the Canal Zone Panama. *Journal of Agricultural Research* 29: 179–193.
- Snyder TE (1925b) New American termites including a new subgenus. *Journal of the Washington Academy of Sciences* 15(7): 152–162.
- Snyder TE (1949) Catalog of the termites (Isoptera) of the world Smithsonian Miscellaneous Collection 112: 1–490.
- Velasco JA, Hurtado-Gómez JP (2014) A new green anole lizard of the “Dactyloa” clade (Squamata: Dactyloidae) from the Magdalena river valley of Colombia. *Zootaxa* 3785(2): 201–216. <https://doi.org/10.11646/zootaxa.3785.2.4>
- Woodburne MO (2010) The Great American Biotic Interchange: dispersals tectonics climate sea level and holding pens. *Journal of Mammalian Evolution* 17(4): 245–264. <https://doi.org/10.1007/s10914-010-9144-8>

The morphology of the immature stages of *Squamapion atomarium* (Kirby, 1808) (Coleoptera, Brentidae) and notes on its life cycle

Krzysztof Pawłęga¹, Jacek Łętowski¹, Ewelina Szwaj², Tomasz Gosławski³

1 Department of Zoology and Animal Ecology, University of Life Sciences in Lublin, Akademicka 13, 20–950 Lublin, Poland **2** Braci Wieniawskich 6/59, 20–844 Lublin, Poland **3** Puławskiego 8/51, 91–021 Łódź, Poland

Corresponding author: *Krzysztof Pawłęga* (krzysztof.pawlega@up.lublin.pl)

Academic editor: *M. Alonso-Zarazaga* | Received 9 May 2019 | Accepted 19 October 2019 | Published 27 November 2019

<http://zoobank.org/F3F32E94-0AB7-49C4-A108-162690F122B4>

Citation: Pawłęga K, Łętowski J, Szwaj E, Gosławski T (2019) The morphology of the immature stages of *Squamapion atomarium* (Kirby, 1808) (Coleoptera, Brentidae) and notes on its life cycle. ZooKeys 892: 143–160. <https://doi.org/10.3897/zookeys.892.36027>

Abstract

The immature stages (egg, mature larva and pupa) of *Squamapion atomarium* (Kirby, 1808), as well as its development cycle and the phenology of its developmental stages, are described for the first time. The larva and pupa of *S. atomarium* have typical morphological features of the subfamily Apioninae. Morphological data on the immature stages were compared with the only fully described *Squamapion* species, *S. elongatum* (Germar, 1817). The larvae of the two species differ in body size and shape, head shape, setae length, the chaetotaxy of the mouthparts, and individual types of setae on the pronotum and thorax. In the case of the pupa, there are also differences in body size and in the type of setae and chaetotaxy of the head, pronotum, metanotum and abdomen.

Keywords

Apioninae, biology, central Europe, egg, host plant, life cycle, morphology, weevil

Introduction

The genus *Squamapion* Bokor, 1923 belongs to the tribe Kalcapiini Alonso-Zarazaga, 1990 in the subfamily Apioninae Schönherr 1823 and family Brentidae Billberg 1820. The adult morphology, ecology, distribution and systematics of the Apionidae

family have been presented in detail by Alonso-Zarazaga (1990, 2011), Petryszak (2004), Marvaldi and Lanteri (2005), Mokrzycki and Wanat (2005), Alonso-Zarazaga and Wanat (2014) and Alonso-Zarazaga et al. (2017). The immature stages of representatives of this family have been described by Scherf (1964), Łętowski (1991), Marvaldi (1999, 2003), Gosik et al. (2010), Wang et al. (2013), Oberprieler et al. (2014), and Łętowski et al. (2015). This genus is known from the Palearctic and Ethiopian regions and is poorly represented in the Oriental region. There are 33 known species in the Palearctic region, 19 in Europe, and only 9 in Poland (Mokrzycki and Wanat 2005; Alonso-Zarazaga 2011; Alonso-Zarazaga et al. 2017). These are herbivorous mono- or oligophagous species feeding on plants from the Lamiaceae family, with a preference for the genera *Salvia* L., *Thymus* L., *Thymbra* L., *Mentha* L., *Origanum* L., *Prunella* L. and *Saccocalyx* Coss. & Durieu. Their larvae bore tunnels inside the roots and stems, occasionally causing galls (Alonso-Zarazaga 1990). Adults have a small body size ranging from 1.10 to 2.70 mm. They are found mainly in dry and thermophilic environments – in non-forested areas and on the edges of forests and bushes (Burakowski et al. 1992).

The biology of only one species and the morphology of its immature stages are known – *Squamapion elongatum* (Germar, 1817) (Łętowski et al. 2015).

This study is a continuation of research on representatives of this genus found in Poland. The authors describe the morphology of the third larval instar and pupa as well as issues concerning the development and ecology of *Squamapion atomarium* (Kirby, 1808).

According to the literature, this species prefers warm, sandy areas and is usually found in xerothermic grasslands (Burakowski et al. 1992). Its host plants are Breckland thyme (*Thymus serpyllum* L.) and broad-leaved thyme (*T. pulegioides* L.). As regards its biology, *S. atomarium* feeds on the upper part of the stem of these plants, causing oval cecidia 2–4 mm long and 2 mm wide (Burakowski et al. 1992).

Material and methods

Insect collection

The research material comprised developmental stages (egg, larvae, and pupa) of *S. atomarium*, isolated in the laboratory from field-collected plants described in the literature as hosts. The choice of study sites was based on faunistic data on the occurrence of *S. atomarium* as well as our own observations of potential habitats in the Lublin region of Poland (Cmoluch 1963, 1971, 1987, 1992; Gosik and Łętowski 2003; Łętowski et al. 2003; Łętowski 2008). The sites were as follows: 1. Okale near Kazimierz Dolny (51°18'11.0"N, 21°53'58.6"E), 2. Bochońnica (51°20'38"N, 22°00'05"E), 3. Lublin-Górki Czechowskie (51°15'47"N, 22°32'03"E), 4. Lublin (51°13'11.50"N, 22°32'04.38"E), 5. Trześniów near Lublin (51°16'20"N, 22°37'04.10"E), 6. Kolonia Pliszczyn (51°17'38"N, 22°37'38"E), 7. the Stawska Góra Reserve near Chełm

(51°22'23"N, 23°24'11"E) and 8. the Żmudź Reserve (51°00'35"N, 23°40'14"E). Immature stages of *S. atomarium* were found at sites 3, 5 and 8. In the remaining sites, despite the presence of host plants, no specimens were found. The material was collected from May to August 2016 and 2017. To obtain immature stages of the species, plants were collected at the sites every 2–3 days. This frequency made it possible to study the development cycle of the species in its natural conditions. Breeding was also conducted in the laboratory. *Squamapion atomarium* adults were collected individually, directly from the host plant and from its immediate surroundings.

Breeding

Adult specimens were placed in plastic containers covered with mesh – separately for *T. serpyllum* L. and *T. pulegioides* L. Wet filter paper was placed on the bottom of the containers to maintain a suitable moisture level, together with thyme. The stems were searched for signs of oviposition and eggs about every three days. Then immature stages were grown in Petri dishes in a growth chamber, in the following conditions: daytime minimum 25 °C, daytime maximum 35 °C, minimum at night 15 °C, maximum at night 20 °C, humidity (60%), light duration – day 14 h, night 10 h. Immature stages were also grown in 125 ml plastic containers stored under room conditions (25 °C with a 14:10 photoperiod). Filter paper soaked in water was placed on the bottom of the container to maintain moisture, together with thyme stems with galls. The closed containers were monitored daily for mould. This method produced better results in terms of larvae survival than the use of the Petri dishes proposed by Scherf (1964). In order to track development and acquire larval stages, 5 stems were randomly selected, the galls were cut open, and developmental stages were isolated from them.

Morphological descriptions

The immature stages obtained by the methods described above were preserved in 70% ethyl alcohol. Two methods were used to prepare microscope slides, as described by Łętowski (1991) and Gosik et al. (2010). To prepare the drawings, we used an OLYMPUS SZX12 and DP72 microscope at magnifications from 200× to 400× and a TESCAN VEGA3LMU scanning electron microscope (SEM) at magnifications from 500× to 2000×. The larvae for SEM images were subjected to critical point drying (CPD). Drawings based on the slides were made using Corel Draw 18.

The terminology of Marvaldi (1999, 2003) and Oberprieler et al. (2014) was used in the morphological descriptions of the larva and pupa for chaetotaxy, and the terminology of Zacharuk (1985) and Marvaldi (1998) for antennae. The number and distribution of setae are given for one side. Measurements of the head (following decapitation) were made on the head capsule, isolated from the body, with the mandibles closed. Measurements were made of 10 L₁, 4 L₂, 15 L₃ and 10 pupae. The larvae were

not separated by gender for the measurements. The mean and standard deviation for each parameter were calculated using Excel.

An analysis was made of the growth of the heads of individual larval instars based on Dyar's law (1890), and the growth rate (GF) was determined based on Bednarz (1953).

Morphological abbreviations

AbI, AbVII, AbVIII, AbIX, AbX – abdominal segments 1, 7–10, **ThI, ThII, ThIII** – thoracic segments 1–3, **prns** pronotal setae, **pda** pedal s., **ps** pedal s., **eus** eusternal s., **lsts** laterosternal s., **prs** prodorsal s., **pds** postdorsal s., **as** alar s., **ss** spicular s., **eps** epipleural s., **ds** dorsal s., **les** lateral epicranial s., **fs** frontal s., **des** dorsal epicranial s., **pes** posterior epicranial s., **at** antenna, **Se** sensorium, **sb** sensillum basiconicum, **ss** sensillum styloconicum, **oc** ocellus, **enc** endocarina. **lrms** labral setae, **cls** clypeus s. **ams** anteromedial s., **als** anterolateral s., **mes** median s., **lr** labral rods., **mds** – dorsal malae s., **dms** dorsal maxillary s., **pfs** palpiferal s., **sts** stipal s., **mpxs** maxillary palp s., **mbs** malar basiventral s., **prms** prelabium s., **pms** postlabium s., **lgs** ligular s., **lbp** labial palpus, **as** apical setae, **ls** lateral s., **pals** posterolateral s., **sos** suborbital s., **rs** rostral s., **fes** femoral s., **ur** urogomphi.

Results

Description of egg

Fig. 1

Measurements (in mm, $N = 5$). Length 0.28 (0.22–0.31), width 0.18 (0.15–0.20).

General. Egg elliptical, shiny, smooth. Chorion soft, delicate (Fig. 1).

Colouration. Pale to dark yellow.

Description of larva

Figs 2–6

Measurements (in mm). First larval instar (L_1) – body length 0.46 (0.39–0.55), width 0.21 (0.19–0.23). Head width 0.13 (0.12–0.14).

Second larval instar (L_2) – body length 0.68 (0.64–0.74). Body widest at abdominal segment III (0.34). Average pronotum width 0.27 (0.15–0.21). Head width 0.19 (0.17–0.21). Stemmata present.

Mature larva (third instar, L_3) – body length 1.36 (1.09–1.72). Body widest at abdominal segment III (0.66, 0.50–0.86). Width of pronotum 0.47 (0.40–0.55). Head width 0.33 (0.30–0.38).

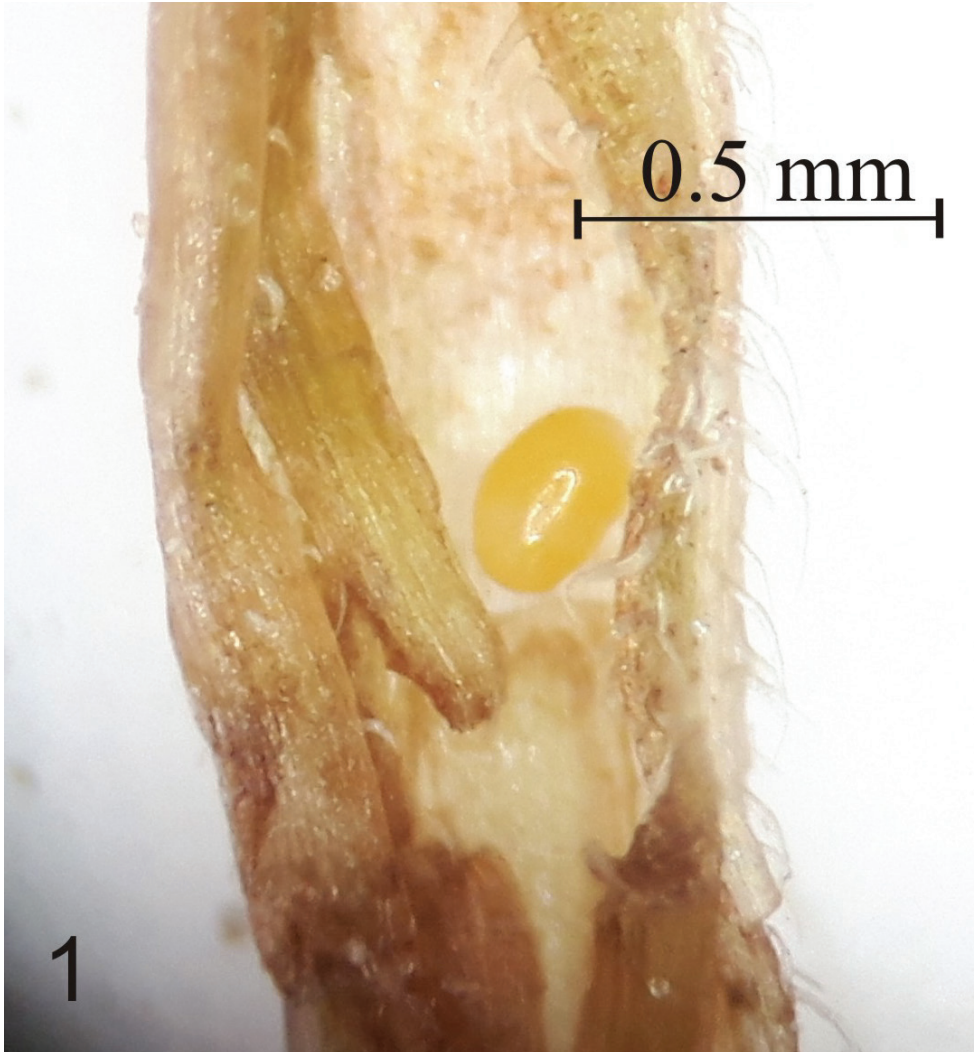


Figure 1. Egg of *Squamapion atomarium*.

General L_3 . Cylindrical, C-shaped, pale yellow with no distinct sclerotizations (Fig. 2). Cuticle microstructure of entire body with many small, sharply pointed cuticular structures. Thoracic and abdominal segments with characteristic, short setae. Body much narrower after abdominal segment VIII.

Head (Fig. 3). Pale yellow, later dark yellow, slightly hidden in prothorax, longer than wide, slightly egg-shaped, widest at $2/5$ of length. Epicranial suture visible. Endocarina (*enc*) distinct, long, together with epicranial suture extends $3/4$ length of head (Fig. 3). End of frontal suture with distinct stemmata. Antennae (*at*) without articulations. Sensorium (*Se*) long, slightly narrowing apically. Antenna with 4 sensillae: 2 *sb* (*sensillum basiconicum*) and 2 *ss* (*sensillum styloconicum*) (Fig. 3). Epicranium with 2

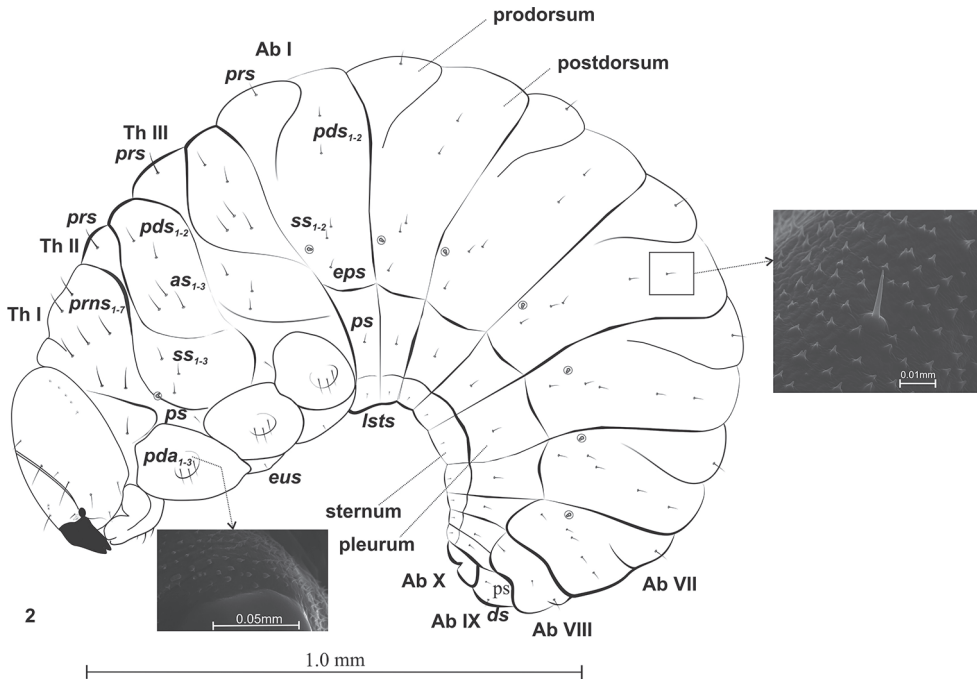


Figure 2. Mature larva (L_3) of *Squamapion atomarium*, lateral view.

lateral epicranial setae (*les*_{1,2}). *Les*₁ more than 4 times longer than *les*₂. Dorsal part of epicranium with 5 visible dorsal setae (*des*_{1–5}), *des*_{1,3–5} situated more or less along frontal suture, *des*₂ on extension of line of *pes* (Fig. 3). *Des*₃ very long, *des*₄ very short and *des*_{1,2,5} short and more or less equidistant. Epicranium with 4 thorn-shaped posterior epicranial setae posterolaterally (*pes*_{1–4}) –very short and more or less equidistant. Frons with 4 frontal setae (*fs*_{1,3–5}) (Fig. 3). *Fs*_{1,3} short (shortest of all *fs*), *fs*₁ situated by endocarina at about 1/3 length of frons, *fs*₃ situated outermost of all *fs*, close to *fs*₄. Setae *fs*₄ long – longest of all *fs*. Setae *fs*₅ slightly above anterior margin of stemmata.

Mouthparts. Labrum – anterior margin slightly arched. Dorsal side with 3 thorn-shaped labral setae (*lrms*), of which *lrms*₂ long and longer than others; *lrms*₁ closer to centre, below mid-height of labrum, *lrms*₂ and *lrms*₃ anterolaterally (Fig. 4a). Epipharynx anteriorly with 2 anteromedial setae (*ams*), of which medial *ams*₁ finger-shaped, outer setae *ams*₂ thorn-shaped (Fig. 4b). Beside *ams*, 2 *als* on epipharynx, arranged more or less diagonally from corner to centre of labrum. *Als*₁ slightly shorter than *als*₂. Both wider at base and narrowing apically. *Mes* digitiform and placed antero-medially. Labral rods (*lr*) present, long, extending well beyond suture (Fig. 4a). Clypeus kidney-shaped, with slightly concave anterior margin. 1 short seta *cls* at lower margin, between them 1 sensillum (*clss*) (Fig. 4a). Mandible massive, highly sclerotization, light to dark brown in colour. Two teeth equal in size, curved. Dorsally 1 pair mandible dorsal setae (*mds*_{1,2}) and 1 sensillum (Fig. 5). Setae close together, one above the other, each sensilla peripherally. *Mds*₂ more than twice longer than *mds*₁.

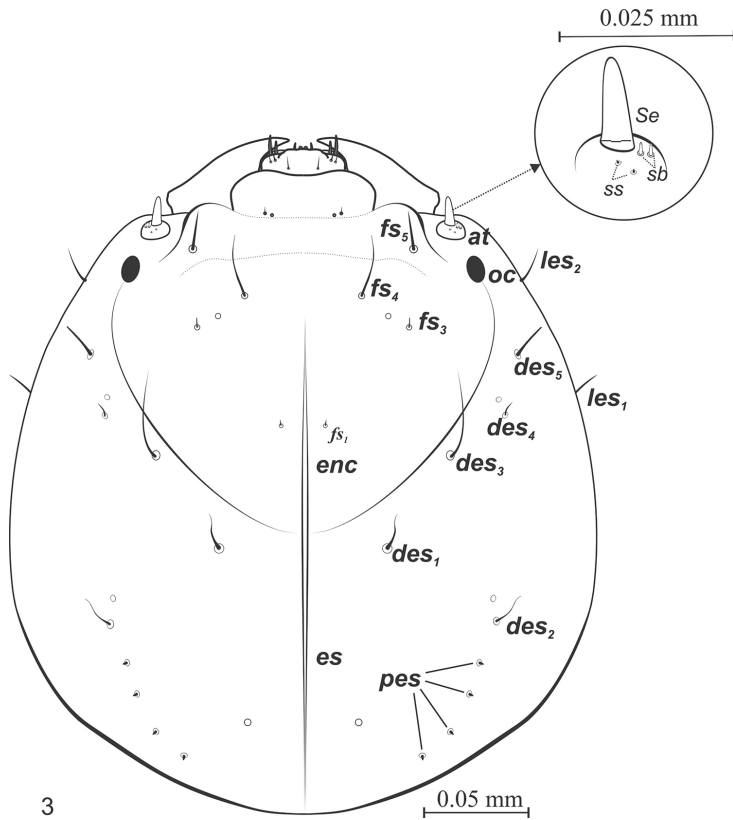
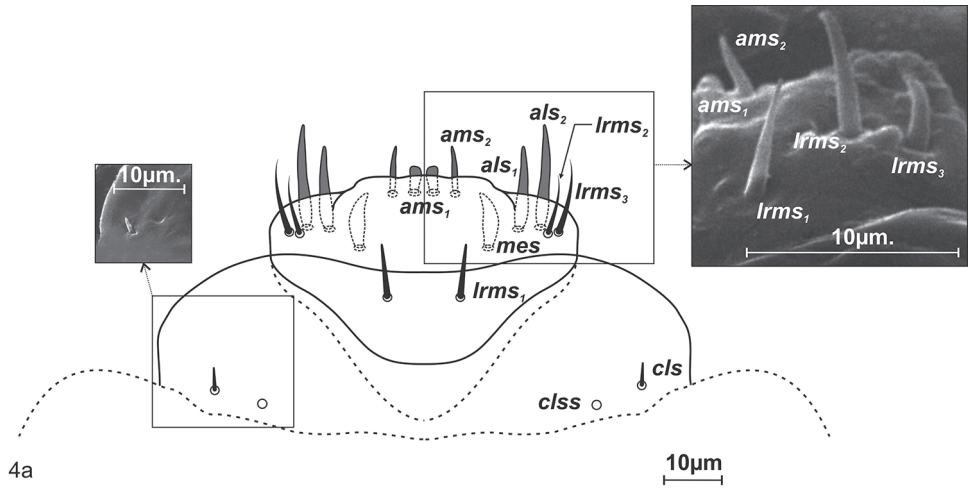


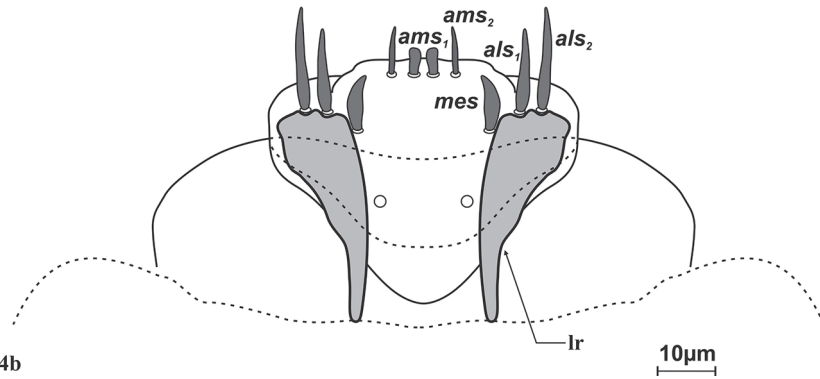
Figure 3. *Squamapion atomarium* (L₃), – epicranium, dorsal view.

Inner margin of inner teeth serrated. Maxillary stipes elongated, widening apically, narrowed at mid-length, with 4 distinct, hair-like setae (Fig. 6). In lower part 1 stipal seta (*stps*). In the upper part palpiferal setae *pfs1* fairly short, placed centrally under maxillary palpus, *pfs2* very long, placed on inner side, basioventral seta (*mbs*) short. Maxillary palpus (*mp*) 2-segmented, distal segment cylindrical, smaller than basal segment, with 10 nodular cuticular tubercles situated apically. Basal segment with rod-shaped sensorium, 1 minute maxillary palp seta (*mpps*) and 1 pore. Malar part of maxilla with 7 dorsal maxillary setae (*dms1–4*, *vms1–3*) clearly visible, finger-shaped setae of equal length in comb-like arrangement.

Labium cup-shaped (Fig. 6). Base of prementum rounded. Postmentum with 3 pairs postmental setae (*pms1–3*), distributed evenly, one over the other, closer to outer part of postmentum, more or less parallel to its edges. First pair setae (*pms1*) situated closest to lower margin, shortest of all *pms*. Above it *pms2*, very long and longest of *pms*, thick, narrowing only at apex. Setae *pms3* situated at 2/3 height of labium, similar in structure to *pms2* but half their length. Labium with Y-shaped premental sclerite situated centrally. 1 pair sensilla at base of arms of this structure. At height of premental sclerite, dorsally, chitinized inverted comma-shaped labial rods with uneven edges.

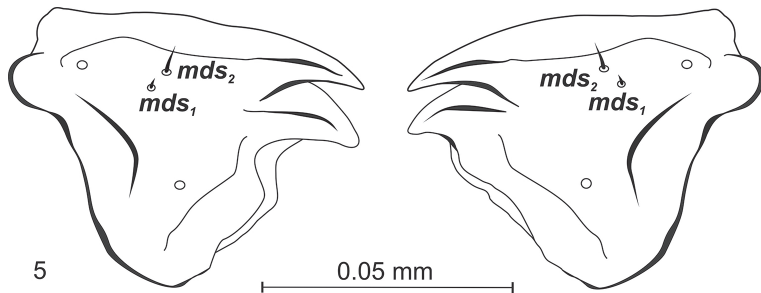


4a



4b

Figure 4. *Squamapion atomarium* (L₃) labrum and clypeus: **a** dorsal view **b** ventral view.



5

Figure 5. *Squamapion atomarium* (L₃) – mandibulae.

Labium with 1 pair simple palpi (*lbp*), with 7 palpillae apically, 1 inner seta at base and 1 outer sensillum. In front of palpi 1 pair long premental setae (*prms*). Behind palpi 2 pairs very short ligular setae (*lgs*) and 1 pair sensilla (Fig. 6).

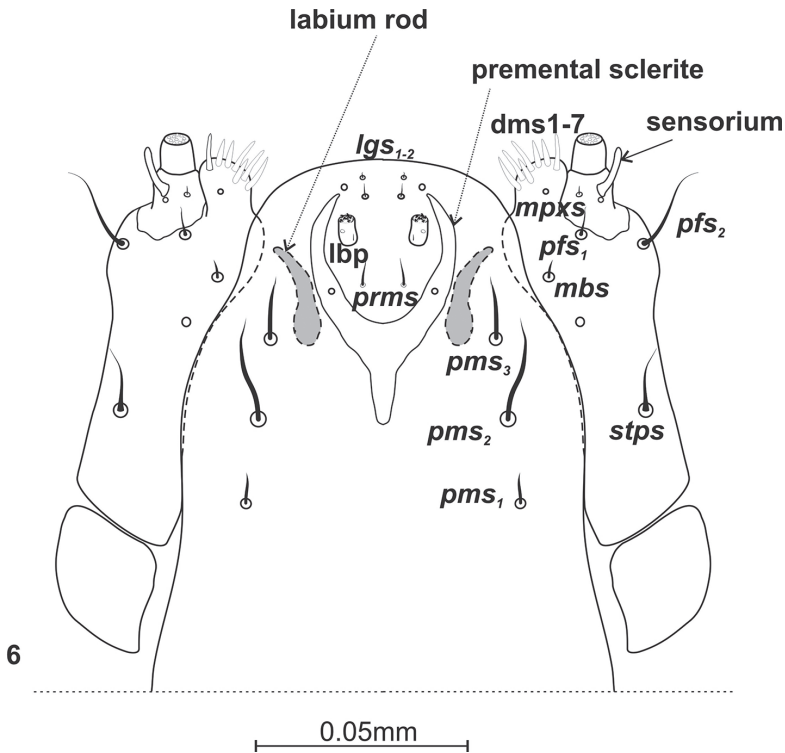


Figure 6. Labium and maxillae (L_3) of *Squamapion atomarium*.

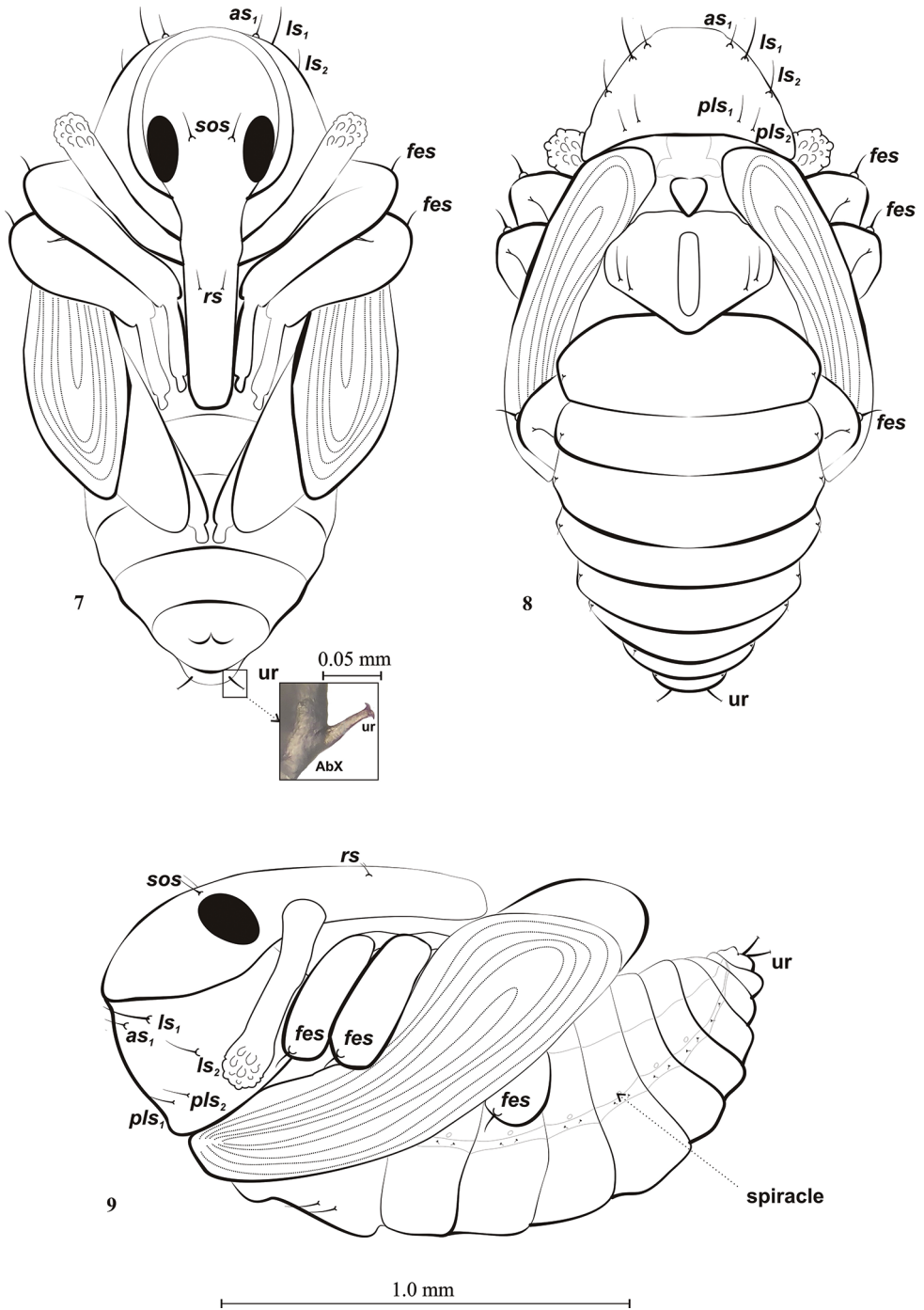
Thorax. Thoracic segments with well visible pedal area. Thoracic setae longer than others. Prothorax with 7 pronotal setae varying in length (*prns*), 1 pleural seta (*ps*) and on pedal area 3 pedal setae (*pda*) (Fig. 2). Meso- and metathorax each with 1 relatively long prodorsal seta (*prs*), 2 postdorsal setae (*pds*), 3 alar setae (*as*), 3 spicular setae (*ss*), 3 *pda* on pedal area and 1 short eusternal seta (*eus*). Thoracic spiracle bicameral, located intersegmentally, between Th.I and Th.II (Fig. 2).

Abdomen. Tergites I–VII with 2 folds and 1 seta (*prs*) on prodorsum. Postdorsum with 2 *pds* and 2 *ss* of varying size; 1 epipleural seta (*eps*) slightly below *ss*. Pleurum with 1 *ps*. Sternum with 1 laterosternal seta (*lsts*). Tergit VIII with gentle folds and with 1 *prs*, 1 dorsal seta (*ds*) and 1 *eps*. Tergit IX without folds, with 1 *ds* and 1 *ps*. Sternum and pleurum of segments VIII–IX with 1 *ps* and 1 *lsts*. Segments I–VII with unicameral spiracles, others without spiracles (Fig. 2).

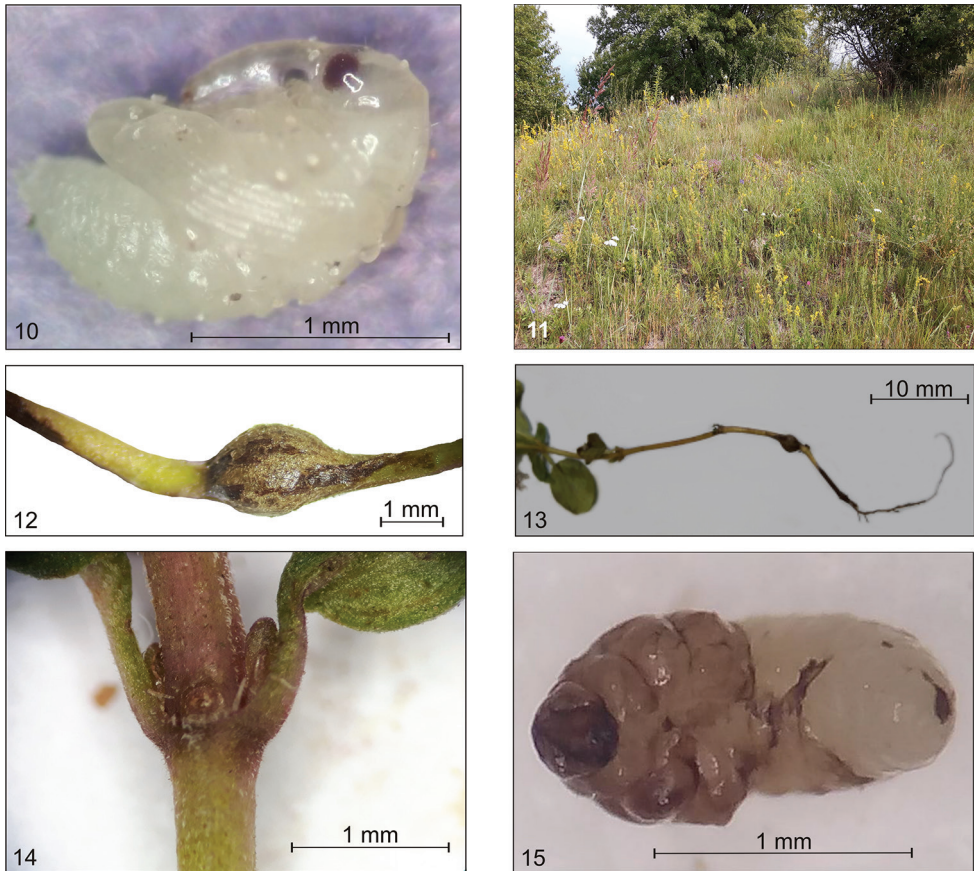
Description of pupa

Figs 7–10

Measurements (in mm). Body length 1.51 (1.24–1.63), width 0.84 (0.72–0.93) (Figs 7–10).



Figures 7–9. Pupa of *Squamapion atomarium* **7** ventral view **8** dorsal view **9** lateral view.



Figures 10–15. *Squamapion atomarium* **10** pupa **11** occurrence environment **12** a gall **13** the most common place to lay eggs at the root collar **14** place for laying eggs **15** larva in prepupal stage for pupation.

Colouration. Colour creamy-white.

Head. Eyes large, with 1 supraorbital seta (*sos*) between them. Rostrum long, extending to end of tarsi of mesolegs, not very wide, with 1 rostral seta (*rs*) below base of antennae, shorter than *sos*. Antennae relatively long, club with conical papillae. Antennae sub-parallel to protibia (Figs 7, 9).

Thorax. Pronotum wider than long; sides with 2 lateral setae – long *ls1* and shorter *ls2*; 1 apical seta on apex (*as*), half length of *ls1* (Figs 7, 8); lower margin with 2 posterolateral setae (*pls1,2*), similar in length to *as1*. Mesonotum without setae. Metanotum with 2 setae, slightly shorter than *ls1* (Figs 8, 9). Each femur with 1 femoral seta (*fes*) on convex base (Figs 8, 9).

Abdomen. Chaetotaxy very sparse. Each segment with 1 short dorsal seta located close to lateral margin. Each of lateral parts of abdominal segments I–VII with 1 pair

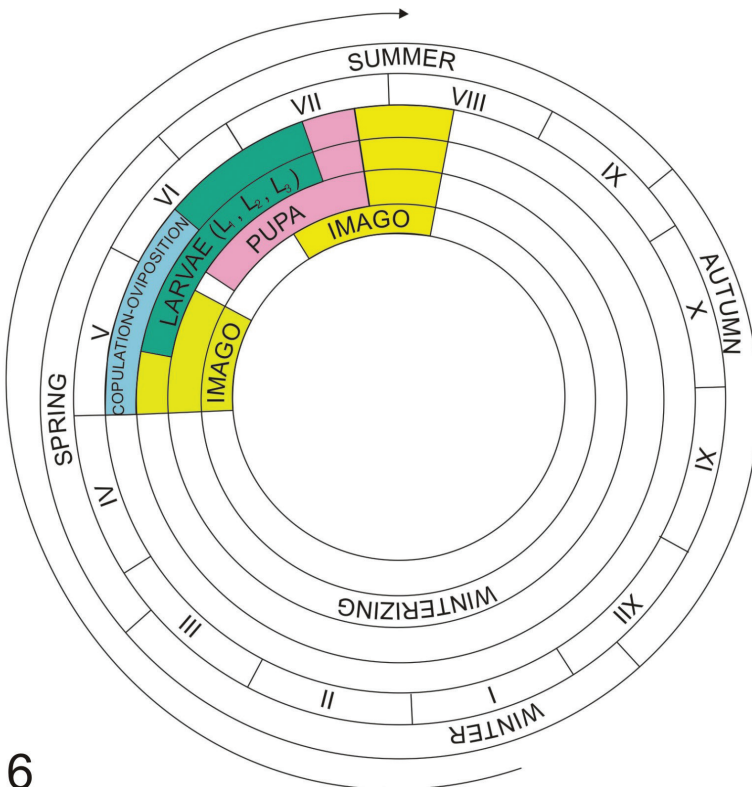
minute lateral setae. Spiracles located between tergites and pleurites, clearly visible on segments I–VI, on others absent (Fig. 9). Segment IX terminally with 1 pair urogomphi (ur) with characteristic ends in form of flattened bifurcation (Fig. 7).

Notes on biology and life cycle

Figs 11–17

Host plant. The life cycle of *S. atomarium* was described based on field data and laboratory observations. *Thymus serpyllum* and *T. pulegioides* were confirmed as host plants (Fig. 11).

Life cycle. Adults, following overwintering and maturation feeding, begin copulation and egg laying in the first half of May. Increased egg laying was observed at the end of May, and single eggs were still noted in early June. Adults usually feed in the evening, by gnawing round holes in the leaf that do not exceed 1 mm in diameter. The fertilized female gnaws a cavity in the stem and lays one egg in it (Fig. 12). Oviposition takes place primarily at the root collar, but it was also observed up to the fourth or fifth node, in both nodes and internodes (Fig. 13). After laying the egg the female does not seal the site with any secretion. The first instar larva (L_1) hatches on average 4 days



16

Figure 16. Life cycle of *Squamapion atomarium*.



Figure 17. Larva of a chalcidoid endoparasitoid found inside the mature larva (L_3) of *Squamapion atomarium*.

after the egg is laid and moults after 10–12 days. The L_1 instar was observed as early as mid-May, but these were isolated specimens. Maximum emergence was observed from the second third of May. L_1 larvae were found until mid-June. The second larval instar (L_2) appeared at the end of May. The activity of L_2 larvae causes distinct galls about 1.32 mm long and about 0.75 mm wide. Furthermore, L_2 gnaws out an opening for oviposition on the opposite side of the groove, but does not gnaw through the skin. The second larval instar lasts on average 10 days, and then the larva moults again. L_3 larvae appeared as early as the last third of June and were noted until mid-July. The average duration of this stage is about 11 days. This stage continues feeding and the gall grows, reaching on average about ca 2.31 in length and ca 1.70 mm in width (Fig. 14). The third larval instar enlarges the opening in the stem. Then pupation takes place (Fig. 15). The pupal stage lasts 2–3 days on average. The first pupae appeared at the end of June. Finally, at a maximum 40 days after the egg is laid, adult individuals appear. An increase in the emergence of adults took place from mid-July. The entire life cycle of *S. atomarium* is presented in the diagram in Figure 16.

Parasitoids. In the second half of July, endoparasitic hymenopterans of the superfamily Chalcidoidea were very active, which is manifested by the high level of parasitism of L_3 larvae. On average 7 of 10 third-instar larvae exhibited symptoms of parasite infection: dark red discolouration on the thoracic tergites and pleurites and swelling of the ab-

dominal segments caused by the growth of the intruder larvae (Fig. 17). The mature larva of the parasitoid usually occupied the space from the second or third thoracic segment to the eighth abdominal segment. The adult larva of the parasite is ca 0.75 mm long and ca 0.56 mm wide. The body of the pupa of the parasitoid is black with a metallic sheen and well chitinized. The parasites brought about the death of L_3 of *S. atomarium*.

Head growth of larval instars and growth factor (GF)

Figs 18, 19

Deviations of the mean dimensions of the heads of individual larval stages from the theoretical dimensions are shown in Figures 18, 19. Analysis of the ratios of the head sizes of larval instars does not clearly result in a single growth factor. GF between L_1 and L_2 is 1.43 and between L_2 and L_3 it is 1.75.

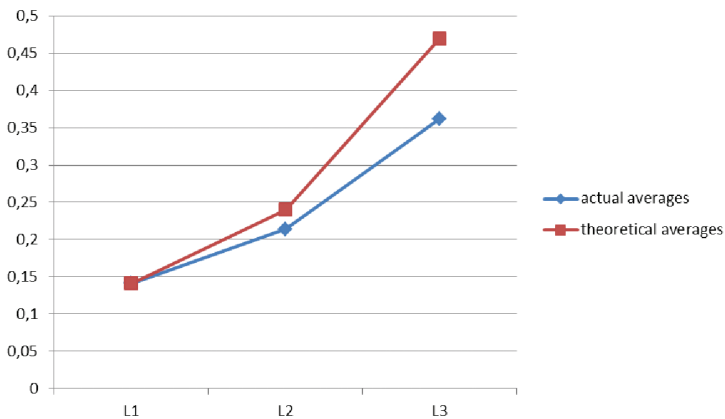


Figure 18. Mean real and average theoretical head lengths of *Squamapion atomarium* larval stages.

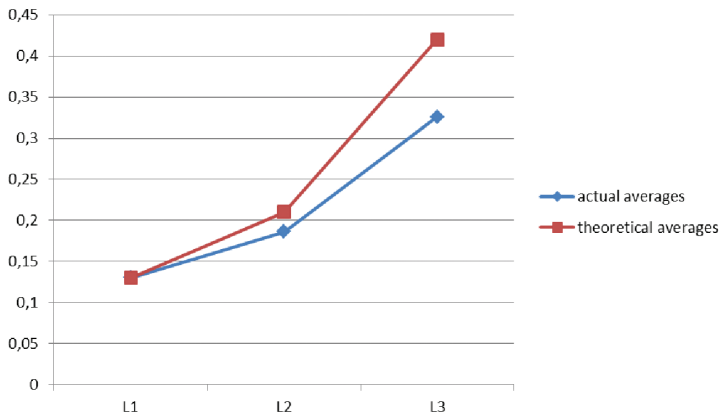


Figure 19. Mean real and average theoretical head widths of *Squamapion atomarium* larval stages.

Discussion

Among species of the genus *Squamapion*, only *S. elongatum* (Germar, 1817) has previously been described, and the existing data on *S. atomarium* concern only its habitat and host plants, with an equal role ascribed to *T. serpyllum* and *T. pulegioides* (Burakowski et al. 1992; Łętowski et al. 2015). The present study has shown that the preferred plant species is broad-leaved thyme (*T. pulegioides*), on which more galls were observed. This is most likely linked to the environment inhabited by *S. atomarium*, where this species of thyme is more common. Another new observation is the site of oviposition and galls. According to Burakowski et al. (1992), the larva feeds on the upper part of the stem. In the present study, the eggs were usually laid in the lower part of the stem.

The morphology of the L₃ larva and pupa of *S. atomarium* does not differ from the typical characters of the subfamily Apioninae (Alonso-Zarazaga and Wanat 2014). These features are the strongly convex and C-shaped body, colour, subglobose head, coronal suture and endocarinal line, clearly visible stemmata close to the frontal suture; numbers of *des*, *les* and *fs*; transverse and trapeziform clypeus with one pair of *cls* and one pair of *clss*; chaetotaxy of the labrum and epipharynx; mandible chaetotaxy; morphology and chaetotaxy of the maxilla and labium; thoracic segments with a prodorsum and postdorsum; very small prodorsum of the pronotum; morphology and chaetotaxy of the pro-, meso- and metanotum, except the number of *as*, with three pairs in *S. atomarium*; mesothoracic spiracles on the membrane between the pro- and mesothorax; and the abdominal morphology and chaetotaxy, except for the presence of *lsts* on the 8th abdominal segment in *S. atomarium*.

Thus the immature stages of the species are generally very similar in their morphology to those described by Łętowski (1991) for *Synapion ebeninum* (Kirby, 1808), *Stenopteraion intermedium* (Eppelsheim, 1875) and *Metatrichapion reflexum* (Gyllenhal, 1833), by Gosik et al. (2010) for *Diplapion confluens* (Kirby, 1808), or by Wang et al. (2013) for *Pseudaspidapion botanicum* Alonso-Zarazaga & Wang, 2011. *Squamapion atomarium* was also confirmed to possess an apomorphic trait of Apioninae emphasized by Marvaldi (2003), namely a lack of spiracles beginning in the eighth abdominal segment. There are differences in body size and in the number and distribution of setae (see Łętowski et al. 2015).

In the comparative analysis of the egg and L₃ larva of *S. atomarium* and *S. elongatum*, the two species are distinguished by differences in the size of both the egg and the L₃ larvae – in *S. atomarium* they are about half the size as in *S. elongatum* (Łętowski et al. 2015). Similar differences are found in the width of the epicranium of the two species, the shape of the head, and some features of their chaetotaxy. The differences are presented in Table 1.

The case of the pupa is similar. There are clearly visible differences between species in body size and chaetotaxy. The body of the pupa of *S. atomarium* is shorter than that of *S. elongatum* (1.5–2.0 times) and has far fewer abdominal setae (Table 2). There are also minor differences in body colour. Similar proportions of body length are found in adults.

The study and descriptions of additional species of the genus *Squamapion* will make it possible to distinguish and describe its generic characters.

Table 1. Character comparison between L₃ *Squamapion atomarium* and *Squamapion elongatum*.

Trait		Species	
		<i>Squamapion atomarium</i>	<i>Squamapion elongatum</i>
Body mm (length/width)		ca 1.36/ca 0.66	ca 2.78/ca 1.24
Setae		shorter, with pointed ends	longer
Head		slightly egg-shaped	oval
Antennae		4 sensilla	2 sensilla
Number of setae on maxillary palpus	basal segment	1 seta, 1 sensillum	1 seta, 2 sensilla
	distal segment	none	1 short sensillum
Labrum/epipharynx	<i>ams</i>	2 pairs (<i>ams1–2</i>)	3 pairs (<i>ams1–3</i>)
	<i>als</i>	2 pairs	3 pairs
	<i>lr</i>	large, widening towards outer margin of epipharynx	narrow
Labium with <i>pms</i>		3 pairs (<i>pms1–3</i>)	2 pairs (<i>pms1</i> and <i>pms3</i>)
Number of conical papillae <i>dms</i>		4	5
Number of setae <i>prns</i> on pronotum		7	5
Number of setae <i>pda</i>		3	2
Number of setae <i>ss</i>		2	3

Table 2. Character comparison between the pupa of *Squamapion atomarium* and *Squamapion elongatum*.

Trait		Species	
		<i>Squamapion atomarium</i>	<i>Squamapion elongatum</i>
Body mm (length/width)		ca 1.51/ca 0.84	ca 2.67/ca 0.94
Colour		creamy-white	whitish-grey
Head setae		1 pair <i>sos</i> , 1 pair <i>rs</i>	1 pair <i>vs</i> , 1 seta <i>rs</i>
Pronotum		1 pair <i>as</i> (<i>as1</i>), 2 pairs <i>ls</i> (<i>ls1,2</i>)	2 pairs <i>as</i> (<i>as1,2</i>), 1 pair <i>ls</i>
Metanotum		2 pairs of setae	3 pairs of setae
Abdomen	lateral part	only 1 pair of setae of I–VII abdominal segments	absent
	dorsal part	absent	AbI–III: 7 pairs,
			AbIV–VI: 5 pairs,
			AbVII: 3 pairs, AbVIII: 1 pair
Urogomphi		flattened bifurcation, straight	crescent-shaped, narrow

Analysis of the growth rate and the ratio of actual and theoretical average head sizes produced some discrepancies that may have been influenced by the fact that the individuals were not divided by sex or collection site, and thus may have represented different populations.

Acknowledgements

The authors would like to thank Professor Bernard Staniec and Jarosław Pawelec of the Maria-Curie Skłodowska University in Lublin for allowing us to take photos using scanning electron microscopy and the CPD procedure. The authors would like to thank the English native Sara Wild – for the correction of the manuscript.

References

- Alonso-Zarazaga MA (1990) Revision of the supraspecific taxa in the Palearctic Apionidae Schoenherr, 1823 (Coleoptera, Curculionoidea) (2. Subfamily Apioninae Schoenherr, 1823: Introduction, keys and descriptions. *Graellsia* 46: 19–156.
- Alonso-Zarazaga MA (2011) Apionidae. In: Löbl I, Smetana A (Eds) *Catalogue of Palearctic Coleoptera* (Vol. 7). Stenstrup, Apollo Books, 373 pp.
- Alonso-Zarazaga MA, Wanat M (2014) Apioninae Schoenherr, 1823. In: Leschen RAB, Beutel RG (Eds) *Handbook of Zoology/ Handbuch der Zoologie, Band 4: Arthropoda, 2. Hälfte: Insecta, Coleoptera, Beetles* (Vol. 3). Morphology and Systematics (Phytophaga). De Gruyter, Berlin, Boston, 395–415.
- Alonso-Zarazaga MA, Barrios H, Borovec R, Bouchard P, Caldara R, Colonnelli E, Gültekin L, Hlavá P, Korotyaev B, Lyal CHC, Machado A, Meregalli M, Pierotti H, Ren L, Sánchez-Ruiz M, Sforzi A, Silfverberg H, Skuhrovec J, Trýzna M, Velázquez de Castro AJ, Yunakov NN (2017) Cooperative catalogue of Palearctic Coleoptera Curculionoidea. *Monografias electrónicas S.E.A.* (Vol. 8), 729 pp.
- Bednarz S (1953) Wzrost głowy larw *Tettigonia viridissima* (Saltatoria, Tettigoniidae) a hipoteza Dyara. *Polskie Pismo Entomologiczne*, Warszawa, T. XXIII, 14: 191–203.
- Burakowski B, Mroczkowski M, Stefańska J (1992) Katalog Fauny Polski. Cz. XXIII, T. 18. Chrzęszcze – Coleoptera. Ryjkowcowate prócz ryjkowców – Curculionoidea prócz Curculionidae. Wydawnictwo Muzeum i Instytut Zoologii PAN, Warszawa, 324 pp.
- Cmoluch Z (1963) Badania nad fauną ryjkowców (Coleoptera, Curculionidae) roślinnych zespołów kserotermicznych południowo-wschodniej części Wyżyny Lubelskiej. *Annales Universitatis Mariae Curie-Skłodowska, sectio C* 17(1): 1–75.
- Cmoluch Z (1971) Studien über Rüsselkäfer (Coleoptera, Curculionidae) xerothermer Pflanzensoziationen der Lubliner Hochebene. *Acta Zoologica Cracoviensia* 16: 29–216.
- Cmoluch Z (1987) Ryjkowce (Coleoptera, Curculionidae) roślinnych zbiorowisk kserotermicznych Białej Góry koło Tomaszowa Lubelskiego. *Annales Universitatis Mariae Curie-Skłodowska, sectio C* 39: 187–197.
- Cmoluch Z (1992) Rüsselkäfer (Coleoptera, Curculionidae) von Polesie Lubelskie. *Annales Universitatis Mariae Curie-Skłodowska, sectio C*, 44 – 1989: 1–64.
- Dyar HG (1890) The number of molts of lepidopterous larvae. *Psyche* 5: 420–422. <https://doi.org/10.1155/1890/23871>
- Gosik R, Łętowski J (2003) Ryjkowcowate (Curculionoidea: Rhinomaceridae, Attelabidae, Apionidae, Curculionidae) użytku ekologicznego „Biała Góra”. *Parki Narodowe i Rezerwy Przyrody* 21(2): 247–266.
- Gosik R, Łętowski J, Kozak E (2010) Morphology of the mature larva and pupa of *Diplapion confuens* (Kirby, 1808) (Coleoptera: Apionidae). *Polish Journal of Entomology* 79: 211–221.
- Łętowski J (1991) Morfologia i biologia trzech gatunków z rodzaju *Apion* Herbst (Apionidae, Coleoptera) uszkadzających sparcetę siewną (*Onobrychis viciaefolia* Scop.). Wydawnictwo Uniwersytetu Marii Curie-Skłodowskiej, 95 pp.
- Łętowski J (2008) The weevils (Curculionoidea) of calcareous habitats of the vicinity of Chełm. *Teka Komisji Ochrony i Kształtowania Środowiska Przyrodniczego OL PAN* 5: 5–125.

- Łętowski J, Gosik R, Czarniawski W, Budzyńska E (2003) Materiały do znajomości ryjkowcowatych (*Curculionoidea*, *Coleoptera*) Kazimierskiego Parku Krajobrazowego. Parki Narodowe i Rezerwy Przyrody 22(2): 227–245.
- Łętowski J, Pawłega K, Ścibior R, Rojek K (2015) The morphology of the preimaginal stages of *Squamapion elongatum* (Germar, 1817) (Coleoptera, Curculionoidea, Apionidae) and notes on its biology. ZooKeys 519: 101–115. <https://doi.org/10.3897/zookeys.519.9134>
- Marvaldi AE (1998) Larvae of Entiminae (Coleoptera: Curculionidae): tribal diagnoses and phylogenetic key, with a proposal about natural groups within Entimini. Entomologica Scandinavica 29: 89–98. <https://doi.org/10.1163/187631298X00212>
- Marvaldi AE (1999) Morfología larval en Curculionidae (Insecta: Coleoptera). Acta Zoológica Lilloana 45(1): 7–24.
- Marvaldi AE (2003) Key to larvae of the South American subfamilies of weevils (Coleoptera: Curculionoidea). Revista Chilena de Historia Natural 76: 603–612. <https://doi.org/10.4067/S0716-078X2003000400005>
- Marvaldi AE, Lanteri AA (2005) Key to higher taxa of South American weevils based on adult characters (Coleoptera, Curculionoidea). Revista Chilena de Historia Natural 78: 65–87. <https://doi.org/10.4067/S0716-078X2005000100006>
- Mokrzycki T, Wanat M (2005) A new checklist of the weevils of Poland (Coleoptera: Curculionoidea). Genus 16(1): 69–117.
- Oberprieler RG, Anderson RS, Marvaldi AE (2014) Curculionoidea Latreille, 1802: Introduction, Phylogeny. In: Leschen RAB, Beutel RG (Eds) Handbook of Zoology (Vol. 3), Walter de Gruyter GmbH, Berlin, Boston, 285–300.
- Petryszak B (2004) Curculionoidea. In: Bogdanowicz W, Chudzicka E, Pilipiuk I, Skibińska E (Eds) Fauna of Poland. Characteristics and Checklist of Species. Museum i Instytut Zoologii PAN (Vol. I). Warszawa, 509 pp.
- Scherf H (1964) Die Entwicklungsstadien der mitteleuropäischen Curculioniden (Morphologie, Bionomie, Ökologie). Verlag Waldemar Kramer, Frankfurt am Main, 335 pp.
- Wanat M (1997) New and little known *Squamapion* species (Coleoptera: Apionidae) from western Palaearctic. Annales Zoologici 47(1/2): 285–295.
- Wang Z, Alonso-Zarazaga MA, Zhou D, Zhang R (2013) A description of preimaginal stages of *Pseudaspidapion botanicum* Alonso-Zarazaga & Wang, 2011 (Apionidae, Curculionoidea). ZooKeys 260: 49–59. <https://doi.org/10.3897/zookeys.260.4450>
- Zacharuk RY (1985) Antennae and sensilla. In: Kerkut GA and Gilbert LI (Eds) Comparative Insects Physiology, Pergamon Press, Oxford, Chemistry and Pharmacology 6: 1–69.